THE UNIVERSITY OF HULL

Robust Fault Tolerant Control of Induction Motor System

Being a thesis submitted for the Degree of PhD

in the University of Hull

by

Zhihuo Wang

Msc (Northwestern Polytechnical University, China)

Bsc (Northwestern Polytechnical University, China)

January 2018

Acknowledgement

Thank Jesus.

Abstract

Research into fault tolerant control (FTC, a set of techniques that are developed to increase plant availability and reduce the risk of safety hazards) for induction motors is motivated by practical concerns including the need for enhanced reliability, improved maintenance operations and reduced cost. Its aim is to prevent that simple faults develop into serious failure. Although, the subject of induction motor control is well known, the main topics in the literature are concerned with scalar and vector control and structural stability. However, induction machines experience various fault scenarios and to meet the above requirements FTC strategies based on existing or more advanced control methods become desirable. Some earlier studies on FTC have addressed particular problems of 3-phase sensor current/voltage FTC, torque FTC, etc. However, the development of these methods lacks a more general understanding of the overall problem of FTC for an induction motor based on a true fault classification of possible fault types.

In order to develop a more general approach to FTC for induction motors, i.e. not just designing specific control approaches for individual induction motor fault scenarios, this thesis has carried out a systematic research on induction motor systems considering the various faults that can typically be present, having either "additive" fault or "multiplicative" effects on the system dynamics, according to whether the faults are sensor or actuator (additive fault) types or component or motor faults (multiplicative fault) types.

To achieve the required objectives, an active approach to FTC is used, making use of fault estimation (FE, an approach that determine the magnitude of a fault signal online) and fault compensation. This approach of FTC/FE considers an integration of the electrical and mechanical dynamics, initially using adaptive and/or sliding mode observers, Linear Parameter Varying (LPV, in which nonlinear systems are locally decomposed into several linear systems scheduled by varying parameters) and then using back-stepping control combined with observer/estimation methods for handling certain forms of nonlinearity.

In conclusion, the thesis proposed an integrated research of induction motor FTC/FE with the consideration of different types of faults and different types of uncertainties, and validated the approaches through simulations and experiments.

Contents

Symbols

0	Zero matrix with compatible dimensions
$\mathbb{R}$	Set of real numbers
$\mathbb{R}^n$	Set of n dimensional real vectors
$\mathbb{R}^{n\times m}$	Set of n by m matrices with elements in $\mathcal{R}$
M^T	The transpose of the matrix M
M^{-1}	The inverse of the invertible matrix M
$M > 0 (M \geq 0)$	M is positive definite (positive semidefinite)
$M < 0 (M \leq 0)$	M is negative definite(negative semidefinite)
λ	An eigenvalue
$\|x\|_1$	L_1 norm of vector $x \in \mathbb{R}^n$, and $\|x\|_1 = \sum_{i=1}^{n} \|x_i\|$
$\|x\|_Q$	$\|x\|_Q = x^T Q x$ with $x \in \mathbb{R}^n$and $Q \in \mathbb{R}^{n\times n}$

List of Figures

Abbreviations

AFTC	Active Fault Tolerant Control
CPLD	Complex Programmable Logic Device
CPU	Central Processing Unit
DSC	Desired State Configuration
DSP	Digital Signal Processor
FD	Fault Diagnosis
FDI	Fault Detection and Identification
FE	Fault Estimation
FPGA	Field Programmable Gate Array
FTC	Fault Tolerant Control
IM	Induction Motor
LMI	Linear Matrix Inequality
LPV	Linear Parameter Varying
LTV	Linear Time Varying
MPC	Model Predictive Control
PFTC	Passive Fault Tolerant Control
PWM	Pulse Width Modulation
SMO	Sliding Mode Observer
SPWM	Sinusoidal PWM
SVPWM	Space Vector PWM
VHDL	Very High Speed Integrated Circuit Hardware Description Language
VSI	Voltage Source Inverter

Chapter 1: Introduction

1.1 Introduction

For centuries, industry developed at a high speed. In developed countries, about half of the electricity is converted into mechanical energy. This energy transformation is usually conducted by induction motors. Compared with the DC motor, induction motors have obvious advantages with regard to ruggedness, convenient maintenance, lower cost etc. (Trzynadlowski, 2000).

The induction motor is the most widely used motor in daily life and industry. It provides power for a variety of mechanical equipment and household appliances. The power capacity of induction motors varies from a few watts to tens of thousands of kilowatts, in order to meet the need of different producing environments. In the world, a large number of electrical equipment use induction motors. In an industrialized country, the use of induction motors typically accounts for 40 to 50 percent of the electricity produced (Thomson & Fenger, 2001). According to the China's Servo Motor Industry Survey and Investment Prospects in 2017 – 2021, the demand for motor applications is increasing steadily, as shown in Figure 1-1.

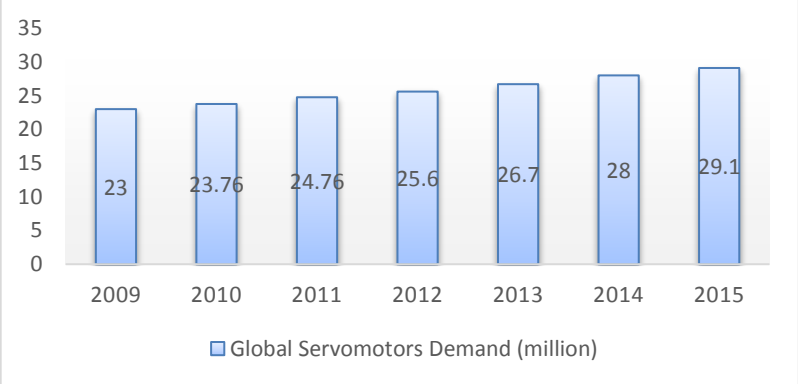

Figure 1-1 The growing global servomotors demand (China's Servo Motor Industry Survey and Investment Prospects in 2017 – 2021)

Induction motor operating efficiency is being pursued in order to limit additional cost of operation. Induction motor failure can lead to a large decrease of efficiency, and even lead to equipment stoppage. It is unacceptable. The following types of conditions greatly affect the performance of induction motor： efficiency accuracy (20% of all possible

conditions), temperature rise (20%), current and torque anomalies due to rotor faults (22.5%). The percentage represent the probality of faults in real world application, it is originally shown in (Agamloh, 2014). In industry, stoppage or shutdowns of induction motor will cause rise of budget for employing motor maintenance team, selecting the best motor-maintenance techniques, and so on. Inevitably, faults in induction motor system certainly raise the necessary expenses.

Based on the above motivations, a lot of work has been done in order to save energy or cost. Since the 1960s, the control of induction motors has been highly valued by researchers, and power systems engineers motivated by the need to optimise machine performance taking account of known physical limitations and application requirements (Lavi & Polge, 1966; Paice, 1968; Hammond & Mokrytzki, 1973; Cornell & Lipo, 1977). For induction motor control, according to Google Scholar approximately 735000 papers are generated in recent 10 years; while focussing specifically on adaptive control, the number of published papers is around 24300. As dynamic system control methods have developed a lot, the induction motors control strategies relates more and more closely with the real system properties. Scientific and engineering research in this field is well motivated by commercial interests, e.g. in manufacturing, automotive engineering, domestic systems, heavy industry, renewable energy etc. The industrial significance of induction motor control has exceeded 80,000 patents (Marino et al., 2010), many based on novel approaches in signal processing. Advanced power electronic devices are also developing at high speed in the case of increasing control range and machine control precision. Digital signal processing methods and devices have become very powerful and have rapidly reducing cost, enabling a wide variety of power electronics devices to meet the control performance requirements (torque, speed, etc.) of modern induction machines (both generators and motors). As a subset of induction machines, induction motors are still widely used in preference to DC motors that may be unlikely to achieve the required performance of the induction motor counter-part (Marino et al., 2010; Chan & Shi, 2011).

Clearly induction motors are very widely used throughout every day engineering systems. Methods of ensuring machine performance in the case of sensor, actuator or component faults remains a challenging subject of both theoretical and applied research. From a control point of view this is the subject of what has become known as Fault Tolerant Control (FTC) in which the faults acting on the motor can be detected or estimated on-line within a “control reconfiguration” action.

The idea of FTC can be stated according to (Patton, 2015): "When unsatisfactory performance or instability happens in the case of actuators, sensors, or components, the methods of fault detection and isolation (FDI), fault detection and diagnosis (FDD), or fault estimation (FE) will be used with FTC to realise active or passive compensation for the closed-loop control system. Then the effects of the faults are reduced or eliminated, which would lead to a safe and reliable operation of the dynamic system."

For example by estimating the signal effect of each fault, the control system can use the estimates to compensate for the fault and reconfigure the control system. The resulting closed-loop system will then be "fault-tolerant" if it can recover the required control action, performance and stability.

A classification of the various forms of FTC systems is given in Chapter 4, where it can be seen that some approaches are based on FDI and system reconfiguration after faults have been detected and isolated. Other methods only use a specially designed feedback system with no diagnosis, detection or estimation of fault – the so-called *passive* approaches. Whereas other methods are based on FE and compensation for the estimated fault(s) using a special control structure. Methods which make use of FDI or FE are known as *active* FTC methods since there are active changes to reconfigure the feedback control and even the system structure.

It turns out that the FDI process prior to system reconfiguration is very complex and hard to implement in a practical system. It works to provide information about the identification of fault scenario but does not supply as much information of fault as FE methods does. FE is more suitable for feedback system requiring accurate fault information. Hence, this PhD thesis focuses entirely on the use of the FE and compensation approach to FTC applied to a study of rotating induction motors (leaving out any consideration of other motor types). The work provides a study specifically on methods for improved reliability according to several system requirements and fault types. The development of methods (with application potential) for dependable motor operation is very much an open area of research and development in which FTC is a very promising approach.

Figure 1-2 shows the outline of the induction motor FTC system using FE, in which the "baseline" control action represents the nominal control system designed in the absence of faults. The FE Observer block is designed to provide a reconstruction or estimation of

the fault signal effects, usually in a manner that takes account of the modelling uncertainty acting on the nominal control design as well as the uncertainty acting on the FE system itself.

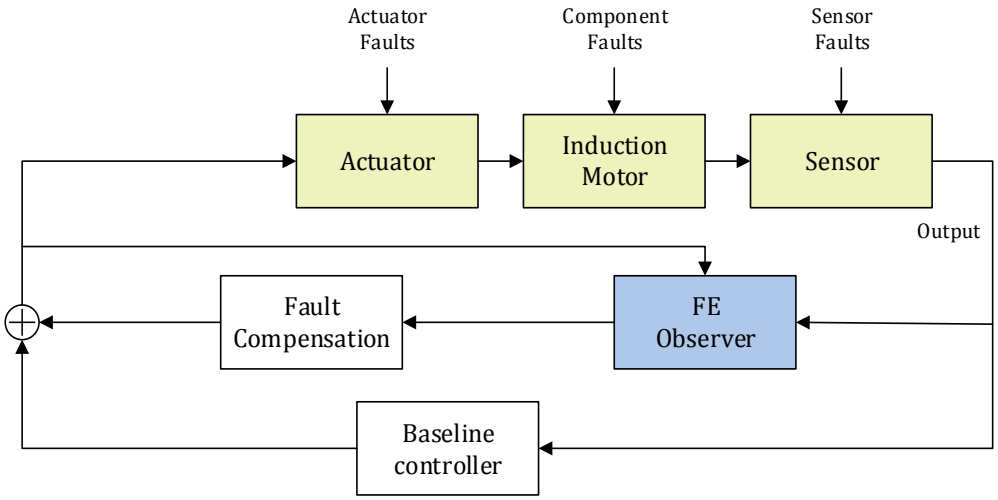

Figure 1-2 Application of FTC on induction motor system

So, what is required for good FTC design and application applied to induction motor systems is (**a**) a modelling approach to model the electro-mechanical operation and behaviour of the machine, (**b**) knowledge of typical faults which occur in the physical system and how they affect the system, and (**c**) based on (**a**) and (**b**) according to the above FTC system architecture. Faults can be considered to occur in the invertor drive system (actuator fault) and/or the measurement system (sensor fault). Fault can also be considered to occur in the induction motor itself (component fault). In the context of this work, variations in load torque are considered as an uncertain signal effect acting on the machine. Other uncertainties arise from the fact that the machine has non-linear dynamics and parameter variation arising from the electromagnetic and electro-mechanical dynamics. To achieve good FTC performance it will be necessary to estimate the faults using FE in the presence of uncertainties and nonlinearities, requiring a robust approach to estimation and control design.

The FDI-based FTC and the FE-based FTC has been introduced in details in Section 4.2 and Section4.3, including both advantages and disadvantages.

After an introduction of the main concepts of the thesis, along with the challenges, aim, objectives, the following sections also summarise the research contributions provided by the work.

1.2 Developments and challenges of induction motor control

With the rapid developments of modern control technology, due to the application of induction motors in different application environments, there are still many problems in control system development and application that remain to solved. This Section summarises the developments, some of which have arisen from real industry-based application problems (Takahashi & Noguchi, 1986; Krzemiński, 1987; Ohtani et al., 1992; Schauder, 1992; Kim et al., 1994; Kioskeridis & Margaris, 1996; Tabbache et al., 2013). Figure 1-3 shows the development of the subject of induction motor control, from a research perspective. Starting from the purely uncontrolled machine, these developments can be broadly summarised under the following headings and definitions.

Uncontrolled induction motor: This means the induction motor system with no control applied (a very common scenario) which is used to supply speed and power requirement with the functions of starting, braking and reversing. Uncontrolled systems still operate with their inefficiency (due to waste of energy) of operation causing investigators to turn to controlled machine types.

Scalar control: This is a control system approach with all dynamical variables considered in steady using simple voltage fed, for current or speed control – common until the 1990's. This allows control of the steady-state speed or torque of the motor, while the magnetic field in the motor is kept at a constant, desired level.

Vector control: This is a field oriented control (3 phases to 2 phases) in which the stator currents of a three-phase induction motor can be expressed as two orthogonal components. The functions of flux control, torque control and speed control can be realised through vector control.

FTC: This is a relatively new approach in induction motor control which combines either FDI or FE and active control (fault compensation/reconfiguration) approaches. The potential advantages are high efficiency because of fault-tolerance ability and reliability. Powerful real applications are readily achievable as a consequence of many advancements in hardware and software platforms available since the late 1990s. The main disadvantage is that there is little or often no physical/hardware redundancy. The only redundancy that can be used arises from estimation/soft sensing. Estimation (combined with control) in

FTC requires the use of robust analysis and design, i.e. taking account of nonlinearity/modelling uncertainty.

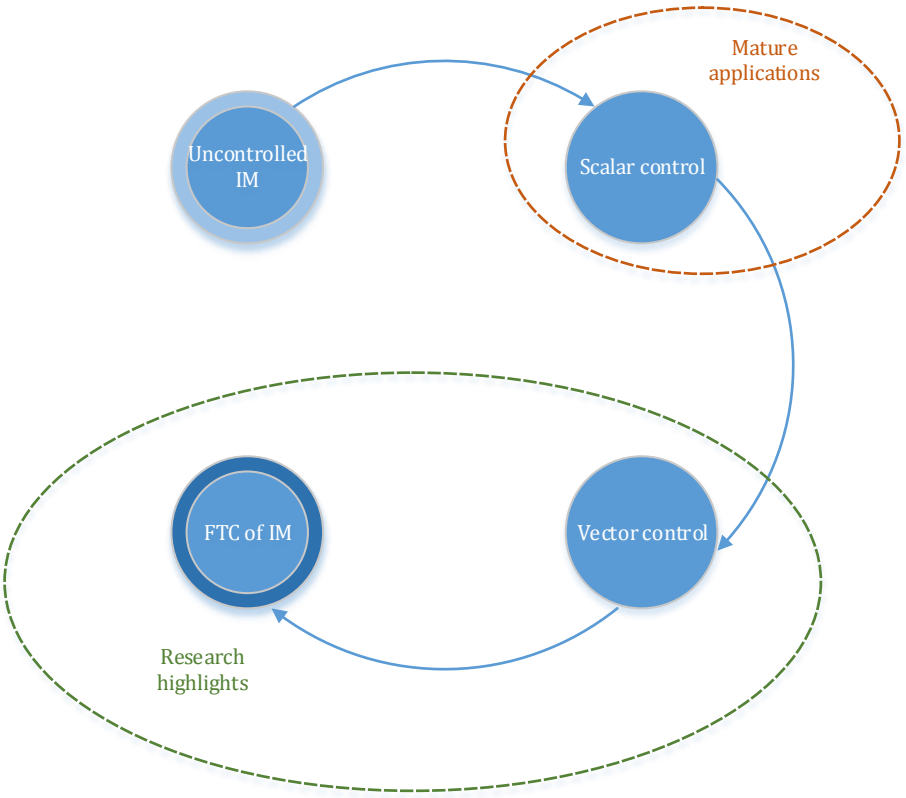

Figure 1-3 Developments of induction motor (IM) control

1.2.1 Problems with uncontrolled induction motor

- **The uncontrolled induction motor**

In most induction motor drives in industrial and home applications, the control aspects are limited to turn-on and turn-off. In a few cases, the machine assists in starting and braking (Trzynadlowski, 2000). In driving the load, the induction motor input is generally a constant stator voltage and frequency. The motor speed is also kept constant, and the load torque is not required to change usually. Practically, this feature is related to the size of the rotor resistance. The smaller the resistance value, the smaller the rotor loss. Considering realistic requirements, efficient induction motors are more in line with modern industrial requirements, such as insensitivity to load changes.

- **Basic faults/shortcomings of uncontrolled induction motor**

The most common induction motor drives are associated with fluid handling machinery, such as pumps, fans, and compressors. The induction motor without the control system looks more cost-effective, but this is not always the case. In many applications, most of the electrical power is wasted. That is, the induction motor provides energy, while some is converted to heat (Trzynadlowski, 2000; Mendrela et al., 2012). Therefore, the improvement of energy conversion efficiency is an important goal for the design of an induction motor control system. This is also an interesting possible direction for future research efforts.

- **Requirement for induction motor control**

Environmental changes affect the motor system performance very much so that the control system should be considered. The sensitivity to power supply voltage variations is a weakness of machines, including uncontrolled induction motor system. Indeed, there is no guarantee that power quality will always be maintained, particularly in under-developed countries (Mendrela et al., 2012). Since the torque generated in the induction motor is dependent on the stator voltage, a sudden drop in voltage can cause the motor to stop. Often, the resulting process interruptions are very expensive. The sensitivity of the induction motor system to voltage changes can be made small through the application of a control system. The situation can be further enhanced by considering the voltage variations as a form of fault or uncertainty and this is one reason to use an FTC system to improve the capability of handling sudden voltage variations.

Based on the above three points, the FE approach is considered a useful and interesting approach to FTC system design. The FTC can be considered to be developed around an essential baseline control function with the FE, which is used to provide good fault information for FTC to achieve fault compensation to enhance the control system operation.

1.2.2 Problems with scalar control and vector control

The simplest approach to induction motor control is to change the structure of the stator windings. Using a “triangular switch”, the starting current can be easily reduced to appropriate levels (Trzynadlowski, 2000). Another type of switch is allowed by changing the number of stator poles (Hammond & Mokrytzki, 1973). The machine variables are considered in steady-state and amplitude and frequency control is used to achieve the

adjustment of the predetermined parameters. This control strategy is referred to as *scalar control* (Marino et al., 2010). However, in modern induction motor control, the stator voltages and currents are being controlled (Bennett et al., 1999; Marino et al., 2010). A rapid change in amplitude or frequency may cause undesirable transient effects, such as interference with normal motor torque. Fortunately, this is not important in low-performance motor control, such as pumps and fans. Therefore, the speed of the motor is usually considered under open-loop control, without the need for speed sensors, although the current sensor can be used for overcurrent protection.

In high performance induction motor systems, the control variables include the torque generated in the motor. The three-phase stator currents are identified as two orthogonal components (a vector), this leads to the so-called *vector control*, which is also known as *field oriented control* (Marino et al., 2010). It can be said that a vector represents the instantaneous value of the corresponding three-phase variables, i.e. the stator current vector can be obtained from all three-phase stator currents. Alternatively, the three-phase currents can be determined from a current vector. Hence, in the vector control method, the vector model of the three-phase motor can be used in the determination of the control algorithms and the control computation. In the transient state of the induction motor system, this method is mainly used to maintain the continuity of the torque (Takahashi & Noguchi, 1986; Schauder, 1992; Kim et al., 1994; Kioskeridis & Margaris, 1996; Nash, 1997).

The field-oriented or vector model makes the control system design more complex it is however a fundamental requirement for 3-phase systems. The scalar control is much simpler, less powerful and does not easily handle the 3-phase problem (Hansen & Debs, 1995). Voltage and current sensors are used more in high-performance motor control, speed and position require sensors in most cases. And almost all of today's induction motor control systems are based on a digital integrated circuit (a microcomputer, a microcontroller, or a digital signal processor). The development of technology has stimulated the interest of many scholars in several directions, especially in improvement in the understanding of induction motor dynamic modelling, as well as in reducing the number of sensors required. Vector control is used to maintain induction motor stability in different applications, and to optimize dynamic characteristics of the system. Also, using vector control, the induction motor model can be described in different mathematical model/coordinate forms (Chan & Shi, 2011). This approach is an important

approach for facilitating an understanding of the ways in which various machine parameters influence the induction motor control and performance.

Vector control is considered as a *baseline control* approach within this thesis. This gives a strong framework for the use of the so-called *strict feedback form* introduced in Chapter 6. This formulation is essential in the model-based approach of back-stepping control used to take account of various machine nonlinearities. The nonlinearities concerned are described in Chapter 2 (Section 2.2.1). It is also interesting to note that this field-oriented modelling approach fits well to the construction of baseline control which is an essential element in active FTC.

1.2.3 Problems with robust FTC of induction motor

This sub-section is concerned with the importance of the use of robust control on the induction motor system.

(Bennett et al., 1999) showed that estimates of torque and flux through the use of state observer methods (e.g. based on bi-linear state structure) can be important for FTC of induction motors. The argument at that time was that measurements of torque and flux had been difficult to achieve, so that estimates of these quantities became important. Recent research is still focused on the research of torque and flux estimation in speed control. For example, a recent design of induction motor sensor-less control is introduced in (Shipurkar et al., 2017), i.e. motors in which the measurement of rotor speed is not available due to sensor failures or on purpose to reduce cost and complexity. In some research on direct torque control, the control variables are induction motor flux and torque, and the requirements for modulators or, tachometers or encoders are removed. Estimation methods are used to feedback the motor speed or motor shaft position (Hinkkanen et al., 2010; Orlowska-Kowalska & Dybkowski, 2010; Zhang et al., 2010; Zhang et al., 2012). However, with these approaches the required steady-state operating conditions may be unstable when large load torque variations and inertial changes are present due to application requirements or environmental changes.

This challenge can be addressed well by considering the use of an unmatched faults/uncertainties description in the modelling of the uncertain machine dynamics. The subject of FTC in the case of unmatched uncertainties is considered in Chapter 6 based on back-stepping control.

In some other model-based induction motor control methods, it is assumed that the rotor flux can be measured and all parameters are known. With this approach, some stability control problems are solved, and the possibility of estimating the rotor speed in the closed-loop control algorithm is addressed. Then under specific load torques and reference signals, the required system global control is obtained, leading to improved system performance (Barut et al., 2007; Lascu et al., 2009; Hinkkanen et al., 2010; Orlowska-Kowalska & Dybkowski, 2010). It would be an interesting challenge to study the adaptive performance of the induction motor system with robustness to both load torque and inertia, assuming that flux measurements are available. This is an interesting topic on adaptive control of induction motors which is addressed in Chapter 7.

1.3 Aim and Objectives

It has been explained that induction motor feedback control algorithm design can be complicated. It is necessary to consider not only the architecture of the FTC strategy (against faults), but also the potential parameter variations or parameter bias errors, i.e. the nonlinearities and uncertainties. The interesting question is what can be considered as faults and alternatively or in a complementary way what can be considered as uncertain system effects. These two – faults and uncertainties – have to some extent some exchangeable properties.

More specifically, to set the scene the induction motor feedback control usually includes two control inputs and two outputs (Marino et al., 2010). The main induction motor output variable is the rotor speed which is required to reach the desired speed quickly and with good dynamic performance. This is a challenging requirement in the event of sensor, actuator or other component (e.g. winding problems) malfunctions or signal interference. Another important output is the rotor flux modulus, through which the induction motor power can be maximized. Furthermore the electromagnetic torque controls the rotor speed, and the electromagnetic torque is an inherently nonlinear function characteristic of the stator current and the rotor flux. The non-linearity involves a number of induction motor parameters, such as load torque and rotor resistance, which vary greatly during induction motor operation (Marino et al., 2010).

The dynamic system nonlinearities imply that parameters of any linearization of the system are changing according to the operation of the motor. Hence, this work considers the effect of parameter uncertainty in induction motor control since when significant

machine model parameter variations exist, the control performance can be compromised or significantly reduced. The feedback control becomes an issue of *robust control* to make sure that the controller design takes account of the parameter sensitivities that affect the performance and the stability, when the parameter variation is bounded (if not bounded it can be regarded as serious fault and substitution is considered) (Patton, 1997b; 1997a). "When sensors malfunction the robustness is also important as methods of ensuring good *fault tolerance* in control action must be capable of providing good discrimination between the effects of faults acting on the system and the effects of modelling uncertainty." (Patton, 2015). In this PhD study the required FTC action is provided through the use of combined fault estimation (FE) and fault compensation within FTC design. Hence in this study FTC design is used to maintain acceptable motor performance when some faults or parameter uncertainties occur.

It must be clear that the machine will cease to function in the presence of total failure of rotor bars, windings etc. unless real redundancy in hardware can be used. In the case of sensor faults some hardware redundancy can be used during motor operation, load torque and resistance parameters will always change, so methods of FDI and FTC must take these changes into account to ensure maximisation of the machine working efficiency and reliably. In order to account effectively for these change effects special fault estimation (FE) methods have been adopted in this thesis to provide a powerful alternative to the FDI function based on linear approximation but using robustness strategies.

Therefore, for this problem, the thesis also provides an important linear approximation approach for FE, i.e. the Linear Parameter Varying (LPV) state observer used in a sliding mode formulation.

Considering the nonlinearities and unmatched faults (which are introduced later in Chapter 7) together, the adaptive back-stepping control algorithm is designed to ensure the stability and robustness of the system, and gain adaption ability to unmatched parameter variation (the load torque), and obtain robustness to uncertainty.

Thesis Aim: The aim of the thesis is focused on the development and design of both linear and nonlinear FE/FTC design techniques, including adaptive observer, sliding mode observer, LPV observer and back-stepping control. The LPV observer approach has been proposed to combine with the sliding mode approach to solve the fault estimation problem within the LPV model framework representation of the nonlinear

induction motor. Considering the unmatched faults/uncertainties and nonlinearities, back-stepping control is designed through the use of Lyapunov theory.

Most of the research is conducted using mathematical modelling and simulation study. However, experimental results have been obtained through a collaboration with the Technical University of Munich. These results are described in Chapter 8.

The **objectives** of the thesis are stated as follows:

- Description and design of state observer approaches based on the 4^{th} order induction motor electrical subsystem (Chapter 5)

  - Adaptive observers and sliding mode observers (SMO) have been used to estimate induction motor fault effects (in simulation) under the assumptions that rotor speed is a constant;
  - Adaptive observer and SMO are extended in to the fast varying fault scenarios with improvement of FE approaches;
  - Both additive faults and multiplicative faults are studied.

- Description and design of LPV observer for the 5^{th} order nonlinear induction motor system (Chapter 6)

  - Induction motor system has been extended into a LPV framework ;
  - LPV sliding mode observer was studied under this condition, where rotor speed is the varying parameter;

- Description and design of back-stepping FTC scheme to account for unmatched uncertainty (arising from nonlinearity).(Chapter 7)

  - Due to the shortcomings (modelling imperfections) of LPV modelling, an adaptive back-stepping control approach has been applied on a nonlinear induction motor system with unmatched faults/uncertainties;

- Experimental design to examine the effectiveness of FTC method (Chapter 8)

  - Based on the adaptive back-stepping control approach, an experimental study of induction motor FTC has been made through a collaboration with the Technical University of Munich;

- Experiment study has been carried out through the use of adaptive back-stepping control, with a consideration of the speed and load torque.

1.4 Summary of contributions and thesis structure

In this thesis, a comprehensive study on induction motor systems with a series of faults has been carried out. The problem arising from observer design and control system design for IM has been systematically studied and evaluated using both linear and nonlinear system theory. A form of adaptive observer and an improved adaptive observer, as well as a sliding mode observer (SMO) and an SMO extension to include linaer parameter variations (LPV) have been used to identify online uncertain parameters. A back-stepping control approach has also been investigated, by considering the nature of the so-called unmatched faults and the nonlinearities between IM currents and rotor flux.

The IM operational performance has been investigated in Chapter 2 in which both linear and nonlinear state space models are introduced for induction motors working under normal conditions. The dynamical models are multivariable and highly nonlinear, especially the torque characteristics, i.e. the nonlinear relationship between the load torque and the rotor speed.

It is found in Chapter 2 that, for quite low load torque or higher load torque, the induction motor maintains a stable operating condition at different rotor speeds. The operating conditions at higher speeds are more likely to remain stable and the operating state at lower speed is more likely to be unstable, while the load torque affects the system performance. Through simulation verification, the characteristics of induction motor obtained in Chapter 2 shows good performance at higher speeds. However, it is not so good at low speed or high load torque and this is due to inaccurate measurements and un-modelled nonlinear factors such as the effect of magnetic saturation.

Once the system with good controllability and observability is established, the design of the FE/FTC is carried out using existing methods. Chapter 3 first discusses the fault modelling and fault-tolerant control of the induction motor. Chapter 4 gives introduction and classification of fault tolerant control methods, focussing on the two methods of (a) sliding mode control and (b) back-stepping control used in Chapters 5,6,7 and 8. Chapter 5 enters into the details of the sliding mode and back-stepping control within the context of fault tolerant control includes the application of an adaptive observer and a sliding

mode observer. In Chapter 6, the sliding mode observer is designed within the LPV framework, which can overcome the nonlinear factors to a certain extent. Finally, in Chapter 7 (Simulation) and Chapter 8 (Experiment), the control design was based on the nonlinear induction motor with adaption to large load torque variation.

Chapter 5 focuses on the design of sensor fault and actuator fault observers and in this simulation study it is assumed that the sensor faults occur in the induction motor stator current sensor. It is shown that an adaptive observer that has been presented in Section 5.2 can simultaneously solve the estimation problems of sensor and actuator faults. Based on the above adaptive observer, an improved adaptive observer is designed in the Section 5.2.4. The optimal solution of the observer design is obtained with optimal H_∞ performance of the system considering noise input. The observer design is improved through the use of the LMI toolbox. Section 5.3.3 introduces the estimation/reconstruction of faults using the sliding mode observer, with the concept of the 'equivalent output injection signal'.

In Chapter 6 an estimation approach based on LPV modelling of an induction motor system is proposed. More accurately, a 4^{th} order electrical system is represented as a linear system when the speed is assumed a constant. However, it is not a constant in real world applications. Therefore, it is necessary to study the nonlinear estimation approaches for this kind of condition. Considering actuator fault and sensor fault, a sliding mode LPV observer is studied. In the design of the observer, the system matrix and a fixed input distribution matrix has been used. The fixed input distribution matrix was used to simplify the process of calculating observer gains and to ensure a stable reduced order sliding motion. In order to reconstruct actuator and sensor fault, the "output error injection signal" was used again in this chapter. Secondly, after the system was transformed into a reduced order system, a second order LMI was formulated to give the observer gains through the Matlab LMI tools.

In Chapter 7, unmatched faults are considered acting on the nonlinear induction motor system. The matched faults enter the system through the same channel as the control input; the unmatched faults/uncertainties enter the system through a different channel from the control input. In this induction motor system, load torque variation ΔT_L is regarded as an unmatched fault. The control aim was to achieve rotor speed and rotor flux tracking with tolerance to the unmatched faults/ uncertainties of the nonlinear system. It was also

verified that the performance of this control system under low speed condition performs as well as at high speed.

Chapter 8 then describes an application of the work developed in Chapter 7. The application study is conducted at the Technical University of Munich through a collaboration with the author. This Chapter is included to demonstrate that the back-stepping design methodology can be applied well in a practical system. The parameters of the induction motor model used in the thesis are the same as those which are known for the real induction motor laboratory system.

Overall, this thesis focuses on research into robust FE/FTC of induction motor systems. Most of the research on induction motor control aims at designing specific control approaches for a specific induction motor problem. However, this thesis proposes a systematic research on induction motor systems and gives conclusions that are more general. As a conclusion, the structure of the thesis is described as in Figure 1-4.

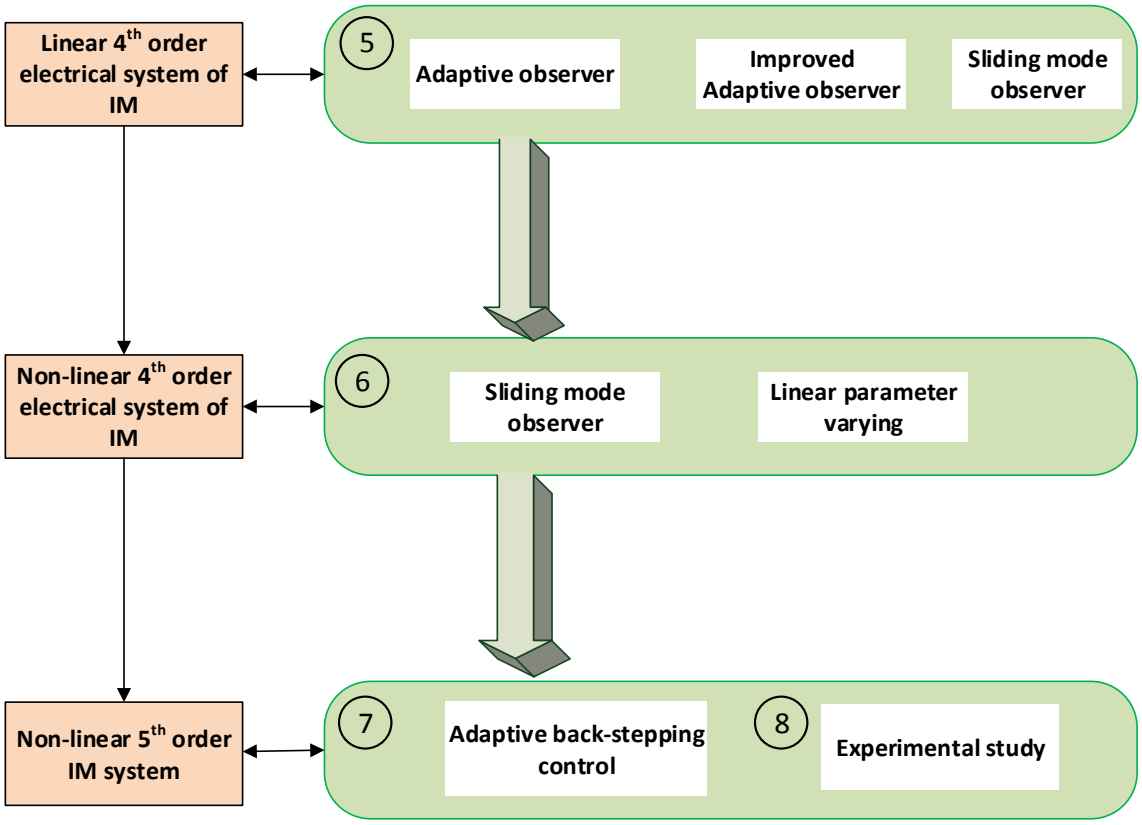

Figure 1-4 Structure of the thesis

Chapter 2: Induction motor modelling and control strategies

In this Chapter, the induction motor construction is outlined. This includes a brief description of the different components of the induction motor. Then different types of induction motor models are described. Finally, the operating properties and model-based motor control strategies are introduced.

Based on the typical three-phase cage induction motor model, which is based on three short-circuited rotor windings, three stator windings and three balanced voltages, two different nonlinear state space models are introduced. Fixed frame and rotating field oriented modelling methods are introduced in this chapter. The study of FTC methods applied to induction motors in Chapter 5, 6, and 7 are all based on these models.

2.1 Induction motor construction

Since 1970s, the focus of research on induction motors has shifted from mechanical properties to electrical characteristics, including instantaneous current and torque, inverter excitation, rectifier inverters, power supply waveform effects, flux and torque regulation, power supply frequency, and so on (Chalmers & Sarkar, 1968; Klingshirn & Jordan, 1968; Lipo & Krause, 1969; Ward & Härer, 1969; Plunkett, 1977).

This Section begins by introducing a typical induction motor construction as well as describing the principle of operation. As an example Figure 2-1 shows an induction motor drive system comprising an induction motor with an induction generator acting as load machine located in the Technical University of Munich (https://www.eal.ei.tum.de/anfahrt/). This platform consists of a 2.2 kW squirrel cage induction motor and a further induction machine that works as load machine. The load machine is driven by a modified ServoStar620 14-kVA inverter. In this platform, the rotor position is measured by a 1024-point encoder (Chen et al., 2013; Wang et al., 2014).

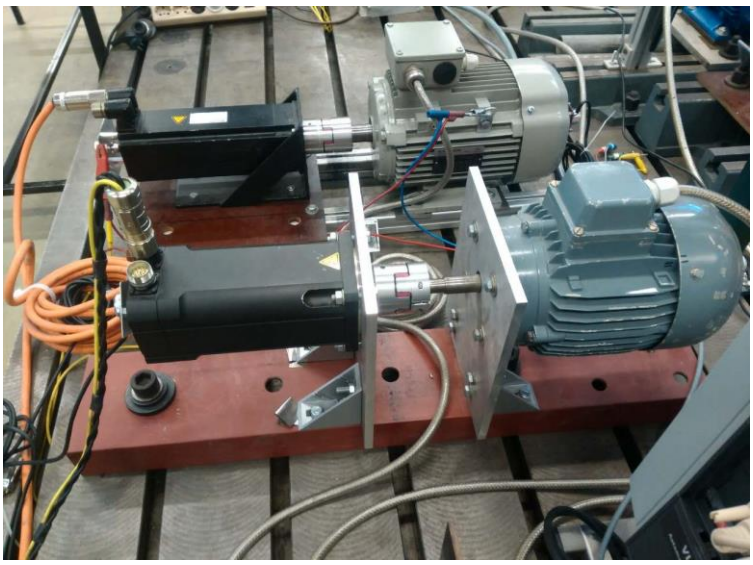

Figure 2-1 Induction motor driving systems (Chen et al., 2013)

The components of the induction motor are stator, rotor and bearing, etc. (Marino et al., 2010; Karmakar et al., 2016b), as shown in Figure 2-2.

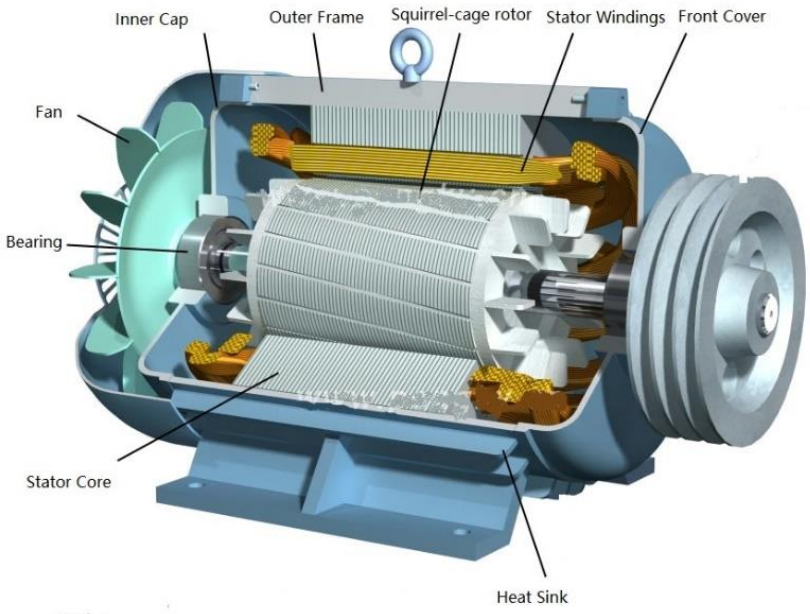

Figure 2-2 Induction motor construction (supplied by TUM)

- **Machine Stator**

The stator is an external stationary part of the motor, which comprises of a cylindrical frame, a magnetic circuit, and an insulated electrical winding. These parts include (I) Cylindrical frame made of cast iron or cast aluminium, may be alloy or welded steel plate;

(II) The magnetic circuit comprises a variety of laminations supported in the cylindrical stator frame, which are grooved alloy steels. The magnetic path is laminated to reduce the eddy current loss and heating; (III) insulated electric windings: For three-phase motors, the stator circuit has three sets of coils, one for each phase. These coils are placed in the grooves of the magnetic circuit stack.

- **Machine Rotor**

The rotor is usually made of a set of grooved sheets. The laminations known as electromagnetic materials are made into a cylindrical form which are insulated from each other. According to the rotor winding structure induction motors are divided into: (I) a squirrel-cage induction motor and (II) a wound rotor type induction motor. In a squirrel-cage induction motor, the rotor includes a set of rods made of copper or aluminium as a rotor conductor embedded in the rotor slot. This gives the rotor a very rugged structure. The ends of the rotor rods are connected to the end ring to form a path. A wound-rotor motor is a type of induction motor where the rotor windings are connected through slip rings to external resistance. Adjusting the resistance allows control of the speed/torque characteristic of the motor.

- **Other components**

In addition to the above two main parts, the induction motor also includes other parts: (I) End Flange: there are two end flanges for supporting both ends of the bearing; (II) Bearing: there are two sets of bearings placed at each end for supporting the rotary shaft; (III) shaft: it is used to transfer the generated torque to the load; (IV) Cooling fan: it is for forced cooling of the stator and rotor; (V) Junction box: it is used to receive electrical signal connection.

2.2 Induction motor state space models

The induction motor system considered in this thesis comprises of two subsystems, i.e. the electrical subsystem and the mechanical subsystem. The modelling presented in this Section is based on the model described in (Marino et al., 1993; Marino et al., 2010). This Section introduces the modelling of the induction motor under different coordinate systems, including the stator reference frame and the rotor flux reference frame. These

two models are used in this thesis in the observer approaches and back-stepping approach respectively, described in Chapters 5, 6 & 7.

2.2.1 State space models

- **Induction motor model**

The three-phase induction motor is based on the principle of electromagnetic induction, that is, when the stator winding is excited by a three-phase symmetrical AC source, a rotating magnetic field will be generated between the stator and the rotor. The rotating magnetic field cuts the rotor winding, generates induced electromotive force and current in the rotor circuit. A mathematical model representation of the 3-phase induction motor can be described as follows (Marino et al., 2010).

Define the stator and rotor 3-phase magnetic flux and current vectors as:

$$\begin{aligned} \psi_s &= [\psi_{s1}, \psi_{s2}, \psi_{s3}]^T \\ \psi_r &= [\psi_{r1}, \psi_{r2}, \psi_{r3}]^T \\ I_s &= [i_{s1}, i_{s2}, i_{s3}]^T \\ I_r &= [i_{r1}, i_{r2}, i_{r3}]^T \end{aligned} \tag{2-1}$$

Then the voltage balance dynamics of the scalar 3-phase motor fluxes of a 1-pole pair induction motor system can be written as follows:

$$\begin{aligned} \frac{d\psi_{s1}}{dt} + R_s i_{s1} &= u_{s1} \\ \frac{d\psi_{s2}}{dt} + R_s i_{s2} &= u_{s2} \\ \frac{d\psi_{s3}}{dt} + R_s i_{s3} &= u_{s3} \\ \frac{d\psi_{r1}}{dt} + R_r i_{r1} &= 0 \end{aligned} \tag{2-2}$$

$$\frac{d\psi_{r2}}{dt} + R_r i_{r2} = 0$$

$$\frac{d\psi_{r3}}{dt} + R_r i_{r3} = 0$$

where the flux vectors should satisfy the assumption of flux linkage of linear magnetic circuits, that is

$$\begin{bmatrix} \psi_s \\ \psi_r \end{bmatrix} = \begin{bmatrix} l_s & l_{s,r} \\ {l_{s,r}}^T & l_r \end{bmatrix} \begin{bmatrix} I_s \\ I_r \end{bmatrix} \quad (2\text{-}3)$$

Where l_s and l_r are the self-inductances of stator and rotor, respectively. $l_{s,r}$ is the mutual inductance for the linkage between the stator and rotor magnetic circuits The relationships between the different inductance value can be seen in (Marino et al., 2010).

- **3 phase to 2 phase transformation principles**

In the subject of induction motor control, the 3-phase current system is transformed into a 2-phase current system sometimes condidering the modelling difficulty and convenience for research. For the induction motor system, a 3-phase current system can be represented within a three-axis coordinate system as shown in Fig 2-3(a). This 3-phase system can be transformed into a 2 axis complex (α, β) reference frame using the Clark transformation (Martins et al., 2007; Marino et al., 2010) as shown in Fig 2-3(b).

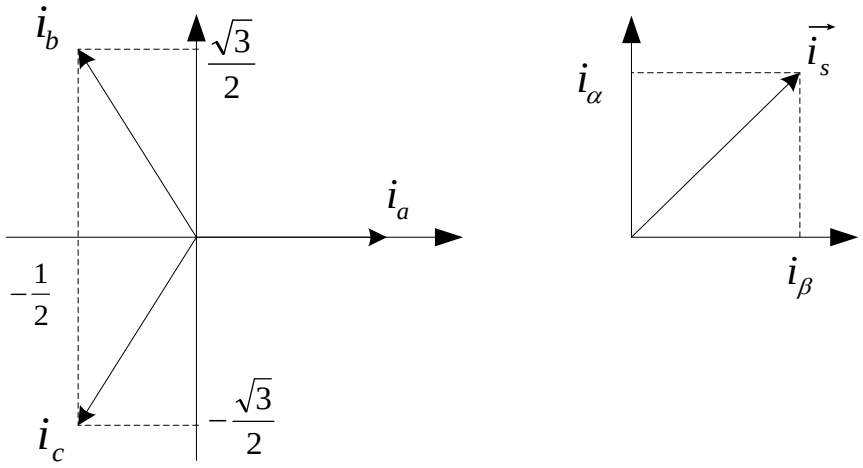

(a).Current system in a three-axis coordinate (a,b,c)

(b).Current system in a complex reference frame (α,β)

Figure 2-3 3-phase to α, β coordinate Clark transformation

The three-phase system with angular frequency ω_0 can be defined in a fixed three-phase coordinate frame as shown in (2-4):

$$i_a = I \cdot \sin(\omega_0 t)$$

$$i_b = I \cdot \sin(\omega_0 t + \frac{2\pi}{3}) \tag{2-4}$$

$$i_c = I \cdot \sin(\omega_0 t + \frac{4\pi}{3})$$

It can be transformed into two-phase system described in the Eq. (2-5):

$$i_s = i_a + a i_b + a^2 i_c$$

$$a = e^{j\frac{2\pi}{3}} = -\frac{1}{2} + j\frac{\sqrt{3}}{2} \tag{2-5}$$

$$a^2 = e^{j\frac{4\pi}{3}} = -\frac{1}{2} - j\frac{\sqrt{3}}{2}$$

The same vector i_s is interpretated in the complex plane using the following transformation (2-6):

$$i_s = i_\alpha + j i_\beta$$

$$i_\alpha = \frac{2}{3}(i_a - \frac{1}{2} i_b - \frac{1}{2} i_c) \tag{2-6}$$

$$i_\beta = \frac{2}{3}(\frac{\sqrt{3}}{2} i_b + \frac{\sqrt{3}}{2} i_c)$$

Sub-index α, β denotes the use of a complex reference frame, it means a stator reference frame in this thesis. To write the transformation in matrix form, Eq. (2-6) can be written as:

$$\begin{bmatrix} i_\alpha \\ i_\beta \end{bmatrix} = \frac{2}{3} \begin{bmatrix} 1 & -\frac{1}{2} & -\frac{1}{2} \\ 0 & \frac{\sqrt{3}}{2} & -\frac{\sqrt{3}}{2} \end{bmatrix} \begin{bmatrix} i_a \\ i_b \\ i_c \end{bmatrix} \tag{2-7}$$

- **2 phase to 2 phase transformation principles**

When the system in α, β coordinates is needed to be transformed to the rotating d, q axis frame, the Park transformation is then used (also known as d, q axis transformation) (Tan & Chang, 1999). Assume that the d, q coordinate system rotates under the rotor flux reference frame against the α, β coordinates with an angle θ, the relationship of the two coordinate systems are thus as follows:

$$\begin{bmatrix} i_d \\ i_q \end{bmatrix} = \begin{bmatrix} \cos(\theta) & \sin(\theta) \\ -\sin(\theta) & \cos(\theta) \end{bmatrix} \begin{bmatrix} i_\alpha \\ i_\beta \end{bmatrix} \tag{2-8}$$

The corresponding inverse transformation from d, q to α, β coordinates is:

$$\begin{bmatrix} i_\alpha \\ i_\beta \end{bmatrix} = \begin{bmatrix} \cos(\theta) & -\sin(\theta) \\ \sin(\theta) & \cos(\theta) \end{bmatrix} \begin{bmatrix} i_d \\ i_q \end{bmatrix} \tag{2-9}$$

As a conclusion of Clark transformation and Park transformation, the following points of view should be stated:

1) From a physical point of view, the Park transform is an equivalent transformation from i_a, i_b, i_c to d, q axis, the stator currents in 3 phase are mapped to the direct axis and the

quadrature axis, i.e. i_d, i_q. For steady state systems, the equivalent i_d, i_q is exactly a constant vector. Therefore, it is unnecessary to take into account the rotating magnetic field produced by the three windings of the stator. Instead, it is convenient to focus on the rotating magnetic field generated by i_d, i_q.

2) The mathematical model of the three-phase induction motor is nonlinear and strongly coupled. When converted into a two-phase mathematical model, the degree of order, nonlinearity and coupling are greatly reduced, which greatly simplifies the control system design. That means the 3-phase variables are transferred into 2-phase variables, including the flux and current of both rotor and stator.

➢ Induction motor modelling under stator reference frame

Let T_e be the electromagnetic torque of the induction motor system and J the moment of inertia of the induction motor. Then according to Eq. (2-10) T_L, R_s, R_r represent the load torque, stator resistance and rotor resistance, respectively. δ is the rotor position with respect to the stator. When the induction motor is running under a balanced condition the sum of currents (of the rotor or stator) vectors in 3 phase equals zero, then the fluxes and torque of a 1-pole induction motor can be written in 2-cordinate form as follows:

$$\begin{aligned} \dot{\psi}_{s\alpha} + R_s i_{s\alpha} &= u_{s\alpha} \\ \dot{\psi}_{s\beta} + R_s i_{s\beta} &= u_{s\beta} \\ \dot{\psi}_{r\alpha} + R_r i_{r\alpha} &= 0 \\ \dot{\psi}_{r\beta} + R_r i_{r\beta} &= 0 \\ \dot{\delta} &= \omega \\ J\dot{\omega} &= T_e - T_L \end{aligned} \tag{2-10}$$

where

$$\begin{bmatrix} i_{r\alpha} \\ i_{r\beta} \end{bmatrix} = \begin{bmatrix} \cos(\delta) & \sin(\delta) \\ -\sin(\delta) & \cos(\delta) \end{bmatrix} \begin{bmatrix} i_{r\alpha} \\ i_{r\beta} \end{bmatrix} \tag{2-11}$$

$$\begin{bmatrix}\psi_{r\alpha}\\ \psi_{r\beta}\end{bmatrix} = \begin{bmatrix}\cos(\delta) & \sin(\delta)\\ -\sin(\delta) & \cos(\delta)\end{bmatrix}\begin{bmatrix}\psi_{r\alpha}\\ \psi_{r\beta}\end{bmatrix}$$

$$T_e = \frac{M}{L_r}(\psi_{r\alpha} i_{s\beta} - \psi_{r\beta} i_{s\alpha})$$

Hence, the nonlinear induction motor model is a combination of the dynamics of the electrical system and mechanical systems. The electrical behaviour of the induction motor system is described in the α, β coordinates in a stationary reference framework with the stator.

The induction motor models are derived in (Marino et al., 2010; Isermann, 2011). For a three-phase induction motor, if voltages and currents of each rotor or stator is expressed, then this leads to a 3-phase expression of the induction motor, which can be found in the Matlab/Simulink manual. However, by transforming the three-phase system into a two-phase system via the combined Clark and Park transformations (the so-called Clark-Park transformation) a considerable simplification can be reached. The resulting 4th order electrical system together with the 1st order mechanical system (speed dynamics) are given as follows:

$$\frac{d\varphi_{r\alpha}}{dt} = -\frac{R_r}{L_r}\varphi_{r\alpha} - n_p\omega\varphi_{r\beta} + \frac{R_r}{L_r}M i_{s\alpha}$$

$$\frac{d\varphi_{r\beta}}{dt} = -\frac{R_r}{L_r}\varphi_{r\beta} + n_p\omega\varphi_{r\alpha} + \frac{R_r}{L_r}M i_{s\beta}$$

$$\begin{aligned}\frac{di_{s\alpha}}{dt} &= \frac{MR_r}{\sigma L_s {L_r}^2}\varphi_{r\alpha} + \frac{n_p R_r}{\sigma L_s L_r}\omega\varphi_{r\beta} - \frac{{L_r}^2 R_s + M^2 R_r}{\sigma L_s {L_r}^2} i_{s\alpha} + \frac{1}{\sigma L_s} u_{s\alpha}\\ \frac{di_{s\beta}}{dt} &= \frac{n_p R_r}{\sigma L_s L_r}\omega\varphi_{r\alpha} + \frac{MR_r}{\sigma L_s {L_r}^2}\varphi_{r\beta} - \frac{{L_r}^2 R_s + M^2 R_r}{\sigma L_s {L_r}^2} i_{s\beta} + \frac{1}{\sigma L_s} u_{s\beta}\end{aligned} \quad (2\text{-}12)$$

$$\dot{\omega} = \frac{n_p M}{J L_r}\left(\varphi_{r\alpha} i_{s\beta} - \varphi_{r\beta} i_{s\alpha}\right) - \frac{T_L}{J}$$

$$T = \frac{n_p M}{L_r}\left(\varphi_{r\alpha} i_{s\beta} - \varphi_{r\beta} i_{s\alpha}\right)$$

where

$\varphi_{r\alpha,\beta}$	rotor flux
$i_{s\alpha,\beta}$	stator current
$L_{r,s}$	inductance
$R_{r,s}$	resistance
M	mutual inductance
$u_{s\alpha,\beta}$	control voltage
ω	rotor speed
n_p	number of pole pairs
σ	it equals $1-\frac{M^2}{L_s L_r}$
T_L	load torque
J	moment of inertia
T_e	Electro-magnetic torque

In the above symbols the subscripts r, s represents the rotor and stator, and α, β represents two axis, respectively.

As shown in (2-12), the mechanical system produces torque to influence the rotation speed of the induction motor. The dynamical behaviour of the rotor speed ω is also determined from Eq. (2-12). The dynamic properties of the induction motor system depend on the load torque and relevant measurable variables. It can be seen that the induction motor model is a highly nonlinear model due to the existence of the products $\varphi_{r\alpha} i_{s\beta}$ and $\varphi_{r\beta} i_{s\alpha}$.

- **Induction motor modelling under rotor flux reference frame**

As described above, the nonlinear induction motor model is composed of a combination of electrical and mechanical systems, which is described in the (α, β) coordinate in a stationary reference framework with the stator. Considering the specific control motivation which is described in the Chapter 6, a transformation is needed in order to give the system a suitable formulation for modelling and estimation/control. The chosen transformation converts the induction motor system into what is known as a *strict feedback form* (Shen & Shi, 2015) which is important when using a method known as back-stepping control (Tan & Chang, 1999).

In the following context, the induction motor model introduced in the stator reference frame is transformed into the rotating rotor flux frame. In other words, a transformation of the (α, β) model in the fixed stator frame coordinates is transformed into a (d, q) frame which rotates with the rotor flux. Under the (d, q) frame this system can be presented as follows:

$$\begin{aligned}
\frac{d\omega}{dt} &= \frac{\mu}{J}\varphi_d i_q - \frac{T_L}{J}, \\
\frac{di_q}{dt} &= -\eta i_q - \beta n_p \omega \varphi_d - n_p \omega i_d - \alpha M \frac{i_q i_d}{\varphi_d} + \frac{1}{\sigma L_s} u_q, \\
\frac{d\varphi_d}{dt} &= -\alpha \varphi_d + \alpha M i_d, \\
\frac{di_d}{dt} &= -\eta i_d - \alpha\beta\varphi_d + n_p \omega i_q + \alpha M \frac{{i_q}^2}{\varphi_d} + \frac{1}{\sigma L_s} u_d, \\
\frac{d\rho}{dt} &= n_p \omega + \alpha M \frac{i_q}{\varphi_d},
\end{aligned} \tag{2-13}$$

where $\eta = \frac{M^2 R_r}{\sigma L_s {L_r}^2} + \frac{R_s}{\sigma L_s}, \rho = arcta\,n\left(\frac{\varphi_\beta}{\varphi_\alpha}\right), \mu = \frac{n_p M}{\mathrm{J} L_r}$.

The (d, q) model described by Eq. (2-13) can be considered as two subsystems. The first subsystem is represented by the first two rows in Eq. (2-13), which is a system with the state vector (ω, i_q) and the control input u_q. The second subsystem is represented by the row 3 and row 4 in Eq. (2-13), which is a system with the state vector (φ_d, i_d) and the control input u_d. The last row of Eq. (2-13) is produced in the transformation of the induction motor state space model, which represent the rotor flux position, therefore $\frac{d\rho}{dt}$ denotes the rotor flux speed.

2.2.2 Types of induction motor parameters

A set of parameters are used according to (Comtet-Varga et al., 1999; Jiang & Staroswiecki, 2002; Chen et al., 2013), it covers the Chapter 5,6 and 7. It is listed in Table 2-1.

Table 2-1 Parameters of IM 1

(Comtet-Varga et al., 1999; Jiang & Staroswiecki, 2002)

Number of pole pairs n_p	2
Stator resistance R_s	10 Ω
Rotor resistance R_r	3.5 Ω
Stator inductance L_s	380 mH
Rotor inductance L_r	300 mH
Mutual inductance M	300 mH
Moment of inertia J	0.02 kg · m^2

This set of parameters and the corresponding model is based on two different points of view which should be taken into consideration when the induction motor model and parameters are applied, as follows.

In this thesis the modelling of the induction motor is used in the context of field-oriented control strategies, this may not be effective in other control approaches. It is necessary to check if the coordinates are transformed properly when a control or estimation approach is applied.

2.3 Operation for healthy induction motor model

This Section introduces the indicators used to compare the performance of the various induction motor systems. The simulation results obtained by Matlab/Simulink simulation are also provided. This study is useful for verifying the induction motor system dynamics and to help the reader to gain an understanding of ways in which the induction motor performance can be determined.

Figures 2-4 to 2-7 shows how a typical induction motor model can be constructed using the Matlab/Simulink platform. The diagrams correspond to the various levels of the overall dynamical system afrter alpha-beta transformation. From Figure 2-5 it is clear that the induction motor has two interacting dynamical subsystems, the electrical system and mechanical systems. The electrical system is represented by the upper part of Figure 2-5, whilst the mechanical system is represented by the lower part of the Smulink diagram. In

this system the load torque can be selected as a constant value and the control voltage input is represented by sine wave.

Table 2-2 Parameters in IM simulink diagram		
vas, vbs, vcs	3-phase stator voltages	V
ids, iqs, idr,iqr	Stator and rotor currents in α and β part	A
phids, phiqs, phidr, phiqr	Stator and rotor flux	Wb
taul	Load torque	N·m
Te	Electromegnetic torque	N·m
omegar	Angular speed	Rad/s
Nr	Rotor Speed	RPM

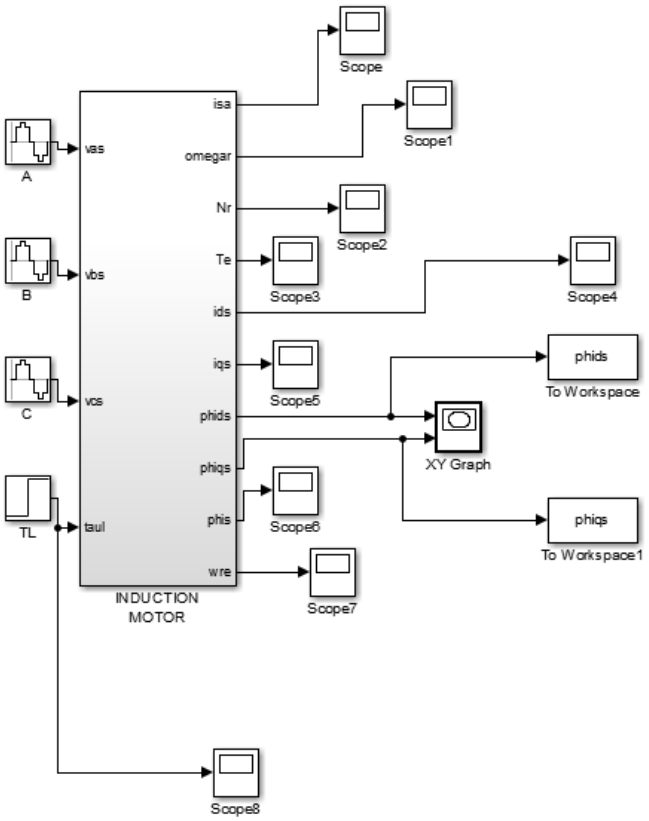

Figure 2-4 Matlab/Simulink model of overall IM Structure

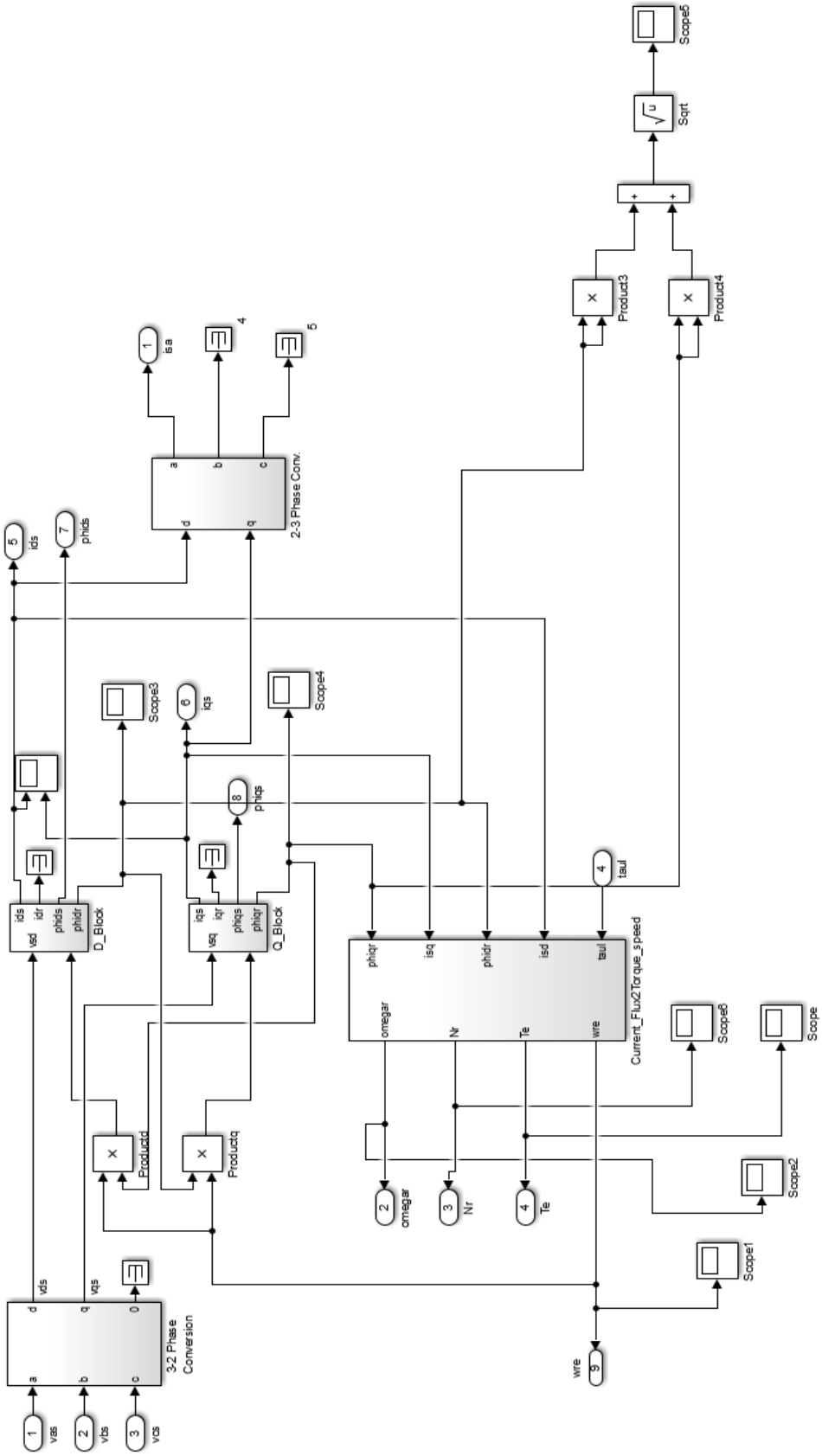

Figure 2-5 Electrical and Mechanical IM Subsystems

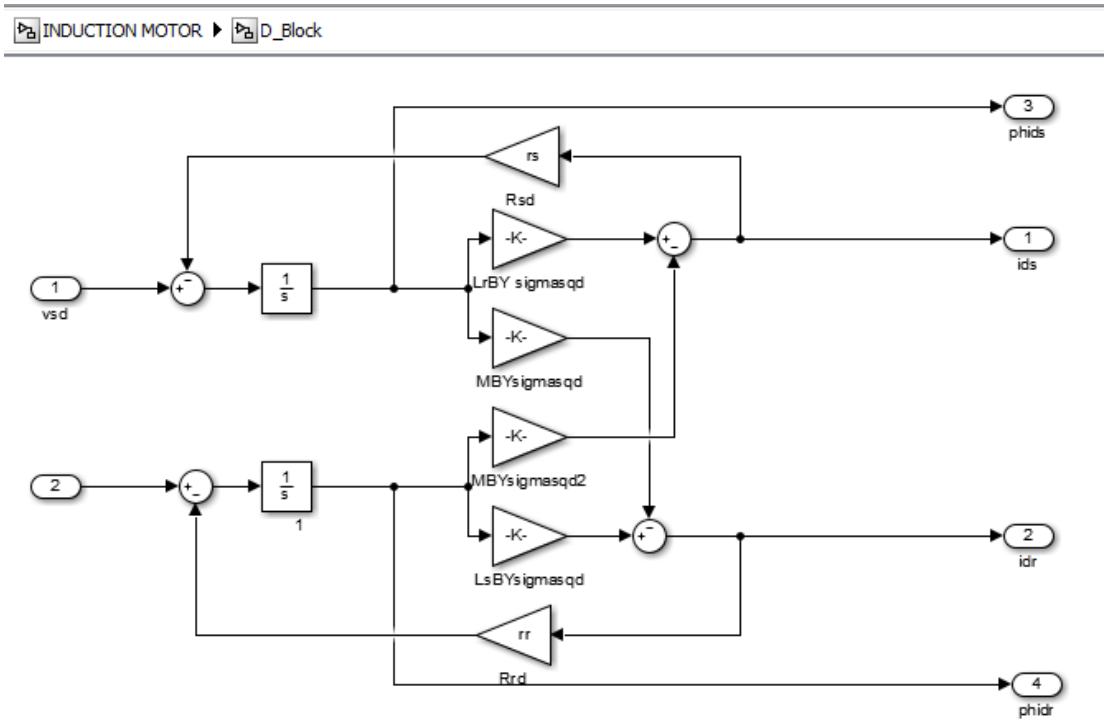

Figure 2-6 α part of IM after transformation

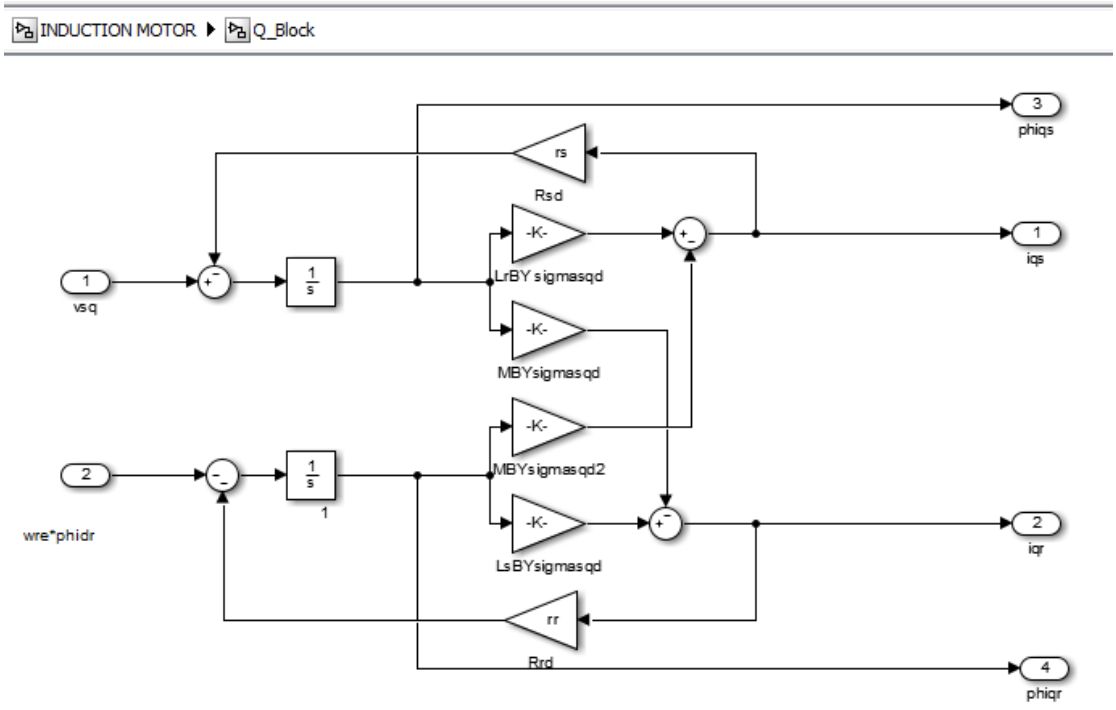

Figure 2-7 β part of IM after transformation

To verify the performance of the induction motor model based on the first set of parameters the simulation has been performed under different speed requirements. The electromagnetic torque and the currents were examined carefully to dtermine the most appropriate starting transient properties. When a certain electromagnetic torque is required and a certain load torque is applied at time t=1s on the system, the properties of speed, electromagnetic torque, single phase stator current, and stator flux are presented below to study the performance of the induction motor system at the start-up stage.

At the start-up stage, there is no external applied load torque to the IM. In the following figures, the load torque is applied when the speed of rotor is increasing.

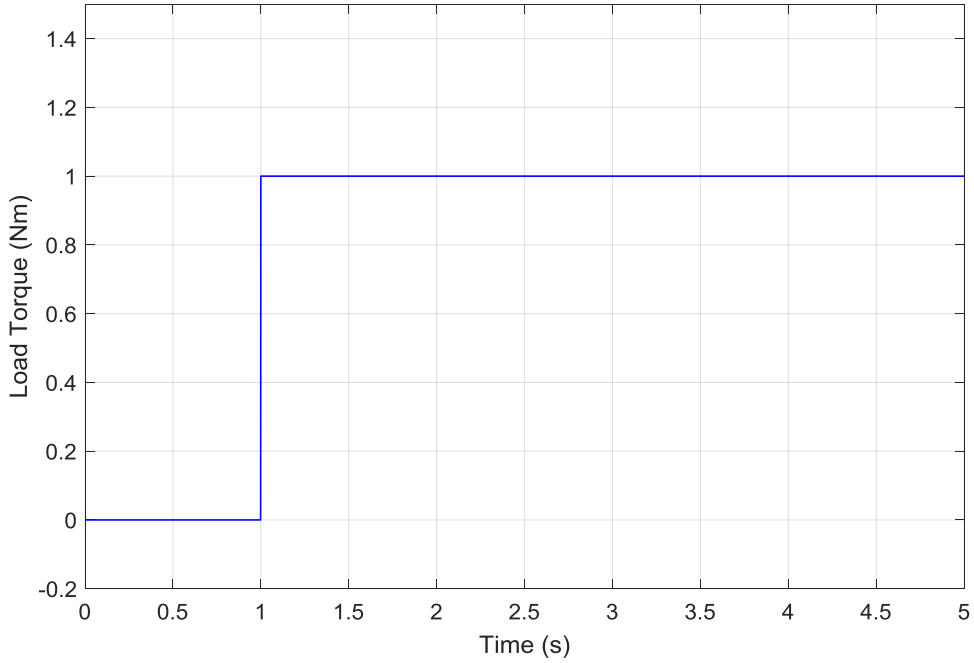

Figure 2-8 Load torque applied at t =1s

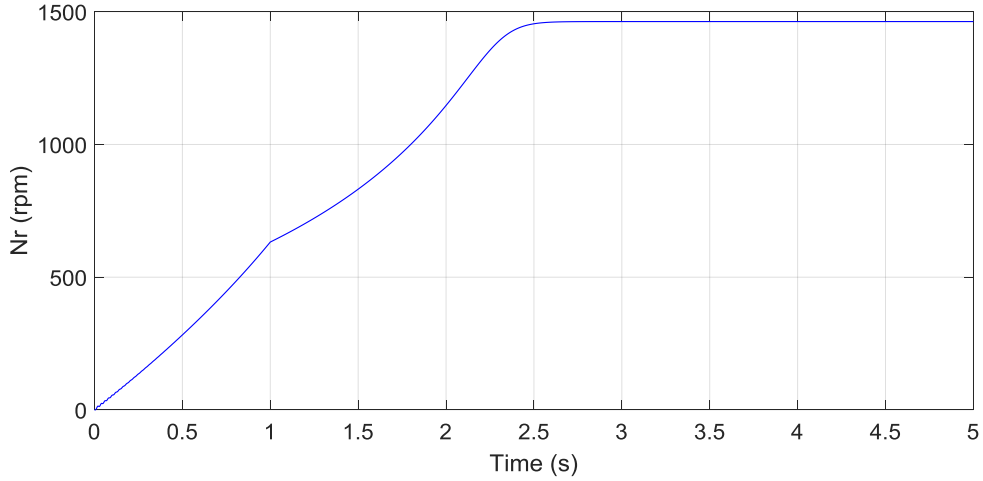

Figure 2-9 Rotor speed

Figure 2-9 shows the speed variation of the induction motor system when a specific level of load torque is applied to this system. In this graph it is shown that the induction motor's speed increases from 0 to 1450 rpm in 2.5s.

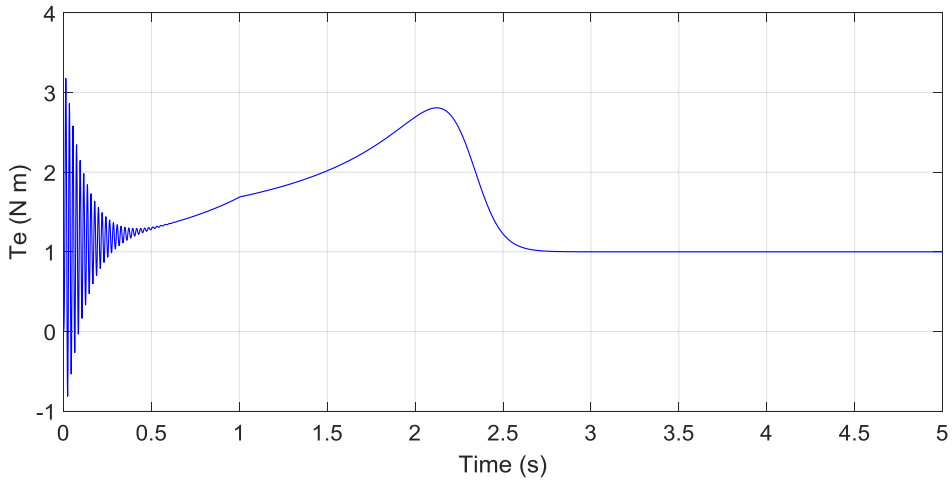

Figure 2-10 Electromagnetic torque

Figure 2-10 shows the electromagnetic torque produced by the induction motor system. This figure shows the result of simulation, but in real induction motor systems, some oscillation is usually observed in this type of response when the stator is fed by a PWM inverter (Matlab manual: Simulate an AC motor drive).

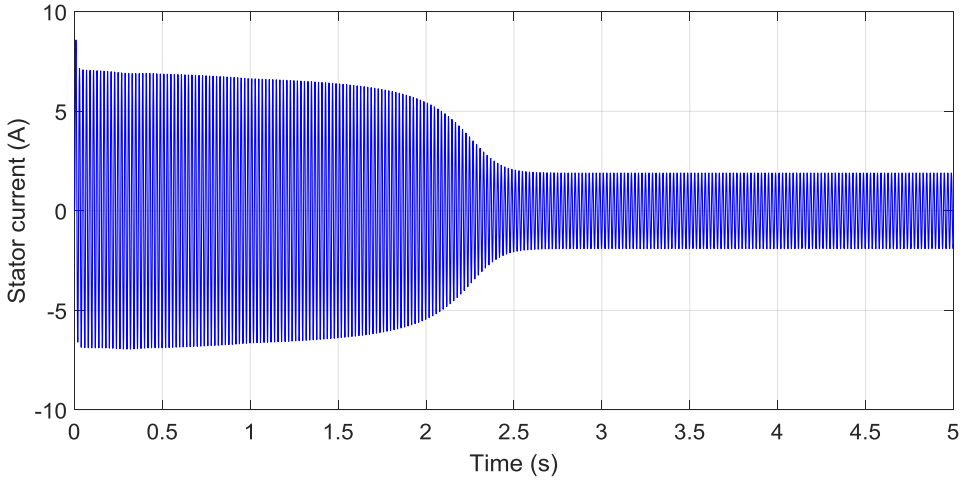

Figure 2-11 Stator current characteristics in α axis

Figure 2-11 shows one of the 3 phases of the stator currents. This graph shows that at the instant t = 1s the load torque changes. In a control system design, the control voltages changes in accordance with the change of load torque and other varying parameters. This result shows that the stator currents react according to the load change.

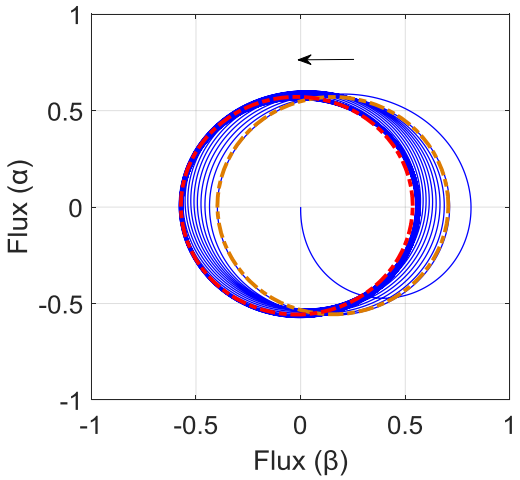

Figure 2-12 Rotor flux trajectories

The Figure 2-12 shows the trajectory of rotor flux vector $(\varphi_{r\alpha}, \varphi_{r\beta})$. Since rotor flux is very important in optimizing the steady state performance and minimizing the steady state power loss, therefore it should be kept at a desired level. As shown in the graph, the rotor flux generated by the induction motor has a drift phenomenon but it can reach a final stable condition. The blue circle represents the flux drift when the 3-phase system is not

balanced due to initialization bias. The red circle shows the nominal situation of the system, which represents the steady state of flux. From the steady state of the flux, the flux drift phenomenon gradually disappear.

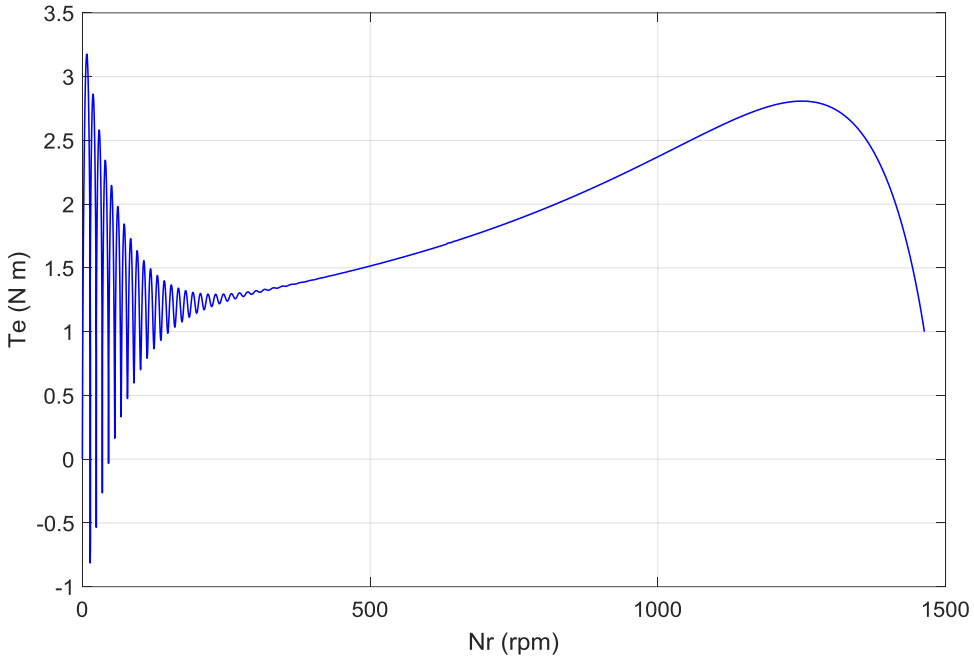

Figure 2-13 Torque-speed characteristic

Figure 13 shows the resulting torque-speed characteristic. In this figure, the electromegnetic torque increase as the speed increase, then the electromegnetic will drop when the speed reached specific level. This high speed area is the high-slip region. The relative speed between rotor and flux field arrives a high value.

FE/FTC of induction motor system will be considered in this model, considering the faults or other uncertain parameters. After the start-up period, the IM system will arrive at a state of stability. If no controller is designed, an energy balance is reached between input voltage and output mechanical energy. The currents and voltages will appear to be stable, changing only if apparent disturbance (temperature, friction, etc.) or load torque is applied. Therefore a FTC stragegy is needed to maintain the stability or keep the system stable under abnormal condition. In other words, the FTC system is responsible for extending the degree of stability of the IM system.

2.4 Industry-based applications of model-based induction motor FE/FTC

Both the FE strategy and the FTC design are model-based approaches based on the assumed IM.

Firstly, model-based control approaches for induction motor control are directly or indirectly based on back electromotive force (EMF) information. Only when the back EMF is enough, the induction motors can work in healthy conditions. The electromagnetic field is in close relationship with flux and velocity while both of them need to be measured. Secondly, through the discussion in Chapter 1, the most recent research on induction motors focuses on fundamental model based approaches on field oriented control and FTC of induction motors. Therefore the focus of this study is to improve the performance of the induction motor system under different fault scenarios by using a number of FE/FTC strategies.

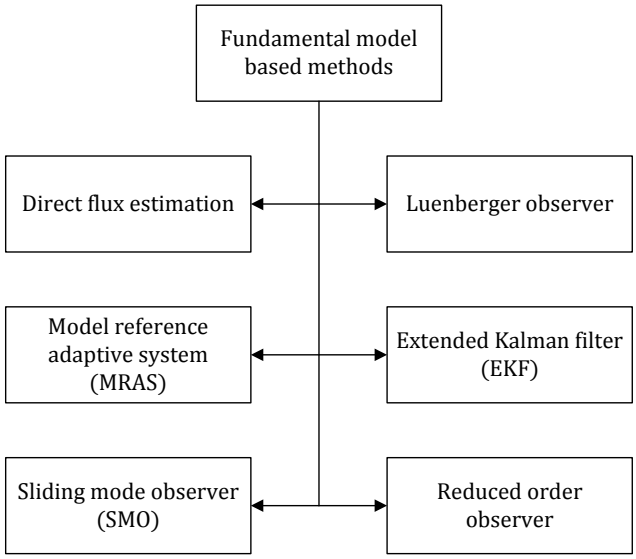

Figure 2-14 Fundamental model based Observer approaches

Direct flux estimation (Kubota et al., 1993; Lascu et al., 1998; Maes & Melkebeek, 2000): In this approach, the rotor position or speed is directly calculated through the use of measured three phase voltages and currents. However, in practice this type of drive system is usually based on current measurements alone. Direct flux estimation is based on the stator voltage equations of the system. A flux calculation equation is obtained

directly by the use of magnitude of stator voltage and position of the stator. The advantage of this method is that it is simple and straightforward.

Model reference adaptive system (MRAS) (Ohnishi et al., 1986; Maiti et al., 2008; Teja et al., 2012): Usually consists of the three parts (1) the reference model, (2) the adaptive controller and (3) the adaptive model. All the parameters of the reference model should be known and it is seen as an ideal model. All the outputs of the reference model and the adaptive model should have the same physical meaning, and the reference model parameters should be as accurate as possible. The control aim is to minimize the error between the reference model and the adaptive model, that is, the difference between the real and estimated values of the position and speed estimation should be small enough.

Luenberger observer (Orlowska-Kowalska, 1989; Kwon et al., 2005; Zhang et al., 2009)**:** the principle of the Luenberger observer is to estimate the output based on the estimated state, then compare the estimated output with measured output, finally correct the system states using this difference. In industrial applications of sensor-less control, a Luenberger observer is assured to be effective by accurate output measurement and accurate parameter setting. Usually, this observer can be ineffective due to measurement noise or parameter variations.

Extended Kalman Filter (EKF) (Zai et al., 1992; Kim et al., 1994; Shi et al., 2002): The EKF was proposed to tackle the noise and disturbance of a system directly when the speed and position estimation was carried out in induction motor control system. In this approach the state space equation of the system is based on currents, flux and speed; and it should be linearized or discretized for the estimation of speed and position.

Sliding mode observer (SMO) (Benchaib et al., 1999; Yan et al., 2000; Lascu et al., 2004): The reason SMO attracts so much attention of researchers is that it has natural robustness to system disturbance and insensitivity to the parameter variations. SMO has been studied in the sensor-less control of induction motor, and it is proved to be effective when the sliding mode manifold is chosen suitably. The stability of this approach can be determined using the Lyapunov approach. Through the application of nonlinear switching function, a SMO is used as a feedback correction item and makes the uncertainty within matched channel of both observation and control system removed.

Reduced order observer (Hinkkanen et al., 2010; Davari et al., 2012): Different from the above full order observer, the reduced order observer works well in the condition when some state variables are unknown. The reduced order observer can be obtained when only some of the state variables are available. In some kind of state space equations of the system, state variables can be available or unavailable, and observer is usually designed for the observation of unavailable variables. In this observer, only the reduced order error system is considered and part of state is required to be available. Reduced order observers have been used in the position and speed estimation of induction motor systems.

2.5 Summary

According to the aim and objectives stated in Chapter 1, this Chapter presents the modelling approaches of the induction motor.

Based on the induction motor construction, two types of models has been developed for the induction motor system in this Chapter, that is $\alpha - \beta$ model under the stator frame and $d - q$ model under the rotor flux frame. The first is used in simulation study of different FE approaches, the second one is used in FTC of induction motor system. Besides the introduction of electrical system and mechanical system of induction motor, and steady state operation properties of the induction motor are described under specific speed and load torque requirements. Each model is modified through the use of the Matlab/Simulink platform. As a highly nonlinear system due to the existence of the product of flux and current, as well as unknown load torque, different parts have also been studied separately. The 4^{th} order electrical subsystem of induction motor will be used in Chapter 4 by applying adaptive observer and sliding mode observer separately. The 5^{th} order nonlinear induction motor model was studied in Chapter 6 based on a linearized parameter approach-LPV. An LPV fault estimation approach for induction motor was studied. In Chapter 7, the nonlinear 5^{th} order induction motor has been studied by using adaptive back-stepping approaches, with the consideration of unmatched faults and specific modelling property - the strict feedback form. After the induction motor modelling, the operation properties of the healthy model and a review of model based control strategies has been given.

Based on the induction motor modelling in this Chapter, a description of typical IM faults and the requirements and challenges of FTC are introduced in Chapters 3 & 4.

Chapter 3: Fault modelling and FTC for Induction motor

3.1 Introduction

In this Chapter, the faults and faults modelling of a nonlinear induction motor is described. This faulty model is based on the mechanical and electrical structure of an induction motor benchmark model proposed in . Fault modelling of the induction motor system has been introduced mathematically. The model in this Chapter is used in the thesis to design the FE/FTC methods for induction motor systems, and in some applications the expression of the induction motor will be changed according to the coordinate changes.

Figure 3-1 presents an overall example scheme of a model-based fault estimation of a speed controlled induction motor stated in (Isermann, 2011). When considering FE and/or FTC for induction motor systems, the fault properties form the basis of the realization of control approaches, so the modelling of a faulty system should be as accurate as possible. In this example case study it can be seen that relatively precise process modelling is required in order to take appropriate account of the fault effects. FE of the induction motor requires sensors to detect measurable state variables and sometimes the rotor speed also needs to be estimated. When using FE within FTC the system can be cobsidered as a field-oriented control system.

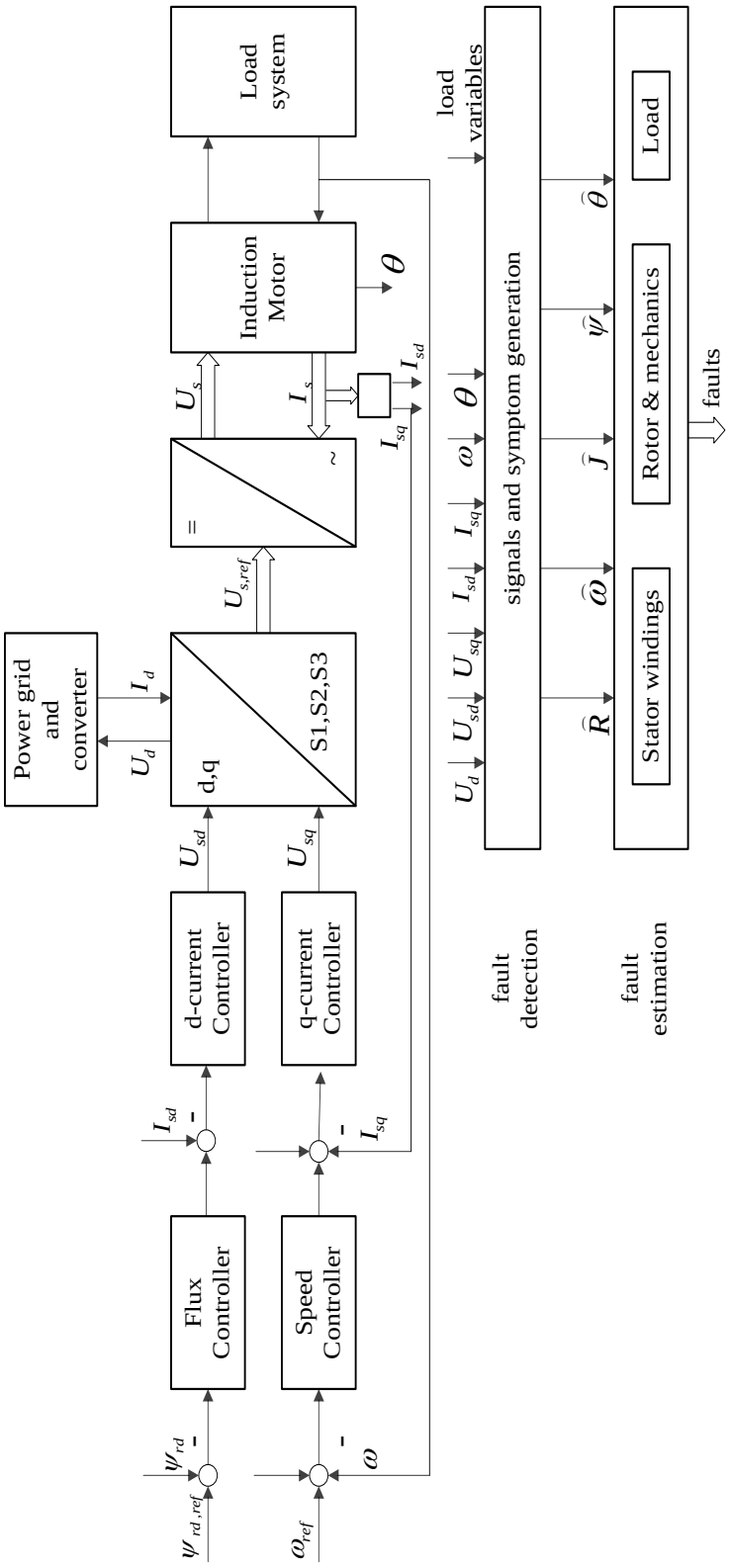

Figure 3-1 Example: Model-based fault estimation of induction motor modified from (Isermann, 2011)

The remainder of this Chapter is organized as follows: The preliminaries of faults, FE and FTC is introduced. Then FDI and FE approaches are described in Section 3.3, Section 3.4 and Section 3.5. The modelling of the induction motor faults will be described in Section 3.6 and Section 3.7. Section 3.8 introduced the need of FE/FTC which is considered in the following chapters of this thesis.

3.2 Preliminaries

In order to help understanding the study, preliminary knowledge about faults, FE and FTC is introduced in the following sections.

3.2.1 Terminology

To facilitate an understanding of some of the concepts in this thesis, it is necessary to make some simple explanations for important technical terms. In the research field of FTC, there are different forms of dynamic system expressions corresponding to different types of control and estimation methods, involving a lot of technical terms. Here it is particualarly of interest to introduce the most important terms, such as those listed below (Isermann & Ballé, 1997; Patton, 1997b; Edwards & Spurgeon, 1998)：

Fault: Unpermitted deviation of at least one characteristic property or parameter of the system from the acceptable, usual standard condition.

Fault Detection: Determination of the faults present in a system and the time of detection.

Fault Isolation: Determination of the kind, location and time of detection of a fault. This follows the fault detection.

Fault identification: Determination of the size-variant and time-variant behaviour of a fault.

Fault Estimation: Determination of magnitude of a fault signal online.

Residual: Fault indicator, based on deviations between measurements and model-equation-based calculations.

Unmatched uncertainty/fault: Any uncertainty/fault which does not lie within the range of the input distribution matrix is described as unmatched uncertainty/fault. Other wise, it is matched uncertainty/fault (see Section 5.1 for more description).

FDI is understood as fault detection and identification or fault detection and isolation; while FDD is used to denote fault detection and diagnosis. In this two concepts, fault diagnosis is said to include fault detection. As a result, only one term of FDI and FDD can be used in one thesis, in order to avoid confusion.

FDD is utilised to determine the type, size, location and occurring time of a fault. Fault detection is absolutely necessary for any practical application (Patton, 1997b; Zhang & Jiang, 2008). And fault identification is needed only when controller reconfiguration is needed. Controller reconfiguration needs to know the fault in detail. Therefore, the fault identification must be considered in a FTC process that means the time response characteristic of each fault should be known, including the size, the occurrence time and location. In this thesis Fault Estimation (FE) is used to give more details about faults of the system, it is included in FDI or FDD.

Residuals are used as an important variable in model based FTC schemes in practical systems. Residuals are generated by comparing the estimated output with the real output, and this knowledge has been widely used in industrial control systems (Chen & Patton, 1999; Zhang & Jiang, 2008). FDI is an important part of FTC, since it determines the information needed in FTC. Fault detection (FD) is to decide whether or not a fault has occurred. When a fault happened the FD part will record the time and supply this information to the FTC part. Fault isolation is responsible to determine the place of a fault. In most recent researches, FE is used more since it is able to get more details of a fault, including time, size etc. Simultaneously, FE determines the types of a fault and the degree of severity (Chen & Patton, 1999; Zhang & Jiang, 2008). Compared with FDI, the difficulties of FE design increases a lot, so FE is a more challenging issue. Furthermore, using the obtained fault information, a fault tolerant controller can be designed to compensate for the effect of the fault.

3.2.2 Fault classification

In order to provide enough faults information, i.e. the kind, size, location and time of fault occurrence, FE can be used as the approach to monitor the faulty conditions of a system. Moreover, as explained in Chapter 1 an AFTC (defined in Chapter 4 in detail) system can be formed by a controller and an FE unit. In this work the FE approach is needed and this subject has been studied and researched in several investigations (Patton, 1997b; Chen & Patton, 1999; Edwards et al., 2000; Jiang & Staroswiecki, 2002; Edwards & Tan, 2006; Zhang et al., 2009; Lan & Patton, 2016).

Generally, faults are classified according to (1) the location and (2) fault characteristics. Faults are classified into sensor faults, actuator faults and component faults in accordance with fault location (Patton, 1997b; Zhang & Jiang, 2008). Figure 3-2 shows the typical fault locations of a system under feedback control.

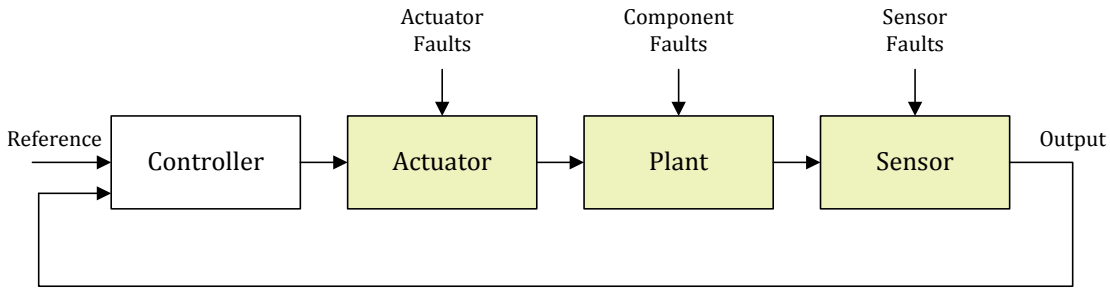

Figure 3-2 Fault classification according to location

Sensor Faults (Patton, 1997b; Chen & Patton, 1999): A feedback control system should be monitored by sensors. Sensor faults may lead to process performance degradation, process shut down or even worse results. Different sensors are adopted for different physical variables measurement, such as the thermometers, anemometers, pressure gauge, accelerometers, and so on. Sensor faults may lead to wrong measurements for these components, in the form of offsets, constant values and so on. The reason for sensor faults could be aging or other physical damage. Faulty sensors may destroy the function of a feedback controller. However, Sensor faults does not affect plant dynamics.

Actuator Faults (Patton, 1997b; Chen & Patton, 1999)**:** Actuators are applied to execute control effort on the target system, any fault within actuator affects the system inputs. For example the faults within valves, motor drives, hydraulic pistons, etc. Actuator fault means that the control effect is changed. An actuator fault could be an additive or multiplicative fault (See Section 5.3.3 for details).

Component Faults (Patton, 1997b; Chen & Patton, 1999)**:** This type of fault indicates the variation of system structure or a variation of system parameter. Component faults may include variations within mass, aerodynamic coefficient, damping constant, friction coefficient, and so on. Generally, these problems come from component failure or damage.

The above fault classification is based on the location of the fault, the following will be based on the dynamic characteristics of the fault itself.

According to the characteristics of faults, the faults are divided into the following 3 types: (1) abrupt faults, (2) incipient faults and (3) intermittent. The fault properties are shown in Figure 3-3.

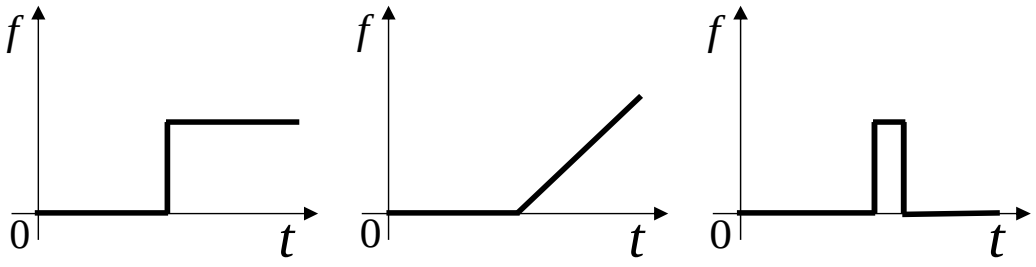

Abrupt fault Incipient fault Intermittent fault

Figure 3-3 Faults classification in time-domain

Abrupt Faults (Isermann & Ballé, 1997; Isermann, 2011): The term “abrupt” here is used to express a sudden fault, usually due to hardware damage to the system or an instantaneous change in a variable. This fault, once generated, has a serious impact on the system performance and system stability. Therefore, the FTC/FE system must respond quickly to abrupt faults.

Incipient Faults (Isermann & Ballé, 1997; Isermann, 2011)**:** Incipient faults represent a slowly changing form of fault. Examples can be component aging or a small change in resistance. This type of fault is not as strong as the above kind of fault, but if it lasts too long a time, it will have a worse effect than the previous fault. Although the incipient fault is hard to detect, it may eventually have a significant impact on the system. Hence, it is important to attempt to detect or estimate incipient faults before they become serious.

Intermittent Fault (Isermann & Ballé, 1997; Isermann, 2011)**:** Intermittent faults lasts for a short duration from generation to disappearance, but the repetition rate is relatively high. One possible cause of this type of fault is intermittent changes in system components or a loose connection in an electronic system.

3.3 Fault diagnosis and isolation

The classification of faults has been discussed in Section 3.2.2. It is necessary to discuss the classification of model based approaches in fault diagnosis (FD).

In a well-known work of (Zhang & Jiang, 2008), FD approaches have been divided into model based methods and data based methods, Figure 3-4 shows the model based approaches. These two types of faults can be divided into either quantitative methods or qualitative methods. Quantitative methods are based on the mathematical model of the physical system. It is clear that in the field of natural sciences, mathematical modelling and mathematical control methods are more accurate and more likely to inspire scholarly interest than qualitative approaches. This thesis focuses on the induction motor system and quantitative methods are used. Quantitative methods are more appropriate in this work, qualitative research methods are not considered. Based on the mathematical model of an induction motor, this thesis studies on control and fault estimation methods, so the research of this thesis belongs to the model-based fault-tolerant control method.

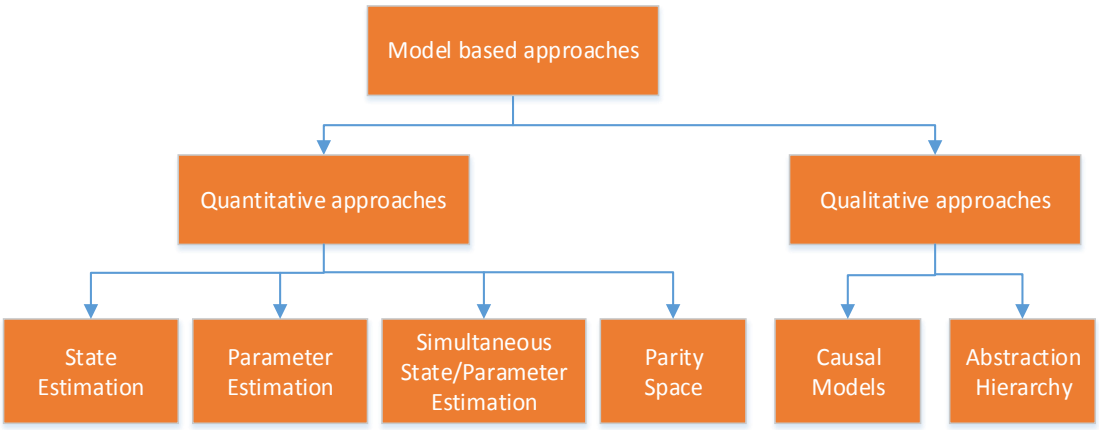

Figure 3-4 Model based FDI approaches (Zhang & Jiang, 2008)

The FDI methods in this thesis are focused on model based mathematical algorithms, the design process depends on the mathematical model of the system. Quantitative methods are the main research methods. The four commonly used quantitative FD approaches are (1) state estimation, (2) parameter estimation, (3) simultaneous state and parameter estimation and (4) parity space (Zhang & Jiang, 2008). The state estimation includes observer-based approaches and Kalman filter approaches. Parameter estimation includes the least-squares, regression analysis and bounding parameter estimation; simultaneous state and parameter estimation involves the approaches of adaptive observers, extended Kalman filters, two-stage Kalman filters and two-step estimation; and the parity space included the state-space-based methods and input-output-based methods (Zhang & Jiang, 2008; Zhang et al., 2009).

The dynamics properties of a system are expressed through the mathematical modelling approaches. The physical meaning of the mathematical model can be explained through detected dynamic performance when FDI is applied. Therefore, the relevant FDI approaches applied on the dynamic system is also quantitative and model based. In some special case, data-based FDI approach can also be applied on model-free conditions.

3.4 Residual-based FDI approaches

The purpose of FDI is to monitor a control system so that each fault can be detected and isolated. Figure 3-5 shows how the FDI function assumes that the controlled system

being monitored has as its inputs the control signal $u(t)$. The closed-loop system has as outputs $y(t)$ and the FDI function involves a residual signal $r(t)$, based on both $u(t)$ and y(t). The function $z = F_1(u, y)$ uses both $u(t)$ and $y(t)$ to drive the function $F_2(z, y)$ whose output $r(t)$ is the "residual" signal $r(t)$. By careful design of $F_1(u, y)$ and $F_2(z, y)$, $r(t)$ can be used to detect if a fault is present using a threshold. A set of specially designed residual can also be used to isolate a fault from other faults so that the fault isolation function can distinguish between faults, as shown in Figure 3-6. Figure 3-7 shows the typical shape of an adaptive threshold for residual evaluation (Chen & Patton, 1999).

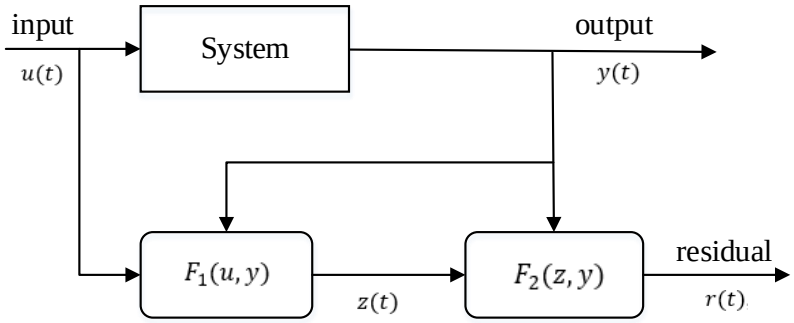

Figure 3-5 Residual generation(Chen & Patton, 1999)

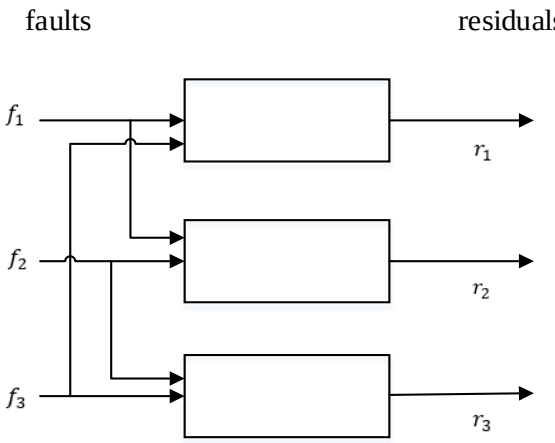

Figure 3-6 Structured residual set (Chen & Patton, 1999)

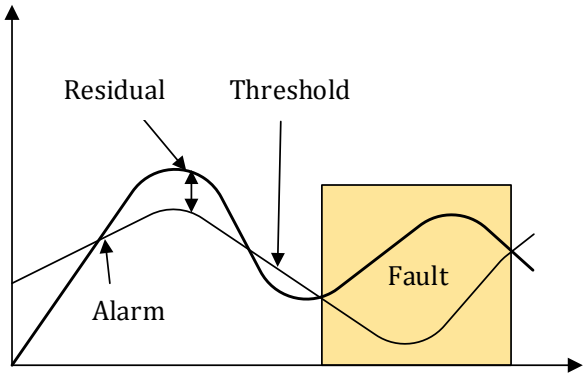

Figure 3-7 Application of threshold (Chen & Patton, 1999)

3.5 Fault estimation approaches

Considering the real fault scenarios and the degree of hardware redundancy in applications, different types of FE observer approaches were introduced in the following context. The most important functions of FE in a closed-loop function are (1) feedback signals generation and (2) use as reference signals of measurements. As a feedback signal, the result of FE can improve control effect; however, it may also bring in time delay and stability problem. There are still huge gaps for FE research.

The adaptive observer, sliding mode observer, neural networks observer, FE filters, iterative learning observer, PI observer and back-stepping observer, etc. are very popular methods (Wang & Daley, 1996; Chen & Patton, 1999; Comtet-Varga et al., 1999; Edwards et al., 2000; Tan & Edwards, 2004; Zhang et al., 2008; Zhang & Jiang, 2008; Chen et al., 2013). The main FE observers are introduced in the following context.

Sliding mode observer (SMO) based FE has been applied in small-vibration or small-friction system a lot. In early applications (Park & Kim, 1991; Shyu & Shieh, 1996) of sliding mode based approaches on induction motor system, the properties of insensitivity or robustness to matched bounded uncertainties were used to maintain operation performance in induction motor system.

Chattering is a shortcoming of this approach, which is caused by the un-modelled dynamics or high frequency component of the control signal in most cases, especially in sliding mode control where the switching of control signal excites un-modelled dynamics (Fridman, 2016; Ventura & Fridman, 2016). The chattering attenuation approaches is of

great importance because this phenomenon is seen as a connection between the theory and the real world application. One way of dealing with chattering is to design an asymptotic observer to eliminate the chattering caused by modelled dynamics; the other way is to reduce the effect of chattering by using a discontinuous control signal within a boundary. Higher-order SMO was proposed to attenuate the chattering phenomenon and was used to improve the robust effect against uncertainty (Laghrouche et al., 2007; Fridman et al., 2008). More recently, frequency domain methods have been used to give analysis of chattering from the angle of amplitude and frequency of predicted self-sustained chattering (Fridman, 2016; Rosales et al., 2016; Ventura & Fridman, 2016). SMO design considering all the problems with balance is presented in some researches (Bartolini et al., 1998; Boiko et al., 2005; Lee & Utkin, 2007).

Neural network fault estimation is capable to do some difficult job but in general observer requires high amount of calculations, therefore it can be easily implemented in PC but not in single chip micro-controller (Theocharis & Petridis, 1994; Kim & Lewis, 1999; Sun et al., 2001; Deng & Yu, 2014; Tayarani-Bathaie et al., 2014; Schmidhuber, 2015). Neural network is designed based on the needs of system, including one-direction design and bi-directional design, and the layers of a network depends on the number of the variables and the depths of the system. Usually a network within 3 layers is called neural network, while a network is of more than 3 layers is called in-depth learning. Except for the layers of the network, the structures of different neural network brings in different performance, for example the recurrent is more welcomed since its structure is more able to simulate real system.

Neural network is implemented more on data processing and patton recognition, NN approach propose more quick and efficient implementation while it is on both GPU and multi-core CPU. Multiple data with single structure can be processed on multi-core CPU, which makes use of the memories of GPU better.

Adaptive observer is known as high-performance with simultaneous state estimation and FE without system performance degradation, which is regarded as an important property. A limitation of adaptive based FE lies in its difficulty to estimate fast time-varying faults although it is suitable for constant fault estimation (Zhang et al., 2008). However, in most practical applications, faults are time varying or even fast time varying. As well as that,

additional conditions are needed sometimes, for example, the strictly positive real (SPR) condition should be considered when adaptive observer are adopted in (Wang & Daley, 1996; Zhang et al., 2008). Compared with SMO, the adaptive observer is closer to real-world application, since the system dynamics has been kept completely and the chattering effect is eliminated. Therefore, a compromise between pursuit of performance and difficulty of realization is considered when tuning adaptive parameters in the study of Chapter 7.

FE filter approach is a method that uses measurements to correct the predicted states online; therefore, it is not a method for tracking a reference signal. As well as that, it may bring in assumptions on fault types (Isermann, 1984; Xu & Rahman, 2003; Chen et al., 2008; Azizi & Khorasani, 2009).

With the above FDI and FE approaches, faults in induction motor should be researched.

3.6 Faults of induction motor systems

Induction motor has very clear advantages, durability, low cost, ease of maintenance, reasonable size, high efficiency, and ease of operation. There have been a number of studies covering reliability, performance and IM failure issues (Hammond & Mokrytzki, 1973; Krzemiński, 1987; Marino et al., 1993; Bennett, 1998; Bennett et al., 1999; Campos-Delgado et al., 2008; Marino et al., 2010). Different types of faults can occur. The most vulnerable parts of induction motors are the bearings, stator windings, rotor bars and shafts. In addition, the air gap between the inner surface of the stator and the outer surface is not uniform and this results in a form of nonlinearity. Non-uniformity in the air gap can either be estimated as a developing fault or treated as a form of uncertainty.

Different induction motor faults can lead to different consequences. Some faults result in induction motor system shutdown or even destruction. For example, resistance overheating leads to automatic protection of the motor. Some of the failures lead to lighter consequences, but can also lead to decreased efficiency. For example, speed and shaft displacement sensor faults may cause an offset to the control target. Faults in an induction motor system can be classified into component faults, sensor faults and actuator faults

(Campos-Delgado et al., 2008; Karmakar et al., 2016b; 2016a) as described in Figure 3-8.

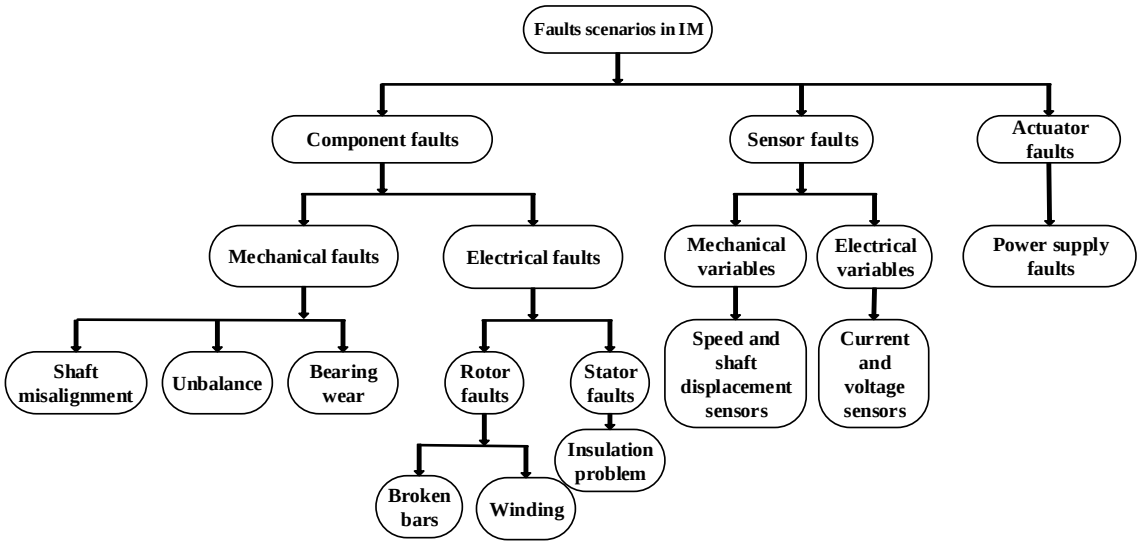

Figure 3-8 Fault conditions in induction motor systems (Campos-Delgado et al., 2008; Karmakar et al., 2016b; 2016a)

3.6.1 Induction motor component faults

Component faults located in the induction motor system arise mainly due to mechanical problems (Karmakar et al., 2016b). These faults are mainly caused by the following: broken bars, winding insulation problems, shaft misalignment, imbalance and bearing wear. These faults cause the system parameters to deviate and trigger multiplicative faults or even change the dynamics of the induction motor system. Generally, faults in the mechanical system require maintenance which is expensive and time-consuming. A number of fault diagnosis and fault estimation methods have been introduced to reduce the impact of these faults (Bennett et al., 1999; Campos-Delgado et al., 2005; Joksimović, 2005). The tasks of these methods are to estimate and compensate the faults before they become too serious.

The most important IM component faults can be summarised as follows:

1) **Broken rotor bar fault** (Trzynadlowski, 2000; Marino et al., 2010; Faiz et al., 2014; Kaikaa et al., 2014; Karmakar et al., 2016b; 2016a)

The main components of a squirrel-cage rotor are the rotor bars and end rings. If one or more bars are broken, the motor is considered to have the possibility of complete machine failure.

In squirrel-cage induction motors, this fault is mainly caused by an asymmetric rotor possibly due to manufacturing defects. The asymmetry that arises in the manufacturing process can lead to uneven stress, which makes it possible to rupture bars during rotor rotation. The heavy end of the rotor will produce centrifugal force, which may lead to additional stress; if the rotor rod is damaged it will cause rotor current asymmetry. This asymmetry cannot be ignored, and if the motor is running for a long time, it is highly likely that the rotor bar will fail. The motor efficiency is reduced, and the motor is partly disabled.

Usually, if a rotor bar mechanical fault occurs, it will gradually lead to other fault effects. For example, if the side bar current is too large, or there is an overheating phenomenon, or serious mechanical damage. The location of the fault consists of a rod, an end ring, or a joint between the rod and end ring. The possibility of a rod and end ring is greater. In addition, the motor running characteristics, may also lead to a fault. Such as the electrical and mechanical properties of the start-up phase (Faiz et al., 2014; Kaikaa et al., 2014; Karmakar et al., 2016a) due to the high rotor acceration during the start-up period.

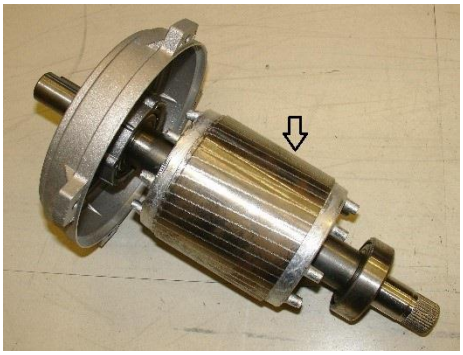

Figure 3-9 Induction motor rotor bars (Karmakar et al., 2016a)

2) **Bearing fault** (Campos-Delgado et al., 2008; Immovilli et al., 2013; Bindu & Thomas, 2014; Leite et al., 2015; Karmakar et al., 2016b)

The role of the bearing in the induction motor is to support the rotor, so that the rotor can be flexible to rotate. The device has a small coefficient of friction; the service life is

affected by the quality of the material, hence it is affected by poor mechanical properties. Each bearing consists of an inner ring, outer ring and ball bearings. The use of lubricating oil will reduce the friction torque. Any damage to the inner, or outer rings or the balls of the bearing is called a bearing failure. In the case of induction motor faults, the bearing is the weakest part of the induction motor. Approximately 41% of induction motor faults are caused by bearing degradation. This is the most significant cause of induction motor faults (Immovilli et al., 2013; Bindu & Thomas, 2014; Leite et al., 2015).

Figure 3-10 Induction motor bearings (Immovilli et al., 2013)

The most possible causes and effects of the bearing faults are listed as follows:

- The load is too large and the load exceeds the elastic limit of the bearing material.
- The temperature is too high, the lubricating oil on the bearing is broken down.
- Fatigue failure. Due to the long-term operation of the bearing, resulting in progressive bearing failure, greatly enhanced vibration and noise.
- Corrosion: This result is produced if the bearing is exposed to corrosive liquids or corrosive gases if the motor is in the working environment.
- Contamination: Lubricants are contaminated with common dirt and particulate matter.
- Lubricant failure: usually used improperly with the lubricant, and the temperature is too high.
- Misalignment of a bearing race or bearing housing will cause unusual and unbalanced loading which will have the effect of damaging the surface of each bearing, giving rise to an increase in friction.

3) **Stator winding fault** (Eftekhari et al., 2013; Shashidhara & Raju, 2013; Drif & Cardoso, 2014; Karmakar et al., 2016b)

The possible causes of this fault is as follows:

- **Stator mechanical failure** - this could caused by the movement of the stator coil and the rotor impinging on the stator. Rotor-to-stator positional deviation and bearing failure can cause the rotor to strike the stator, and the impact force will cause the stator stack to pierce the coil outside the insulation. In addition, high-intensity vibration may cause an open circuit fault in the stator windings.
- **Stator voltage transients** - Instantaneous voltage changes can reduce the life of the stator windings and, in severe cases, may cause inter-turn short circuit or ground faults.
- **Overheating** - too high a temperature will cause the stator winding insulation performance to deteriorate. High ambient temperature, obstruction of the ventilation, a variety of reasons caused by over large currents can result in high temperature conditions. If the motor starts and stops several times in a short time, the insulation performance of the windings may decrease gradually. Breakdown of insulation will cause abnormal temperature, resistance and current variations.
- **Contamination** - if the motor runs in a dirty environment, it may have the following bad consequences. Foreign matter may reduce the cooling rate, thereby reducing the insulation life. Foreign matter will also impede the flow of air; the heat generated will increase the winding temperature, thereby reducing the life of insulating materials.
- **Stator winding short-circuit** - If over-current heating or short-circuits occur in the stator windings, the rotationg flux will be weakened. These stator winding faults can lead to decreased rotor torque and even complete failure of the machine to operate. Even for a well-designed motor, these failures are difficult to avoid. Winding failure is the most common stator fault. Approximately 30% of the induction motor faults involve stator winding malfunctions. It includes the turn-to-turn short circuit faults, coil-to-coil short circuit faults, phase-to-phase short circuit faults, coil-to-ground short circuit faults , short circuit between turns of different phases, and open-circuit faults (Eftekhari et al., 2013; Shashidhara & Raju, 2013; Drif & Cardoso, 2014).

4) **Single phase fault** (Trzynadlowski, 2000; Marino et al., 2010; Bindu & Thomas, 2014; Drif & Cardoso, 2014)

Single-phase faults can be defined as electrical faults, caused either by a power electronics malfunction, a short circuit in one phase winding or a discconnection. For a three-phase induction motor, a single-phase fault will result in loss of torque, unbalanace, motor vibration and sometimes over-heating of the stator windings (Bindu & Thomas, 2014; Guzman et al., 2014).

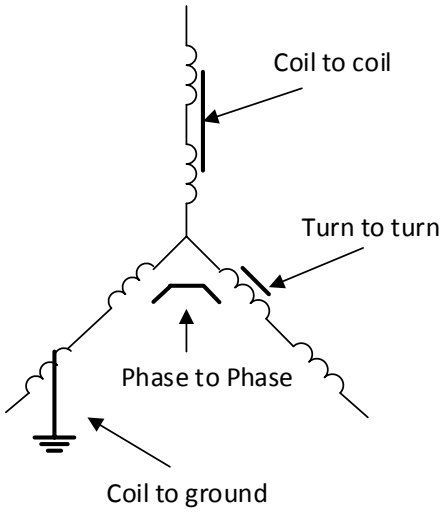

Figure 3-11 Induction motor single phase faults

In sumary, the most common types of IM faults are broken rotor bar faults, bearing faults, stator winding faults, and single phase faults. The signals used to detect and estimate the fault effects are considered to be stator currents, rotor flux, rotor speed, electromechanical torque, load torque. As a starting point the fault analysis should be based on linear dynamic system modelling, estimation and control. However when considering field-oriented rotating coordinates, it is important to use non-linear modelling.

3.6.2 Induction motor sensor faults

There are a number of important sensors to monitor the performance and health of the IM system as well as provide necessary information for the feedback control. As the IM is an electro-mechanical system, both electrical and mechanical sensors are expected, including the speed and shaft displacement sensors, current and voltage sensors etc. Normally, these sensors provide real-time speed, current, and voltage signals for motor

feedback control. In some cases, however, the signals provided by the sensors can become inaccurate due to either the changing working environment or sensor faults (Schoen et al., 1995; Benbouzid, 2000; Lopez-Toribio et al., 2000; Nandi et al., 2005; Siddique et al., 2005; Romero et al., 2010).

Environmental factors can be possible causes of sensor faults. Changes in environmental factors affect sensor accuracy, for example unusual temperature variations. Other examples of adverse environmental factors causing breakdown of sensor operation are (i) poor working conditions such as dust or excessive moisture or (ii) the presence of strong extraneous magnetic fields (an electromagnetic compatibility problem).

Sensor faults may arise from mechanical/electrical problems. The failure of speed and current sensors is not uncommon, possibly due to noise, open circuit etc. Unlike the DC motor, the induction motor current is coupled with speed, inductance and flux, etc. This coupling results in a change in one axis current and a transient disturbance in the other currents. This results in an error in the measured and actual values, which reduces the performance of the drive system (Kommuri et al., 2014; Chakraborty & Verma, 2015).

3.6.3 Induction motor actuator faults

An inverter drive is a type of adjustable-speed drive used in electro-mechanical drive systems to control AC motor speed and torque by varying motor input frequency and voltage. They are fed by three phase power supplies (Kastha & Bose, 1994; Filippetti et al., 2000; Mendes & Cardoso, 2006). Inverters as widely used in motor control systems are divided into voltage source inverters and current source inverters, which provide a stable power supply for motor systems. Any abmornal signal, such as time-delay, large noise will cause control inaccuracy. This type of fault should be taken into consideration in time once it happened.

Hence according to their action in the IM system a 3-phase invertor acts as an actuator. Hence, actuator faults that can arise in an IM system are either related to the power supply itself or malfunction in an invertor circuit. These actuator faults will induce an ineffective control voltage or an unbalanced control voltage to the IM. In more detail these faults are caused by (Campos-Delgado et al., 2008; Chen et al., 2016):

- unbalanced power supply between the different phases (F1),
- line-to-ground short-circuit (F2),
- open circuit gate to base drive power semiconductor (F3),
- short circuits in power supply system (F4),

In the condition of faults F1 and F2 the induction motor will operate with a performance deterioration. Fault F3 will result in no control voltage, which seriously reduces the inverter operating efficiency. Faults F4 will start the induction motor self-protection mechanism (depending on the type of motor), so that the motor stops running.

3.7 Modelling of induction motor faults

The overall induction motor system model is a 5th order nonlinear model, the details of the nonlinear system is described in Chapter 2. As shown in (2-12) and (2-13), the induction motor nonlinearities mainly lies within the coupling among the rotor speed, rotor flux and currents, which is a highly nonlinear function of $\omega, \varphi_{r\alpha}, \varphi_{r\beta}, i_{s\alpha}, i_{s\beta}, T_L$, and J.

Model-based control approaches, i.e. FTC/FE can be applied on the mathematical model of this system. The 5th nonlinear induction motor model is deducted from (2-12) and (2-13) into state space form:

$$\begin{aligned} \dot{x}(\mathrm{t}) &= f(x(t), u(t), d(t)) \\ y(t) &= Cx(t) \end{aligned} \tag{3-1}$$

in which $x = [\varphi_{r\alpha} \quad \varphi_{r\beta} \quad i_{s\alpha} \quad i_{s\beta} \quad \omega]^T$, $y = [i_{s\alpha} \quad i_{s\beta} \quad \omega]^T$, $u = [u_{s\alpha} \quad u_{s\beta}]^T$ and the signal d includes the effect of any nonlinearities, load torque uncertainty. Sensor detected parameters are used in the FTC/FE system which is reflected in the matrix C. When a current sensors is used, C becomes:

$$C = \begin{bmatrix} 0 & 0 & 1 & 0 & 0 \\ 0 & 0 & 0 & 1 & 0 \\ 0 & 0 & 0 & 0 & 1 \end{bmatrix}$$

A model-based control system can be designed based on the induction motor model described in (2-12). However, this is only designed in the fault-free condition when faults are not considered.

As outlined in Section 3.6.1, Section 3.6.2 and Section 3.6.3, there are three types of faults that need to be considered in a dynamic system: (1) sensor faults, (2) actuator faults and (3) component faults. Either one of the three types of fault model can be combined with (2-12) to design an FTC/FE system for induction motors.

The following Sections combine the research of model-based FTC/FE approaches with the modelling approaches of the above three types of faults. For example, different types of faults can be used with the system (2-12) in the FTC/FE system in order to deal with multiple faults condition. For both actuator and sensor fault, (2-12) is used to design an FTC/FE system in order to deal with both actuator and sensor faults in induction motors.

Based on several types of tests described in (Campos-Delgado et al., 2008; Isermann, 2011), four different faults are now selected to show the estimation of additive and multiplicative faults of the induction motor system. The faults can be summarized as:

1) A current sensor offset fault ΔI which leads to a change of stator current $i_{s\alpha}$ or $i_{s\beta}$;
2) An offset fault in the speed sensor ω which leads to a change of the speed measurement;
3) A change of inertia value and load torque;
4) A multiplicative change of the armature resistance R.

Table 3-1 Induction motor faults classification

Additive faults	current sensor offset fault	ΔI
	speed sensor offset fault	$\Delta\omega$
Multiplicative faults	change of load torque	ΔT_L
	armature resistance	ΔR

3.7.1 Induction motor sensor faults

An induction motor model with sensor faults is used in FTC/FE for induction motor sensor faults. This model can be expressed as follows:

$$\dot{x}(\mathrm{t}) = f(x(\mathrm{t}), u(\mathrm{t}), d(\mathrm{t}))$$
$$y(\mathrm{t}) = Cx(\mathrm{t}) + f_s(\mathrm{t}) \tag{3-2}$$

in which $f_s(\mathrm{t})$ is a vector representing the sensor faults.

As shown in (3-2), the modelling of actuator and sensor fault are all regarded as additive faults. Multiplicative faults are also considered in this thesis as the sliding mode observer is introduced in Chapter 5. The multiplicative sensor fault can be transformed into additive sensor fault. (Sami & Patton, 2012; Shaker & Patton, 2014).

3.7.2 Induction motor actuator faults

Actuator faults in induction motor systems are also researched through FTC/FE approaches in the remaining of this thesis. This model can be expressed as follows:

$$\dot{x}(\mathrm{t}) = f(x(\mathrm{t}), u(\mathrm{t}) + f_a(\mathrm{t}), d(\mathrm{t}))$$
$$y(\mathrm{t}) = Cx(\mathrm{t}) \tag{3-3}$$

where $f_a(\mathrm{t})$ represents the actuator fault.

The actuator fault is a type of additive fault to the induction motor system. A multiplicative actuator fault representing gain factor errors in the actuator can also be considered as follows:

$$\dot{x}(\mathrm{t}) = f(x(\mathrm{t}), (1 + \Delta)u(\mathrm{t}), d(\mathrm{t}))$$
$$y(\mathrm{t}) = Cx(\mathrm{t}) \tag{3-4}$$

where $-1 \leq \Delta \leq 1$ is the scaled multiplicative fault (this range is realistic considering a likely real fault condition). Both additive and multiplicative faults are estimated using an FE observer and the fault can be compensated by the FTC system.

3.7.3 Induction motor component faults

Component faults include the faults within the function range of states, inputs, etc. therefore they affect system stability. An induction motor with component faults can be described as:

$$\dot{x}(\mathrm{t}) = f(x(\mathrm{t}), u(\mathrm{t}), d(\mathrm{t})) + f_c(x(\mathrm{t}), u(\mathrm{t}), d(\mathrm{t}))$$
$$y(\mathrm{t}) = Cx(\mathrm{t}) \tag{3-5}$$

where $f_c(x(\mathrm{t}), u(\mathrm{t}), d(\mathrm{t}))$ represents the component faults.

3.7.4 Effects of multiple induction motor faults

The effects of multiple induction motor faults can be considered as follows when FTC/FE are designed for both actuator faults and sensor faulst:

$$\dot{x}(\mathrm{t}) = f\big(x(\mathrm{t}), u(\mathrm{t}) + f_a(\mathrm{t}), d(\mathrm{t})\big)$$
$$y(\mathrm{t}) = Cx(\mathrm{t}) + f_s(\mathrm{t}) \tag{3-6}$$

3.8 The need for FE/FTC

The introduction of IM modelling in Chapter 2 and the presentation of faults in Chapter 3 implies that the problem of Faults and FTC remains a very open problem. Therefore, this Section discussed the need for FE/FTC, as applied to IM systems.

- **Theoretical needs**

Fault estimation (FE) is applied in fault detection with robustness to uncertainty in various frameworks (Mangoubi et al., 1992; Stoustrup & H Niemann, 2002). In real-world application, the more accurate information of faults means less budget or more money saved. Therefore, the type, size, location and time of fault occurrence should be given as accurately as possible. Considering the robustness ability of FE observer approaches, H_∞ optimization is a good approach with multi-objective design. In this thesis, the FE approach is designed to provide fault information for fault compensation within AFTC schemes.

- **Practical requirements**

This thesis combines the theory of induction motor fault modelling and FTC/FE, and classical theories are cited and summarized. With the development of FTC/FE, the FTC design for induction motor has attracted more and more attention with the **requirement**

of safety, reliability, maintainability and sustainability (Filippetti et al., 2000; Marino et al., 2010; Chen et al., 2013; Tabbache et al., 2013; Shipurkar et al., 2017).

Using an FE method, the faulty components, actuators or sensors can be identified and the control system can be reconfigured by using suitable FTC strategies. **Fault compensation** can be achieved using an FE observer, the estimated faults can be effectively compensated in the control system. On the other hand, the utilization of FE/FTC is a huge **compensation for the hardware redundancy**. Especially when the FE is so popular in industrial application, the hardware design should cooperate well with the control algorithm design, although the hardware redundancy is not always enough for real-world application.

3.9 Summary

Based on the induction motor modelling in Chapter 2, this Chapter introduces the fault modelling background as well as the concepts of FE and FTC for induction motor.

There are a series of induction motor faults, such as rotor broken bar, stator faults, single phasing, bearing faults, unbalanced power supply, short circuit in different parts, etc. These are discussed along with causes and effects. This Chapter gives a general description of induction motor faults, including the phenomenon and physical reasons, and then give classification of the faults we want to research. With regard to the classification of sensor faults, actuator faults and component faults, it can also be classified into additive faults and multiplicative faults according to the way it works on the system and the place it works on system. The modelling of induction motor faults is presented in this Chapter, including modelling for actuator, sensor and component faults. Then, various FTC/FE methods are reviewed. In Chapter 5, adaptive observer and sliding mode observer are used to estimate the sensor fault, actuator fault and component fault. It is shown in Chapter 6 & 7 that the LPV approach and back-stepping control approach provides approaches for nonlinear induction motor FTC/FE.

Chapter 4 introduces the active FTC (AFTC) concept by outlining the various methods and focussing on FDI-based reconfiguration and FE-based fault compensation.

Chapter 4: Approaches to active FTC

4.1 The FTC concept and classification of methods

According to (Patton, 2015) "FTC is a strategy in control systems architecture and design to ensure that a closed-loop system can continue acceptable operation in the face of bounded actuator, sensor or process faults. The goal of FTC design must ensure that the closed-loop system maintains satisfactory stability and acceptable performance during either one or more fault actions. When prescribed stability and closed-loop performance indices are maintained despite the action of faults the system is said to be "fault-tolerant" and the control scheme that ensures the fault tolerance is the fault tolerant controller."

There are mainly two types of fault-tolerant control, namely passive fault tolerant control (PFTC) and active fault tolerant control (AFTC) according to the difference of the control structure, i.e. through the use of fixed control structure or reconfigurable control structure (Zhang & Jiang, 2006; 2008), as outlined briefly in Chapter 1.

The PFTC structure is based on a fixed controller which minimize the effect of the fault over control effect (Zhang & Jiang, 2008; Xiao-Zheng & Guang-Hong, 2009; Lan & Patton, 2017). The degree of freedom of the controller design is not always good, and as the controller is designed to mimize the effect of a fault, its tolerance for uncertainty is limited (Patton, 1997a). PFTC does not require on-line fault information, it is usually designed off-line based on robust control theory, such as linear optimization and linear matrix inequalities (LMI), Quantitative feedback theory, H_∞ theory, nonlinear regulation theory or methods based on absolute stability (Patton, 1997b; 1997a; Zhang & Jiang, 2008). Since PFTC is known as an off-line control design based on certain *priori* knowledge of the faults, it is considered able to handle only a very limited range of fault scenarios.

AFTC has two conceptual steps to provide the system with fault tolerant capability:

1) Construct a scheme to detect or estimate faults robustly. This mechanism must be capable of isolating or locating the fault within the system. When there are no faults

present a baseline controller attenuates disturbances and ensures good stability and closed-loop tracking performance.

2) Adapt or reconfigure/restructure the controller parameters so that the required closed-loop system performance can be maintained even in the presence of bounded faults.

An AFTC control system can be divided into four main parts or functions (as shown in Figure 4-1):

1) A reconfigurable *baseline* controller;
2) A FDI scheme for fault detection/isolation or fault estimation (FE);
3) A controller reconfiguration mechanism;
4) A command/reference governor.

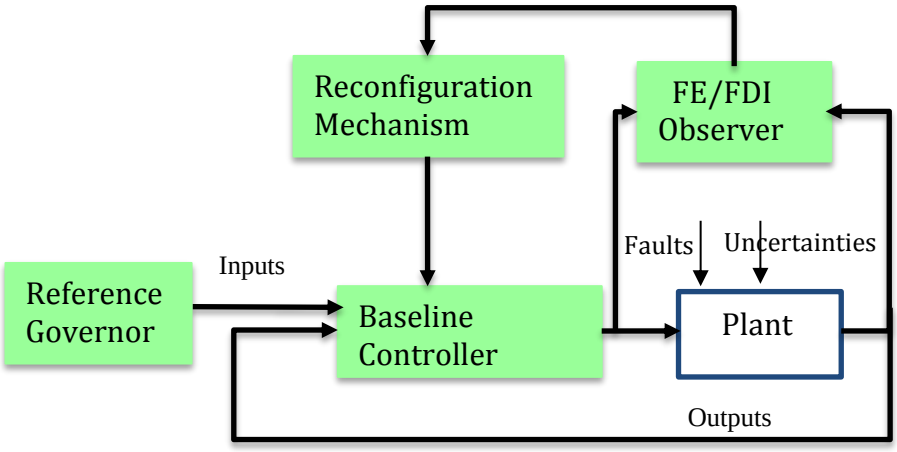

Figure 4-1 The component functions of an AFTC system

In the papers (Patton, 1997b; Zhang & Jiang, 2008; Patton, 2015), according to the evolution of FTC, AFTC is classified according to mathematical design tools, design approaches, reconfiguration mechanisms and type of systems dealt with. Until 20 years ago, the FDI procedure was mainly used for system monitoring but during the last 20 years attempts have been made to use the FDI function in reconfigurable control or AFTC. However, more recently real-time FE has gradually taken over from the use of FDI for both fault monitoring and AFTC (Oudghiri et al., 2008; Odgaard & Johnson, 2013; Yin et al., 2014).

This Chapter provides a classification of FTC methods, focussing on AFTC. In particular the use of FE within FTC as a form of AFTC is described briefly as it forms the background to the work in Chapters 5, 6 & 7.

Figure 4-2 shows a classification and development of all FTC approaches. The red line line shows the area of the diagram that is relevant to the methods used in the thesis. In particular, the work in the thesis makes use of AFTC with the fault information provided by an FE or adption mechanism. The FE/adaption function replces the formerly used FDI function. Estimates from the FE are used to compensate the effect of the fault from the baseline controller. Control allocation works to allocate from faulty actuator to healthy actuator, fault hiding acts to hide fault from dynamic systems, controller redesign requires new parameter design for new controllers.

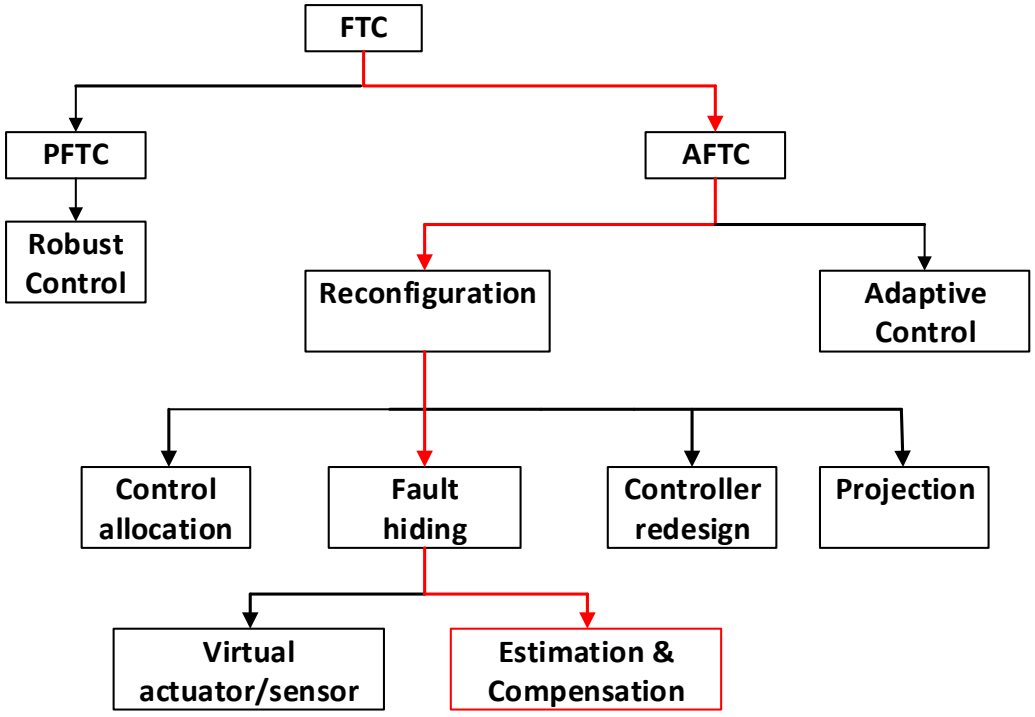

Figure 4-2 Classification of FTC methods (Zhang & Jiang, 2008)

In this thesis, AFTC has been chosen as the control approach and several FE approaches are involved in the design. Therefore, AFTC applied on an induction motor system is realized with FE based reconfigurable control.

4.2 FTC/reconfiguration based on FDI

As discussed in Section 3.3 the concept of considering the FDI function to operate within a closed-loop control system is very well known (shown in Figure 4-3) and it is especially important to consider the effect of system uncertainty on the robustness of FDI. This was first shown by (Patton, 1997b) and the main ideas were later extended by (Comtet-Varga et al., 1999; Blanke et al., 2006; Ding, 2009; Isermann, 2011).

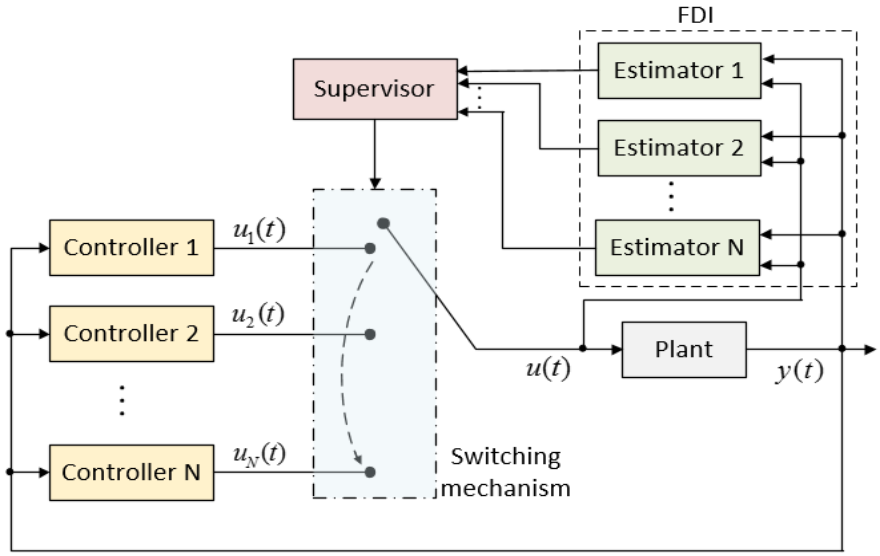

Figure 4-3 FDI based FTC

However, these early studies on integration of control and FDI do not represent the truly integrated design of FDI with AFTC described by (Lan and Patton, 2017).

Figure 4-3 shows the integration of FDI within the system feedback control loop. The FDI function (described in Section 3.3) generates residual signals which are used to detect the presence of faults and isolate one fault from another. The reconfiguration function then requires a decision mechanism to decide, based on the FDI, whether the system needs to be reconfigured or not. This decision function is a supervisory role which is actually a form of AI software. Hence, the automatic supervisor causes a switching operation to occur as the system is switched between one controller to another (removing the presence of the faulty component, sensor etc.). The FDI function also introduces an unknown time-delay as the time to detect a fault depends on the amount of noise or uncertainty in the system and also depends on the level of the threshold applied to each residual signal.

It can therefore be seen that the resulting FDI-based reconfiguration AFTC system is considerably more complex to design and implement in a practical system involving both switched feedback and unknown time-delay as well as model uncertainty and the presence of noise.

Figure 4-3 shows that the reconfiguration system has N (the number of nodes) FDI residual estimators with N corresponding controllers (each corresponding to a fault-free control configuration). For different fault scenarios, the specific FDI functions and controllers are designed offline, with only the FDI function and decision/switching computed on-line.

The above approach of FDI and FTC is required to realize robust closed-loop stability, robust residual performance, stable reconfiguration, and good performance in the presence of variable time-delay and uncertainty (Lan & Patton, 2016); however, its disadvantages are obvious. Due to the existence of switching mechanism and the resulting requirement for multi-objective design it is very difficult to take account of the modelling uncertainties as well as the uncertainty due to the controller switching,

These difficulties and disadvantages mean that, in the view of the author, it is better to use the alternative approach to AFTC making use of combined FE and fault compensation.

4.3 FTC/reconfiguration based on FE

The fault tolerant operation of AFTC is summarized as follows (Patton, 1997b; Blanke et al., 2006; Zhang & Jiang, 2008; Lan & Patton, 2015; Patton, 2015):

Supply the dynamic system with a FE scheme and use the fault information (fault estimates) as input for the post-fault closed-loop system.

The baseline controller is used to ensure stability or tracking performance when faults are not acting on the system.

“Fault hiding” is used to describe the action of hiding the fault effect (fault estimate(s)) from the baseline controller by inserting a reconfiguration block between the plant and baseline controller. Through the use of this extra block, the dynamic system can be

reconfigured and the baseline controller can also be reconfigured, hence the AFTC function is complete (Lan & Patton, 2017).

Compared with PFTC, AFTC is a topic of wider range of applications. The FE and FTC scheme can be integrated into one control system design and is designed as a powerful method for achieving robust closed-loop FTC system design, taking account of parametric uncertainty and admissible performance (Sami & Patton, 2013; Feng et al., 2014; Lan & Patton, 2015; Shi & Patton, 2015; Tan & Patton, 2015; Lan & Patton, 2016).

The problems concerned with AFTC methods stem mainly from system modelling errors, nonlinearities, and parametric uncertainty. Hence, the main challenges for AFTC design are as follows:

- How can the fault information be reconstructed from the dynamic changes when uncertainties exist in the system?
- How can the closed-loop FTC be designed to have acceptable performance and good robustness to uncertainty?

The first question is very well researched in the AFTC design subject, because accurate fault information is always important for control system design. Hence, it is known that the fault estimation performance should also be designed against the effect of system uncertainty (Patton, 1997b). As shown in the paper (Lan & Patton, 2016), the design of a joint FE and FTC system can be achieved in an integrated structure to achieve high joint robustness performance in FE and FTC, where bi-directional uncertainties are involved (in both control and estimation).

The second question considers the AFTC problem of a dynamic system with fault/uncertainty. This means that the FE, or adaption schemes, or other robust approaches should be designed for FTC, sometimes they should be designed together to consider the coupling effect in the AFTC design (Zhang & Jiang, 2006).

4.4 FE-based AFTC architectures

AFTC, which is also known as reconfigurable control, is based on controller design using online information from state and fault estimation observers, or from a switching mechamism involving FDI as shown in Figure 4-3.

This kind of controller compensates for the faults and uncertainties of the system with higher degree of design freedom than the PFTC approach. The design methods of this thesis all belong to the category of AFTC.

Figure 4-4 shows the idea that if a fault or uncertainty occurs in the system, a state observer system will quickly perform the FE function to provide real-time information (state and fault estimates) for the on-line adjustment of the controller. The reconfigurable controller utilizes real-time fault information and state variable information to reconstruct the controller parameters, which are adapted to the current dynamics and static characteristics of the system, thus ensuring the stability of the closed-loop system. The reference signal is designed to adjust the tracking objectives or the control aims by operators online (Zhang & Jiang, 2008).

According to the above structure, the design objectives are as follows:

1) The observer must be able to estimate the state variables and fault signals as accurately as possible.
2) The reconfigurable controller must have guaranteed feedback stability under all considered fault conditions.
3) The control accuracy of the AFTC system for the given fault conditions must be maximized using performance robustness.

The purpose of the FE observer is:

1) To detect whether the fault has occurred and the time of fault occurrence.
2) To detect the magnitude and dynamic characteristics of the fault.
3) Provide a robust estimate of the fault that can be used for fault compensation in the AFTC system.

Figure 4-4 shows the structure of a AFTC system implemented using FE. The FE function can be combined with approaches such as predictive control (Morari & Lee, 1999; Deshpande et al., 2009; Feng, 2014), sliding mode control (Edwards & Spurgeon, 1998; Edwards & Tan, 2006), LPV structures (Shi & Patton, 2014), multiple-model based approaches (Sami & Patton, 2012), etc.

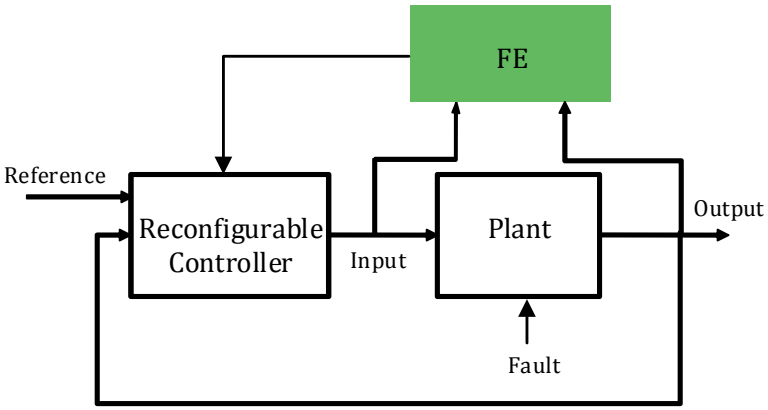

Figure 4-4 AFTC with FE

4.5 Summary

This Chapter introduces several fault compensation approaches to FTC including the essential requirements of an AFTC system. The motivation of fault compensation based FTC is to make use of FE.

Following this, Chapter 5 is concerned with the development of two FE schemes for IM systems, based on a linear system approach applied to the 4th order IM model described in Section 2.2. The first uses the so called adaptive observer for actuator and sensor fault estimation, for cases in which the faults contain constant signals. For the case of time-varying faults the sliding mode observer is considered. As well as that, SMO is used to estimate multiplicative faults by considering these as time-varying aditive faults.

Chapter 6 extends the FE work in Chapter 5 into a time-varying or LPV framework. The LPV modelling strategy is used as this represents a time-varying linear representation of the true non-linear system.

Chapter 7 describes an AFTC design strategy using adaptive back-stepping applied on a 5th order induction motor system. In this approach, both significant nonlinearity arising

from coupling between flux and currents is taken into account. The IM inertia and load torque are considered to be varying so that an adaptive method is described. The load torque is considered as an unmatched fault which is accounted for usign the back-stepping control method.

Chapter 5: Observer based FE for electrical subsystem of induction motor

5.1 Introduction

As described in Chapter 2 the induction motor is an electro-mechanical system that can be modelled as two interacting electrical and mechanical subsystems. As an electro-mechanical system it seems natural to attempt to deal separately with (a) electrical faults and (b) mechanical related faults. However, it turns out that the machine rotation speed ω is the "scheduling" variable that determines the amount of coupling between these two subsystems. So that, in fact if the rotating speed is a constant the two subsystems can be considered separately. It then also follows that if the speed is slowly varying the two subsystems are approximately decoupled. Hence, using the assumption that the rotation speed is slowly changing or constant the electrical system faults maybe estimated using the 4 electrical state equations of Eq. 2-12.

Chapter 6 extends the FE problem developed in this Chapter to the parameter-varying case using a Linear Parameter Varying (LPV) formulation. In the LPV case the limitation of considering only small changes in ω is dropped since the parameter-varying structure encompasses the full range of speed variations of the machine.

Therefore, this Chapter provides the basic background to this problem using the two methods of adaptive state observer and sliding mode observer, respectively, in preparation for the LPV description given in Chapter 6.

As discussed in Section 3.3 FDI residuals have been traditionally used to detect and isolate faults in dynamical systems. A threshold level is chosen and applied to the residual signal so that when a fault occurs the threshold can be exceeded by the residual, providing a detection flag. A set of residuals can be used to determine which fault has occurred, the so-called fault isolation problem of FDI. However, for FTC the FDI residual approach leads to a very complex way of reconfiguring the system, subsequent to a fault. Recent research (Lan & Patton, 2015; 2016; 2017) has shown clearly that the FDI approach can be superseded in a powerful way by fault estimation or FE. There is now a mature body

of knowledge about FE methods that have been developed to provide robustness to modelling uncertainty (Chen & Patton, 1996; 1999; Ding et al., 2000; Zhang et al., 2002; Jiang et al., 2004; Yan & Edwards, 2007). In fact, the tasks of fault detection and fault isolation are automatically included together in FE since the aim is to estimate the fault signal accurately. Once the fault signal has been estimated the location of the fault in the system is known by the setting up of the estimation problem, i.e. the location of the fault is always known as this is implicitly known in the FE problem. Furthermore, the fault estimates can be used in a much more direct way for FTC using the approach known as FE and fault compensation control, as summarised in Section 3.3. The FDI approach is not used in this thesis and attention now turns to the FE process itself, how it is achieved and a brief description of the main FE methods known in the literature.

In fact, in most of the FE processes the fault estimation is carried out using a state observer in which the system states and the faults are estimated together in an augmented observer structure. For example, FE can be achieved using linear state observers (Shi & Patton, 2014), adaptive state observers (Ekramian et al., 2013), non-linear observers (Garcia & Frank, 1997), sliding mode observers (Edwards et al., 2000) and even using neural networks (Theocharis & Petridis, 1994).

The one exception to the "augmented observer rule (Shi & Patton, 2015)" is the sliding mode observer (SMO) in which the fault estimate is achieved using the so-called output injection signal, which is actually not a state variable and the SMO is not an augmented observer (Edwards et al., 2000).

Another powerful approach is the adaptive observer based FE (Wang & Daley, 1996; Zhang et al., 2008; Zhang & Jiang, 2008; Boulkroune et al., 2014) which has been found to be effective for some classes of parameter-varying or non-linear systems (Xiao et al., 2012; Fan et al., 2013).

Neural networks can also be used to mimic the state observer role as they can be trained to model the input-output and/or dynamic behaviour of a system. There have been many attempts to use neural networks for state and fault estimation. However, it is hard to understand how to take into account the various factors of faults, parameter changes and modelling uncertainty when using a neural network (Sonmez et al., 2006; Khoob, 2008; Rehman & Mohandes, 2008). This is because, in a neural network approach, one

characteristics of a dynamic system is usually represented by one parameter. It is difficult to use a separate parameter to represent fault as in model-based fault estimation approach.

Section 5.2 considers FE for both sensor fault and actuator fault cases. Two methods have been used for FE, in relation to the electrical system faults, based on the 4th order induction motor system of Eq. 2-12, assuming that the rotation speed ω is constant. In the case of Algorithm 1 it is assumed that the faults are constant (i.e. have no dynamics). Algorithm 2 considers both the fault dynamics and fast-varying fault scenarios. Following this and as a novel contribution in this thesis an adaptive observer is described in Section 5.2.3 whose adaptive parameters are solved using a matrix inequality (LMI) formulation. LMI is used as the optimization is "multi-objective", in which the objectives are (a) optimize the robustness of the estimation to modelling error or disturbance; (b) minimize the error of the fault estimates for time varying faults; (c) optimize the stability of the adaptive observer. All the required parameters are designed together off-line and the observer is adaptive as the fault dynamics are included in the design.

After introducing the adaptive FE observer described by (Jiang & Staroswiecki, 2002) and improved adaptive FE observer is proposed in Section 5.2.3. This new design strategy considers an $H\infty$ approach (within the gain design) to achieve suitable robust performance. This study involves a multi-objective LMI design in which the objectives are the adaption gains, the maximization of the observer stability and the $H\infty$ minimization of sensitivity to uncertainty (robustness problem).

In Section 5.3, sensor faults, actuator faults and component fault (multiplicative fault) are considered in which the SMO is used as the FE approach. In all three case the sensor, actuator and multiplicative faults are considered as so-called "matched" faults. It is important to note here that the multiplicative faults can be expressed as a special form of additive fault structure, as discussed in Section 5.3.3.

Definition of the meaning of "matched faults" or "matched uncertainty"

In a dynamic system which is expressed as $\dot{x}(t) = Ax(t) + Bu(t) + D\xi(t,x)$ where $R(D) \subset R(B)$, $\xi(t,x)$ is understood as matched uncertainty. In other words, uncertainty which lies within the range space of the control input distribution matrix B is described

as matched uncertainty. Otherwise, the uncertainty is said to be unmatched (Edwards & Spurgeon, 1998).

An outline of the structure of the Sections of this Chapter is shown in Figure 5-1.

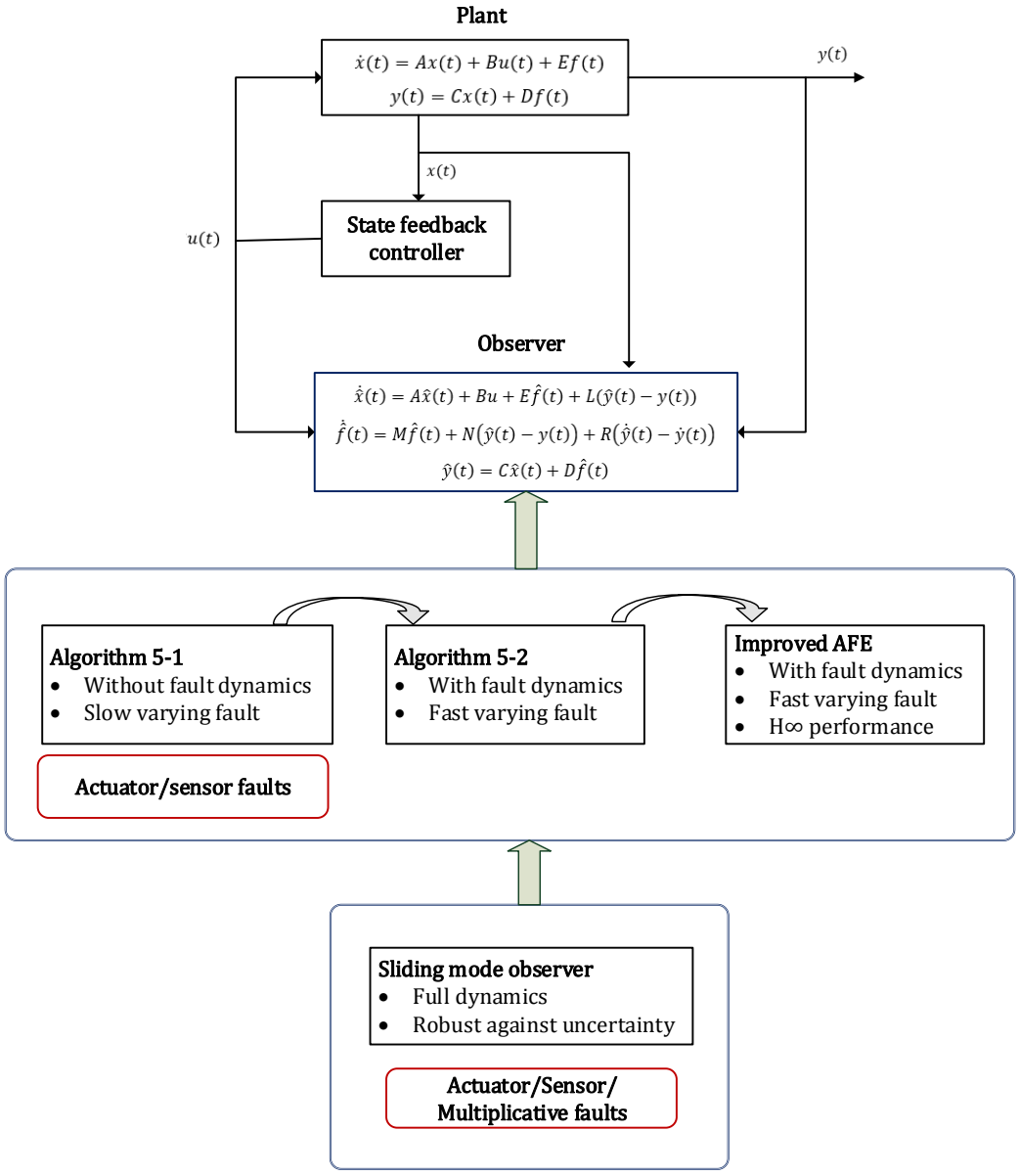

Figure 5-1 Observer-based FE for linear system

5.2 FE using adaptive observer

In this Section, the adaptive observer and an improved adaptive observer are presented. Both of the FE approaches are designed for sensor faults and actuator faults estimation based on the original work of (Wang & Daley, 1996). The main function of the FE observer approach is to provide all the fault information, which is very useful for system fault compensation or reconfiguration. FE can be used on uncertain systems, such as the induction motor system with parametric variations. Going further, a number of FE/FTC approaches have been applied on induction motor systems during the past two decades (Kubota et al., 1993; Lascu et al., 1998; Chan & Shi, 2011; Eftekhari et al., 2013; Chakraborty & Verma, 2015). However, there are still some open problems for the application of FE on induction motors, especially when sensor or actuator faults occur, which can make the operation become potentially hazardous. For example, if the invertor circuit has a "power supply" fault the voltage and current levels in this unit could become excessive with the probable risk of fire and further system damage. Although there are protection mechanisms it is clear that the complexity of these can be reduced by estimating the fault effects before they become serious. Therefore, it is essential to consider both the application performance and control requirements. The pursuit of the implementation of FE without degradation or loss of performance is an interesting application area of continuing research.

5.2.1 Development of adaptive observer for FE

Here the development of an adaptive approach to observer FE, following the work of (Wang & Daley, 1996; Jiang & Staroswiecki, 2002; Zhang et al., 2008), is described in the context of application to the induction motor system.

In the work of (Wang & Daley, 1996) an adaptive observer technique was presented for state estimation and actuator fault estimation in linear systems. The adaptive observer is designed to perform FE for abrupt faults with robustness to parametric uncertainty. The problem considered is one of linear system dynamics but with time-varying faults, i.e. the fault evolution in time can be described by a dynamical system. Hence, the appropriate state observer has a fixed gain matrix corresponding to the state estimation observer subsystem but becomes adaptive due to the fault dynamics, So a part of the gain matrix

is time-varying and this FE observer system can be referred to as an adaptive observer according to the fault dynamics. At the observer design stage it is important to consider the convergence rate of the fault estimates. However, this original approach is difficult to use in practice due to the assumption made by (Wang & Daley, 1996) that the faults should have constant values.

Based on the above problems, two novel approaches were developed in (Jiang & Staroswiecki, 2002) for the estimation of both actuator and sensor faults. In their work, the shape of the fault signals can be estimated and used more precisely. This is considered in this study as more useful approach for fault accommodation in the induction motor system.

Consider the induction motor system model (see also Section 2.2.1):

$$\begin{bmatrix} \dot{\varphi}_{r\alpha} \\ \dot{\varphi}_{r\beta} \\ i_{s\alpha} \\ i_{s\beta} \end{bmatrix} = \begin{bmatrix} -\frac{R_r}{L_r} & -n_p\omega & \frac{R_r}{L_r}M & 0 \\ n_p\omega & -\frac{R_r}{L_r} & 0 & \frac{R_r}{L_r}M \\ \frac{MR_r}{\sigma L_s {L_r}^2} & \frac{n_p R_r}{\sigma L_s L_r}\omega & -\frac{{L_r}^2 R_s + M^2 R_r}{\sigma L_s {L_r}^2} & 0 \\ \frac{n_p R_r}{\sigma L_s L_r}\omega & \frac{MR_r}{\sigma L_s {L_r}^2}\omega & 0 & -\frac{{L_r}^2 R_s + M^2 R_r}{\sigma L_s {L_r}^2} \end{bmatrix} \begin{bmatrix} \varphi_{r\alpha} \\ \varphi_{r\beta} \\ i_{s\alpha} \\ i_{s\beta} \end{bmatrix} + \begin{bmatrix} 0 & 0 \\ 0 & 0 \\ \frac{1}{\sigma L_s} & 0 \\ 0 & \frac{1}{\sigma L_s} \end{bmatrix} \begin{bmatrix} u_{s\alpha} \\ u_{s\beta} \end{bmatrix}$$

This 4th order electrical system of the induction motor is described based on the α *and* β coordinate transformation. The electrical system is different from the mechanical system in the following aspects: (1) electrical signal properties are different from mechanical related variables; (2) the coupling part can be investigated separately, since the electrical and mechanical systems are coupled through only one 1st order system, where only the electromagnetic torque is coupled with the electrical system (rotor flux and stator currents). The work described in this Chapter neglects this coupling through the assumption that rotor speed is a constant value.

Consider the stator current with abnormal bias (fault), and the following derivation of the abnormal bias (fault) with dynamics as follows.

$$\frac{d\hat{f}(t)}{dt} = M\hat{f}(t) + N\big(\hat{y}(t) - y(t)\big) + R\big(\dot{\hat{y}}(t) - \dot{y}(t)\big)$$

$\hat{f}(t)$ and $\hat{y}(t)$ are the estimated fault and estimated output signals respectively. $\dot{\hat{y}}(t)$ and $\dot{y}(t)$ are the derivatives of the estimated and actual outputs, respectively. M, N, R are the adaption matrices to be designed. This dynamic system fault reflects the signal processing ability of the adaptive observer proposed originally in (Jiang & Staroswiecki, 2002), since it considers not only the outputs but also the estimated faults and the faults dynamics.

One FE observer is designed to provide accurate fault signals; an improved approach aims to improve the former FE observer design with the H_∞ approach to achieve suitable robust performance.

Hence, this Chapter applies these two observer FE structures to a 4th order induction motor system model, in linearised form based on the model description given in Section 2.2.1. When considering the case when the rotor speed is assumed to be constant, the appropriate system is actually linear. The background work in the literature (Jiang & Staroswiecki, 2002) has stimulated the development of some new ideas about how to design the induction motor control system in the case of weakening of this constant speed assumption, i.e. for the more general case of variable rotation speed (i.e based on the 4th-order nonlinear mechanical system of Section 2.2.1).

The strategy adopted here is based on the work of (Zhang et al., 2008) in which a feasible algorithm was explored to design the gain parameters of a FE state observer using an LMI multi-objective strategy. In the (Zhang et al., 2008) work, an adaptive observer is used which is not based on knowledge of the fault dynamics. In this thesis, a similar LMI strategy has been adopted for the adaptive FE observer taking into account the fault dynamics, with application to the induction motor system. This new design approach is capable of generating improved estimation results compared with the first two approaches introduced in this Section.

5.2.2 General problem statement

Here, a system with both sensor fault and actuator fault is presented, and an adaptive observer is proposed to tackle this problem of actuator fault and sensor fault estimation.

Consider a linear dynamic system：

$$\dot{x}(t) = Ax(t) + Bu(t) + Ef(t) \quad (5\text{-}1)$$

$$y(t) = Cx(t) + Df(t) \quad (5\text{-}2)$$

where the state is $x \in R^n$, the input is $u \in R^m$, and the output is $y \in R^r$. The pair (A, C) is observable and $rank(C) = r, rank(D) = q, q \leq r$. Each additive fault $f(t) \in R^q$ is assumed to behave smoothly when the fault occurs. The matrices E, D are distribution matrices giving the distribition of the faults into the state and output equations, respectively.

In this approach, the fault dynamics has been considered in the FE process. And this approach is able to finish both states and faults estimation simultaneously.

Following the work of (Wang & Daley, 1996) the following augmented observer systems can be used to estimate both the states $x(t)$ and faults $f(t)$:

$$\dot{\hat{x}}(t) = A\hat{x}(t) + Bu + E\hat{f}(t) + L(\hat{y}(t) - y(t)) \quad (5\text{-}3)$$

$$\dot{\hat{f}}(t) = M\hat{f}(t) + N\big(\hat{y}(t) - y(t)\big) + R\big(\dot{\hat{y}}(t) - \dot{y}(t)\big) \quad (5\text{-}4)$$

$$\hat{y}(t) = C\hat{x}(t) + D\hat{f}(t) \quad (5\text{-}5)$$

where $\hat{x}(t) \in R^n$ is the state estimate, $\hat{y} \in R^r$ is the output estimate, $\hat{f}(t) \in R^q$ is the fault estimate, and L, M, N, R are matrices of appropriate dimensions to be designed to provide optimal fault estimation $\hat{f}(t)$.

Remark 5-1:

It is assumed that this type of observer is designed with fixed gain matrices *N* and *R*, and a time-varying fault matrix $\hat{f}(t)$. The time-varying nature of the fault is the reason why this FE observer is referred to as an adaptive observer. Eq. (5-4) means that, in this

observer, the FE design makes use of a fixed stable matrix *M* and the fault dynamics are taken into account. Due to the derivative of the output error, the dynamics of the fault are considered using the matrix *R*. The choice of matrices *M* and *R* work together to introduce the full dynamics of the fault, which is the special purpose of this FE approach.

5.2.3 AFE design for linear systems

The state $e_x(t)$ and fault $e_f(t)$ estimation errors are defined as follows:

$$e_x(t) = \hat{x}(t) - x(t), \;\; e_f(t) = \hat{f}(t) - f(t) \tag{5-6}$$

Using (5-6) and equations (5-1) to (5-5), it then follows that the appropriate dynamical system representration of the augmented observer is given (in terms of the estimation errors) as follows:

$$\dot{e}_x(t) = (A + LC)e_x(t) + (E + LD)e_f(t) \tag{5-7}$$

$$\begin{aligned}(I - RD)\dot{e}_f(t) = {} & [NC - RC(A + LC)]e_x(t) \\ & + [ND + RC(E + LD)]e_f(t) - \dot{f}\end{aligned} \tag{5-8}$$

Hence in (5-7) and (5-8), e_x, e_f are states variables. It is then convenient to define:

$$\dot{\varphi} = \tilde{A}\varphi + \tilde{B}\dot{f} \tag{5-9}$$

where:

$$\varphi = \begin{bmatrix} e_x \\ e_f \end{bmatrix}$$

$$\tilde{A} = \begin{bmatrix} A + LC & E + LC \\ (I - S)^{-1}[NC + SD^{+}C(A + LC)] & (I - S)^{-1}[ND + SD^{+}C(E + LD)] \end{bmatrix}$$

$$\tilde{B}_1 = \begin{bmatrix} 0 \\ -(I - S)^{-1} \end{bmatrix}$$

$$S = RD$$

D^{+} is the left-inverse of D. Then the augmented estimation system (sates and faults) can be designed through appropriate computation of matrices L, N, S to satisfy stability, i.e.

with $\widetilde{A}$ a Hurwitz matrix (negative real part eigenvalues). The following assumptions provide two solutions for the design of L, N, S.

Assumption 5-1 (Jiang & Staroswiecki, 2002):

There exists a pair of positive definite symmetric matrices *P, Q*, such that the following Lyapunov matrix inequality holds:

$$(A - ED^{+}C)^{T}P + P(A - ED^{+}C) + 2C^{T}DD^{+}C \leq -Q \qquad (5\text{-}10)$$

Remark 5-2:

This assumption comes from the stability of $\tilde{A}$ according to Lyapunov inequality. The aim of the *Algorithm 5-1* and *Algorithm 5-2* is to achieve the estimation of both the faults and states; the matrices L, N, S should satisfy the condition that $\tilde{A}$ is stable. L, N, S will be designed through the proposed two algorithms in the following context. In both of the algorithms the *Assumption 5-1* should be true.

The *Assumption 5-1* can be applied in real systems, such as the induction motor electrical system described in this thesis. In this case, if the matrix $(A - ED^{+}C)$ is stable, for a given $Q > 0$, then there is a symmetric and positive definite solution P to (5-10) according to Lyapunov theory. That means, for any values of parameters in (5-1) and (5-2), if the above assumption is satisfied and the form of the system is able to fit in the system given at the beginning of this Section, then the adaptive estimation approach is applicable.

Algorithm 5-1 (Jiang & Staroswiecki, 2002):

When the matrices L, N, S are suitably chosen, under the Assumption 5-1, the system matrix $\tilde{A}$ can be asymptotically stable. Then the following matrices can be given as:

$$L = (P^{-1}C^{T}D - E)D^{+}$$

$$N = -GD^{T} - \epsilon G[D^{+}C(A + LC)]C^{-}$$

$$S = \epsilon I_{q}$$

where C^- is the right-inverse of the matrix *C*, D^+ is the left-inverse of the matrix *D*, and ϵ is a constant such that:

$$\epsilon[D^+C(E - AC^-D)] < D^TD, \epsilon \neq 0, \epsilon \neq 1 \quad (5\text{-}11)$$

Algorithm 5-2 (Jiang & Staroswiecki, 2002):

Under Assumption 5-1, when the matrices L, N, S are chosen to make the system matrix $\tilde{A}$ asymptotically stable, then the following solutions exist:

$$L = (P^{-1}C^TD - E)D^+$$

$$N = -GD^T$$

$$S = 0$$

where $G = G^T > 0$ is a weighting matrix.

Remark 5-3:

In Algorithm 5-1, in which the fault dynamics is kept when a non-zero parameter ϵ is considered. In Algorithm 5-2, the special condition of $S = 0$ means that the fault dynamics are not represented. However, in these circumstances the FE will be very appropriate if the faults are assumed constant.

Remark 5-4:

Different from the design given by Algorithm 5-2, Algorithm 5-1 enlarged the degree of freedom when designing the parameter ϵ which is calculated through (5-11). Through the design, fault dynamics can be estimated.

5.2.4 Improved AFE design using a LMI-based approach

In this Section the Bounded Real Lemma (BRL) for continuous-time systems is introduced, as shown in *Lemma 5-1*. This Lemma helps to transform the H_∞ suboptimal constraints into a matrix inequality. Then this Section is divided into the following Steps:

Step 1: Transfer function generation

In order to consider the LTI system:

$$\begin{aligned} \dot{x}(t) &= Ax(t) + N_1 w(t) \\ z(t) &= Cx(t) + N_2 w(t) \end{aligned} \tag{5-12}$$

where $x(t)\,\epsilon\,R^n$ are state variables of the system, and $w(t)\,\epsilon\,R^q$ are external disturbances input and $z(t)\,\epsilon\,R^n$ are the measured outputs.

Considering the Laplace transform of (5-12), it is easy to get

$$\begin{aligned} \mathrm{X}(s) &= (sI - A)^{-1} N_1 W(s) \\ Z(s) &= C\mathrm{X}(s) + N_2 W(s) \end{aligned} \tag{5-13}$$

Put $C\mathrm{X}(s)$ in to the second equation of (5-13), then the following equation can be deduced:

$$T(s) := \frac{Z(s)}{W(s)} = N_2 + C(sI - A)^{-1} N_1 \tag{5-14}$$

Step 2: Analysis of BRL

The control or estimation problem of the LTI system is transformed into an optimal problem of (5-14), only through the optimization of the disturbance with regard to the measured output can be minimized. The BRL is introduced as follows:

Lemma 5-1 (Apkarian & Gahinet, 1995):

Consider a continuous-time transfer function $T(s)$ (not necessarily minimal) of realization $T(s) = N_2 + C(sI - A)^{-1} N_1$. The following statements are equivalent:

- **a)** $\|N_2 + C(sI - A)^{-1} N_1\|_\infty < \gamma$ and A is stable in the continuous-time sense $(Re(\lambda_i(A)) < 0)$;
- **b)** there exists a symmetric positive definite solution P to the LMI:

$$\begin{pmatrix} A^T P + PA & PN_1 & C^T \\ {N_1}^T P & -\gamma I & {N_2}^T \\ C & N_2 & -\gamma I \end{pmatrix} < 0 \qquad (5\text{-}15)$$

The (a) and (b) statements of BRL are equivalent and this has been proved in (Gahinet & Apkarian, 1994).

Remark 5-5:

As pointed out in the proof of the sufficiency and necessarity (Gahinet & Apkarian, 1994; Apkarian & Gahinet, 1995), one important property of this approach should be pointed out: The system of (5-12) is of a Linear Fractional Transformational form as shown in Section 6.2.3 when the system is seen as a vertice of the LFT form of an LPV system. Accordingly, this approach is directly applied on the LFT dependent system to generate a *Controller* or *Observer*.

Consider the system (5-12), with transfer function $T(s) = N_2 + C(sI - A)^{-1}N_1$. The H_∞ norm of $T(s)$ is defined as

$$\|T(s)\|_\infty = sup_\omega \sigma_{max}(T(j\omega))$$

This is the peak of the maximum singular value of the system frequency response.

According to *Lemma 5-1*, when $\|T(s)\|_\infty < \gamma$, the system is asymptotically stable if and only if there exists a symmetrical positive definite matrix *P*.

Then through solving the following optimal problem:

$$min\,\gamma$$

$$\begin{bmatrix} A^T P + PA & PN_1 & C^T \\ P^T X & -\gamma I & {N_2}^T \\ C & N_2 & -\gamma I \end{bmatrix} < 0 \qquad (5\text{-}16)$$

$$P > 0$$

The solution of the optimal performance analysis problem of the system can be obtained. The optimal value of the problem (5-14) is therefore the optimal H_∞ performance of the system (5-12).

The above optimal problem shown in (5-16) can be understood as follows. ***Convexity*** of the solvability condition (5-16) is synthesis feasibility of these constraints, it is concluded as LMIs problem in the work of (Apkarian & Gahinet, 1995; Apkarian et al., 1995). The reserch in this Section is so called "Scaled H_∞ control" problem, it can be used to identify the design matrix without loss of generality. This theory study solved the control or observation problem of the system using the LMI-based solvability condition. This approach can be extended into "gain-scheduled H_∞ control " which is similar to the work in Chapter 6.

Since this problem is a convex optimization problem with linear matrix inequality constraints and linear objective functions, it can be solved using the mincx solver in the LMI toolbox of Matlab.

Remark 5-6:

By using the improved AFE approach, Assumption 5-1 has been removed. There is more freedom to design the matrices *P*, *Q* and the fault dynamics are retained. Also, the FE observer is designed under the guarantee of H_∞ robust performance. Therefore, the FE effect, stability and robust performance are guaranteed.

Step 3: Application to error system (5-9)

Considering Eq. (5-9), and the output equation can be formulated as $z = \tilde{C}\varphi = e_f$ when $\tilde{C} = [0 \quad I]$ with appropriate dimensions.

$$\begin{aligned} \dot{\varphi} &= \tilde{A}\varphi + \tilde{B}\dot{f} \\ z &= \tilde{C}\varphi \end{aligned} \tag{5-17}$$

Consider the system transformation and Lemma BRL, the LMI can be formulated as

$$\begin{bmatrix} \tilde{A}^T\tilde{P} + \tilde{P}\tilde{A} & \tilde{P}\tilde{B} & \tilde{C}^T \\ \tilde{B}^T\tilde{P} & -\gamma I & 0 \\ \tilde{C} & 0 & -\gamma I \end{bmatrix} < 0$$

where $\tilde{P}$ is symmetric positive definite matrix.

The FE proplem is turned into a stability problem with minimization of the effect of fault derivative.

5.2.5 Simulation study

The AFE and the improved AFE strategies in Section 5.2.3 and Section 5.2.4 are simulated and tested on the electrical system of the induction motor presented in Eq. 2-12.

Figure 5-2 and Figure 5-3 shows the Matlab/Simulink structure for the simulation. For both of the figures, the simulation structure is formed by (1) the linear system and (2) the observation system. The fault scenarios is controlled manually by a switching component, which is shown at the top of each figure. The noise, uncertain parameters and the baseline feedback control signals are applied on the system through a gain matrix, which are shown as different gain values in the Simulink. These parameters is the inputs of the system, and the output includes the system outputs and the observer outputs. The system output is applied as an input for observer, while the observation outputs is what we desire- the fault estimation results. In each of the simulation figure, the estimation results are compared with the reference signals.

Table 5-1 shows the realization of the improved adaptive fault estimation approach, which involves the convexity problem solvability. Therefore, it is concluded as a LMI problem and it is solved using the coding regulations of LMI tools (included in the Matlab platform).

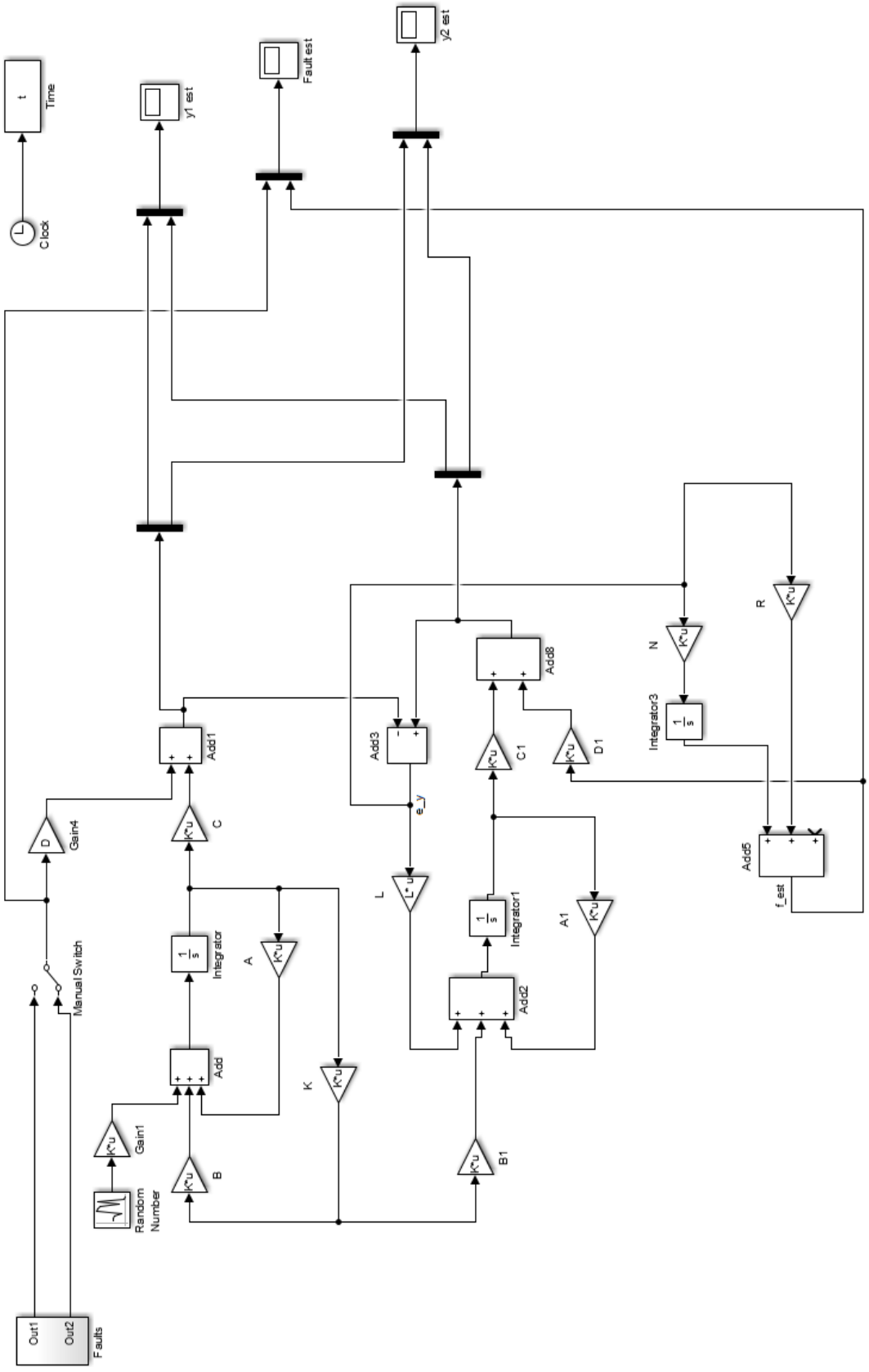

Figure 5-2 Matlab/Simulink structure for Algorithm 5-1 & Algorithm 5-2

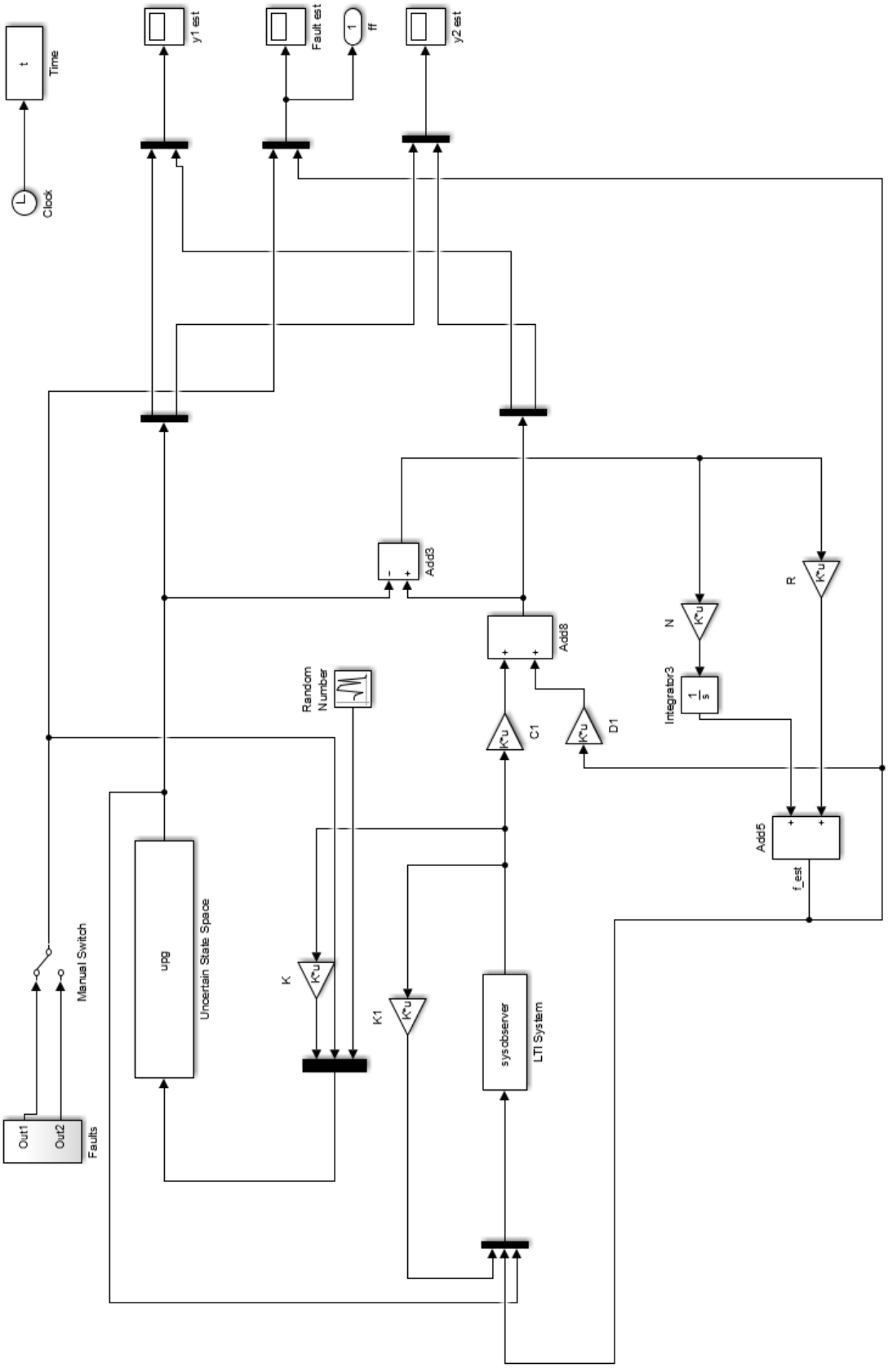

Figure 5-3 Matlab/Simulink structure for improved AFE

Table 5-1 Code for improved AFE observer

```
function [vecobserver,R,N] = getobserver(A,B,C,D)

E=[0.1;0.1;0;0];

R = [0 1]; % Assume R*D=0

setlmis([]);

Y = lmivar(2,[4 2]);
P = lmivar(1,[4 1]);
Z = lmivar(2,[1 2]);

%pos (1,1)
lmiterm([1 1 1 Y],1,C,'s');
lmiterm([1 1 1 P],1,A,'s');
% lmiterm([1 1 1 P],1,A);
% lmiterm([1 1 1 P],A',1);
% lmiterm([1 1 1 Y],1,C);
% lmiterm([1 1 1 -Y],C',1);

%pos (1,2)
lmiterm([1 1 2 P],1,E);
lmiterm([1 1 2 Y],1,D);
lmiterm([1 1 2 -Z],C',1);

%pos (2,2)
% lmiterm([1 2 2 Z],1,D);
% lmiterm([1 2 2 -Z],D',1);
lmiterm([1 2 2 Z],1,D,'s');

%pos (2,3)
lmiterm([1 2 3 0],1);

%pos (2,4)
lmiterm([1 2 4 0],1);

%pos (3,3)
lmiterm([1 3 3 0],-1); % gama is chosen to be 1 here.

%pos (4,4)
lmiterm([1 4 4 0],-1); % gama is chosen to be 1 here.

% lmiterm([-2 1 1 P],1,1); % P>I
% lmiterm([2 1 1 0],1);

lmiterm([-2 1 1 P],1,1); % P>0
% lmiterm([2 1 1 0],0);

lmis = getlmis;
[tmin,feas] = feasp(lmis);

Y = dec2mat(lmis,feas,Y);
P = dec2mat(lmis,feas,P);
```

```
Z = dec2mat(lmis,feas,Z);

L = inv(P)*Y;
N = Z; % Q*N = Z, assume Q = I

% [K,S1,e1] = lqr(A,B,eye(4),eye(2));

%====Create observer system====================

vecobserver = ss(A+L*C,[B E+L*D -L],eye(4),zeros(4,5));
```

The nominal parameters (See Table 2-1) of the induction motor electrical system are chosen as follows: $\omega_r = 500$ rpm, $R_s = 10\ \Omega, L_s = 0.38\ H, R_r = 3.5\ \Omega, L_r = 0.3\ H, n_p = 2, M = 0.3$ H. By calculation, it is easy to obtain the system matrices as follows:

$$A = \begin{bmatrix} -11.7 & -1000 & 3.5 & 0 \\ 1000 & -11.7 & 0 & 3.5 \\ 291.7 & 25000 & -168.3 & 0 \\ -25000 & 291.7 & 0 & -168.3 \end{bmatrix},$$

$$B = \begin{bmatrix} 0 & 0 \\ 0 & 0 \\ 12.5 & 0 \\ 0 & 12.5 \end{bmatrix},$$

$$C = \begin{bmatrix} 0 & 0 & 1 & 0 \\ 0 & 0 & 0 & 1 \end{bmatrix},$$

$$D = \begin{bmatrix} 1 \\ 0 \end{bmatrix},$$

$$E = 0.$$

In this simulation, it is assumed that the sensor faults occur in the induction motor stator current measure $i_{s\alpha}$. Two types of sensor faults are considered as follows:

$$f_1(t) = \begin{cases} 0, & 0 \le \mathrm{t} < 5\ (\mathrm{sec}) \\ 0.4, & 5 \le \mathrm{t} < 15\ (\mathrm{sec}) \\ 0.8, & 15 \le \mathrm{t} < 30\ (\mathrm{sec}) \\ 1.2, & 30 \le \mathrm{t} < 45\ (\mathrm{sec}) \\ 0.2, & 45 \le \mathrm{t} < 50\ (\mathrm{sec}) \end{cases}$$

$$f_2(t) = \begin{cases} 0, & 0 \le \mathrm{t} < 10\ (\mathrm{sec}) \\ sin(t), & 10 \le \mathrm{t} \le 50\ (\mathrm{sec}) \end{cases}$$

It is easy to check that Assumption 5-1 is satisfied for this model, so the two adaptive observer methods proposed in Section 5.2.3 is applicable. According to Remark 5-4, the Algorithm 5-2 keeps the fault dynamics compared with Algorithm 5-1 theoretically, so simulation results of Algorithm 5-2 and the Improved AFE method are given.

For the simulation of Algorithm 5-2,

$$P = \begin{bmatrix} 17.743 & 0.631 & 0.458 & 0.022 \\ 0.631 & 10.235 & 0.028 & 0.158 \\ 0.458 & 0.028 & 0.018 & 5.247\mathrm{e}-04 \\ 0.022 & 0.158 & 5.247\mathrm{e}-04 & 0.006 \end{bmatrix}$$

$$L = \begin{bmatrix} -3.9318 & 0 \\ -0.3209 & 0 \\ 152.150 & 0 \\ 9.361 & 0 \end{bmatrix}$$

$$N = [-3.385 \quad 0]$$

$$S = 0.02$$

For the simulation of the Improved AFE method,

$$P = \begin{bmatrix} 154.709 & 11.511 & 4.499 & 0.442 \\ 11.511 & 75.366 & 0.479 & 1.326 \\ 4.499 & 0.479 & 0.182 & 0.011 \\ 0.442 & 1.326 & 0.011 & 74.566 \end{bmatrix}$$

$$L = \begin{bmatrix} 4.166 & 4.302\mathrm{e}+04 \\ 0.274 & -93.205 \\ -143.940 & -1.065\mathrm{e}+06 \\ 0.008 & 64.806 \end{bmatrix}$$

$$N = [-23.161 \quad -1.283]$$

$$S = 0.02$$

The simulation results are described within Section 5.4 in order to make comparison between the three different fault estimation approaches.

5.3 FE using sliding mode observer

The estimation (reconstruction) of actuator or sensor fault using SMO is provided in the work of (Edwards et al., 2000), where the concept of the "output injection signal" is proposed to estimate (reconstruct) faults. This *output injection signal* is produced when the discontinuous switching function is selected and output errors are forced into the sliding mode manifold. This work was further developed by (Tan & Edwards, 2002) who considered the case of multiplicative faults. The work on robust estimation/reconstruction of sensor faults, actuator faults and multiplicative faults was developed further by (Tan & Edwards, 2003; Edwards & Tan, 2006). In this Section, the Edwards & Spurgeon SMO is applied to the 4^{th} order system of the induction motor described in Section 5.4. This Chapter consideres the FE of actuator faults, sensor faults and component faults corresponding to the IM system.

5.3.1 SMO preliminaries

Based on the *Utkin Observer* (Drakunov & Utkin, 1995) and *Walcott-Żak observer* (Walcott & Zak, 1987; Walcott & Zak, 1988), in (Edwards et al., 2000) a sliding mode observer had been designed for fault detection. The concept of "equivalent output injection" was constructed to reconstruct fault signals. This method considered two kinds of faults: actuator faults and sensor faults.

Considering that the additive faults were widely studied in the area of FDI, the paper (Tan & Edwards, 2004) considered component failures in a system, that are described as multiplicative faults. This paper applied the concept of *equivalent output error injection* in sliding mode control (SMC). It provides control effort by designing a discontinuous function.

The SMO cannot be used to estimate unmatched faults; however, its natural robustness against uncertainty within the matched channel gives inspiration of SMO design for typical faults, i.e. sensor fault, actuator fault and multiplicative fault. The necessity and sufficiency proof of robustness against matched uncertainty is introduced in (Edwards & Spurgeon, 1994; Edwards & Spurgeon, 1998). Therefore, the fault reconstruction that is

closely related to the equivalent injection signal is not affected by the matched parameter variations.

In this Section, the Edwards & Spurgeon observer is applied to the induction motor system.

5.3.2 Edwards & Spurgeon SMO design

Consider the general expression of a linear system with a class of matched uncertainty/fault described by:

$$\dot{x}(t) = Ax(t) + Bu(t) + D\xi(t, x, u)$$
$$y(t) = Cx(t) \tag{5-18}$$

where $A \epsilon R^{n\times n}, B \epsilon R^{n\times m}, C \epsilon R^{p\times n}$ and $D \epsilon R^{n\times q}$ where $p \geq q$.

Considering the following assumptions 5-2 which are used to guarantee that the system (5-18) can be transformed into a canonical form in which the SMO is applicable. This was first proposed in the Utkin Observer design and later was utilised in (Edwards & Spurgeon, 1994) to a more general case in which dynamic system uncertainty was considered.

Assumption 5-2:

1) The pair (A, C) is observable;
2) The matrices B, C, D are of full rank;
3) The function $\xi: R_+ \times R^n \times R^m \rightarrow R^q$ is assumed to have bounded unknown parameter so that:

$$\|\xi(t, x, u)\| \leq r_1\|u\| + \alpha(t, y) \tag{5-19}$$

where: r_1 is a known scalar and $\alpha: R_+ \times R^p \rightarrow R_+$ is a known function. It is a boundary for matched uncertainty or fault.

4) $rank(CD) = rank(D) = q$ and the zeros of the system model given by the triple (A, D, C) are in the left-hand complex plane, that is:

$$\begin{bmatrix} sI - A & D \\ C & 0 \end{bmatrix} = n + q \tag{5-20}$$

For all *s* such that $R(s) \geq 0$. The conditions of (2) and (3) in *Assumption 5-2* guarantees the existence of bounded matched fault/uncertainty. The condition (1) of *Assumption 5-2* acts as a necessary condition of an observer for the dynamic system. The condition (4) of *Assumption 5-2* ensures the existence of a canonical form of the dynamic system (which is described in the following *Step 1*, and guarantees an observer with sufficient robustness against matched uncertainty or FE against matched faults.

Step 1: Canonical form formulation

In the first step, there is a linear transform of the observer form, from the nominal form into canonical form:$x \mapsto T_0 x$, the relevant matrix becomes:

$$T_0 = \begin{bmatrix} N_0^T \\ C \end{bmatrix}, CT_0^{-1} = [0 \quad I_p] \tag{5-21}$$

where $N_0^T \in R^{n\times(m-p)}$ represent the null space of C.

Therefore through the following transformation:

$$T_0 A T_0^{-1} = \begin{bmatrix} A_{11} & A_{12} \\ A_{21} & A_{22} \end{bmatrix} \ and \ T_0 B = \begin{bmatrix} B_1 \\ B_2 \end{bmatrix} \tag{5-22}$$

The system state is decomposed into two components, expressed using $x_1(t)$ and $x_2(t)$. The system is then represented as in (5-23), which is in the space of (x_1, y).

Therefore, the new coordinate system can be written as:

$$\begin{aligned} \dot{x}_1(t) &= A_{11}x_1(t) + A_{12}y(t) + B_1 u(t) \\ \dot{y}(t) &= A_{21}x_1(t) + A_{22}y(t) + B_2 u(t) + D_2\xi(t, x, u) \\ y(t) &= x_2(t) \end{aligned} \tag{5-23}$$

where $x_1 \epsilon R^{n-p}, B \epsilon R^p$ and the matrix A_{11} has stable eigenvalues. (Edwards and Spurgeon, 1998).

Remark 5-7:

Through this transformation, the effect of the matched uncertainty/fault $\xi(t,x,u)$ in Eq. (5-15) is transformed into the output channel as shown in Eq. (5-23). This is convenient for the next action, i.e. the switching function design within (5-24) appears in the same channel as matched uncertainty/fault of the dynamic system (5-23). The effect of matched fault/uncertainty is removed within SMO design. A good transformation means the system order is reduced. The switching function is designed to tackle matched uncertainty/faults in the process of reaching sliding motion, while the linear approach can be used on unmatched fault/uncertainty in the process of maintaining sliding motion.

The transformation of Eq. (5-21) and (5-22) originally comes from the work of Utkin Observer, in which the dynamic system is expressed into a system with state variable (x_1, y). Then, the Walcott-Żak observer considered the condition of matched uncertainty $f(t,x,u) = D\xi(t,x,u)$ and developed observer generation algorithm based Walcott-Żak observer pair. Based on this work, Edwards, Spurgeon and Patton proposed a further synthesis approach of a discontinuous observer. The SMO is designed to estimate matched faults if and only if the dynamic system satisfies Assumption 5-2 (4), and the proof of this property can be found in (Edwards & Spurgeon, 1994; Edwards & Spurgeon, 1998).

Step 2: SMO formulation

Consider an observer of the form:

$$\begin{aligned} \dot{\hat{x}}_1(t) &= A_{11}\hat{x}_1(t) + A_{12}\hat{y}(t) + B_1 u(t) - A_{12}e_y(t) \\ \dot{\hat{y}}(t) &= A_{21}\hat{x}_1(t) + A_{22}\hat{y}(t) + B_2 u(t) - (A_{22} - A_{22}^s)e_y(t) + v \end{aligned} \tag{5-24}$$

where A_{22}^s is a stable design matrix and $e_y = \hat{y}(t) - y(t)$. The switching part of observer v is designed as:

$$v = \begin{cases} -\rho(t,y,u)\|D_2\| \dfrac{P_2 e_y}{\|P_2 e_y\|} & \text{if } e_y \neq 0 \\ 0 & \text{otherwise} \end{cases} \tag{5-25}$$

where P_2 is a symmetric positive definite matrix.

The scalar function $\rho(t, y, u)$, like the one given in the original formulation of the Walcott-Żak observer (Walcott & Zak, 1988), should be chosen so that it is larger than the upper bound of the fault:

$$\rho(t, y, u) \geq \alpha(y, u, t) + \gamma_0 \tag{5-26}$$

where γ_0 is a positive scalar.

The above equation (5-23) reduces the order of the problem. If the state estimation error $e_1 = \hat{x}_1 - x_1$, the error system can be written as:

$$\begin{aligned} \dot{e}_1(t) &= A_{11} e_1(t) \\ \dot{e}_y(t) &= A_{21} e_1(t) + A_{22}^s e_y(t) + v - D_2 \xi \end{aligned} \tag{5-27}$$

Consider the Lyapunov function of

$$V(e_1, e_y) = e_1^T P_1 e_1 + e_y^T P_2 e_y \tag{5-28}$$

and the following Lyapunov equation

$$A_{22}^{s\,T} P_2 + P_2 A_{22}^s = -Q \tag{5-29}$$

where A_{22}^s is seen as intermediate variables since it does not affect the estimation result, that is, it doesn't appear at the output injection signal.

The error system written within (5-27) can be proved to be quadratically stable. The proof process can be found in (Edwards & Spurgeon, 1994; Edwards & Spurgeon, 1998).

Consider the hyperplane given as

$$\mathcal{S}_0 = \{e \in R^n : Ce = 0\} \tag{5-30}$$

and the Lyapunov function

$$V(e_y) = e_y^T P_2 e_y \tag{5-31}$$

It is proved that the output error e_y convergence to zero in finite time and the sliding motion takes place on $\mathcal{S}_0$ in finite time.

Hence, the Edwards and Spurgeon observer structure is summarized as:

$$\dot{\hat{x}}(t) = A\hat{x}(t) + Bu(t) - G_l Ce(t) + G_n v \tag{5-32}$$

where the linear gain is:

$$G_l = T_0^{-1}\begin{bmatrix} A_{12} \\ A_{22} - A_{22}^s \end{bmatrix} \tag{5-33}$$

and the switching nonlinear gain is:

$$G_n = \|G_2\| T_0^{-1}\begin{bmatrix} 0 \\ I_p \end{bmatrix} \tag{5-34}$$

With

$$v = \begin{cases} -\rho(t,y,u)\dfrac{P_2 Ce}{\|P_2 Ce\|} & if\ Ce \neq 0 \\ 0 & otherwise \end{cases} \tag{5-35}$$

Remark 5-8:

In the observer design in Eq. (5-32), v is discontinuous about the hyperplane in Eq. (5-30). G_l , $G_n \in R^{n\times p}$ are appropriate matrix which are produced in the process of forcing the sliding motion out to the hyperplane in the presence of matched uncertainty. Quadratic stability of the error system (5-27) using the SMO (5-32) is proved in (Edwards & Spurgeon, 1994; Edwards & Spurgeon, 1998).

In the following context, the reconstruction (estimation) of a matched actuator or sensor fault is introduced. Moreover, as a contribution to the approach, considering the the presence of component faults within the induction motor, the component fault reconstruction is introduced.

5.3.3 Fault reconstruction (estimation)

The SMO is an important approach for fault reconstruction/estimation based on the concept of the equivalent 'output error injection signals' proposed in (Edwards & Spurgeon, 1998; Edwards et al., 2000). Consider a nominal linear system with faults given by:

$$\begin{aligned} \dot{x}(t) &= Ax(t) + Bu(t) + Df_a(t) \\ y(t) &= Cx(t) + f_s(t) \end{aligned} \tag{5-36}$$

where: $A \in R^{n\times n}, B \in R^{n\times m}, C \in R^{p\times n}, D \in R^{n\times q}$ satisfying $n > p \geq q$. And the matrices *B, C* and *D* are full rank. $f_a(t)$ and $f_s(t)$ are the functions that represent actuator and sensor faults respectively. *Assumption 5-2* is applicable to this dynamic system with additive fault. However, it is assumed that only $y(t)$ and $u(t)$ are measurable, whereas the states of the system are unknown (only when $n = p$, all state variable will be known).

- **Actuator fault estimation**

In Section 5.3.2 a SMO is designed corresponding to a constructed sliding mode. Once a sliding motion is constructed, $e_y = 0$ and $\dot{e}_y = 0$. Subsequently, from (5-27) it follows that:

$$0 = A_{21}e_1(t) - D_2f_a(t) + v_{eq} \tag{5-37}$$

The equivalent output injection signal is introduced and expressed as v_{eq}. Equivalent output injection represents the behaviour and influence of discontinuous variables and represents the effort required to maintain the sliding mode (Drakunov & Utkin, 1992). From (5-26), and if A_{11} is stable, then it is obvious that $e_1(t) \to 0$ and so that it is shown:

$$v_{eq} \to D_2f_a(t) \tag{5-38}$$

As v_{eq} is a discontinuous signal, an appropriate approximation must be used in order to recover the equivalent output injection. The discontinuous component in (5-35) is replaced by the continuous approximation:

$$v_\delta = -\rho\|D_2\|\frac{P_2 e_y}{\|P_2 e_y\| + \delta} \tag{5-39}$$

where δ is a small positive scalar.

Considering Eq. (5-39), if δ is small enough then the equivalent output injection can be estimated as accurately as possible. Since $rank(D_2) = q$ then it is found from (5-38) that

$$f_a(t) \approx -\rho\|D_2\|(D_2^T D_2)^{-1} D_2^T \frac{P_2 e_y}{\|P_2 e_y\| + \delta} \tag{5-40}$$

The estimation of the actuator fault can be calculated online through the application of the output estimation error of e_y.

- **Sensor fault estimation**

Consider the case when $f_a(t) = 0$ but $f_s(t) \neq 0$. Since the output of the system is represented by (5-36), it follows that:

$$y(t) = x_2(t) + f_s(t) \tag{5-41}$$

and therefore $e_y = e_2 - f_s$. The state estimation error in the observer is now given by:

$$\dot{e}_1(t) = A_{11} e_1(t) + A_{12} f_s(t) \tag{5-42}$$

$$\dot{e}_y(t) = A_{21} e_1(t) + A_{22}^s e_y(t) - \dot{f}_s(t) + A_{22} f_s(t) + v \tag{5-43}$$

The sliding mode can be reached with the existence of disturbance of $f_s(t)$ and $\dot{f}_s(t)$ if the nonlinear gain ρ is designed properly. Once a sliding motion can be reached and maintained considering (5-42) and (5-43), the following equation exists.

$$0 = A_{21} e_1 - \dot{f}_s(t) + A_{22} f_s(t) + v_{eq} \tag{5-44}$$

For a slow varying fault, it is appropriate that

$$v_{eq} \approx -(A_{22} - A_{21} A_{11}^{-1} A_{12}) f_s \tag{5-45}$$

- **Component fault estimation**

In order to use the FE approach in Section 5.3.3 on component fault estimation, the component fault is transformed into additive fault in this approach. A system with multiplicative faults is researched with FE approaches.

Here the transformation from multiplicative fault to additive fault will be introduced. Consider a system with multiplicative fault in the system matrix described as:

$$\dot{x}(t) = (A + \Delta A)x(t) + Bu(t) + E_a d_a(t) \quad (5\text{-}46)$$

$$y(t) = C(x) \quad (5\text{-}47)$$

And it can be rewritten in the actuator additive fault format:

$$\dot{x}(t) = Ax(t) + Bu(t) + E_a d_a(t) + F_m f_m(x,t) \quad (5\text{-}48)$$

$$y(t) = C(x) \quad (5\text{-}49)$$

where:

$$F_m f_m(x,t) = \Delta A x(t) \quad (5\text{-}50)$$

In general formulation, F_m is a matrix whose columns represent the fixed fault dimensions. $f_m(x,t)$ is the re-constructed faults. The transformation will be used to estimate the resistance fault scenario described in the Section 5.3.4.

The changes of system component parameters are presented as multiplicative component faults which are hard to estimate using observer based methods since the faults are expressed using the product of the system state variable and faults. Hence, an approach is used to transform the multiplicative fault into an additive fault format acting on the system states, which has been presented in Section 5.3.3. Following this transformation, it is straightforward to use SMO introduced in Section 5.3.3.

Remark 5-9:

In the research on component fault estimation, SMO is designed for induction motor FE. The existence of component fault/multiplicative fault within induction motor, i.e. resistance variation or state current bias, etc., inspired the idea of component fault FE.

Hence, the component fault FE is applied on the 4^{th} order electrical system as shown in Section 2.2.1.

5.3.4 Simulation study

When the above FE approach is used for FE of the component fault, both additive and multiplicative faults are considered. For the electrical system of the induction motor with resistance fault (which is seen as a component fault).

Figure 5-4 shows the simulation structure within Matlab/Simulink, it is composed of the system and the observer design. However, not all the equations can be expressed in the Simulink because fault estimation may be calculated using m file, it depends on the situation.

Table 5-2 shows the coding for the calculation for sensor fault which is used in the following scenario, combining with the use of main function and Simulink.

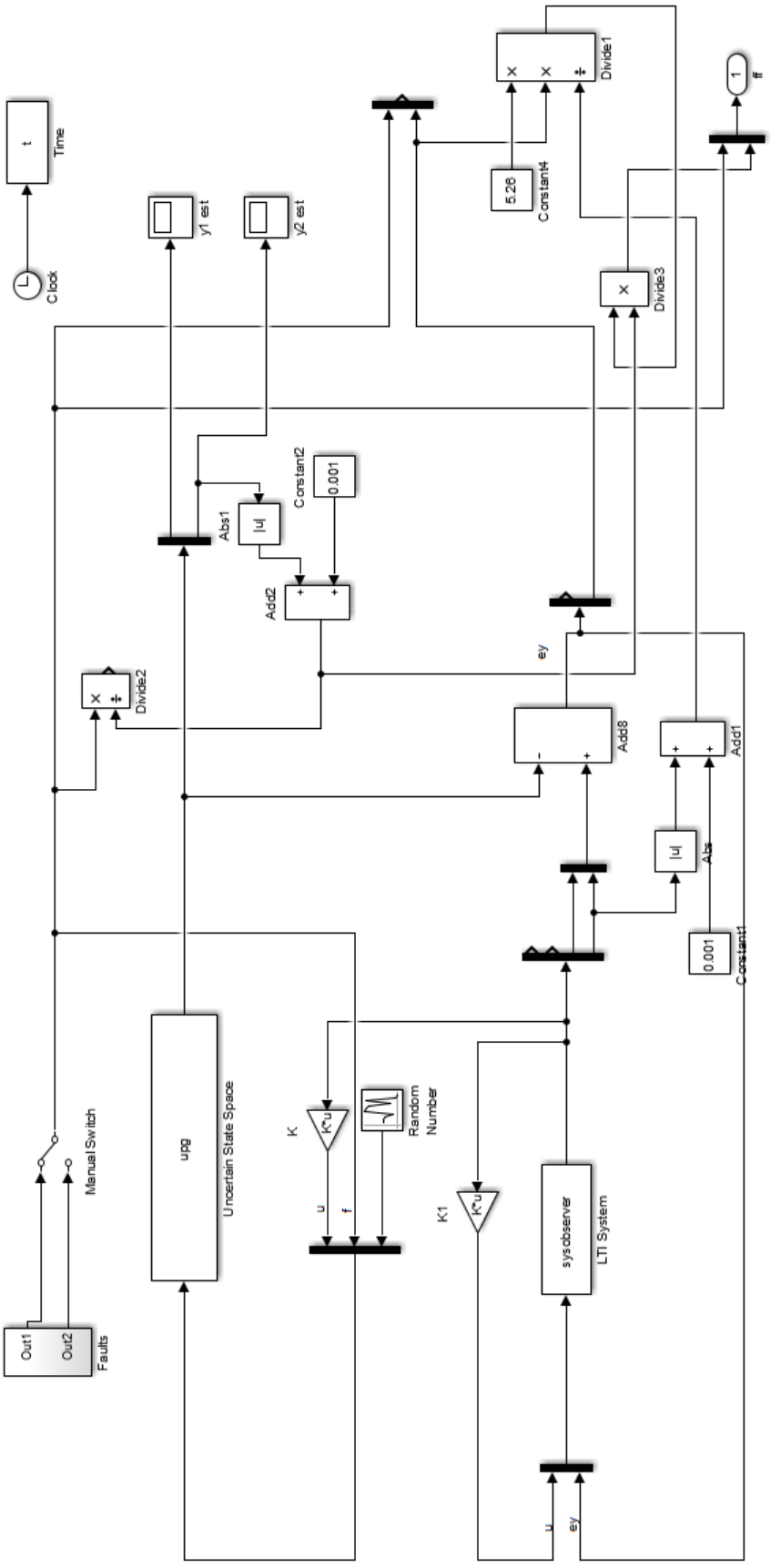

Figure 5-4 Matlab/Simulink structure for Sliding Mode Observer

Table 5-2 Code for Sliding Mode Observer

```
clear all
%%=====================================================
%% System description matrix
%%=====================================================
A=[-11.7 -1000 3.5 0;
    1000 -11.7 0 3.5;
    291.7 25000 -168.3 0;
    -25000 291.7 0 -168.3];
B=[0 0;0 0;12.5 0;0 12.5];
% B=[0 0 12.5 12.5];
C=[0 0 1 0;0 0 0 1];
D=[1;0];
% E=[0.1;0.1;0;0];
E=[0;0;0;0];

%%=====================================================
%% Create uncertain system
%%=====================================================
p1 = ureal('p1',1000,'Range',[900 1100]);
Ap=[-11.7 -1000 3.5 0;
    p1 -11.7 0 3.5;
    291.7 25000 -168.3 0;
    -25000 291.7 0 -168.3];
Bp=[0 0;0 0;12.5 0;0 12.5];
Df=[0.1;0.1;0;0];
upg = uss(Ap,[Bp E Df],C,[zeros(2,2) D zeros(2,1)]);

%%=====================================================
%% Baseline controller
%%=====================================================
[K,S1,e1] = lqr(A,B,eye(4),eye(2));

ff = [];  %% Initialization
gg = [];
hh = [];
hold on;

%%=====================================================
%% Call the observer function
%%=====================================================
sysobserver = getsmobserver(A,B);

%%=====================================================
%% Find the Simulink and start
%%=====================================================
uvars = ufind('fault_est_of_polytopic_uncertain_system');
uval = usample(uvars);

[t,x,y] = sim('fault_est_of_polytopic_uncertain_system');


%%=====================================================
%% SMO
%%=====================================================

function vecobserver = getsmobserver(A,B)
```

```
A22s = [-11 0; 0 -12];
P2 = lyap(A22s',eye(2));

A11 = [-11.7 -1000; 1000 -11.7];
A12 = [3.5 0; 0 3.5];
A21 = [291.7 25000; -25000 291.7];
A22 = [-168.3 0; 0 -168.3];
G1 = [A12; (A22 - A22s)];
G2 = G1 - [0 0;0 0;P2];

Ee = inv(A22 - A21*(inv(A11))*A12)*P2;

vecobserver = ss(A,[B -G2],eye(4),zeros(4,4));
```

In the component fault case (multiplicative fault) of a linear system where R is the fault to be estimated,

$$A+\Delta A=\begin{bmatrix} -\frac{R_r}{L_r} & -\omega_r & R_r & 0 \\ \omega_r & -\frac{R_r}{L_r} & 0 & R_r \\ \frac{R_r}{L_l L_r} & \frac{\omega_r}{L_l} & -\frac{R+f}{L_l} & 0 \\ -\frac{\omega_r}{L_l} & \frac{R_r}{L_l L_r} & 0 & -\frac{R+f}{L_l} \end{bmatrix}$$

Hence, ΔA is expressed as:

$$\Delta A=\begin{bmatrix} 0 & 0 & 0 & 0 \\ 0 & 0 & 0 & 0 \\ 0 & 0 & -\frac{f}{L_l} & 0 \\ 0 & 0 & 0 & -\frac{f}{L_l} \end{bmatrix}$$

According to the conclusion in Section 5.3.3, it is easy to obtain:

$$F_m f_m(x,t)=\Delta A x(t)=\begin{bmatrix} 0 & 0 & 0 & 0 \\ 0 & 0 & 0 & 0 \\ 0 & 0 & -\frac{f}{L_l} & 0 \\ 0 & 0 & 0 & -\frac{f}{L_l} \end{bmatrix}\begin{bmatrix} \emptyset_{r\alpha} \\ \emptyset_{r\beta} \\ I_{s\alpha} \\ I_{s\beta} \end{bmatrix}$$

$$= \begin{bmatrix} 0 & 0 & 0 & 0 \\ 0 & 0 & 0 & 0 \\ 0 & 0 & -\frac{1}{L_l} & 0 \\ 0 & 0 & 0 & -\frac{1}{L_l} \end{bmatrix} f \begin{bmatrix} \emptyset_{r\alpha} \\ \emptyset_{r\beta} \\ I_{s\alpha} \\ I_{s\beta} \end{bmatrix}$$

$$= \begin{bmatrix} 0 & 0 \\ 0 & 0 \\ -\frac{1}{L_l} & 0 \\ 0 & -\frac{1}{L_l} \end{bmatrix} f \begin{bmatrix} I_{s\alpha} \\ I_{s\beta} \end{bmatrix}$$

$$F_m = \begin{bmatrix} 0 & 0 \\ 0 & 0 \\ -\frac{1}{L_l} & 0 \\ 0 & -\frac{1}{L_l} \end{bmatrix}, f_m(x,t) = f \begin{bmatrix} I_{s\alpha} \\ I_{s\beta} \end{bmatrix}.$$

So far, the multiplicative fault in the system resistance is reorganized as an additive fault. It is noticed that $R(F_m) \subset R(B)$ that is, the unmatched multiplicative fault has been fitted into a matched condition. Then the fault $f \begin{bmatrix} I_{s\alpha} \\ I_{s\beta} \end{bmatrix}$ is estimated using the sliding mode observer, simultaneously $\begin{bmatrix} \hat{I}_{s\alpha} \\ \hat{I}_{s\beta} \end{bmatrix}$ is estimated. So it is easy to calculate the fault estimation $\hat{f}_m(x,t) = \hat{f} \begin{bmatrix} \hat{I}_{s\alpha} \\ \hat{I}_{s\beta} \end{bmatrix}$.

In Section 5.4.3, both constant and time-varying faults are considered for the multiplicative fault (component fault) estimation. The reference fault signal setting is changed and the fault type is also different. This is done in order to make the problem description more general. The magnitude of the faults are different as shown, in order to show the application of the approach under different fault shapes and different magnitudes.

Remark 5-10:

The robustness of SMO against matched uncertainty/fault is verified in this Section, the SMO for matched fault estimation is satisfactory.

5.4 Comparison of fault estimation performance using three approaches

5.4.1 Result of sensor fault estimation

In this Section, the comparison of fault estimation performance using three different approaches are illustrated in the following context. Figure 5-5 and Figure 5-8 are the results of Adaptive Observer; Figure 5-6 and Figure 5-9 are the results of Improved Adaptive Observer (Improved AFE); Figure 5-7 and Figure 5-10 are the results of Sliding Mode Observer (SMO). The general input of the system except for the control input are shown in the following table.

	Noise	Uncertainty	Fault
Adaptive Observer	√	×	√
Improved AFE	√	√	√
Sliding Mode Observer	√	√	√

Figure 5-5 and Figure 5-8 shows the results of simulation from Algorithm 5-2, which take into consideration of fault dynamics, which is not considered in the Algorithm 5-1. Figure 5-8 shows the estimation of the time-varying sensor fault. Figure 5-6 and Figure 5-9 reflect the performance of the estimation based on the Improved AFE using an LMI-based approach. This approach considers the synthesis feasibility of a convexity problem, it involves the comprehensive performance of the system under the consideration of estimation accuracy, robustness, etc. In the following figures, the Figure 5-6 and Figure 5-9 shows better estimation accuracy of the observation methods than that is shown in Figure 5-5 and Figure 5-8.

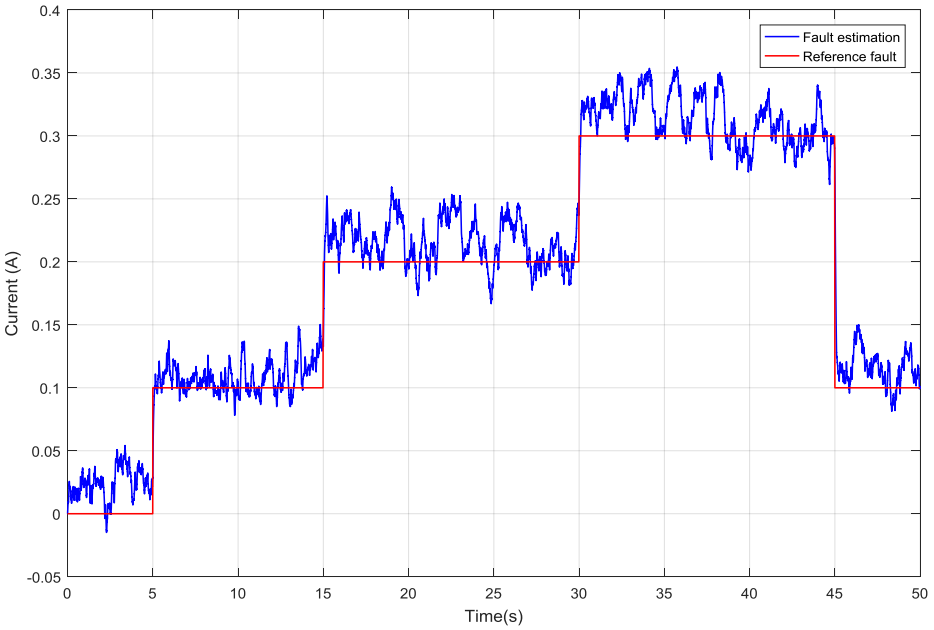

Figure 5-5 Fault estimation using Adaptive Observer

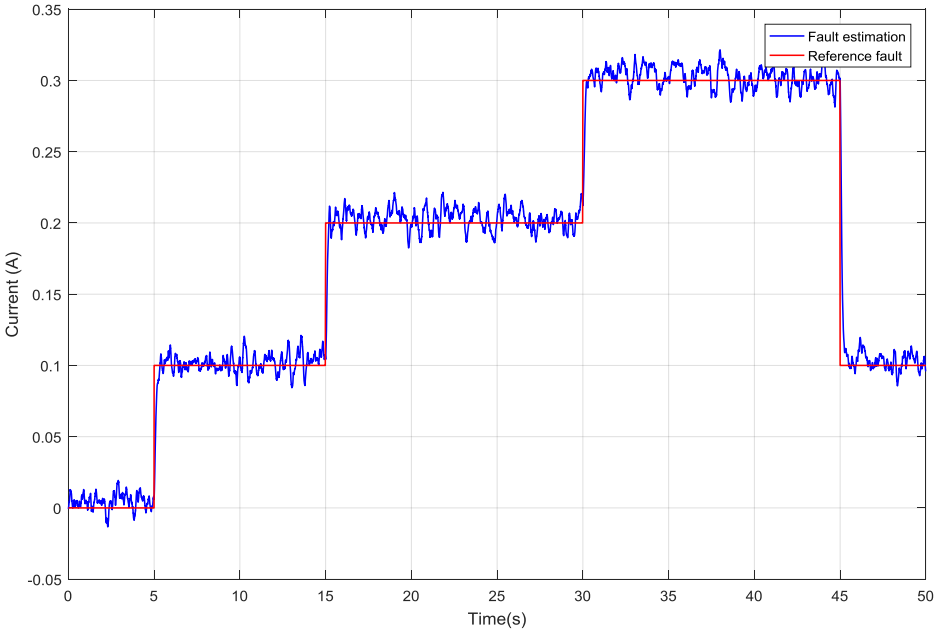

Figure 5-6 Fault estimation using Improved Adaptive Observer

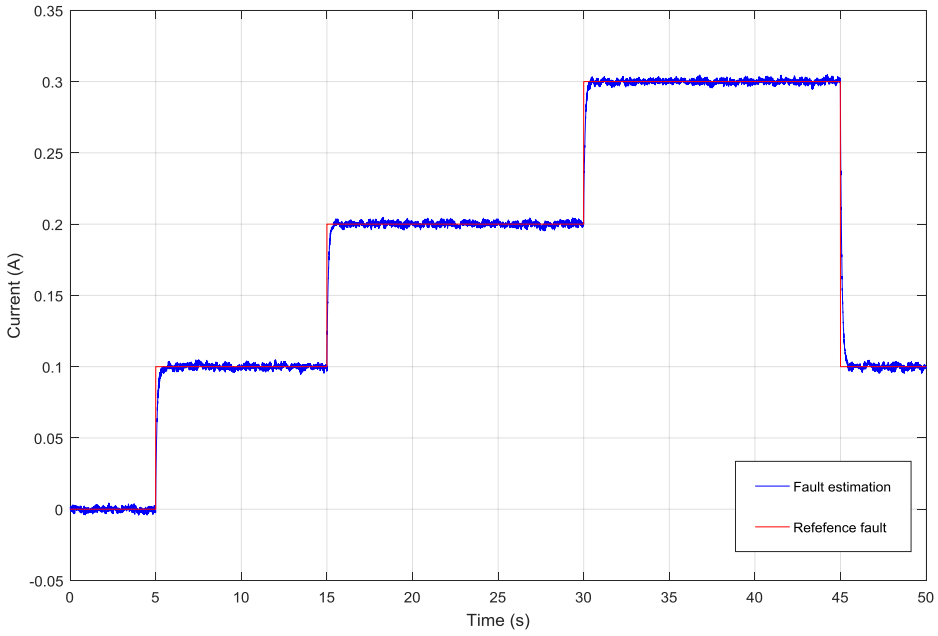

Figure 5-7 Fault estimation using SMO

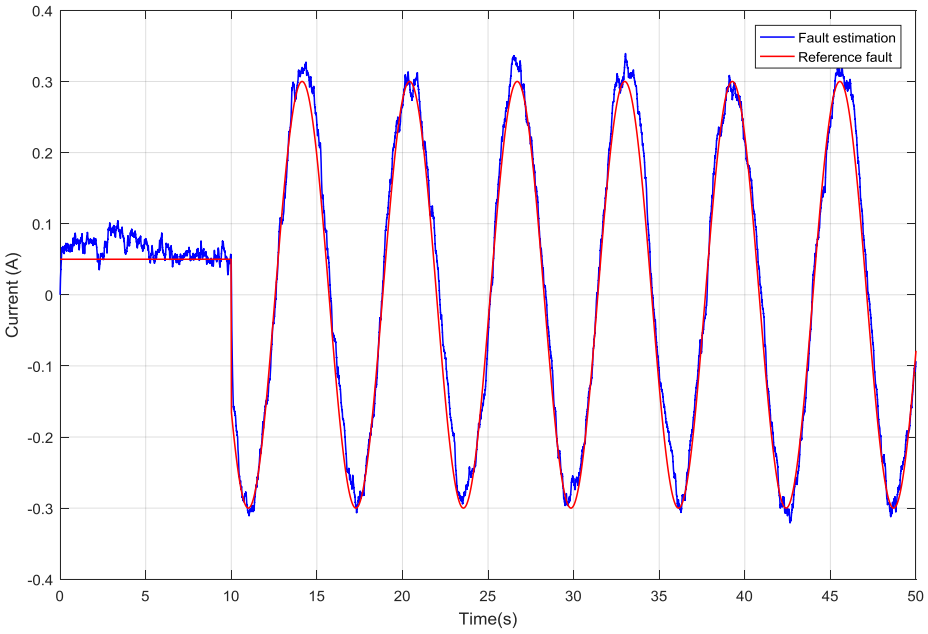

Figure 5-8 Fault estimation using Adaptive Observer

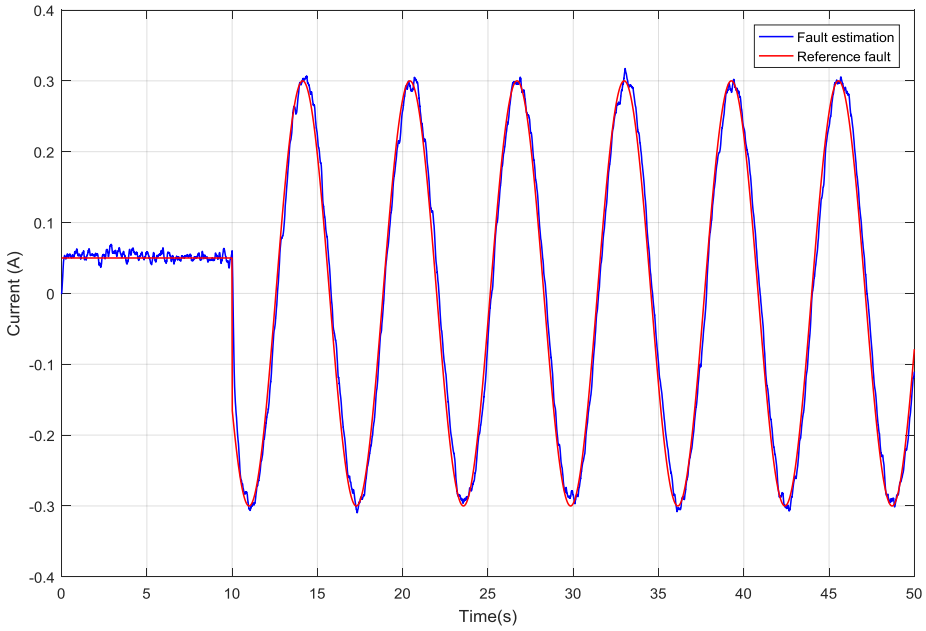

Figure 5-9 Fault estimation using Improved Adaptive Observer

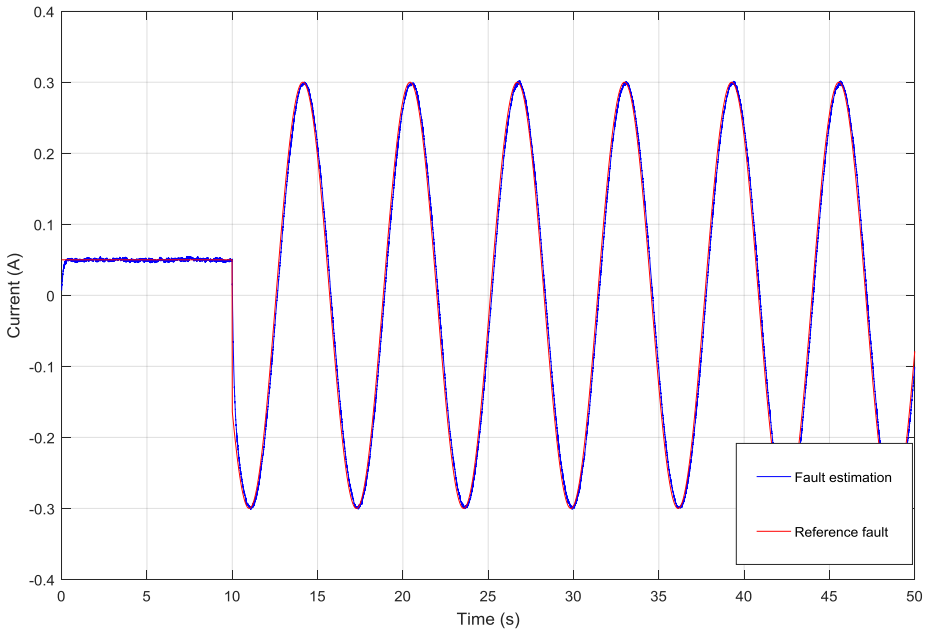

Figure 5-10 Fault estimation using SMO

5.4.2 Result of actuator fault estimation

Since we use the controlled voltage variation as the faulty signal, so the actuator fault is represented in sine wave considering the dynamic property of control signal. In this group of simulation results, the parameter setting is the same as in Section 5.4.1. Other types of faulty scenarios are not considered simutaneously. Figure 5-11, 5-12 and Figure 5-13 represent the fault estimation using Adaptive Observer, Improved Adaptive Observer, and Sliding Mode Observer respectively. Only in the Adaptive Observer, there exist obviously bias with the estimation signal. This is due to the separate design steps with this adaptive approach, i.e. the gain parameters of the observer are designed seperately, which caused the accumulation of faulty signals or bias. But this effect is solved through the robust design with both the improved adaptive observer and the SMO.

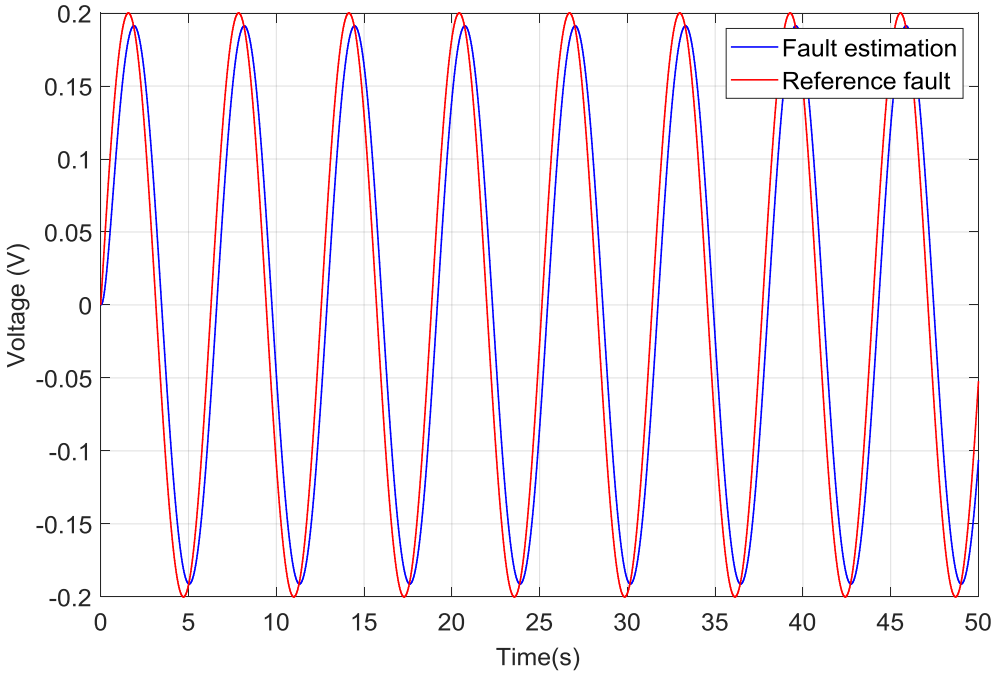

Figure 5-11 Fault estimation using Adaptive Observer

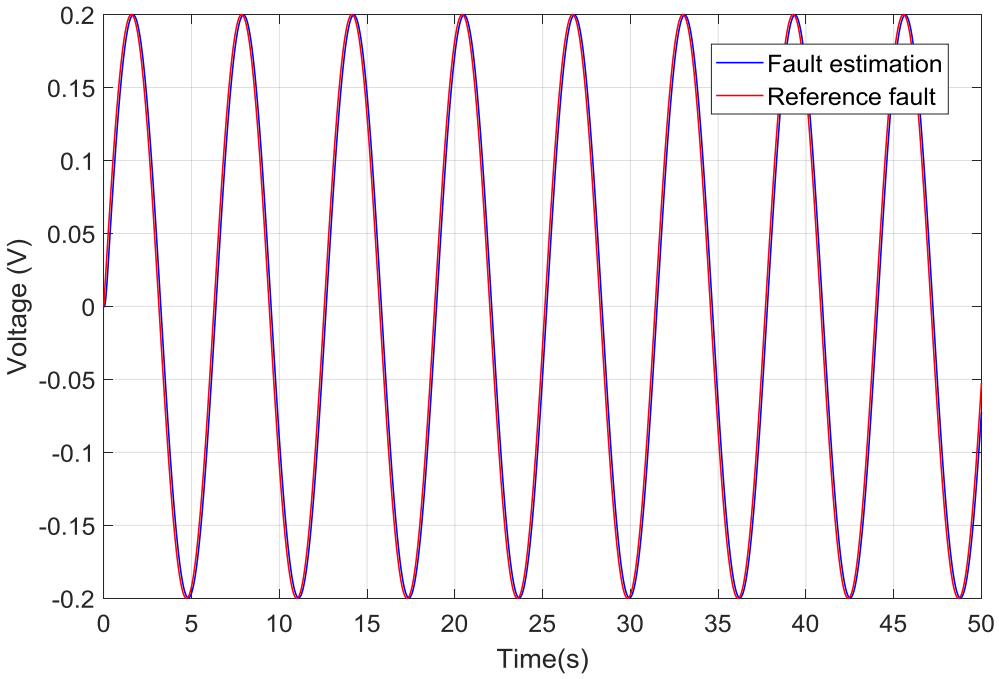

Figure 5-12 Fault estimation using Improved Adaptive Observer

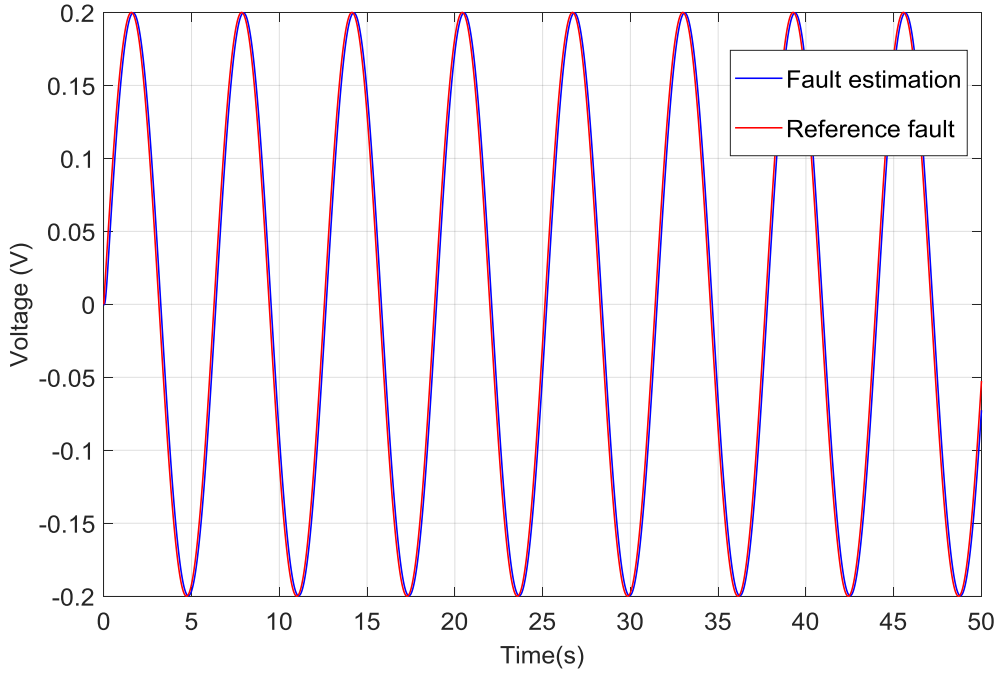

Figure 5-13 Fault estimation using SMO

5.4.3 Result of component fault estimation

Compared with the FE for a constant fault, the varying fault estimation shows a bias away from the reference fault signals. The larger the reference, the larger the bias appearing in the FE results, due to the existence of the discontinuous component of SMO.

However, both of the FE results for the constant and time-varying faults show the robustness of the SMO. This illustrates the capability of this SMO method to estimate the matched uncertainty or matched fault (in this case the matched fault is considered).

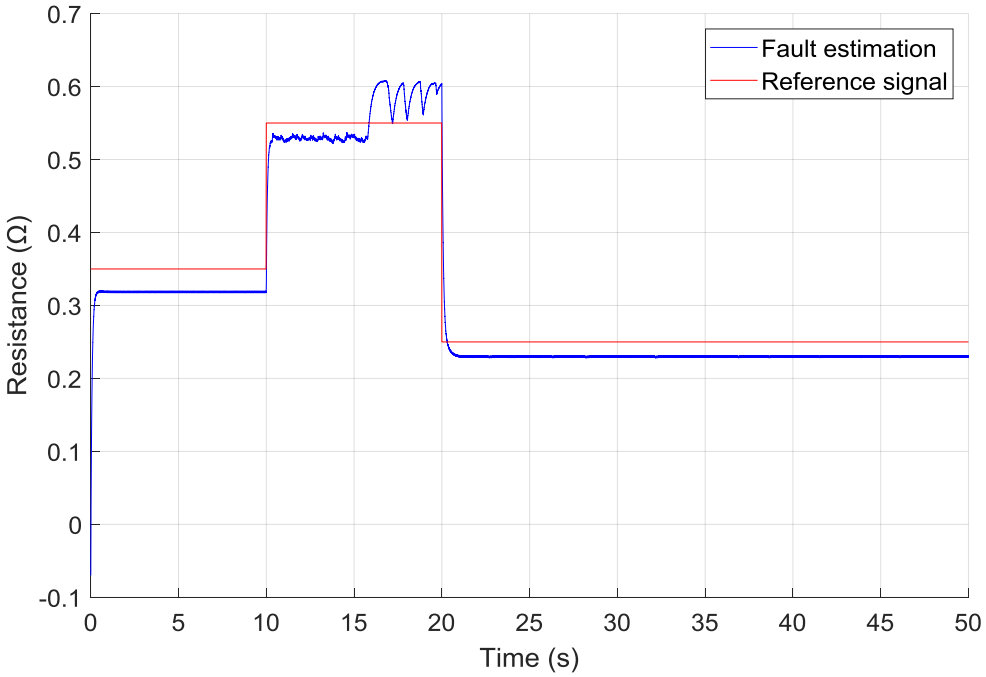

Figure 5-14 Fault estimation using Adaptive Observer (1)

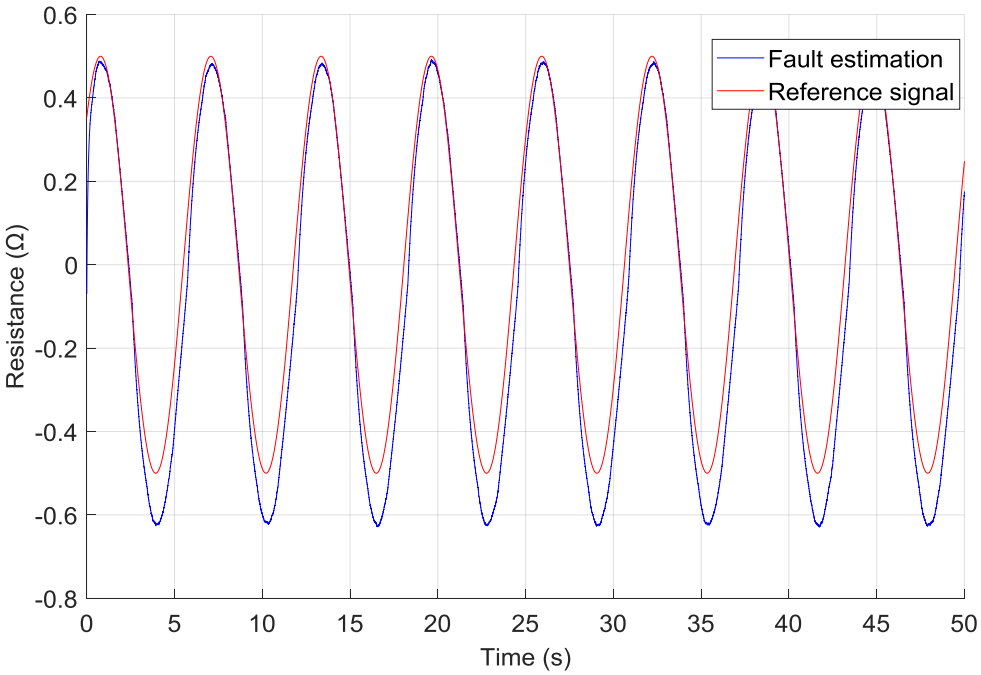

Figure 5-15 Fault estimation using Adaptive Observer (2)

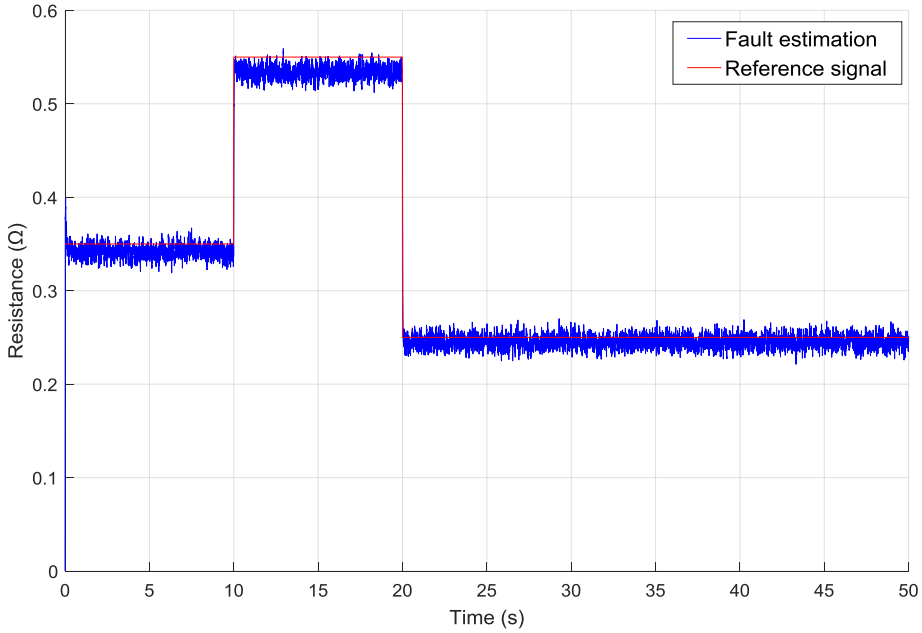

Figure 5-16 Fault estimation using SMO (1)

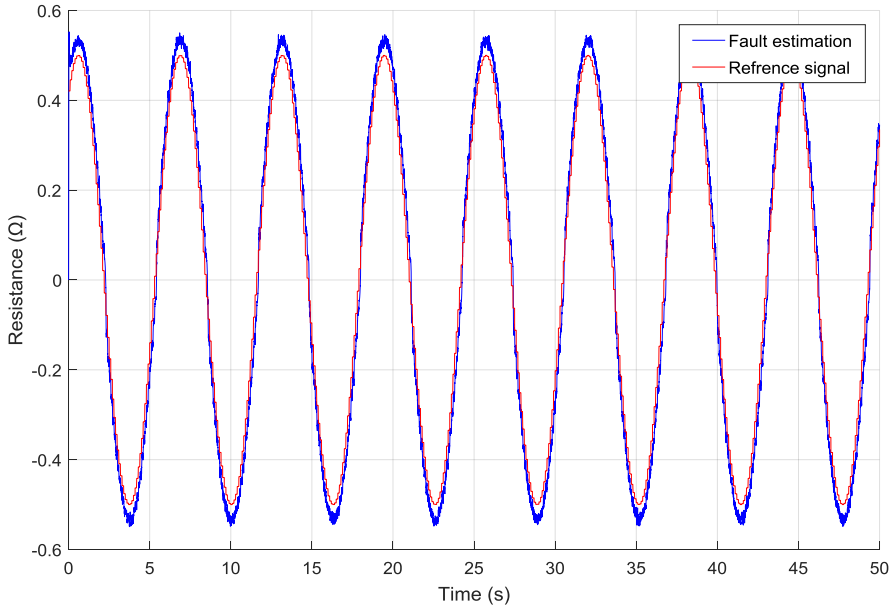

Figure 5-17 Fault estimation using SMO (2)

The performance of three different approaches are concluded as shown in the following table, it includes the performance of estimation accuracy and robustness. Some of the performance is found through the design process, such as the Improved AFE, it is a robust design; and some of the performance is wide-known and just verified here, such as the natural robustness property of SMO. The estimation accuracy is found through the comparison of different results of three different FE approaches.

Performance / Observer Type	Computation	Fault estimation	Robustness within matched channel
Adaptive Observer	Medium	Fault estimation with consideration of fault dynamics	No robust design considered.
Improved AFE	Low	An overall solution with consideration of fault dynamics, uncertainty and noise.	Robust design with good performance.

Sliding Mode Observer	Low (if sliding surface is suitable)	The most accurate one.	Natural robustness.

5.5 Summary

In this Chapter, a linear adaptive observer technique has been developed for FE in the electrical system of induction motor; and an improved AFE algorithm using LMI approaches is proposed based on the above approach. The improved AFE brings in robust property against uncertain parameters. Then the 3rd FE approach-SMO is proposed, which brings in natural robustness against uncertain parameters. In the simulation of these three approaches, the IM paremeters are unified, the fault scenarios are unified, and a comparison of the performance of these three FE approaches are made in a separate section. As well as that, the SMO is a vital approach which will be considered in LPV system of Chapter 6, therefore, a component fault (multiplicative fault) is considered in SMO seperately.

The above research is conducted on the 4th order electrical system of IM, in the coming Chapter 6, the assumption that the rotor speed is constant will be cancelled. The IM is constructed as a LPV system by local linearization. The LPV approach is used as the modelling approach and a SMO is used as FE approach.

Chapter 6: LPV FE for a nonlinear induction motor

6.1 Introduction

Chapter 5 outlines two main design approaches, the adaptive FE observer and the SMO for estimation of actuator, sensor and component faults, applied to linear systems with input disturbance and faults that are either constant (or slowly varying) or are time-varying. The approaches are applied on the linearised 4 electrical state equations of Eq.2-12, with an assumption that the machine rotation speed ω is a constant value. However, this assumption does not hold when the speed is required to be time-varying, according to practical requirements. By way of an extension to the work in Chapter 5 this Chapter picks up the Linear Parameter Varying (LPV) concept introduced briefly in Chapter 4.

Hence, this Chapter considers systems with parameter variations considered within a linear time-varying system framework, via LPV. The FE using the SMO introduced in Chapter 5 is extended into the LPV framework by considering the machine rotation speed ω as a varying "scheduling" parameter. The justification for using the LPV framework is that it is a powerful way of extending the linear system concepts, including design for: stability, robustness, time performance, etc. There are some early studies of applying LPV to induction motor systems. One background study considers an LPV approach to estimate the rotor magnetic flux vector based on tracking requirements in the presence of high nonlinearities (Prempain et al., 2002). In (Hasegawa et al., 2003), LPV is used to design a full-order observer for an induction motor taking core loss into account. In these studies it is shown that the LPV formulation acts as a valuable modelling approach for observer design applied to induction motor systems.

Section 6-1 shows that there are 3 approaches of implementing LPV modelling. They can be regarded as two thoughts in dealing with LPV system. In one thought it is convenient to develop an LMI model based on the linearization about operating points, where linear theory can be applied conveniently. This is a traditional view of a time-varying system that is identified as a set of linear systems with each one corresponding to one operating

point. The second thought for LPV system is more often used, this is the so-called affine expression of a nonlinear system in which the locally time-varying linear system description is described as a function of the scheduling or affine parameter. The focus in this work is on the affine approach which is further subdivided into three specific methods: (a) General LPV systems, (b) Polytopic LPV systems and (c) Linear Fractional Transformation (LFT).

Estimation approaches have been designed in order to fit within an LPV framework (Shi & Patton, 2014; Shi & Patton, 2015). In early papers about the LPV approach (Becker & Packard, 1994; Yu et al., 2002; Lu & Wu, 2004), parameter-dependent problems for LPV systems were presented. In later research, various observer-based methods were proposed to give good FE performance using LMI tools (Chen & Saif, 2006; Choi, 2007; Wang et al., 2007). A solvability condition was formulated as an LMI problem, and nonlinearity and uncertainty turned out to depend convexly on varying parameters (Gahinet & Apkarian, 1994). Hence, the main challenge to the use of LPV for observer based FE design is the guarantee of convexity. *Convexity* is defined within the context of multi-objective optimization in Section 5.2.4 (after Remark 5-5). Convexity may not be guaranteed when the system includes certain parameters and even scheduling parameter(s). In further work of (Apkarian & Gahinet, 1995; Agamloh, 2014; Emedi & Karimi, 2014; Narita et al., 2017), an LPV strategy was proposed to guarantee convexity using an LMI solution based on affine parameter dependence. This stategy of (Gahinet and Apkarian, 1995) has been developed by many investigators and applied to a variety of control and estimation problems, eg. for sliding mode control and also the SMO (see Sections 5.3 and 6.5 for more discussion).

There are several advantages of using the LPV modelling framework as follows.

(1), One advantage of LPV expression for nonlinear system is that, the linear approaches for LTI system can be easily applied. For example, state observers and state/output feedback controllers, etc. can often be extended to fit within an LPV system (Apkarian et al., 1995; Pellanda et al., 2002; Shi & Patton, 2014). The LPV form of system is able to tolerate large parameter variations and has good local control performance during operation.

(2), Some robust approaches can be extended to fit into the LPV framework, such as the H_∞ technique and LMIs (Gahinet & Apkarian, 1994; Apkarian & Gahinet, 1995). The idea in the work of (Khamari et al., 2011) uses H_∞ and LMI tools within a polytopic LPV model of an induction motor system, where the rotor speed is the scheduling parameter. In their work the rotor speed ω is a varying parameter measured online so that no linearization with regard to operation points is required.

(3), FE based observer design can be integrated into an FTC system. The paper by (Prempain et al., 2002) shows how to construct an LPV framework for both FE and FTC. In this example, once again the rotor speed is seen as a scheduling parameter, which is used to solve a tracking problem of a nonlinear induction motor system.

This Chapter focuses on the SMO based FE extension into an LPV framework. Actuator and sensor faults of the 4 electrical state equations of Eq.2-12 are considered as the induction motor model system, where the rotor speed ω is a varying parameter.

6.2 Definition of an LPV system

A linear time-invariant (LTI) system is an appropriate modelling approach to represent a nominal state space model. However, since there are usually uncertainties in a dynamic system, i.e. dynamic uncertainty and parametric uncertainty. In order to encompass some of the uncertainty and parameter variations, a dynamic system can also be expressed as a linear time-varying (LTV) system (Apkarian & Gahinet, 1995), as follows:

$$\begin{aligned} \dot{x}(t) &= A(t)x(t) + B(t)u(t) \\ y(t) &= C(t)x(t) + D(t)u(t) \end{aligned} \tag{6-1}$$

where $A(t), B(t), C(t), D(t)$ are time-varying system matrix, $x(t)$ is the state variables, $u(t)$ is the control input, $y(t)$ is the output.

To deal with the nonlinearity in a dynamic system, the LPV affine system can be developed as follows, in which a time-varying scheduling parameter vector $\theta(t)$ is required to vary within certain range of variation. The LTI system then has affine dependence based on $\theta(t)$ represented as:

$$\dot{x}(t) = A\big(\theta(t)\big)x(t) + B\big(\theta(t)\big)u(t)$$
$$y(t) = C\big(\theta(t)\big)x(t) + D\big(\theta(t)\big)u(t) \qquad (6\text{-}2)$$

In the induction motor system, the rotor speed ω is considered as scheduling parameter. In the induction motor introduced in Section 2.2.1, the state variables like flux, currents, etc. can be estimated on-line. A polytopic approach can be used in which a set of vertices of a specific polytope can be shown to represent the main features (stability, etc) of points lying within the polytope (Apkarian & Gahinet, 1995).

However, in this current work the LPV approach is applied to state observer design for the FE problem. The fault reconstruction refers to the result of weighted combination of various LPV fault estimators. The basic ideas of the observer-based FE for LPV systems can be expressed in Figure 6-1, using an example of a time-varying or nonlinear plant with disturbance inputs as well as actuator and sensor faults.

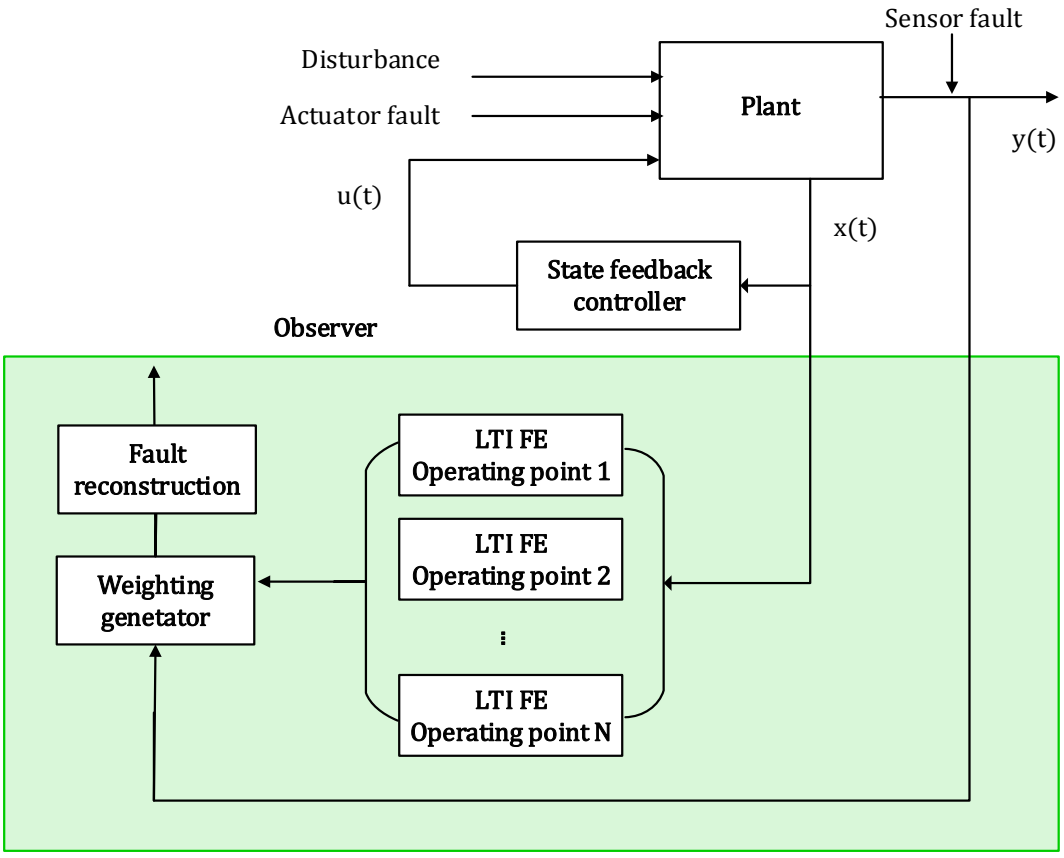

Figure 6-1 Polytopic LPV observer for actuator and sensor fault estimation

Based on different parameter forms, 3 LPV modelling methods are explained below and examples are given to illustrate the main concepts.

6.2.1 General LPV system

For different LPV systems, the form of expression is different; the method used in research can vary significantly. The most common LPV system is generally expressed in the following form (Gahinet & Apkarian, 1994; Oliveira & Peres, 2005). For example consider the following system:

$$\dot{x}(t) = A(\theta(t))x(t) \tag{6-3}$$

where $x(t) \in R^n$ is the time-varying state variable vector of the LPV system. In addition, $\theta(t)$ is the time-varying *scheduling* parameter vector. There is a hypothesis for such a system that the matrix A is generally dependent on the parameters of the time-varying vector $\theta(t)$ and must be bounded. There are many ways for this kind of system to relate to the parameters in $\theta(t)$, such as via polynomials, rational, and exponential, and so on.

Typically, if an LPV system is polynomial-dependent on the time-varying parameters, the matrix $A(\theta(t))$ with affine dependency on θ(t) can be expressed as:

$$A(\theta(t)) = A_0 + \sum_{1}^{i} A_i \theta^{\alpha_i} \tag{6-4}$$

where θ^{α_i} is a multi-index notation (Apkarian et al., 1995).

The affine LPV system gives a more general expression of an LPV system, the assumptions and other restrictions become less significant. Based on this style other LPV forms can be derived from. An ordinary LPV system can take full advantage of the appropriate output variables, and then change the original system into polynomial or affine descriptor LPV systems. In this way, a LPV system is able to describe a more general dynamic system.

Example 6-1 (Briat, 2014)

A main idea of the General form of LPV system is illustrated through the following example.

Consider a 1st order LPV system given by

$$\dot{x}(t) = \left(\frac{\rho(t)}{\rho(t)^2 + 1} - 1\right)x(t) \tag{6-5}$$

where $\rho(t)$ is a scalar valued continuous function of time bounded by $\rho(t) \in [-1,1]$. Through a particular transformation, the system (6-5) is expressed as the following descriptor LPV system, which can be found in (Briat, 2014):

$$\begin{gathered} \dot{x} = -x - y_1 + y_3 \\ \rho x + y_1 + y_3 = 0 \\ -\rho y_1 + y_2 + \rho y_3 = 0 \\ -\rho y_2 + y_3 = 0 \end{gathered} \tag{6-6}$$

$$\begin{bmatrix} 1 & 0 & 0 & 0 \\ 0 & 0 & 0 & 0 \\ 0 & 0 & 0 & 0 \\ 0 & 0 & 0 & 0 \end{bmatrix} \begin{bmatrix} \dot{x} \\ \dot{y}_1 \\ \dot{y}_2 \\ \dot{y}_3 \end{bmatrix} = \begin{bmatrix} -1 & -1 & 0 & 1 \\ \rho & 1 & 0 & 1 \\ 0 & -\rho & 1 & \rho \\ 0 & 0 & -\rho & 1 \end{bmatrix} \begin{bmatrix} x \\ y_1 \\ y_2 \\ y_3 \end{bmatrix}$$

The same example is used in the study of the LFT form of LPV system in Section 6.2.3

6.2.2 Polytopic LPV system

In addition to the General form of LPV system, the Polytopic LPV system can also be used to express a system model with uncertain parameters. Unlike the previous expression, the polytopic LPV system is expressed as a time-varying convex combination of LTI systems. This property of the polytopic LPV system is more convenient for determining stability proofs.

In a polytopic LPV system (Gahinet & Apkarian, 1994; Apkarian & Gahinet, 1995; Prempain et al., 2002; Khamari et al., 2011), the convex property can be expressed in detail as follows. Consider the system (6-7) which has parameter dependency in the state as well as input and output parameters:

$$\dot{x}(t) = A(\theta(t))x(t) + B(\theta(t))u(t) \tag{6-7}$$

$$y(t) = C(\theta(t))x(t) + D(\theta(t))u(t)$$

where

$$\begin{pmatrix} A(\theta) & B(\theta) \\ C(\theta) & D(\theta) \end{pmatrix} := \left\{ \begin{pmatrix} A_i & B_i \\ C_i & D_i \end{pmatrix}, i = 1, \dots r \right\} \tag{6-8}$$

From (Apkarian & Gahinet, 1995) the system matrix $\begin{pmatrix} A(\theta) & B(\theta) \\ C(\theta) & D(\theta) \end{pmatrix}$ can be expressed as a linear combination of systems at different operating points as:

$$\begin{pmatrix} A(\theta) & B(\theta) \\ C(\theta) & D(\theta) \end{pmatrix} = \sum_{i=1}^{r} \alpha_i \begin{pmatrix} \mathrm{A}_i & B_i \\ C_i & D_i \end{pmatrix} \tag{6-9}$$

where $\alpha_i \geq 0$ and $\sum_{i=1}^{r} \alpha_i = 1$.

Any non-linear system can be represented by a variety of LPV systems to a certain degree of accuracy. In some important points, the values of the time-varying parameters can determine the immediate state of the system, that is, defined as a vertex; by selecting multiple vertices to form a polyhedron, the nonlinear system can be expressed by linear systems (Apkarian & Gahinet, 1995).

Figure 6-2 shows the convex hull of a polytopic LPV system in which a set of vertices of operating points are included within the polyhedron (Briat, 2014). In other words, when a so called "Scaled H_∞ control" problem in extended into a so called "gain-scheduled H_∞ control" problem, the integrated control or estimation problem is formulated into LMIs based convex problem. The solvability of convex problem can be tackled only if the convex problem stands, that is, the scheduling parameter should lie in the range of convex hull.

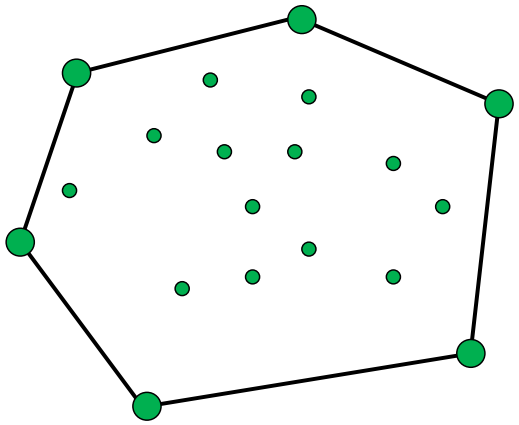

Figure 6-2 Convex representation of LPV system

Example 6-2 (Briat, 2014)

An example of a polynomial LPV system is considered as (Briat, 2014):

$$\dot{x}(t) = (A_0 + A_1\rho(t) + A_2\rho(t)^2)x(t) \tag{6-10}$$

where $\rho(t) \in [-1,1]$. For the given area of the time-varying parameter, it is necessary to determine the values of terms $\rho(t)$ and $\rho(t)^2$. The corresponding value range is given by:

$$S := (\rho(t),\ \rho(t)^2) \tag{6-11}$$

where $\rho(t)^2 \in [0,1]$

Considering the time-varying parameters, the convex area of the system is generated as follows:

$$\begin{pmatrix} \rho(t) \\ \rho(t)^2 \end{pmatrix} \subset S_e := \left\{\begin{bmatrix} -1 \\ 0 \end{bmatrix}, \begin{bmatrix} 1 \\ 0 \end{bmatrix}, \begin{bmatrix} -1 \\ 1 \end{bmatrix}, \begin{bmatrix} 1 \\ 1 \end{bmatrix}\right\} \tag{6-12}$$

The non-linear system corresponding to the polyhedron can be expressed as $[-1,1] \times [0,1]$. By the concept of a polytopic LPV system, within the set S_e this nonlinear system can be described as a polytopic system:

$$\dot{x}(t) = [A_0 + A_1 \sum_{i=1}^{4} (-1)^i \gamma_i(t) + A_2(\gamma_3(t) + \gamma_4(t))]x(t)$$

with

$$\rho(t) = \sum_{i=1}^{4} (-1)^i \gamma_i(t) = \big(\gamma_1(t) + \gamma_3(t)\big)(-1) + \big(\gamma_2(t) + \gamma_4(t)\big)(1) \tag{6-13}$$

$$\rho(t)^2 = \big(\gamma_3(t) + \gamma_4(t)\big) = \gamma_3(t)(-1)^2 + \gamma_4(t)(1)^2$$

and from this $\rho(t)$ and $\rho(t)^2$ can be expressed as:

$$\begin{pmatrix} \rho(t) \\ \rho(t)^2 \end{pmatrix} = \gamma_1(t)\begin{pmatrix} -1 \\ 0 \end{pmatrix} + \gamma_2(t)\begin{pmatrix} 1 \\ 0 \end{pmatrix} + \gamma_3(t)\begin{pmatrix} -1 \\ 1 \end{pmatrix} + \gamma_4(t)\begin{pmatrix} 1 \\ 1 \end{pmatrix}$$

6.2.3 LFT form of LPV system

The LPV system in LFT form is used to represent the two subsystems of the interconnected LPV system, and is usually used in the robust control of uncertain systems (Apkarian et al., 1995; Apkarian & Adams, 2000). In this form, the system uncertainty can be expressed separately, since the system is divided into two parts comprising the deterministic (certain) system and the uncertainty. Early studies of interconnection systems originate from the study of faults caused by unexplained faults in control systems (Gahinet & Apkarian, 1994; Garcia & Frank, 1997).

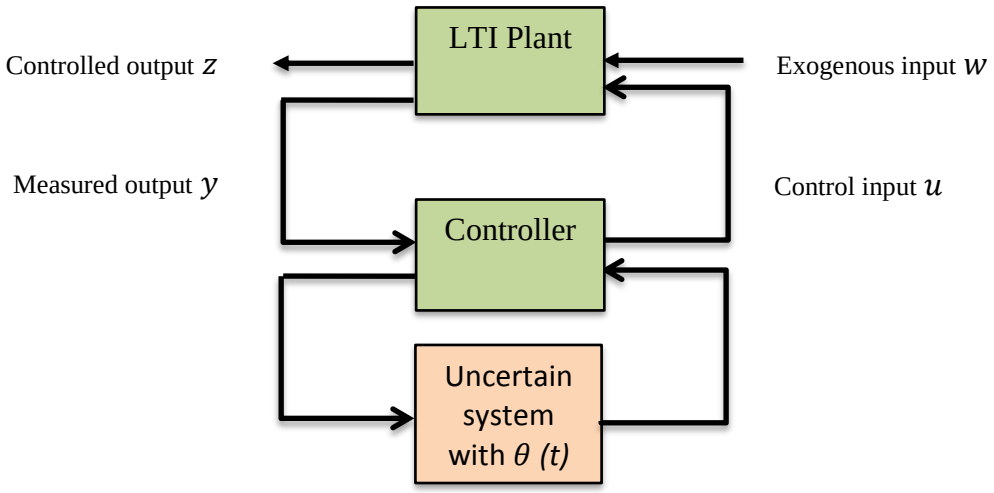

Figure 6-3 LFT system mapping from w to z (Apkarian & Gahinet, 1995)

The core idea of LFT is to rewrite complex uncertain systems into two subsystems of interconnection, including a simple deterministic part and an uncertain part. The deterministic part should have some easy-to-handle aspects such as linearity, temporal invariance, etc.; uncertain parts include time-varying items, non-linearity, etc. Due to the progress of the research of LPV considering H_∞ performance, the LPV system in the form of LFT has received more attention than other types of LPV forms introduced in this Chapter (Casella & Lovera, 2008; Ballesteros & Bohn, 2011).

An LFT-form of LPV system is illustrated in Figure 6-3, which can also be described using the following formulation:

$$\begin{aligned} \dot{x}(t) &= Ax(t) + N_1 w(t) \\ z(t) &= Cx(t) + N_2 w(t) \\ w(t) &= \Theta\big(\rho(t)\big) z(t) \end{aligned} \tag{6-14}$$

where $x(t)$ represents system state variables, $w(t)$ and $z(t)$ represent the connections between the linear system and the parameter-dependent component $\theta(t)$.

The above formula clearly reflects the two parts of the LPV system interconnection, the linear part (A, N_1, C, N_2) and the non-linear time-varying part $\theta(t)$. There may be several expressions for the LFT form of LPV for a given nonlinear system, but usually a minimum expression is sought to minimize the coupling and complexity of the interconnected subsystems of the system (Apkarian & Gahinet, 1995; Apkarian et al., 1995; Apkarian & Adams, 2000).

Example 6-3 (Briat, 2014)

Consider a similar scalar LPV system given in Example 6-1:

$$\dot{x}(t) = \left(\frac{\rho_2(t)}{\rho_1(t)^2 + 1} - 3\right) x(t) \tag{6-15}$$

According to (6-14), the LFT representation of this case can be as follows, of which the mathematical derivation can be found in (Briat, 2014):

$$\begin{bmatrix} \dot{x} \\ z_0 \\ z_1 \\ z_2 \end{bmatrix} = \begin{bmatrix} \tilde{A} & B \\ C & D \end{bmatrix} \begin{bmatrix} x \\ \omega_0 \\ \omega_1 \\ \omega_2 \end{bmatrix}$$

with

$$\begin{bmatrix} \tilde{A} & B \\ C & D \end{bmatrix} = \begin{bmatrix} -3 & 1 & 0 & 1 \\ 1 & 0 & 0 & 0 \\ 0 & 0 & 0 & -1 \\ 0 & 0 & -1 & 0 \end{bmatrix} \text{ and } \begin{bmatrix} \omega_0 \\ \omega_1 \\ \omega_2 \end{bmatrix} = \begin{bmatrix} \rho_2 & 0 & 0 \\ 0 & \rho_1 & 0 \\ 0 & 0 & \rho_1 \end{bmatrix} \begin{bmatrix} z_0 \\ z_1 \\ z_2 \end{bmatrix} \tag{6-16}$$

Then

$$A(\rho) = \frac{\rho_2(t)}{\rho_1(t)^2 + 1} - 3$$

$$= -3 + \begin{bmatrix} 1 \\ 0 \\ 0 \end{bmatrix} \begin{bmatrix} 1 & 0 & 0 \\ 0 & 1 & -\rho_1 \\ 0 & -\rho_1 & 1 \end{bmatrix}^{-1} \begin{bmatrix} \rho_2 \\ 0 \\ 0 \end{bmatrix}$$

$$= \tilde{A} + B(I - \theta(\rho)D)^{-1}\theta(\rho)C$$

From this example, it is straightforward to find that the LPV system can be expressed using the LFT form with rational dependence on time-varying parameters. As discussed in Section 5.2.4, this form of system is within the solvability of BRL. This form is also explained in (Apkarian & Gahinet, 1995; Apkarian et al., 1995) as a suboptimal H_∞ problem within the LPV framework. Also, methods of transforming a General LPV form into an LFT form can be found in (Pfifer, 2013; Cai et al., 2014).

6.3 LPV based FE approaches

There are two popular ways of dealing with the problem of FE for a LPV system: the H_∞ theory based LPV observer and sliding mode LPV observer. Based on these two approaches, the induction motor system simulation was considered in the research of this thesis, although the study of the SMO approach is also demonstrated in Section 6.5.

Using H_∞ theory, the design of a controller has been introduced in (Gahinet & Apkarian, 1994; Apkarian & Gahinet, 1995; Apkarian et al., 1995). This approach has also been

used in the study of estimation methods, state observers, FE, etc. (Shi & Patton, 2014; Shi & Patton, 2015). In this class of LPV systems, the state-space matrices are fixed functions of the time-varying parameters. In fact, this problem has been concluded as a convex problem based on the vertex property of a polytopic LPV system, which has been introduced in Section 6.2. The general polytope expression of a LPV system can be expressed as in Figure 6-4. In this approach, the estimation design is guaranteed by H_∞ performance with a vector of time-varying parameters. Section 6.5 shows how this solution is derived as a LMI problem.

Hence, the resulting estimation observer is time-varying along with the varying parameter vector $\rho(t)$. The trajectory of $\rho(t)$ is also known as a *parameter trajectory (Oliveira & Peres, 2005).* Compared with classical LPV approaches stated in (Shamma & Athans, 1991), the appearance of this approach proposes a different method to guarantee the stability and performance along all the possible trajectories of the time-varying parameters.

The LPV extension of the SMO estimator has been fully described in (Alwi et al., 2012; Alwi & Edwards, 2014), all their work is based on the original studies by (Edwards & Spurgeon, 1998; Edwards et al., 2000).

In this work a SMO for fault reconstruction belonging to a class of LPV systems has been designed, which can be used to tackle the problem of sensor and actuator fault estimation of an LPV system. A fixed input distribution matrix and a time-varing matrix was used in the observer design. One of the motivations for the design of this approach is that it is able to guarantee the stability and the robustness against faults and disturbance over a wide range of parametric operating conditions. Another reason is that the LPV approach provides a good compromise between local LTI methods and a total nonlinear design approach. Of course, the most important reason is that the induction motor system can be expressed correctly through the use of this approach and gives satisfactory results.

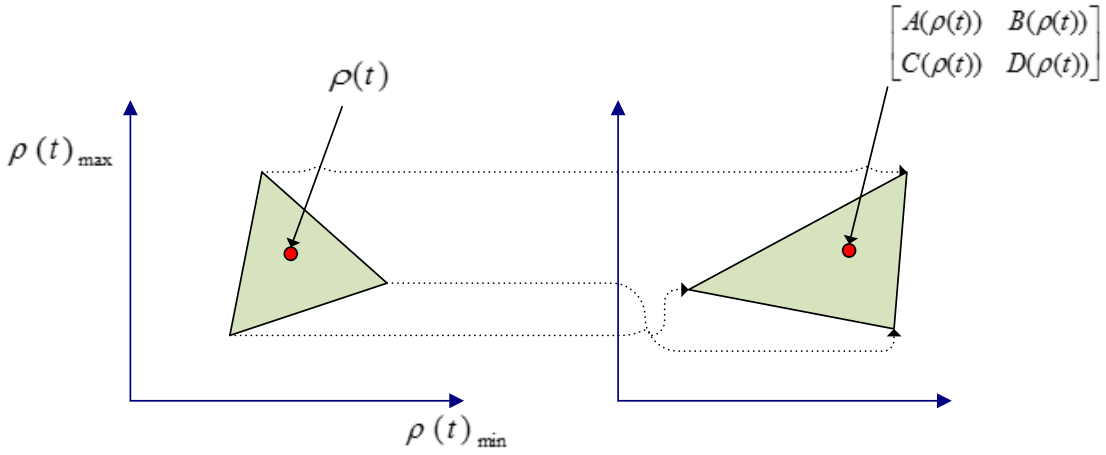

Figure 6-4 Polytope of a LPV system dependent on varying parameter $\rho(t)$

6.4 Problem statement

In the study of the induction motor system, a 4th order electrical system has been seen as a linear system when the rotating speed ω is assumed to be constant. However, it is clearly not constant in most applications. So when considering the rotation speed as a varying parameter, it is necessary to study the FE approaches for a nonlinear system.

For the system considered here, a general LPV model with actuator and sensor faults is expressed as follows (Alwi et al., 2012; Alwi & Edwards, 2014):

$$\dot{x}(t) = A(\rho)x(t) + B(\rho)u(t) + F_1(\rho)f_a(t) \quad (6\text{-}17)$$

$$y(t) = Cx(t) + F_2 f_s(t) \quad (6\text{-}18)$$

where the dimension of system matrices, actuator faults and the sensor faults should satisfies the dimension requirements in the following part. $A(\rho) \in R^{n\times n}, B(\rho) \in R^{n\times m}, F_1(\rho) \in R^{n\times q}$ are the dimensions of the system matrices with varying parameters, $C \in R^{p\times n}$ is the dimension of the output distribution matrix. $F_2 \in R^{p\times n}, rank(F_2) = r \leq p$. $f_a(t) \in R^q$, $f_s(t) \in R^r$ represent the dimensions of the actuator and sensor faults, respectively. It should be noted that when $f_a(t) \neq 0$, it means there exists an actuator fault; while $f_a(t) = 0$, means the absence of an actuator fault. When $f_s(t) \neq 0$, a sensor fault is indicated. When $f_s(t) = 0$, it means there is no sensor fault.

Assumption 6-1 (Edwards et al., 2000):

1) The system described by equations (5-17) and (5-18) is observable;
2) The time-varying parameter $\rho(t)$ is measurable;
3) The system order is n, the number of the measured outputs p and the number of independent actuator faults q are assumed to satisfy $n > p \geq q$.
4) Rule (4) of Assumption 5-2.

The (1) and (2) of *Assumption 6-1* guarantees that the system is observable and the varying parameter is detectable online. (3) and (4) of *Assumption 6-1* ensures the existence of a canonical form of the dynamic system in the following context.

The LPV system can be described as a time-varying state space model based on one of the mathematical expression approaches in Section 6.2.

6.5 A sliding mode LPV observer design

The theory of the sliding mode LPV observer is described in Section 5.3, based on work by (Alwi et al., 2012). In this thesis, the approaches are developed into the FE application for the induction motor system which is described in Section 2.2.1. The approach is applied in two types of fault estimation scenarios, the actuator fault estimation and the sensor fault estimation. One should bear in mind that the robust FE results are developed in order to use in a FTC system, based on fault compensation. However, the FTC problem is deloped in Chapter 7. Athough this Section discusses the use of FE using SMO, the FTC system described in Chapter 7 makes use of a more suitable approach based on adaption to model uncertainty.

The FE problem with an LPV system modelling framework is summarised in the equations (6-17) and (6-18), when the actuator fault is considered, whilst the sensor fault is assumed to be zero, i.e. $f_a(t) \neq 0, f_s(t) = 0$. Because sensor fault is transformed into actuator fault scenario and dealt with. $F_1(\rho)$ is divided into two parts, including a constant part and a time-varying part, that is R and $E(\rho)$. R is a fixed matrix and $E(\rho)$ is a matrix with varying parameters. In the observer design for the induction motor system, the speed is considered to be the only varying parameter of the LPV system. Due to the coupling of

the speed and other system state variables, the varying parameter does exist in different parts of the system and appears as nonlinear components.

$$F_1(\rho) = RE(\rho) \tag{6-19}$$

where $R \in R^{n\times q}, E(\rho) \in R^{q\times q}$. $E(\rho)$ is assumed invertible for all $\rho \in \Omega$. $F_1(\rho)$ is subdivided into the summation of constant matrix and a time-varing matrix. Consequently, it helps to construct "virtual fault signals" which will be shown in Section 6.5.1 and Section of 6.5.2.

By subsituting Eq. (6-19) into Eq. (6-17), the system equation can be written as follows:

$$\dot{x}(t) = A(\rho)x(t) + B(\rho)u(t) + RE(\rho)f_a(t) \tag{6-20}$$

where $E(\rho)f_a(t) \coloneqq f_v(t,\rho)$, $f_v(t,\rho)$: $R_+ \times R^d \to R^q$ represents the virtual faults which are to be estimated by this approach. The invertibility of $E(\rho)$ for all $\rho \in \Omega$ implies that the real actuator fault is estimated through the estimation of $f_v(t,\rho)$, the virtual fault acts as a intermediate variable. As introduced in Section 5.3.2 it is assumed that the fault is bounded, i.e.

$$\|f_v(t,\rho)\| < r_1(\rho)\|u\| + \varphi(t,y,\rho) \tag{6-21}$$

where the $r_1(\rho) \in R_+, \varphi \in R_+$ are known functions. y represents the measured output described in Eq. (6-18). The physical meaning of equation (6-21) is that the fault to be observed/estimated is bounded within a prescribed range (corresponding to the physical/practical application problem) (Alwi et al., 2012; Alwi & Edwards, 2014).

An observer structure is described here (Alwi et al., 2012; Alwi & Edwards, 2014) for the estimation of each of the actuator and sensor faults (considered separately). The LPV estimator structure is as follows (this observer structure is of the same form which is considered in Section 5.3.2), based on the system Eqs. (6-17) and (6-18):

$$\dot{\hat{x}}(t) = A(\rho)\hat{x}(t) + B(\rho)u(t) - G_l(\rho)e_y(t) + G_n v(t) \tag{6-22}$$

where $G_l(\rho) \in R^{n\times p}, G_n \in R^{n\times q}$ are appropriate distribution matrices and $v(t)$ represents the discontinuous switched component used to maintain the sliding motion

(Edwards et al., 2000). The *switching component* is introduced after the regular form generation (*Step 1*) and the canonical form feneration (*Step 2*), because it is an important variable in forcing the reachability of the motion in accordance with the hyperplane. In this process, fault reconstruction can be finished by maintaining the sliding motion on the manifold through a switching mechanism. It is finished within the process of producing "equivalent output error injection" in Section 5.3.3. Since the objective is to force the output error to zero in finite time, it is necessary to derive the following output estimation error:

$$e_y(t) = \hat{y}(t) - y(t) \tag{6-23}$$

where $\hat{y}(t) = C\hat{e}(t)$. If this output error reaches zero in finite time, then a sliding motion is said to have been reached on the sliding hyperplane, as described by (6-24).

The formulation for the reconstruction of the actuator faults and sensor faults of the LPV system is now developed using the "equivalent output injection", as stated in Section 5.3.3. In this process the sliding motion is maintained on the sliding surface.

As discussed above, appropriate switching causes the motion of the estimation error system to be maintained within the sliding hyperplane (or sliding manifold) (Edwards & Spurgeon, 1998; Edwards et al., 2000). The switching action of the observer feedback is defined in Section 6.5.1 and causes the motion to remain within the sliding manifold.

This switching motion is maintained by the nonlinear switching part $v(t)$ introduced in (6-22).

$$S = \{e \in R^n : Ce = 0\} \tag{6-24}$$

Remark 6-1:

1) The design of the Observer shown in Eq. (6-22) constructs a sliding mode observer with output error requirements, that is, sliding motion takes place and forces the output error to zero within finite time.
2) This form of SMO is able to form a reduced order output error system considering the system in Eq. (6-20), the transformation is conducted in following Step 1 and Step 2.

In the above process, the states error system is kept quadratically stable as shown in Eq. (6-37) where the details is explained.

6.5.1 Actuator fault estimation

The SMO is designed in the following 4 steps: Regular form generation, Canonical form generation, Affine form generation and fault reconstruction. The process is shown as follows.

Step 1: Regular form generation

Hereby, the definition of estimation error is $e(t) = \hat{x}(t) - x(t)$, so it is not hard to get the error system from (6-20) and (6-22):

$$\dot{e}(t) = A(\rho)e(t) - G_l(\rho)e_y(t) + G_n v(t) - Rf_v(t,\rho) \tag{6-25}$$

According to a linear change of coordinates $x(t) \to Tx(t)$ described in Section 5.3.2, it is easy to obtain a new expression of the output:

$$y(t) = [0 \quad T]\begin{bmatrix} x_1(t) \\ x_2(t) \end{bmatrix} \tag{6-26}$$

This is because the existance of the 4th rule of Assumption 6-1 and Eq. (6-19), R is a fixed matrix and CR is full rank, therefore, Eq. (6-26) holds.

And the fault distribution matrix R as shown in Eq. (6-27) helps with the transformation in Step 1.

$$R = \begin{bmatrix} 0 \\ R_2 \end{bmatrix} = \begin{bmatrix} 0 \\ 0 \\ R_0 \end{bmatrix} \tag{6-27}$$

where $T \in R^{p\times p}$ is orthogonal, $R_2 \in R^{p\times q}$, and $R_0 \in R^{q\times q}$ is non-singular (invertable). Based on the above transformation and the definitions, the states estimation error system (6-25) is illustrated by the following equation:

$$\begin{bmatrix}\dot{e}_1(t)\\ \dot{e}_2(t)\end{bmatrix}=\begin{bmatrix}A_{11}(\rho) & A_{12}(\rho)\\ A_{21}(\rho) & A_{22}(\rho)\end{bmatrix}\begin{bmatrix}e_1(t)\\ e_2(t)\end{bmatrix}-\begin{bmatrix}G_{l1}(\rho)\\ G_{l2}(\rho)\end{bmatrix}e_y(t)+\begin{bmatrix}G_{n1}\\ G_{n2}\end{bmatrix}v(t)-\begin{bmatrix}0\\ R_2\end{bmatrix}f_v(t,\rho) \quad (6\text{-}28)$$

Where $e_1 \in R^{n-p}$ and $e_2 \in R^p$.

This step separated the "virtual faults" as shown in the lower part of Eq. (6-28). The next step is to sepetate the switching function from the system, making sure that it works only on the lower part of Eq.(6-28).

Step 2: Canonical form generation

Hereby a second transformation is taken into consideration, this is called the Canonical form generation.

$$\tilde{e}(t)=\begin{bmatrix}\tilde{e}_1(t)\\ e_y(t)\end{bmatrix}=T_L\begin{bmatrix}e_1(t)\\ e_2(t)\end{bmatrix}=\begin{bmatrix}e_1(t)+Le_y(t)\\ e_y(t)\end{bmatrix} \quad (6\text{-}29)$$

where $T_L \in R^{n\times n}$ is given by

$$T_L=\begin{bmatrix}I & L\\ 0 & T\end{bmatrix} \quad (6\text{-}30)$$

where $L \in R^{(n-p)\times p}$. The design of matrix L is flexible according to the order of the system. If the system of Eq. (6-28) can be seen as two subsystems described by two parts of equations, the aim of this transformation of Eq. (6-29) is to make sure that the effect of the discontinuous switching component works only on the lower part of system in Eq. (6-28). The output error can be expressed as follows:

$$e_y(t)=[0 \quad I]\tilde{e}(t) \quad (6\text{-}31)$$

L has the following structure:

$$L=[L_1 \quad 0] \quad (6\text{-}32)$$

Through the transformation, the gain matrix related to the output injection signal is expressed in Eq. (6-33).

$$\tilde{G}_n = T_L G_n = \begin{bmatrix} 0 \\ I_p \end{bmatrix} \tag{6-33}$$

Through the above transformation, Eq. (6-28) can be rewriten as:

$$\begin{bmatrix} \dot{\tilde{e}}_1(t) \\ \dot{e}_y(t) \end{bmatrix} = \begin{bmatrix} \tilde{A}_{11}(\rho) & \tilde{A}_{12}(\rho) \\ \tilde{A}_{21}(\rho) & \tilde{A}_{22}(\rho) \end{bmatrix} \begin{bmatrix} \tilde{e}_1(t) \\ e_y(t) \end{bmatrix} - \begin{bmatrix} 0 \\ \tilde{R}_2 \end{bmatrix} f_v(t,\rho) - \begin{bmatrix} \tilde{G}_{l1} \\ \tilde{G}_{l2} \end{bmatrix} e_y(t) + \begin{bmatrix} 0 \\ I \end{bmatrix} v(t) \tag{6-34}$$

where $\tilde{A}(\rho) = T_L A(\rho) T_L^{-1}, \tilde{R} = T_L R$.

It can be seen that the discontinuous switching component only affects the second subsystem of Eq. (6-34). Furthermore, the distribution matrix of $v(t)$ is transferred from a variable matrix to a fixed matrix. It benefits the design process in Eq. (6-36). From Eq. (6-27) and Eq. (6-32), $LR_2 = 0$ can be attained. Define $\tilde{R}_2 = LR_2$ and

$$e_y(t) = \tilde{C}\tilde{e}(t) = [0 \quad I_p]\tilde{e}(t) \tag{6-35}$$

Step 3: Affine form generation

The matrix $\tilde{A}(\rho)$ can be expressed in details (Alwi et al., 2012; Alwi & Edwards, 2014):

$$\begin{aligned} \tilde{A}(\rho) &= \begin{bmatrix} \tilde{A}_{11}(\rho) & \tilde{A}_{12}(\rho) \\ \tilde{A}_{21}(\rho) & \tilde{A}_{22}(\rho) \end{bmatrix} \\ &= \begin{bmatrix} A_{11}(\rho) + LA_{21}(\rho) & A_{12}(\rho)T^{-1} + LA_{22}(\rho)T^{-1} - \tilde{A}_{11}(\rho)LT^{-1} \\ TA_{21}(\rho) & TA_{22}(\rho)T^{-1} - TA_{21}(\rho)LT^{-1} \end{bmatrix} \end{aligned} \tag{6-36}$$

Based on (6-32), the block $\tilde{A}_{11}(\rho)$ of (6-36) can be expressed as:

$$\tilde{A}_{11}(\rho) = A_{11}(\rho) + L_1 A_{211}(\rho) \tag{6-37}$$

where $A_{211} \in R^{(p-q)\times(n-p)}$ is the top $(p-q)$ rows of $A_{211}(\rho)$. The next step is to realise the quadratical stability of $\tilde{A}_{11}(\rho)$ through the design of the matrix L_1. That is to design suitable L_1 and a symmetric positive matrix P_1 to make the following inequality holds for all $\rho \in \Omega$.

$$\tilde{A}_{11}(\rho)^T P_1 + P_1 \tilde{A}_{11}(\rho) < 0 \tag{6-38}$$

Choose the observer gain $\tilde{G}_l(\rho)$ for the system (6-34):

$$\tilde{G}_l(\rho) = \begin{bmatrix} \tilde{G}_{l1}(\rho) \\ \tilde{G}_{l2}(\rho) \end{bmatrix} = \begin{bmatrix} \tilde{A}_{12}(\rho) \\ \tilde{A}_{22}(\rho) - \tilde{A}_{22}^s \end{bmatrix} \tag{6-39}$$

where

$$\tilde{A}_{22}^s = -k_2 I_p \tag{6-40}$$

k_2 is positive scalar and is to be designed. The matrix $\tilde{A}_{22}^s$, as explained in Section 5.3.2, works as a stability design matrix but does not contribute to the fault reconstruction. Putting (6-39) into (6-34), the following equation is obtained:

$$\begin{bmatrix} \dot{\tilde{e}}_1(t) \\ \dot{e}_y(t) \end{bmatrix} = \begin{bmatrix} \tilde{A}_{11}(\rho) & 0 \\ \tilde{A}_{21}(\rho) & -k_2 I_p \end{bmatrix} \begin{bmatrix} \tilde{e}_1(t) \\ e_y(t) \end{bmatrix} - \begin{bmatrix} 0 \\ \tilde{R}_2 \end{bmatrix} f_v(t, \rho) + \begin{bmatrix} 0 \\ I \end{bmatrix} v(t) \tag{6-41}$$

Remark 6-1:

Through the first coordinate transformation as shown in (6-26), the "regular form" of the sliding mode observer has been obtained. Through the second canonical form coordinate transformation as shown in (6-29) and the affine coordinate transformation as shown in (6-39), the upper part of Eq. (6-28) is transformed into Eq. (6-41). The problem turns into a problem of stability of $\tilde{A}_{11}(\rho)$, and it can be solved through the design of the matrix L_1, that means that $\tilde{e}_1(t)$ goes to zero in finite time. However, it ensures the stability for the upper part of Eqs. (6-28). Hence, the second subsystem of Eqs. (6-41) is handled in a straightfoward way.

Step 4: Sliding mode fault reconstruction

The fault reconstruction using "output injection signal" is conducted in the following context. This process is used in estimating the actuator faults and sensor faults. In order to calculate each estimated fault separately, it is necessary to consider the function of each component of $v(t)$ separately (Alwi et al., 2012; Alwi & Edwards, 2014). The *jth* component of $v(t)$ is defined as:

$$v_j(t) = -k_1 sign\left(e_{y,j}(t)\right)\left|e_{y,j}(t)\right|^{\frac{1}{2}} + z_j(t) \tag{6-42}$$

$$\dot{z}_j(t) = -k_3 sign\left(e_{y,j}(t)\right) - k_4 e_{y,j}(t) \tag{6-43}$$

Combining the lower part of $\dot{e}_y(t)$ in (6-41), with (6-42) and (6-43), the equations of the error system can be written individually and expressed in a set of equations as follows:

$$\dot{e}_{y,j}(t) = \tilde{\xi}_j(t) - k_2 e_{y,j}(t) - \tilde{R}_{2,j} f_v(t,\rho) + v_j(t) \tag{6-44}$$

where $\tilde{R}_{2,j}$ is the *jth* component of $\tilde{R}_2$. And

$$\dot{\tilde{\xi}}_j(t) = \tilde{A}_{21,j}(\rho)\tilde{e}_1(t) \tag{6-45}$$

$\tilde{A}_{21,j}(\rho)$ is the *jth* row of $\tilde{A}_{21}(\rho)$. From (6-42) to (6-44) we can get:

$$\begin{aligned}\dot{e}_{y,j}(t) = -k_1 sign\left(e_{y,j}(t)\right)\left|e_{y,j}(t)\right|^{\frac{1}{2}} - k_2 e_{y,j}(t) + z_j(t) \\ + \tilde{\xi}_j(t) - \tilde{R}_{2,j} f_v(t,\rho)\end{aligned} \tag{6-46}$$

$$\dot{z}_j(t) = -k_3 sign\left(e_{y,j}(t)\right) - k_4 e_{y,j}(t) \tag{6-47}$$

Where $j = 1,2 \ldots, p$. Define the following equation:

$$\tilde{z}_j(t) \coloneqq z_j(t) + \tilde{\xi}_j(t) - \tilde{R}_{2,j} f_v(t,\rho) \tag{6-48}$$

Then (6-46) and (6-47) can be expressed as:

$$\dot{e}_{y,j}(t) = -k_1 sign\left(e_{y,j}(t)\right)\left|e_{y,j}(t)\right|^{\frac{1}{2}} - k_2 e_{y,j}(t) + \tilde{z}_j(t) \tag{6-49}$$

$$\dot{\tilde{z}}_j(t) = -k_3 sign\left(e_{y,j}(t)\right) - k_4 e_{y,j}(t) + \varphi_i(t) \tag{6-50}$$

where

$$\varphi_i(t) = \dot{\tilde{\xi}}_j(t) - \tilde{R}_{2,j}\dot{f}_v(t,\rho) \tag{6-51}$$

It is not difficult to obtain:

$$
\begin{aligned}
|\varphi_i(t)| &< \left\|\dot{\tilde{\xi}}_j(t)\right\| + \left\|\tilde{R}_{2,j}\right\|\left\|\dot{f}_v(t,\rho)\right\| \\
&\leq \left\|\frac{\partial \tilde{A}_{21,j}}{\partial \rho}\right\| \|\dot{\rho}\|\|\tilde{e}_1(t)\| + \left\|\tilde{A}_{21,j}\right\|\left\|\dot{\tilde{e}}_1(t)\right\| \\
&+ \left\|\tilde{R}_{2,j}\right\|\left\|\dot{f}_v(t,\rho)\right\|
\end{aligned} \tag{6-52}
$$

Provided the upper part system of the system (6-41) is stable, then $\|\tilde{e}_1(t)\|$ and $\left\|\dot{\tilde{e}}_1(t)\right\|$ are bounded. Assuming $\left\|\dot{f}_v(t,\rho)\right\|$ is bounded, $\tilde{A}_{21}(\rho)$ is affine to ρ, the LPV parameter varying rate $\dot{\rho}$ is bounded. When a large enough parameter ε is chosen, then the inequality $|\varphi_i(t)| < \varepsilon$ holds. In fact, the expressions (6-49) and (6-50) can be seen as a super-twisting algorithm, which can be found in (Moreno & Osorio, 2008). In this reference the parameter setting is defined as follows:

$$k_1 > 2\sqrt{\varepsilon} \tag{6-53}$$

$$k_2 > 0 \tag{6-54}$$

$$k_3 > \varepsilon \tag{6-55}$$

$$k_4 > \frac{(k_2)^2((k_1)^3 + \frac{5}{4}(k_1)^2 + \frac{5}{2}(k_3 - \varepsilon))}{k_1(k_3 - \varepsilon)} \tag{6-56}$$

And after finite time, $e_{y,j} = \dot{e}_{y,j} = 0$ will be attained according to the conclusions in (Moreno & Osorio, 2008). Therefore, in (6-49), $\tilde{z}_j(t) = 0$ will be obtained in finite time. From its definition in (6-48),

$$z_j(t) = \tilde{R}_{2,j} f_v(t,\rho) - \tilde{\xi}_j(t) \tag{6-57}$$

From the upper equations in (6-41), $\dot{\tilde{e}}_1(t) = \tilde{A}_{11}(\rho)\tilde{e}_1(t)$. Since $\tilde{A}_{11}(\rho)$ is quadratically stable, then $\tilde{e}_1(t) \to 0$. Then from (6-45) and (6-57), it is obvious:

$$z(t) \to \tilde{R}_2 f_v(t,\rho) \tag{6-58}$$

where $z(t) = \left[z_1, z_2 \ldots z_p\right]^T$ is described in (6-43). Then the virtual fault $f_v(t,\rho)$ can be estimated through

$$\hat{f}_v(t) = \tilde{R}_2^{\dagger} z(t) \tag{6-59}$$

where $\tilde{R}_2^{\dagger}$ is the pseudo-inverse of $\tilde{R}_2$, that is $\tilde{R}_2^{\dagger} = (\tilde{R}_2^T \tilde{R}_2)^{-1} \tilde{R}_2^T$. Note that $\tilde{R}_2$ is full rank and $E(\rho)$ is invertible. Therefore, by using $E(\rho) f_a(t) \coloneqq f_v(t, \rho)$, which has been defined before, the actuator fault estimation of a LPV system can be expressed as follows:

$$\hat{f}_a(t) = E(\rho)^{-1} \hat{f}_v(t) \tag{6-60}$$

Through (6-59) the estimation of a LPV system can be expressed as follows:

$$\hat{f}_a(t) = E(\rho)^{-1} \tilde{R}_2^{\dagger} z(t) \tag{6-61}$$

In this Section, the fault reconstruction is conducted in a scalar way, which makes the calculation clear and easy to be applied using hardware description language.

6.5.2 Sensor fault estimation

Considering the LPV system with sensor fault represented by the equations:

$$\dot{x}(t) = A(\rho)x(t) + B(\rho)u(t) \tag{6-62}$$

$$y(t) = Cx(t) + F_2 f_s(t) \tag{6-63}$$

where $f_s(t) \in R^r$ represents sensor faults and $F_2 \in R^{p \times r}$. The output equation can be rewritten as (6-64) to express the nominal and faulty parts separately.

$$y(t) = \begin{bmatrix} y_1(t) \\ y_2(t) \end{bmatrix} = \begin{bmatrix} C_1 \\ C_2 \end{bmatrix} x(t) + \begin{bmatrix} 0 \\ I \end{bmatrix} f_s(t) \tag{6-64}$$

where $C_1 \in R^{(p-r) \times n}, C_2 \in R^{r \times n}, C = \begin{bmatrix} C_1 \\ C_2 \end{bmatrix}, F_2 = \begin{bmatrix} 0 \\ I \end{bmatrix}$. Now reconstruct the faulty part in order to estimate $f_s(t)$. A new state $z_f(t) \in R^r$ is constructed:

$$\dot{z}_f(t) = -A_f z_f(t) + A_f y_2(t) \tag{6-65}$$

where the $-A_f \in R^{r \times r}$ is a stable matrix. Put the expression of $y_2(t)$ from (6-64) into (6-65), the new system can be written as:

$$\begin{bmatrix} \dot{x}(t) \\ \dot{z}_f(t) \end{bmatrix} = \begin{bmatrix} A(\rho) & 0 \\ A_f C_2 & -A_f \end{bmatrix} \begin{bmatrix} x(t) \\ z_f(t) \end{bmatrix} + \begin{bmatrix} B(\rho) \\ 0 \end{bmatrix} u(t) + \begin{bmatrix} 0 \\ A_f \end{bmatrix} f_s(t) \tag{6-66}$$

where $x_a = \begin{bmatrix} x(t) \\ z_f(t) \end{bmatrix}$, $A_a(\rho) = \begin{bmatrix} A(\rho) & 0 \\ A_f C_2 & -A_f \end{bmatrix}, B_a(\rho) = \begin{bmatrix} B(\rho) \\ 0 \end{bmatrix}, F_a = \begin{bmatrix} 0 \\ A_f \end{bmatrix}$. Then replace $y_2(t)$ in (6-64) with (6-65),

$$\begin{bmatrix} y_1(t) \\ z_f(t) \end{bmatrix} = \begin{bmatrix} C_1 & 0 \\ 0 & I_r \end{bmatrix} \begin{bmatrix} x(t) \\ z_f(t) \end{bmatrix} \tag{6-67}$$

The new system formed by (6-66) and (6-67) is in the same form as Eq. (6-20). By replacing $(A(\rho), R, C)$ in Section 6.5.1 with $A_a(\rho), F_a, C_a$, an observer can be constructed as in Section 6.5.1 the same way, a further transformation needed is stated in (Alwi et al., 2012).

6.6 Case study for the induction motor system

In this Section an induction motor system with control voltage signal bias (which is demonstrrated in Figure 6-5) will be dealt with using the LPV sliding mode observer described in this Chapter. The induction motor model has been introduced in detail in the Chapter 3. The parameter setting for this motor has also been described in Chapter 2. This simulation was carried out using Matlab and Simulink. The original induction motor plant was described as a 4th order nonlinear system with parameters of induction motor 1 described in Section 2.2.1. But in this Chapter it is described as a LPV plant with a varying parameter: the rotor speed ω. Due to the special structure of the induction motor state space equation, LPV modelling is not required.

The state variables of the system are $[\varphi_{r\alpha}, \varphi_{r\beta}, i_{s\alpha}, i_{s\beta}]^{\mathrm{T}}$(which represent the α, β axis rotor flux and α, β axis state currents). The inputs of the system are $[u_{s\alpha}, u_{s\beta}]$ (which represent the α, β axis voltage). In this simulation study the outputs of the LPV system are $[\, i_{s\alpha}, i_{s\beta}]^T$. In this case the power supply fault occur in the β axis voltage $u_{s\beta}$. The state space model is described by

$$\begin{bmatrix}\dot{\varphi}_{r\alpha}\\ \dot{\varphi}_{r\beta}\\ i_{s\alpha}\\ i_{s\beta}\end{bmatrix}=\begin{bmatrix} -\frac{R_r}{L_r} & -n_p\omega & \frac{R_r}{L_r}M & 0\\ -n_p\omega & -\frac{R_r}{L_r} & 0 & \frac{R_r}{L_r}M\\ \frac{MR_r}{\sigma L_s {L_r}^2} & \frac{n_p R_r}{\sigma L_s L_r}\omega & -\frac{{L_r}^2 R_s+M^2R_r}{\sigma L_s {L_r}^2} & 0\\ -\frac{n_p R_r}{\sigma L_s L_r}\omega & \frac{MR_r}{\sigma L_s {L_r}^2} & 0 & -\frac{{L_r}^2 R_s+M^2R_r}{\sigma L_s {L_r}^2}\end{bmatrix} \quad (6\text{-}68)$$

$$\cdot\begin{bmatrix}\varphi_{r\alpha}\\ \varphi_{r\beta}\\ i_{s\alpha}\\ i_{s\beta}\end{bmatrix}+\begin{bmatrix}0 & 0\\ 0 & 0\\ -\frac{1}{\sigma L_s} & 0\\ 0 & -\frac{1}{\sigma L_s}\end{bmatrix}\cdot\begin{bmatrix}u_{s\alpha}\\ u_{s\beta}\end{bmatrix}$$

With the varying parameter $\rho=\omega$, the LPV model of the electrical system is given by

$$A(\rho)=A_0+A_1(\rho) \quad (6\text{-}69)$$

$$B(\rho)=B_0+B_1(\rho) \quad (6\text{-}70)$$

where

$$A_0=\begin{bmatrix}-11.7 & 0 & 3.5 & 0\\ 0 & -11.7 & 0 & 3.5\\ 291.7 & 0 & -168.3 & 0\\ 0 & 291.7 & 0 & -168.3\end{bmatrix}$$

$$A_1(\rho)=\begin{bmatrix}0 & -4\rho & 0 & 0\\ 4\rho & 0 & 0 & 0\\ 0 & 50\rho & 0 & 0\\ -50\rho & 0 & 0 & 0\end{bmatrix}$$

$$B(\rho) = \begin{bmatrix} 0 & 0 \\ 0 & 0 \\ 12.5 & 0 \\ 0 & 12.5 \end{bmatrix}$$

$$C = \begin{bmatrix} 0 & 0 & 1 & 0 \\ 0 & 0 & 0 & 1 \end{bmatrix}$$

$$F_1(\rho) = \begin{bmatrix} 0 \\ 0 \\ 0 \\ 1 \end{bmatrix} \cdot 12.5$$

This satisfies $rank(CD) = 1$, and it is full rank.

In order to design the LPV observer, it is necessary to calculate the inequality (6-36) first. At the same time, $P_1 > 0$, while $L_1 \in R^{2\times1}, P_1 \in R^{2\times2}$. The Matlab function "msfsyn" was used to solve the inequality (6-36) and $P_1 > 0$ together. The range of the varying parameter, i.e. the rotor speed varies beetween 0 and 1500 rpm. Through the calculation, the following result is produced:

$$L_1 = \begin{bmatrix} 0.9145 \\ 1.0214 \end{bmatrix}$$

$$P_1 = \begin{bmatrix} 0.9842 \times 10^{-5} & 0 \\ 0 & 1.0012 \times 10^{-5} \end{bmatrix}$$

The design of the matrix P_1 is shown in Eq. (6-40)

$$\tilde{A}_{22}^{s} = -I_2$$

where

$$k_3 = 1$$

As shown in Eq. (6-31), G_n can be expressed as $G_n = T_0^{-1}T_L^{-1}\tilde{G}_n$, then G_n is

$$G_n = \begin{bmatrix} -0.9145 & 0 \\ 0 & 1.0214 \\ 1 & 0 \\ 0 & 1 \end{bmatrix}$$

The corresponding individual gains are:

$$k_1 = 0.56, k_2 = 1.41, k_4 = 6.16$$

Based on the above parameter settings, the fault reconstruction results are shown in Section 6.6.1 and Section 6.6.2. The fault considered in this Chapter is an additive actuator fault, i.e. the power supply fault occurs in the β axis voltage $u_{s\beta}$. The simulation results are able to show almost perfect performance of the fault reconstruction.

Remark 6-2:

This approach is an extension application based on the work of Chapter 5. The "output injection signal" is used to reconstruct the actuator and sensor faults in the induction motor system. The differences between the contributions of Chapter 6 and Chapter 5 are:

1) This Chapter is based on the nonlinear system, though the LPV is regarded as a linear time-varying application under the LPV framework;
2) This Chapter considers the induction motor rotor speed ω as a varying parameter, which introduces system coupling factors, rendering the non-linear simulation closer to the real induction motor system.

6.6.1 Result of sensor fault estimation

In the sensor fault estimation, the Figure 6-5(a) and 6-6(a) reflect the estimation effect while the Figure 6-5(b) and 6-6(b) show the zoom figure in specific time window to show the fault estimation effect under different speed scenarios. The current sensor fault estimation is more accurate when the fault signal is small enough. The estimation error becomes larger when reference fault signal turns larger. This phenomenon is reflected in the corresponding (a) figures.

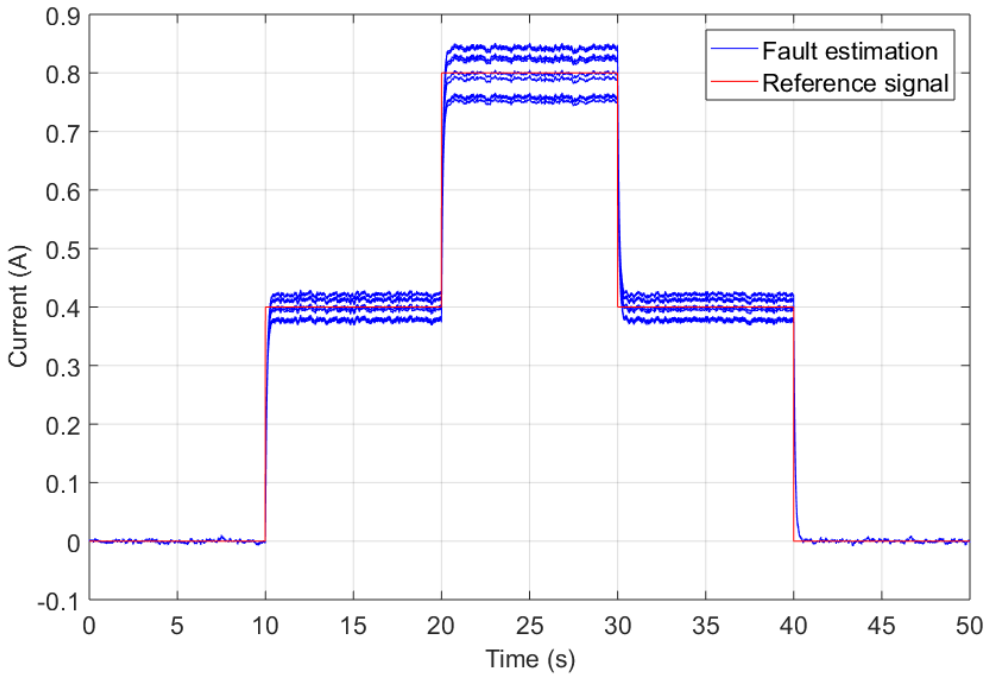

Figure 6-5(a) Fault reconstruction in current sensor fault

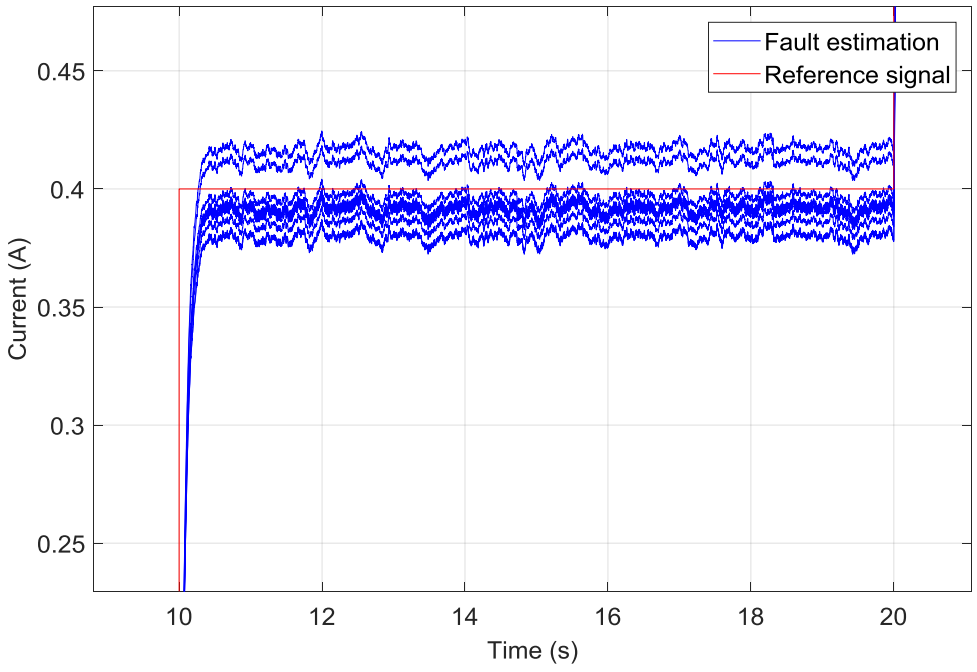

Figure 6-5(b) Fault reconstruction in current sensor fault (Zoom figure)

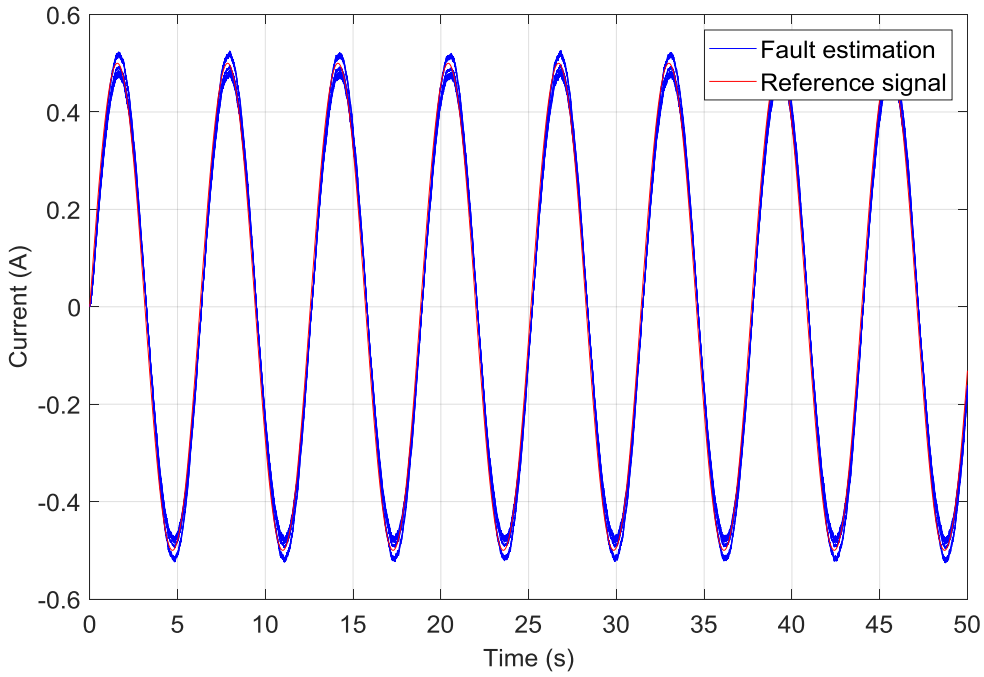

Figure 6-6(a) Fault reconstruction in current sensor fault

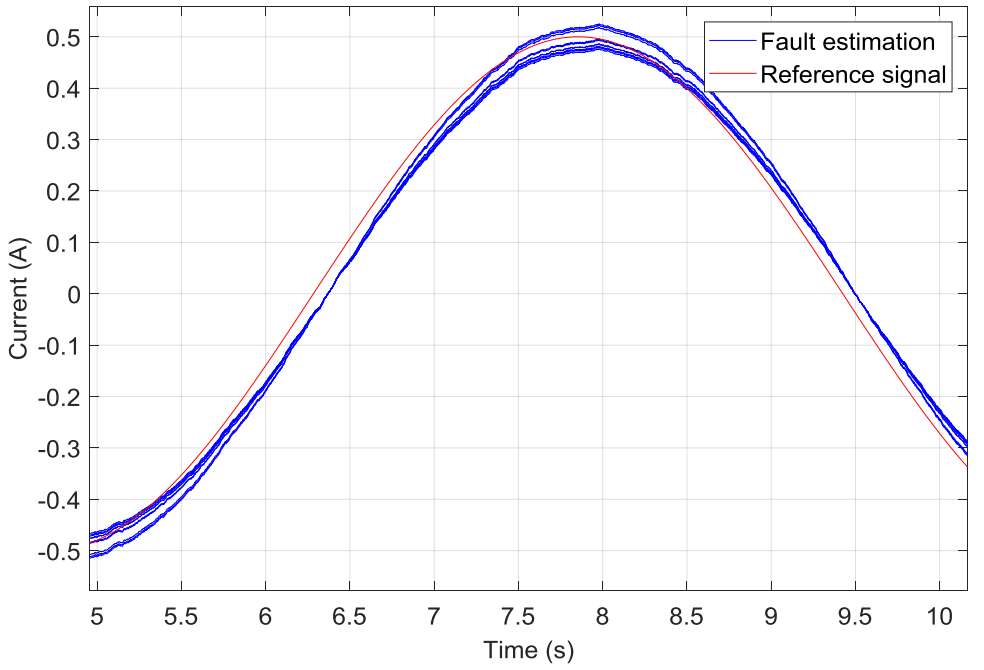

Figure 6-6(b) Fault reconstruction in current sensor fault (Zoom figure)

6.6.2 Result of actuator fault estimation

The Figure 6-7(a) and 6-8(a) represents the estimation of actuator fault, and the Figure 6-7(b) and 6-8(b) represents the zoom figure of these two figures. The result reflects the high robustness property of SMO against uncertainty within matched channel. The zoom figures show that the actuator fault estimation under different speed variation keeps stable .

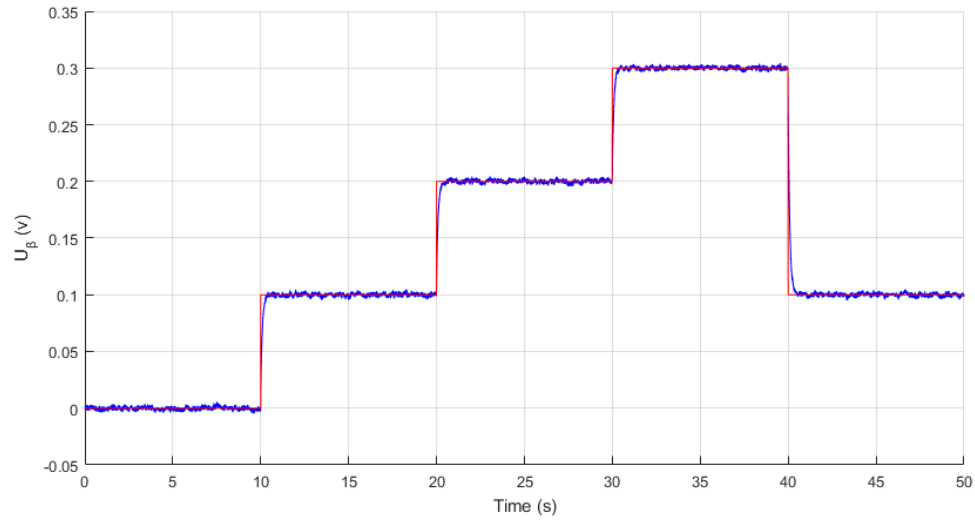

Figure 6-7(a) Fault reconstruction in β axis voltage $u_{s\beta}$

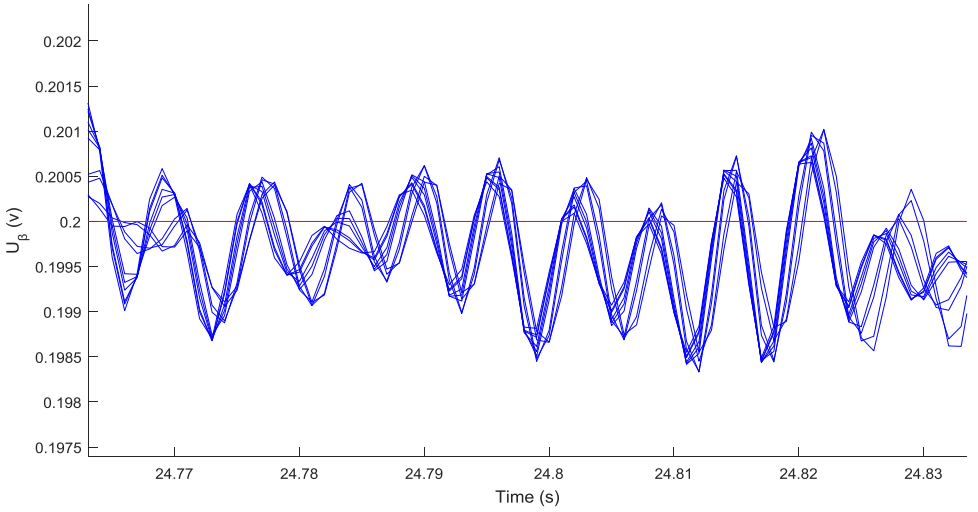

Figure 6-7(b) Fault reconstruction at different vertices in β axis voltage $u_{s\beta}$ (Zoom figure)

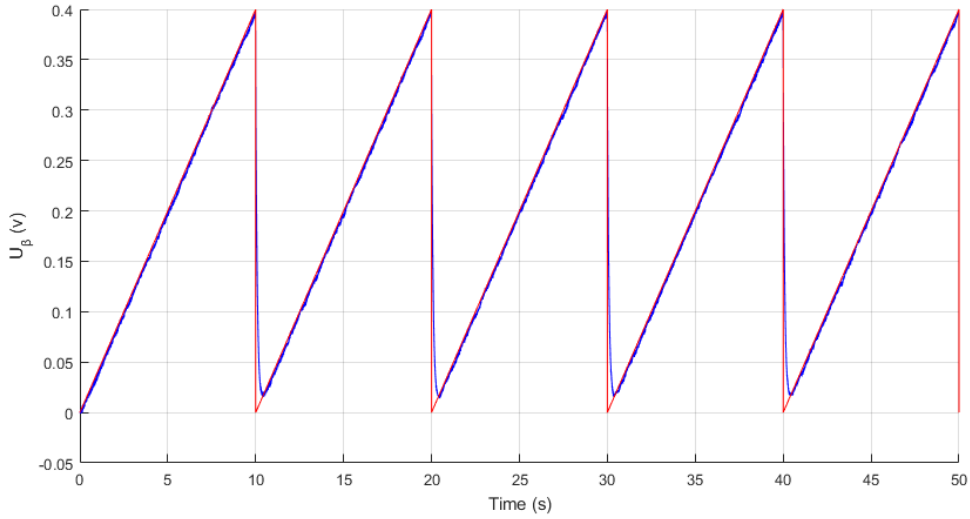

Figure 6-8(a) Fault reconstruction in β axis voltage $u_{s\beta}$

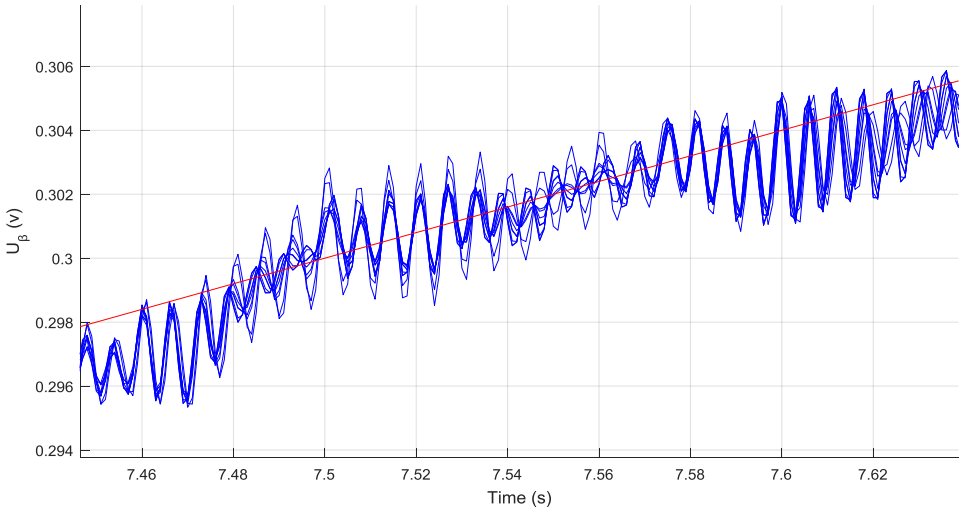

Figure 6-8(b) Fault reconstruction at different vertices in β axis voltage $u_{s\beta}$ (Zoom figure)

6.7 Summary

In this Chapter an LPV estimation approach is introduced using the 4th order nonlinear induction motor system when considering the rotor speed ω as a varying parameter. It is applied in the design of the actuator and sensor fault estimation. At this stage the work does not include FTC.

It is importat to note first of all that the typical types of LPV expressions have been given using simple examples to show the properties of the methods. The main LPV system types are summarised as the General LPV system, the Polytopic LPV system and the LFT form LPV systems.

Secondly, the sliding mode LPV observer is described. In the observer design, the system matrices $A(\rho), B(\rho), D(\rho)$ and a fixed input distribution matrix R have been used. The fixed input distribution matrix R was used to simplify the process of calculating the observer gains L_1, P_1, G_n and to ensure a stable reduced order sliding motion. In order to reconstruct the actuator and sensor faults, the "output error injection signal" was used again in this Chapter. The power of this estimation approach as applied to the induction motor non-linear system with sensor faults, it is shown in a case study.

Thirdly, after the system is transformed into a reduced order system, a second order LMI is formulated to generate the observer gains by using the Matlab LMI toolbox. As the case study for this Chapter, an induction motor system with a power supply fault in the stator voltage has been studied at the end of this Chapter to show potential of using LPV estimation approach. The LPV formulation is used as a form of "bridge" between the linear estimation (considering the linear system without parameter changes) and the nonlinear estimation.

Chapter 7 develops the fully nonlinear induction motor system with strong coupling nonlinearity based on the $d-q$ coordinate system. Unmatched faults are considered in the application of the adaptive back-stepping control approach. The aim of Chapter 7 is to develop an AFTC strategy for induction motor fault tolerant control based on the adaptive back-stepping control.

Chapter 7: Adaptive back-stepping FTC of a nonlinear induction motor

7.1 Introduction

Chapter 5 introduces two FE approaches, adaptive estimation and sliding mode estimation for potential application to an induction motor system. The limitation of the study in Chapter 5 is that only a linear induction motor model is considered, i.e. the rotation speed ω is considered constant. This is clearly not representative of the real system in which ω is usually allowed to vary (e.g. from start-up, a stopping procedure or because of speed set point changes which depend on the application).

Chapter 6 presents the LPV sliding mode FE approach for the LPV considering the rotation speed ω variations of the nonlinear induction motor system. It is shown that there are advantages of using the LPV approach, however the main limitation is that the nonlinear dynamics of the machine are not sufficiently represented. This is especially true when there exist faults or uncertainties in the system. However, the LPV modelling strategy can handle the challenges which arise from discriminating between the faults and uncertainties when either or both are matched or unmatched. The meaning and significance of matching in this context is defined in Section 5.1.

In this Chapter, an adaptive back-stepping control approach is used to develop on FTC structure which can be applied to the nonlinear induction motor system. In the truly non-linear system some faults/uncertainties are present in the system as unmatched signal effects for which the concepts described in Chapters 5 and 6 are not directly applicable. By applying adaptive back-stepping control a form of AFTC is produced to solve the matching/unmatching problems associated with the uncertainty/faults.

The purpose of the adaptive back-stepping FTC is to examine the effectiveness and performance of this algorithm with the task of speed tracking, as well as the performance with low-speed variations.

At the beginning of this Chapter, properties of the back-stepping approach are introduced, and a simple numerical example is given as a tutorial introduction to the subject. The performance of the nonlinear induction motor system under different speed conditions is examined carefully. Results are given to illustrate the effects of the control design, demonstrating that the back-stepping approach meets the desired FTC objectives.

7.2 Background of back-stepping FTC

The basic concept of back-stepping control is to divide a complex nonlinear system into subsystems with suitable dimensions. According to the design using a Lyapunov function and virtual control input, and repeated appication of the back-stepping process, the final control law is generated to maintain overall system stability. This approach uses a Lyapunov strategy together with adaptive approach. Based on the back-stepping structure considered in combination with the other approaches, it is usually used to solve the problems of (1) nonlinear system control, (2) nonlinear system with uncertain parameter variations, and (3) nonlinear system control with both unmatched uncertainty/faults.

- **Back-stepping approach preliminaries**

Based on the fault scenarios presented in Chapter 3, additive faults i.e. sensor, actuator faults are studied through FE approaches, i.e. the Adaptive observer and SMO. However, from the standpoint of control, the faults can be divided into matched and unmatched faults, as summarised in Section 3.2.1. Back-stepping is a good alternative for dealing with system control with unmatched fault since it is able to divide a system into subsystems, then realize control locally and globally step by step (Koshkouei & Zinober, 2000a; Estrada & Fridman, 2010a; Estrada & Fridman, 2010b; Yao et al., 2014). The application of backstepping should satisfy a strict feedback form or semi-strict feedback form (as defined after the following example) (Tan & Chang, 1999), it is shown as follows:

$$\dot{\boldsymbol{x}} = f_0(\boldsymbol{x}) + g_0(\boldsymbol{x})z_1 + \Delta_0(x,t)$$

$$\dot{z}_1 = f_1(\boldsymbol{x}, z_1) + g_1(\boldsymbol{x}, z_1)z_2 + \Delta_1(x,t)$$

...

$$\dot{z}_n = f_n(\boldsymbol{x}, z_1, \dots z_n) + g_n(\boldsymbol{x}, z_1, \dots z_n)u + \Delta_n(x, t)$$

where $\boldsymbol{x}$ is the state variable, u is the control input, f_i are the unknown smooth functions of $\boldsymbol{x}, z_1, \dots z_n$. The back-stepping components $z_1, \dots z_n$ are state variables of subsystems. $\Delta_i(x, t)$ is disturbance component. The system is strict feedback form if $\Delta_i(x, t) = 0$, other wise it is semi-strict feedback form.

In order to deal with the control problem of a nonlinear system with unmatched fault, the paper (Estrada & Fridman, 2010a) proposed a new algorithm based on block control and higher order sliding mode control. In principle, the paper adopts the back-stepping approach as a framework, with a combination of sliding mode control, to realize the robust control with regard to a dynamic system with unmatched faults. The dynamic system in this paper is divided into several subsystems and therefore virtual control signals are designed for each subsystem. Considering the unmatched fault, a higher order sliding mode controller is used in one of the subsystems to tackle the unmatched fault. In (Koshkouei & Zinober, 2000b) an adaptive back-stepping algorithm has been proposed for a class of nonlinear uncertain systems with disturbances, and it can be converted to a semi-strict feedback form. In this method the adaptive design appears in both the back-stepping and sliding mode control design process, which makes the algorithm suitable for a nonlinear system with both unmatched and matched uncertainty. In other words, this paper proposed an integrated control system design with regard to different types of faults.

Two inspirations are as follows: (1) Use back-stepping as a framework to tackle unmatched faults; (2) Deal with different types of fault/uncertainty together (including unmatched faults). The back-stepping control structure is illustrated in Figure 7-1.

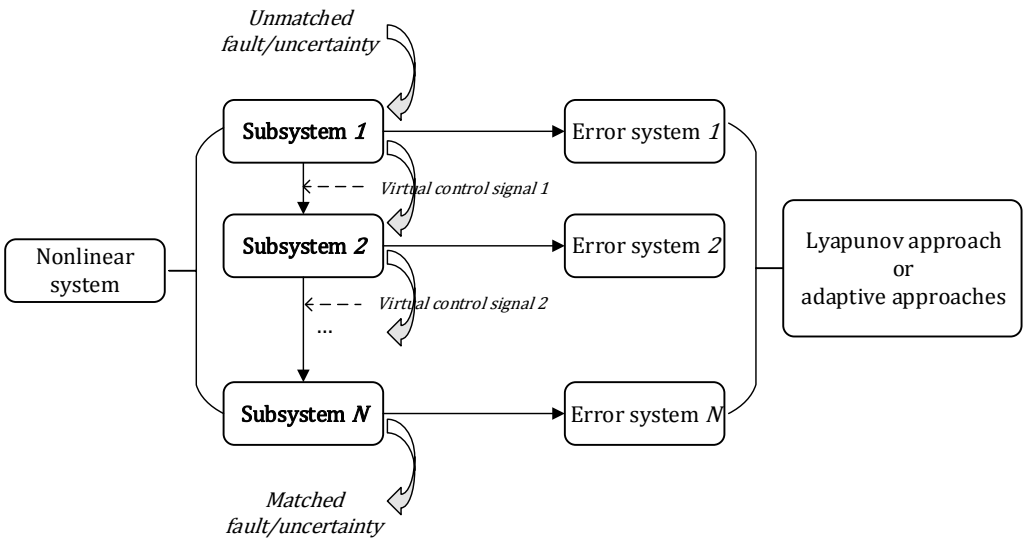

Figure 7-1 Unmatched Fault/uncertainty compensation through back-stepping

The back-stepping control approach has been applied on induction motor systems in the work of (Shieh & Shyu, 1999; Tan & Chang, 1999; Lin et al., 2002), where the speed, flux, and torque are always control aims. In these works, control performance and robustness properties against unmatched faults are regarded as an important evaluation. In this thesis, the back-stepping approach is considered to realize FTC for the nonlinear induction motor system considering unmatched fault.

- **Nonlinear system control**

In back-stepping control, the basic idea is to divide the nonlinear system into several subsystems if it satisfies the strict or semi-strict feedback form. In each step of the back-stepping control the Lyapunov approach is applied, the local subsystem stabilization is realized step by step, so that finally global stabilization is realized.

In an induction motor system with both mechanical and electrical subsystems, there are highly coupled components between the two systems which should be taken into account in estimation and control designs where non-linearity and faults are considered. An important example, is the coupling of rotor flux with rotor speed variations. Even more significantly this coupling causes strong nonlinear effects simultaneously in different regions of system operation. This is taken seriously by researchers considering the speed requirements and state variables, under the consideration of uncertainty/fault (Hasegawa et al., 2003; Campos-Delgado et al., 2005; Barut et al., 2007; Hinkkanen et al., 2010).

- **Nonlinear system control with matched/unmatched uncertainty/fault**

Based on the purely nonlinear system control, it is necessary to consider more about the nonlinear system with uncertain parameters. Generally, there are two methods to deal with unceratin parameters: (1) Use control robust approaches to minimize the effect of uncertain parameters; (2) Use control methods that encompass the dynamics corresponding to uncertain parameters.

If robustness against uncertainty is within the nonlinear system control, the back-stepping approach can be applied using robust approaches. For example, SMC can be applied on the nonlinear system control with robustness since SMC handles matched uncertainty in a natural way, this is discussed in Section 5.3.1.

In a nonlinear system control, if uncertainty/fault dynamics are to be considered (see Chapter 5: Adaptive FE design considering fault dynamics), in this case, only robustness against bounded uncertainty need not be considered. For example, the dynamics of the load torque variation (unmatched fault) of the induction motor is taken into consideration using the back-stepping approach.

7.3 Problem formulation of induction motor control

7.3.1 Challenges of induction motor FTC

The induction motor has been widely applied across almost all the industrial fields, since it is a good candidate for electrical power train with low cost and high reliability.

Induction motor control techniques focused on pursuing good speed, position and torque control performance under highly nonlinear and coupled conditions. But the control performance of the induction motor is still influenced by uncertainties and disturbances, which are usually composed of unpredictable parameter variations, external load disturbances, and system nonlinearities (Chen & Patton, 1999). Therefore, various studies have been carried out on induction motor control, such as predictive control, adaptive control, robust control, fuzzy control and direct torque control (Bennett, 1998; Raisemche et al., 2014). Although a lot of effort has been spent on solving these problems by using

advanced control algorithms, the efficient and effective combinations with industrial induction motor has yet to be developed.

For industry application, sensor-less control is the most popular topic in motor control under industry backgrounds; researchers pursue good system performance and high efficiency by reducing the use of pulse width modulation (PWM) modulator and speed measurement components (Kim & Youn, 2002; Vogelsberger et al., 2010). The most important control strategies for this topic are focused on finding new ways to tackle problems in field oriented control (FOC), direct torque control (DTC) and predictive torque control (PTC). Both FOC and DTC can be used to achieve good performance at steady and transient states, and PTC is also able to present similar performance and is seen as a strong alternative in electrical drive systems. PTC has large amounts of calculation compared with DTC and FOC (Stando et al., 2014). But nearly all the methods rely on the use of speed encoder and measurement sensors, though the dependence is different between each other. So various observer based approaches have been applied, such as extended Kalman filter (EKF), neural networks, reduced order observer, model reference adaptive system (MRAS) (Chen et al., 2013) etc. A major concern on fault tolerant ability of sensor-less control is to continue to grow (Wang et al., 2014; Morawiec, 2015).

As discussed in Section 3.2 induction motor faults are mainly caused by over-current, resistance variation，over-heating, dirt, moisture and vibration (Fekih, 2008). Faults due to these factors may cause nonlinear changes of the motor parameters, including load torque offset, resistance variations and sensor measurement offsets, and so on (Bennett et al., 1999; Soualhi et al., 2013). In this Chapter, unmatched faults or uncertainties are considered to act on the system via different channels. According to definition of a matched fault (see Section 3.2), the stator resistance variation naturally satisfies the so-called matching condition since it acts on the control inputs. The load torque offset applied on the system is an unmatched fault since it does not act on the channel of control input and does not satisfy the matching condition (Tan & Chang, 1999; Campos-Delgado et al., 2008).

Considering the electrical and mechanical faults, as well as the nonlinearities in the induction motor system, an approach is considered to take care of these factors

simultaneously. The above statements concern the development of induction motor fault tolerant control. The Aim of this Chapter is to provide an effective back-stepping fault tolerant control algorithm for a nonlinear induction motor system with unmatched faults or uncertainties. The purpose of this algorithm is to provide fault tolerant capability for industrial induction motor applications.

This Chapter is structured as follows: Section 7.3 gives a problem description of the induction motor system used in this study; Sections 7.4.1, 7.4.2, 7.4.3 present the design of the adaptive back-stepping FTC. The simulation results of Section 7.5, show the FTC performance under different speed conditions. A comparison has been made corresponding to the various conditions leading to a Summary in Section 7.6.

7.3.2 Field oriented transformation of induction motor model

The nonlinear induction motor model is composed of an electrical system and a mechanical system, which has been given in detail is the Chapter 3. The electrical behaviour of the induction motor system is described in the (α, β) coordinate in a stationary reference framework with the stator. In this context, the well-known induction motor Park model is given in Section 3.2.2. Through this transformation, (α, β) model in the fixed stator frame is transformed into a (d, q) coordinate which rotates with the rotor flux. A strict feedback form is formed during this transformation (Shen & Shi, 2015), which is introduced in Section 7.2. It allows the use of back-stepping control on the induction motor system:

$$\frac{d\omega}{dt} = \frac{\mu}{J}\varphi_d i_q - \frac{T_L}{J}, \tag{7-1}$$

$$\frac{di_q}{dt} = -\eta i_q - \beta n_p \omega \varphi_d - n_p \omega i_d - \alpha M \frac{i_q i_d}{\varphi_d} + \frac{1}{\sigma L_s} u_q, \tag{7-2}$$

$$\frac{d\varphi_d}{dt} = -\alpha \varphi_d + \alpha M i_d, \tag{7-3}$$

$$\frac{di_d}{dt} = -\eta i_d - \alpha\beta \varphi_d + n_p \omega i_q + \alpha M \frac{{i_q}^2}{\varphi_d} + \frac{1}{\sigma L_s} u_d, \tag{7-4}$$

$$\frac{d\rho}{dt} = n_p \omega + \alpha M \frac{i_q}{\varphi_d}, \tag{7-5}$$

where $\eta = \frac{M^2 R_r}{\sigma L_s {L_r}^2} + \frac{R_s}{\sigma L_s}, \rho = arctan(\frac{\varphi_\beta}{\varphi_\alpha})$.

The (d, q) model described by (7-1) to (7-5) is seen as two subsystems. The first subsystem is formed by (7-1) and (7-2), which is a system with the state vector (ω, i_q) and the control input u_q. The second subsystem is formed by (7-3) and (7-4), which is a system with the state vector (φ_d, i_d) and the control input u_d. The equation (7-5) is produced in the transformation of the IM system, which can be ignored here.

Assumption 7-1:

The states i_q, i_d, φ_d are measureable (where $\varphi_q = 0$ through the $d - q$ transformation).

7.3.3 Problem statement

In this Chapter, unmatched faults are considered acting on the nonlinear induction motor system. According to the definition of unmatched faults (Campos-Delgado et al., 2008), The matched faults enter the system through the same channel as the control input; the unmatched faults enter the system through different channel with the control input.

Actually, the stator resistance variation R_s naturally satisfies the so-called matching condition since it acts on the control inputs. Load torque offset T_L applied on the system is an unmatched fault since it does not act on same channel as the control input and hence it does not satisfy the matching condition (Tan and Chang, 1999; Campos-Delgado et al., 2008). In the induction motor model introduced above, the ordinary matched fault and the unmatched fault is defined as follows:

As shown in Fig. 7-1, the control objectives of this Chapter are to achieve rotor speed and rotor flux tracking with tolerance to the unmatched faults and disturbance arising from the nonlinear system. It is also important to verify the performance of this control system under low speed operation, and compare this with the performance at high speeds.

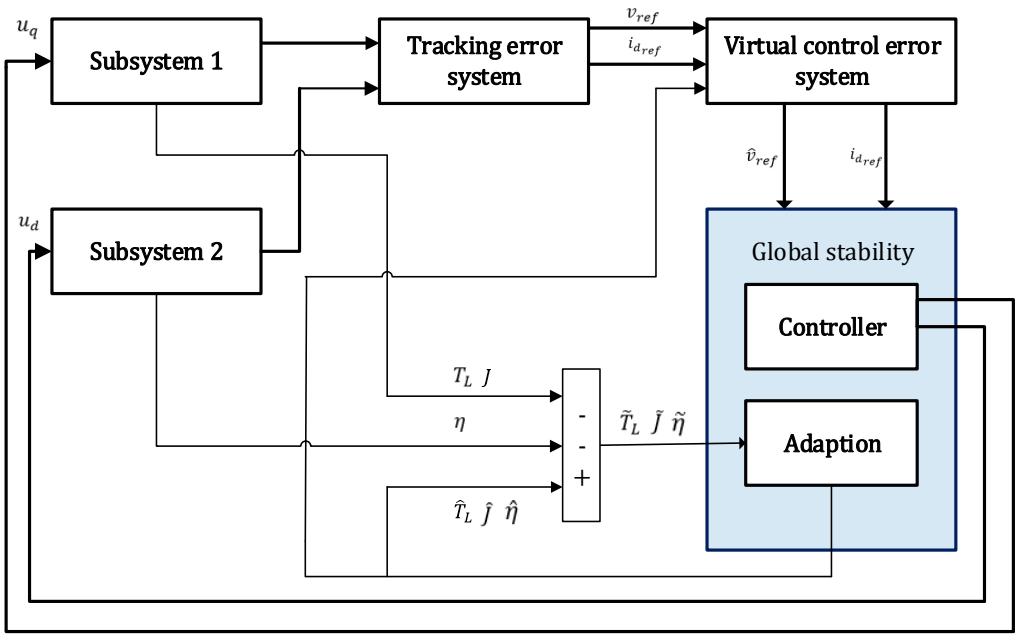

Figure 7-2 Adaptive back-stepping control of the induction motor system

The implementation and performance analysis of the adaptive back-stepping control is described in the following Sections.

There are several important points which should be noticed as follows:

1) An assumption has been made when this model is applied on the research of Chapter 6, which states that the states i_q, i_d, φ_d are measureable, where $\varphi_q = 0$ through the $d-q$ transformation.
2) The absolute value of the rotor flux speed $\frac{d\rho}{dt}$ minus rotor speed ω is usually named as the slip speed, which is proportional to the electromagnetic torque T and inversely proportional to the flux φ_d.
3) This field-oriented model described in Eq.(2-12) is advantageous for the implementation of some control algorithms, because the control variables (u_d, u_q) act on the currents (i_d, i_q) directly; for example, in the back-stepping control algorithm, the currents (i_d, i_q) can be considered as a pair of elements within an intermediate control vector.

7.4 Back-stepping control design

Based on the nonlinear system expressed in new coordinates, here the back-stepping approach is adopted to construct the FTC scheme for the nonlinear induction motor system. The rotor speed ω and the rotor flux φ_d is required to track the required trajectories. In the back-stepping control algorithm which will be introduced as follows, the nonlinearity of the induction motor system can be solved through the use of "Virtual control signals". In the controller design, the system has been divided into several subsystems. That means the multiple input multiple output system is divided into several single input single output systems.

7.4.1 Virtual control inputs generation (Step 1)

Based on the two subsystems described through Section (7.5), the back-stepping design is introduced as follows. In the first step, tracking errors and its dynamic systems are defined and suitable virtual control signals have to be decided.

The tracking errors for rotor speed and rotor flux has been defined as:

$$e_1 = \omega_{ref} - \omega \, , e_3 = \varphi_{ref} - \varphi_d$$

Hence, the error dynamic system can be described as

$$\dot{e_1} = \dot{\omega}_{ref} - \dot{\omega} = \dot{\omega}_{ref} - \frac{\mu}{J}\varphi_d i_q + \frac{T_L}{J}, \tag{7-6}$$

$$\dot{e_3} = \dot{\varphi}_{ref} - \dot{\varphi}_d = \dot{\varphi}_{ref} + \alpha\varphi_d - \alpha M i_d. \tag{7-7}$$

For the two subsystems, we choose $\varphi_d i_q$ and i_d as the *virtual control* signals. When the parameters *J* and T_L are known, the Lyapunov function related to the rotor speed and flux errors are defined as follows,

$$V_1 = \frac{1}{2}[{e_1}^2 + {e_3}^2] \tag{7-8}$$

Then (7-8) will be stabilized by

$$v_{ref} = (\varphi_d i_q)_{ref} = \frac{J}{\mu}\left[k_1 e_1 + \dot{\omega}_{ref} + \frac{T_L}{J}\right] \tag{7-9}$$

$$i_{d_{ref}} = \frac{1}{\alpha M}\left[k_3 e_3 + \dot{\varphi}_{ref} + \alpha\varphi_d\right]. \tag{7-10}$$

which will finish the proof of the following inequality by choosing suitable coefficients,

$$\dot{V}_1 = -k_1 {e_1}^2 - k_3 {e_3}^2 < 0. \tag{7-11}$$

with $k_1 > 0, k_3 > 0$ (the coefficients to be designed), the tracking can be realized when J and T_L are known. However, if they are unknown, it is necessary to consider the following form,

$$\hat{v}_{ref} = \frac{\hat{J}}{\mu}\left[k_1 e_1 + \dot{\omega}_{ref} + \frac{\hat{T}_L}{J}\right], \tag{7-12}$$

$$\mathrm{i}_{\mathrm{d_{ref}}} = \frac{1}{\alpha M}\left[k_3 e_3 + \dot{\varphi}_{ref} + \alpha\varphi_d\right]. \tag{7-13}$$

As stated in (7-12) and (7-13), the equivalent stator current references are given and the stator currents references should ensure the stator current control.

In the next step, the estimation of J and T_L are considered since they are uncertain paramters. The error functions of virtual control signals and its dynamic equations is to be deduced, in order to derive the error of the unknown parameters.

7.4.2 Currents control design (Step 2)

In Step 1, a stable dynamic speed and flux tracking error is assured, if and only if the virtual control errors are considered. Only through the use of the "virtual control signal", the subsystem can be designed sepetately. This forms the basis of the global stability design in the final step.

Define the error of virtual control signal,

$$e_2 = \hat{v}_{ref} - \varphi_d i_q = \frac{\hat{J}}{\mu}\left[k_1 e_1 + \dot{\omega}_{ref}\right] + \frac{\hat{T}_L}{J} - \varphi_d i_q, \tag{7-14}$$

$$e_4 = i_{d_{ref}} - i_d = \frac{1}{\alpha M}\left[k_3 e_3 + \dot{\varphi}_{ref} + \alpha\varphi_d\right] - i_d. \tag{7-15}$$

Then the error system is expressed as

$$\dot{e_1} = -k_1 e_1 + \frac{\mu}{J} e_2 + \frac{\tilde{J}}{J}\left[k_1 e_1 + \dot{\omega}_{ref}\right] - \frac{\tilde{T}_L}{J}, \tag{7-16}$$

$$\dot{e_3} = -k_3 e_3 + \alpha M e_4. \tag{7-17}$$

The dynamic system for errors e_2, e_4 are described as in (7-18) and (7-19), where the state voltages u_d, u_q are included, as follows

$$\begin{aligned} \dot{e}_2 &= \frac{\dot{\hat{J}}}{\mu}\left[k_1 e_1 + \dot{\omega}_{ref}\right] + \frac{\hat{J}}{\mu}\left[k_1 \dot{e}_1 + \ddot{\omega}_{ref}\right] + \frac{\dot{\tilde{T}}_L}{J} - \dot{\varphi}_d i_q - \varphi_d i_q \\ &= \varphi_1 - \frac{1}{\sigma L_s}\varphi_d u_q + \frac{\tilde{J}}{J}\varphi_2 + \frac{\tilde{T}_L}{J}\varphi_3 - \varphi_d i_q \tilde{\eta}, \end{aligned} \tag{7-18}$$

$$\dot{e}_4 = \frac{1}{\alpha M}\left[k_3 \dot{e}_3 + \ddot{\varphi}_{ref} + \alpha\dot{\varphi}_d\right] - i_d = \varphi_4 - \frac{1}{\sigma L_s} u_d - i_q \tilde{\eta}. \tag{7-19}$$

where

$$\begin{aligned} \varphi_1 = \frac{\dot{\hat{J}}}{\mu}\left[k_1 e_1 + \dot{\omega}_{ref}\right] + k_1 e_2 + \frac{\hat{J}}{\mu}\left[-{k_1}^2 e_1 + \ddot{\omega}_{ref}\right] + \frac{\dot{\tilde{T}}_L}{\mu} \\ - \left[-\alpha\varphi_d + \alpha M i_d\right] i_q \\ - \varphi_d\left[-\hat{\eta} i_q - \beta n_p \omega \varphi_d - n_p \omega i_d - \alpha M \frac{i_q i_d}{\varphi_d}\right] \end{aligned} \tag{7-20}$$

$$\varphi_2 = k_1 e_2 - \frac{k_1}{\mu}\hat{J}\left[k_1 e_1 + \dot{\omega}_{ref}\right], \tag{7-21}$$

$$\varphi_3 = -\frac{k_1}{\mu}\hat{J}, \tag{7-22}$$

$$\begin{aligned} \varphi_4 = \frac{1}{\alpha M}\left[k_3(-k_3 e_3 + \alpha M e_4) + \ddot{\varphi}_{ref} + \alpha(-\alpha\varphi_d + \alpha M i_d)\right] \\ - \left[-\hat{\eta} i_d + \alpha\beta\varphi_d + n_p \omega i_q + \alpha M \frac{{i_q}^2}{\varphi_d}\right]. \end{aligned} \tag{7-23}$$

In order to design the adaption and control algorithms together in the final step, it is necessary to take the actual control inputs u_d, u_q, as well as the matched and unmatched

faults into consideration in the final step. The Lyapunov approach is used to derive the actual control signals and those design parameters, i.e. $k_1, k_2, k_3, k_4, \gamma_1, \gamma_2, \gamma_3$ in the next step. It should be noted that k_1, k_2, k_3, k_4 arise from subsystem stability design, whilst $\gamma_1, \gamma_2, \gamma_3$ only involves within the adaption law design.

7.4.3 Global stability design using Lyapunov approach (Step 3)

To stabilize the whole system and obtain the control law and adaption law, a second Lyapunov function is designed based on the errors of speed, rotor flux and stator currents.

$$V = \frac{1}{2}\left[\sum_{j=1}^{j=4} {e_j}^2 + \frac{1}{\gamma_1 J}\tilde{J}^2 + \frac{1}{\gamma_2 J}{\tilde{T}_L}^2 + \frac{1}{\gamma_3 J}\tilde{\eta}^2\right]. \tag{7-24}$$

$\gamma_1, \gamma_2, \gamma_3$ are positive design parameters,

$$\begin{aligned}
\dot{V} = \sum_{j=1}^{j=4} e_j \dot{e}_j + \frac{\tilde{J}}{\gamma_1 J}\dot{\hat{J}} + \frac{\tilde{T}_L}{\gamma_2 J}\dot{\hat{T}}_L + \frac{\tilde{\eta}}{\gamma_3 J}\dot{\hat{\eta}} \\
= \sum_{j=1}^{j=4} k_j {e_j}^2 + \frac{\mu}{J} e_1 e_2 \\
+ e_2\left[k_2 e_2 + \varphi_1 - \frac{1}{\sigma L_s}\varphi_d u_q\right] \\
+ e_4\left[\alpha M e_3 + k_4 e_4 + \varphi_4 - \frac{1}{\sigma L_s} u_d\right] \\
+ \frac{\tilde{J}}{J}\left[-e_1\left(k_1 e_1 + \dot{\omega}_{ref}\right) + e_2\varphi_2 + \frac{1}{\gamma_1}\dot{\hat{J}}\right] \\
+ \frac{\tilde{T}_L}{J}\left[-e_1 + e_2\varphi_3 + \frac{1}{\gamma_2}\dot{\hat{T}}_L\right] \\
+ \frac{\tilde{\eta}}{J}\left[\frac{\dot{\hat{\eta}}}{\gamma_3} - J e_2 \varphi_d i_q - J e_4 i_d\right]
\end{aligned} \tag{7-25}$$

k_2, k_4 are also positive design constants. Hence, the controller follows as:

$$u_q = \frac{\sigma L_s}{\varphi_d}[k_2 e_2 + \varphi_1] \tag{7-26}$$

$$u_d = \sigma L_s[\alpha M e_3 + k_4 e_4 + \varphi_4]. \tag{7-27}$$

To ensure that the (7-25) is negative definite, the adaption law of the faults is set up as follows.

$$\dot{\hat{J}} = -\gamma_1\left[-e_1\left(k_1 e_1 + \dot{\omega}_{ref}\right) + e_2\varphi_2\right], \tag{7-28}$$

$$\dot{\hat{T}}_L = -\gamma_2[-e_1 + e_2\varphi_3], \tag{7-29}$$

$$\dot{\hat{\eta}} = \gamma_3 J\left[e_2\varphi_d i_q + e_4 i_d\right]. \tag{7-30}$$

where the $\hat{R}_s$ is given by using

$$\hat{\eta} = \frac{M^2 R_r}{\sigma L_s {L_r}^2} + \frac{\hat{R}_s}{\sigma L_s} \tag{7-31}$$

7.5 Simulation study for the induction motor system

7.5.1 Simulation structure

All the simulations are carried out based on the induction motor system described in Table 7-2. The simulation is divided into two parts in accordance with high and low rotor speed regions of operation.

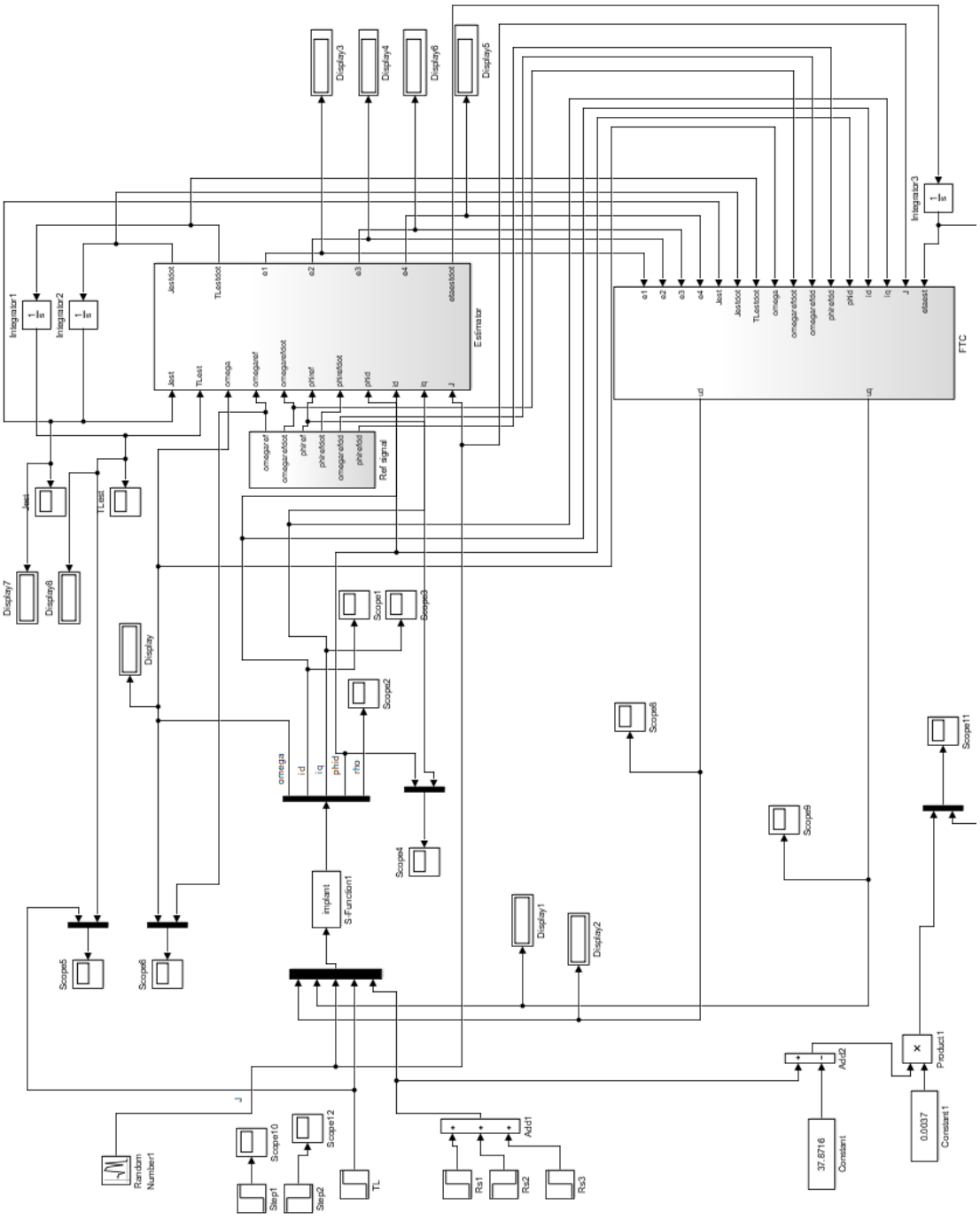

Figure 7-3 Simulink model of Back-stepping control

Considering the efficiency of the simulation, part of the simulation is realized in m file. The plant model is expressed in S-Function format as shown in Table 7-1.

Table 7-1 IM model expressed in S-Function

```
function [sys,x0,str,ts]=implant(t,x,u,flag)
switch flag,
case 0,
    [sys,x0,str,ts]=mdlInitializeSizes;
case 1,
    sys=mdlDerivatives(t,x,u);
case 3,
    sys=mdlOutputs(t,x,u);
case {2, 4, 9 },
    sys = [];
otherwise
    error(['Unhandled flag =',num2str(flag)]);
  end
function [sys,x0,str,ts]=mdlInitializeSizes
sizes = simsizes;
sizes.NumContStates  = 5;
sizes.NumDiscStates  = 0;
sizes.NumOutputs     = 5;
sizes.NumInputs      = 5;
sizes.DirFeedthrough = 0;
sizes.NumSampleTimes = 0;
sys=simsizes(sizes);
x0=[0.5,1,1,1,1];
str=[];
ts=[];
function sys=mdlDerivatives(t,x,u)

%
% rs=0.18; %Stator resistance
% rr=0.15; %Rotor resistance
% Ls=0.0699;%Stator inductance
% Lr=0.0699;%Rotor inductance
% M=0.068; % Mutual inductance
% np=1;

%%%%%%%%%%%%%%%%%% 2018.4.6 %%%%%%%%%%%%%%%%
np=2;
rs=10;
rr=3.5; %Rotor resistance
Ls=0.38;%Stator inductance
Lr=0.30;%Rotor inductance
M=0.30; % Mutual inductance
%%%%%%%%%%%%%%%%%% 2018.4.6 %%%%%%%%%%%%%%%%

sigma1=((Ls*Lr)-(M*M))/(Lr*Ls);
alpha=rr/Lr;
beta=M/(sigma1*Lr*Ls);
% eta=M*M*rr/(sigma1*Lr*Lr*Ls)+rs/(sigma1*Ls);
mu=np*M/(Lr*u(3));   % J_u(3) TL_u(4)

sys(1)=(mu/u(3))*x(3)*x(2)-(u(4)/u(3));
sys(2)=-u(5)*x(2)-beta*np*x(1)*x(3)-np*x(1)*x(4)-
alpha*M*x(2)*x(4)/x(3)+u(2)/(sigma1*Ls);
sys(3)=-alpha*x(3)+alpha*M*x(4);
sys(4)=-
u(5)*x(4)+alpha*beta*x(3)+np*x(1)*x(2)+alpha*M*x(2)*x(2)/x(3)
```

```
+u(1)/(sigma1*Ls);
sys(5)=np*x(1)+alpha*M*x(2)/x(3);

function sys=mdlOutputs(t,x,u)

sys(1)=x(1);  %% omega
sys(2)=x(4);  %% id
sys(3)=x(2);  %% iq
sys(4)=x(3);  %% phid
sys(5)=x(5);  %% rho
```

For the high speed condition, the speed reference signal is required to reach 140 rad/s at t=1s, and it changes to 160 rad/s at t=5s, then rises to 180rad/s at t=9s. For the low speed condition, the speed reference signal is required to reach 10 rad/s at t=1s, and it changes to 20 rad/s at t=5s, then rises to 30rad/s at t=9s. In the simulation, a speed reference signal will be given at t=1s, t=5s respectively. At t=2s, a load torque is applied, which is unknown to the controller.

The induction motor system performance is illustrated using the following simulation results.

7.5.2 Simulation result at high speed

Figures 7-4 to Figure 7-6 illustrate the induction motor performance in the high speed area, the reference speed is given in Figure 7-5. Figure 7-6 shows that the steady-state characteristics of currents at both d axis and q axis are stable, which means the system is stable. However, there is an obvious overshoot in the state variable i_q when the time speed requirement changes at t=1s. In order to prevent severe practical limitations in industrial induction motor experiments, magnitude limitations are usually applied.

7.5.2.1 The matched component fault and unmatched fault estimation

Figure 7-4 illustrates the adaption performance with regard to the matched fault R_s and the unmatched fault T_L. The red line is the reference signal for both R_s and T_L, the estimation result is given by the blue line. The estimation of the moment of inertia J is not given since it is too small to be estimated accurately. On the other hand, this also shows that variations in J will not affect the system performance in contrast to the effects of variations in load torque ΔT_L and stator resistance ΔR_s .

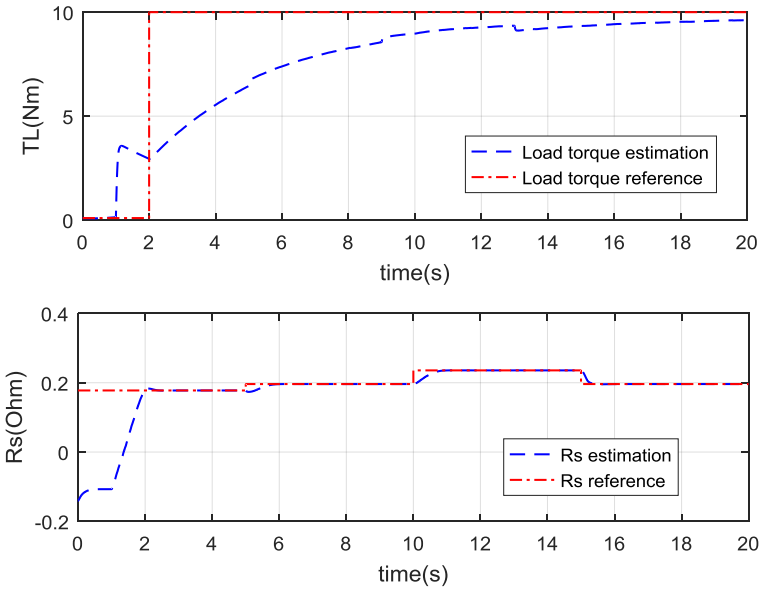

Figure 7-4 Adaption performance of induction motor at high speed area

7.5.2.2 The speed control and state observation

Figure 7-5 illustrates good tracking performance of the rotor speed ω and rotor flux φ_d with tolerance to the unmatched/matched uncertain parameters. As the speed increases, the rotor flux magnitude is realtively reduced according to the field weakening rule (Tan, 1999). However, in real system experiments, this value is obtained by experience, which is useful in this case since the assumption that the flux is measurable should be removed. Since flux measurement is usaully infeasible, flux estimation would need a separate design. This would involve another area of research that is not considered here.

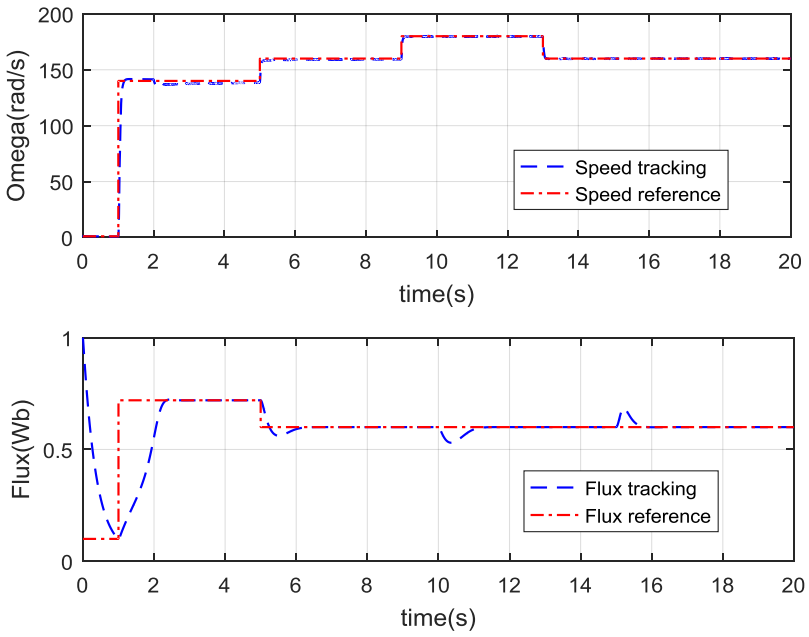

Figure 7-5 Tracking performance of induction motor at high speed

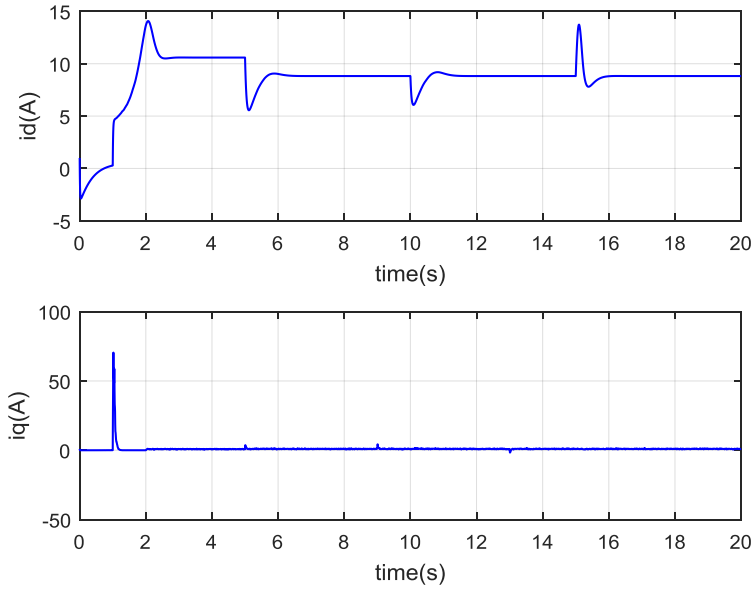

Figure 7-6 State variables (currents) of induction motor at high speed

7.5.3 Simulation result at low speed

Figures 7-7 to Figure 7-10 describe the induction motor performance in the low speed area. Figure 7-9 shows that the steady-state characteristics of currents at both d axis and q axis are stable, which means that the system is stable. Furthermore, the i_q current

overshoot present in Figure 7-6 disappears when the time speed requirement changes at t=1s. This means that the induction motor system is stable and the algorithm can be applied on a real application, at low speed.

7.5.3.1 The matched component fault and unmatched fault estimation

Figure 7-7 illustrates the estimation performance, including a good estimation of both the matched fault R_s and the unmatched fault T_L. Compared with Figure 7-4, the estimation of the uncertain parameter is better considering time delay and accuracy.

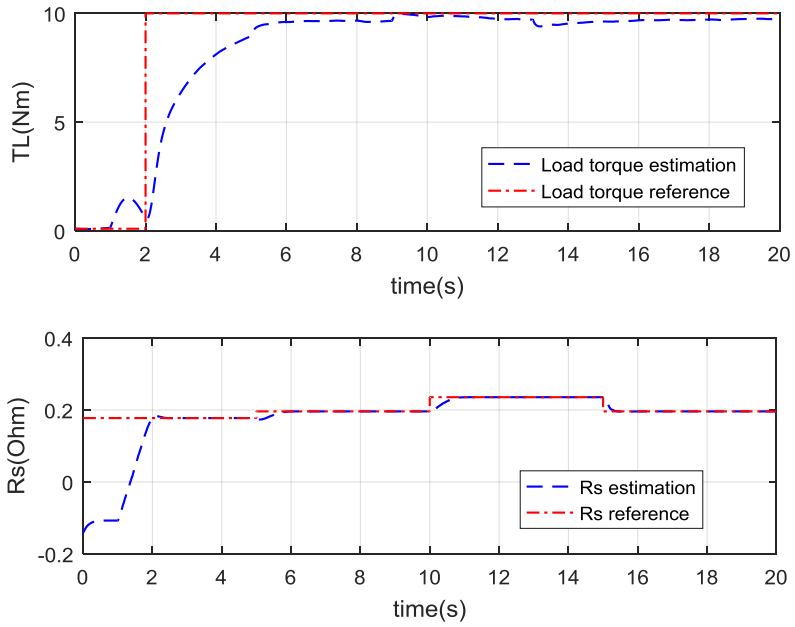

Figure 7-7 Adaption performance of the induction motor at low speed

7.5.3.2 The speed control and state observation

Figure 7-8 also presents a good tracking performance of rotor speed and rotor flux with tolerance to the matched faults, unmatched faults, and disturbances. It is easy to find the obvious change in the rotor speed ω when the unmatched uncertain parameter load torque T_L is applied. In other words, the control is sensitive to the load torque variations considering a set of parameter uncertainties, i.e. including load torque T_L, moment of inertia J, stator resistance R_s.

What is more important is that the speed maintains good control action after a short time (about 1s) of the load torque change. This shows clearly that the back-stepping control is stable (in simulation) for the induction motor under low-speed operation.

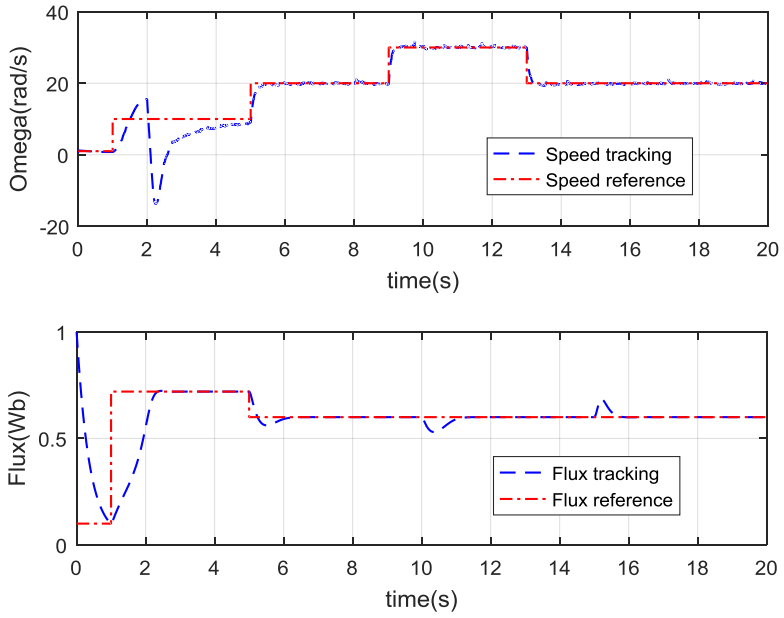

Figure 7-8 Tracking performance of the induction motor at low speed

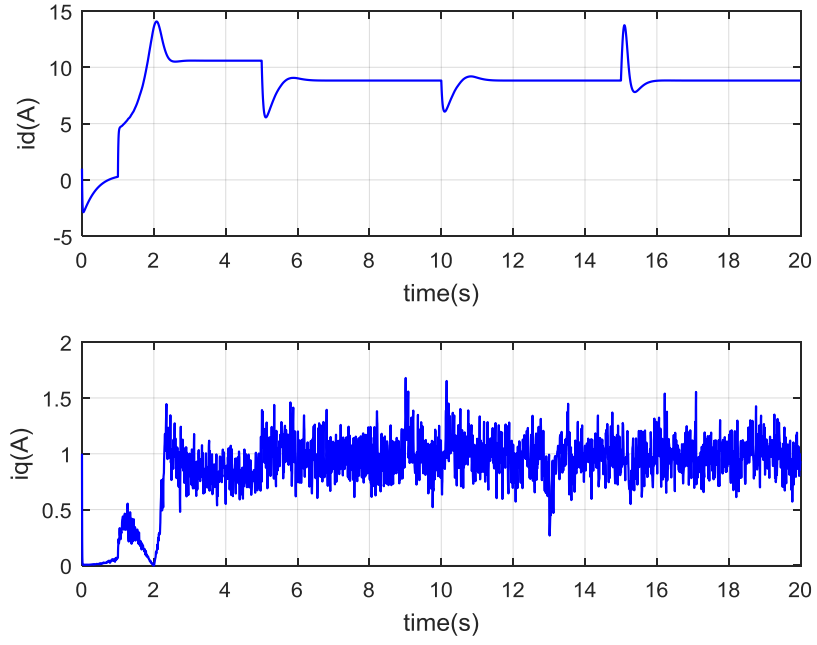

Figure 7-9 State variables (currents) of induction motor at low speed

7.5.4 The actuator effort (controller) under faulty scenario

Figure 7-10 includes an illustration of the control inputs at the d and q channels; they vary in acceptable ranges, both u_d and u_q are smooth and reasonable. Through the 2-3 phase transformation of the control input signal in Figure 7-11, it is under stable consition.

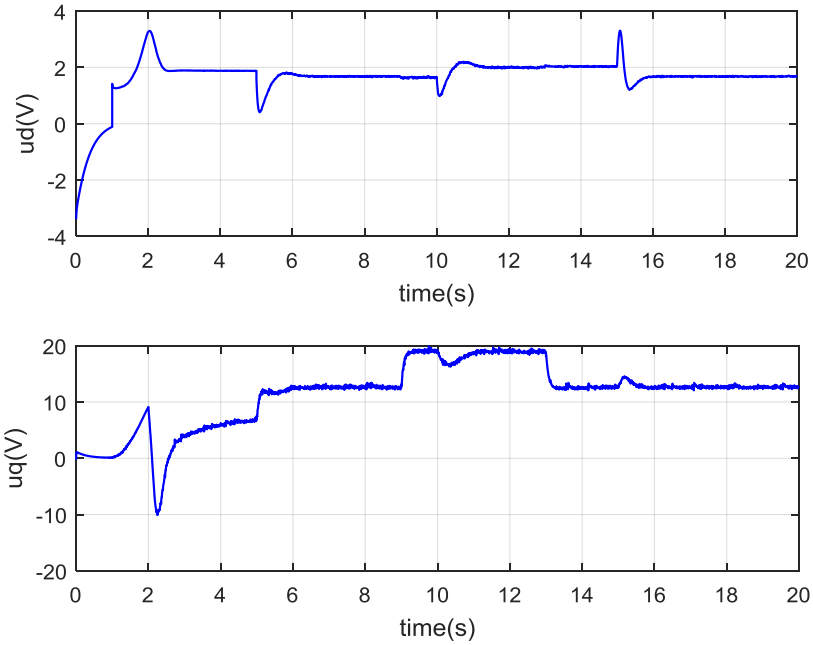

Figure 7-10 Control inputs for the induction motor at low speed

All the above simulation results include the dynamic response of the induction motor in different channels. The following signals present the control signals in 3-phase conditions. From Figure 7-11 it can be seen that the control effort works well on the system as the speed requirements changes.

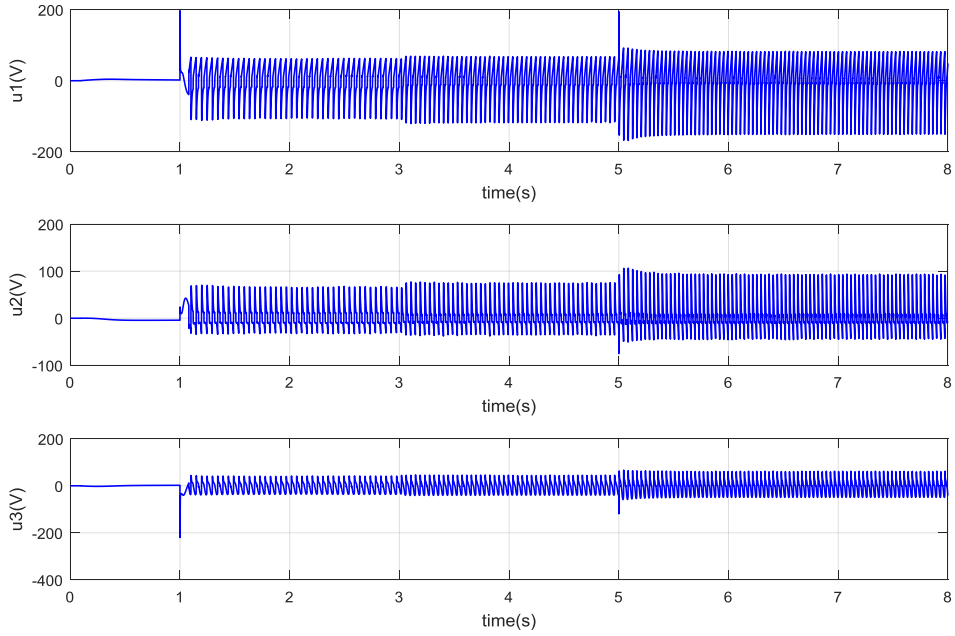

Figure 7-11 Control input in 3 phases

A comparison is made between different induction motor performances at high speed and at low speed. The results shows that good speed and flux tracking performance can be obtained at both high and low speed. The simulation results reveal that at low speed the at the d and q axis currents stay in a reasonable range whilst at high speed the current variations are not satisfactory. Accordingly, abnormal overshoot appears in the control signal u_d at high speed condition and this disappears at low speed. This result shows clearly that this Algorithm has good application on future induction motor experiments.

During the process of parameter tuning for the low speed case, the estimation performance is not the focus because the steady-state performance of the currents i_d and i_q and system stability are the most important issues. However, the simulation results carried out at low speed show better performance than those at high speed. This means that the adaptive back-stepping algorithm has natural advantages on induction motor system control for low speed operation. In other words, it satisfies the conditions for industrial experiments in the future experimental research.

7.6 Summary

The back-stepping FTC approach are introduced for a nonlinear system with strong coupling or unmatched uncertainties. The main challenges of applying this startegy to the induction motor FTC are discussed, focusing on problems arising from nonlinearity and unmatched uncertainty. An adaptive back-stepping control is designed for a nonlinear induction motor system with unmatched faults or uncertainties, where the matched condition is not the main focus. Field-oriented transformation of the (α, β) model from the fixed stator frame coordinate to a (d, q) coordinate system which rotates with the rotor is carried out. Based on the nonlinear system expressed in new coordinates, the adaptive back-stepping approach to used. Simulation results show that the induction motor performance at both varying low and high speed demonstrate good performance. The state variable (currents) at low speed satisfy the requirements for industrial induction motor application. Future research work can be carried out on integrated design by using back-stepping controller together with the use of a back-stepping observer.

Based on the above work, Chapter 8 discusses the experimental study based on the work of Chapter 7. The application study has been carried out at the Technical University of Munich by Dr. Zhe Chen in close collaboration with the author.

Chapter 8: Experimental Implementation

8.1 Introduction

The test-bench composed of hardware and software is introduced in this Chapter. The experimental implementation is based on the induction motor control strategies demonstrated in Chapter 7. There are two types of induction motor motion control systems, including *Field Programmable Gate Array (FPGA)* and *Digital Signal Processor (DSP)*. Considering the requirement of sampling frequency, FPGA-based controller is chosen using *Very High Speed Integrated Circuit Hardware Description Language (VHDL)* as programming language (Chen et al., 2013; Chen et al., 2014; Wang et al., 2014). The reasons for using FPGA based controller is as follows:

1) A significant difference between DSP and FPGA is that FPGA uses a flexible hardware structure, which FPGA programming is conducted in accordance with applications. DSP has fixed hardware structure, i.e. transistors memory, peripheral structures and invariable connections. DSP actions (such as addition, multiplication, I/O control, etc.) are predefined, where operations are processed in a sequential manner;
2) FPGA operations are not predefined. This process is designed using VHDL simultaneously. Parallel processing ability is one of the most important features that separate FPGA from DSP and make FPGA superior in induction motor control;
3) Consider a control system which requires processing large data at high speed. An FPGA is capable of appropriate parallel processing for this task. FPGA can be used to process large data with few clock cycle and hence the user has the freedom to determine the device hardware configuration. This is impossible with DSP applications since data flow is limited by the (16-bit, 32 bit, etc.) processor bus architecture and processing speed.

In this test-bench, FPGA and Central Processing Unit (CPU) work together to control an induction motor system, where complex control algorithms can be implemented. The resulting analysis is presented in Section 8.5.

8.2 Experimental test-bench

The proposed control of the induction motor system has been verified on this experimental test-bench, which is located at the Institute for Electrical Drive System and Power Electronics of the Technical University of Munich. The whole test-bench is illustrated in the Figure 8-1, the induction motor drive system is given in the Figure 8-2. It is formed by two 2.2 kW squirrel-cage induction machines. One of the machines uses a Danfoss VLT FC-302 3.0 KW inverter as driver, this is a load machine. The induction machine under control is driven by a SERVOSTAR620 14 kVA inverter. A real-time computer system (1.4 GHz) is used. A 1024-points incremental encoder is used to measure the rotor position (Chen et al., 2013; Wang et al., 2014).

Table 8-1 List of Test-bench items

Items	Specification	Number
Squirrel-cage induction machine (Danfoss VLT FC-302 3.0 KW inverter)	2.2 kW	1
Squirrel-cage induction machine (SERVOSTAR620 14 kVA inverter)	2.2 kW	1
Real-time computer system	1.4 GHz	1
Incremental encoder	1024-points	1

The parameters of the main motor are given in Chapter 2. In this Section, the test-bench structure, space vector PWM implementation and resolver demodulation will be introduced.

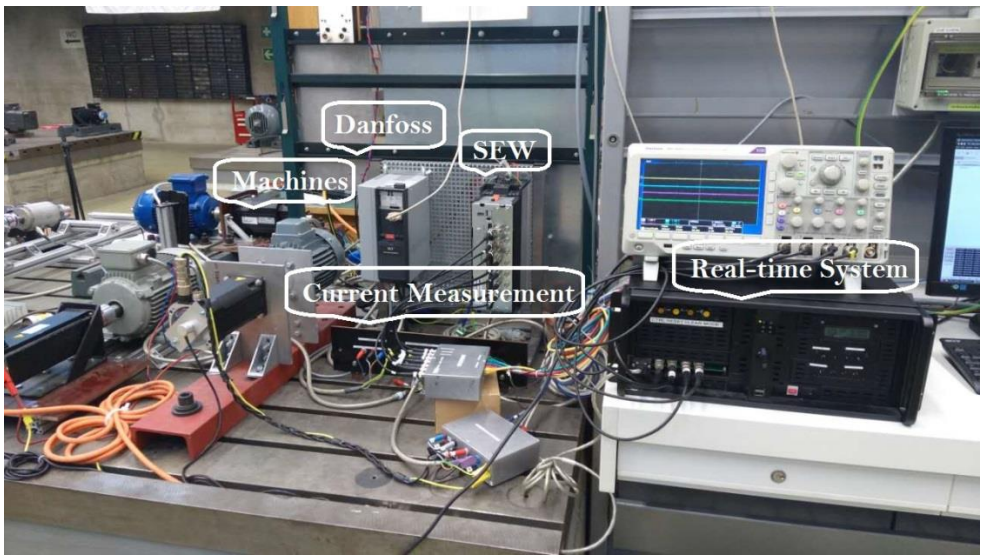

Figure 8-1 The whole testbench

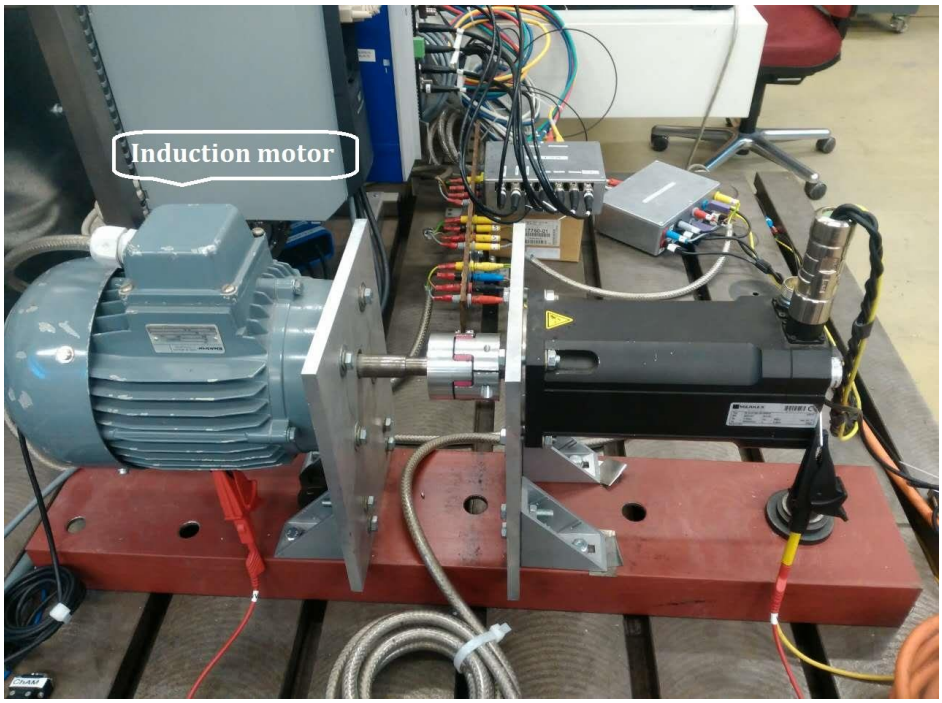

Figure 8-2 The induction motor drive system

8.2.1 Test-bench structure

The real time system of the test-bench is formed of a CPU (Core 2 Duo), an FPGA (Cyclone 3) and a *Complex Programmable Logic Device* (CPLD), which is shown in Figure 8-3 (Chen et al., 2013; Wang et al., 2014).

Since the CPU is capable of performing quickly operations on floating point data, it is responsible for FPGA configuration and control algorithm realization. FPGA is seen as a coprocessor, FPGA works together with core processor - CPU. FPGA is mainly responsible for signal sampling, signal pre-processing, output signal shaping, and so on.

For example, the configuration of the system peripherals (for example, A/D, D/A, etc.) are completed by the FPGA.

The induction motor control system uses the characteristics of parallel computing of FPGA, as well as the operation flexibility. When the CPU and FPGA works together, CPU receives a 16kHz interrupt signal generated by the FPGA. In order to decode the control signals sent by the CPU to the FPGA, as well as to provide an interface for the PWM signal, a CPLD is designed as an intermediate device between the CPU module and the FPGA module. It is the default configuration of the real-time system, however, it is flexible to change the configuration if experimental requirements change. In some cases FPGA can replace the CPU in order to handle specific tasks, which is mainly determined by the complexity of calculation and application objectives.

As illustrated in Figure 8-3 (Chen et al., 2013; Wang et al., 2014), FPGA includes seven modules which are driven by four different clocks, it helps to improve the properties of compatibility of device requiring different excitations. The Phase-Locked-Loop module of FPGA is responsible for producing these four clocks and for using them on different modules. In order to ensure efficient data exchange between the CPU and the FPGA synchronously, the communication module runs at 20MHz.

In the next Section the method of transferring Matlab / Simulink into C code and VHDL code are introduced.

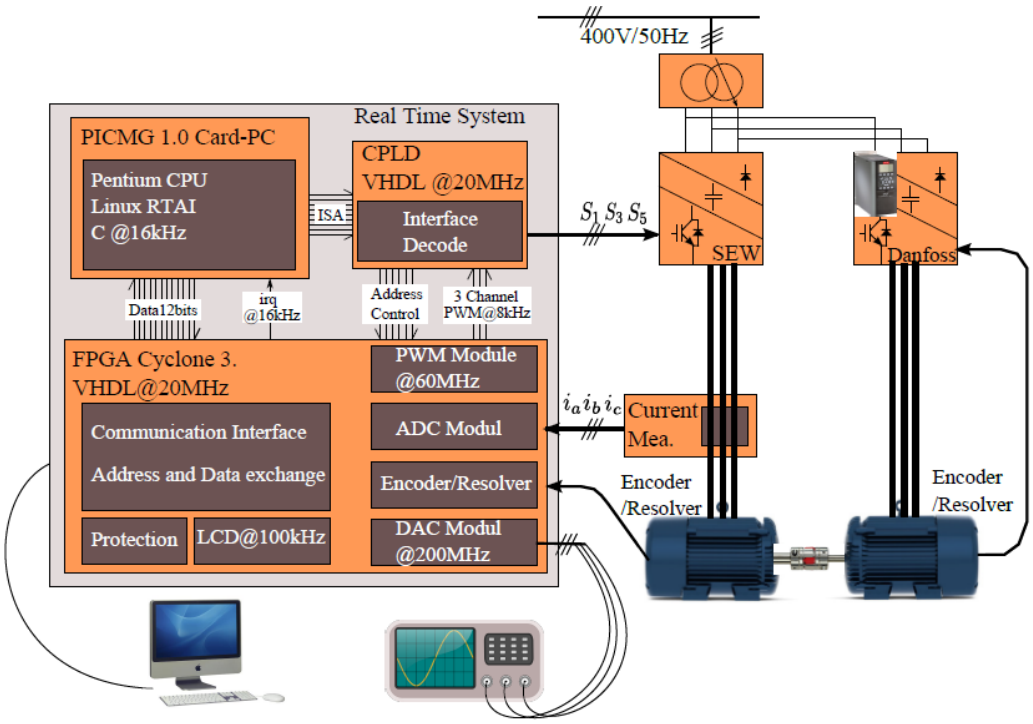

Figure 8-3 Hardware setup (Chen et al., 2013)

8.2.2 Space Vector PWM implementation

In a control system based on *Voltage Source Inverter (VSI)*, PWM technology is widely used. There are two main types of PWM, the *Sinusoidal PWM (SPWM*) and *Space Vector PWM (SVPWM)* (Beig et al., 2007; Naderi & Rahmati, 2008).

The SPWM generates a PWM signal by making a comparison of the sinusoidal modulation signal and the triangular carrier signal. The algorithms applied is easy to be implemented. However, it only uses 78.6% of the DC link voltage, and some compensation is required to increase the ratio (Chen et al., 2013). As a good alternative, SVPWM is proved to be more efficient compared with SPWM, though it is difficult to implement. It is able to reach 90.6% efficiency of the DC link, but reduce voltage and current harmonics with obvious symmetrical waveform of the PWM (Chen et al., 2013). The FPGA has a PWM top-module that contains an SPWM generators and a DSC generator. In practice, it is able to implement SVPWM in the CPU since the CPU is very advantageous in dealing with complex algorithms.

Although the limited sampling frequency of the CPU and the sequential data processing mechanism lead to delay of the PWM signal, the FPGA is able to deal with parallel data computing. So it has much higher sampling frequency than the CPU. Therefore, through the design of FPGA-based SVPWM generator, the performance and flexibility of real-time systems can be improved. This improvement is in accordance with the following two aspects: **(1)** If the CPU is used as core processor, its computational burden can be releaved; **(2)** It is able to make FPGA functions completely independent of CPU, then FPGA can be used as the core processor. Therefore, control algorithms with input signals and output signals can be dealt with by the FPGA.

Although SVPWM is more powerful in functions compared with SPWM, it has some disadvantages on implementations. SVPWM generator makes use of more computing resources.

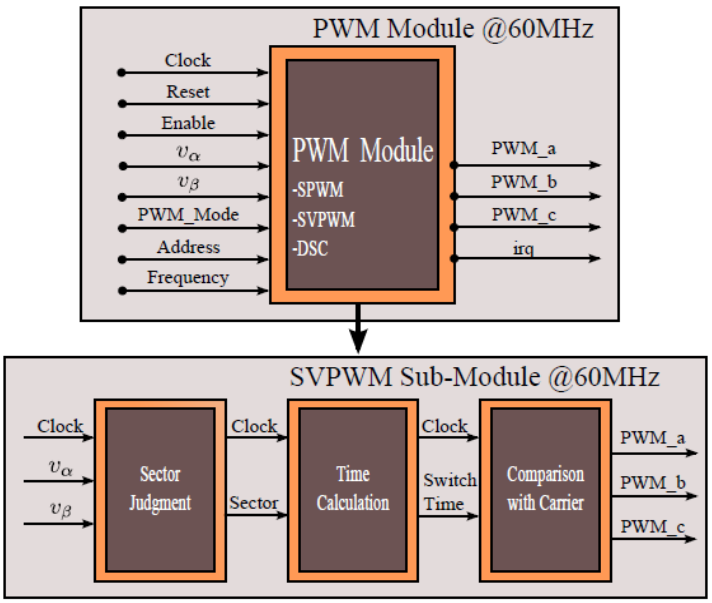

Figure 8-4 PWM module and SVPWM sub-module in FPGA

In Figure 8-4, the PWM top-module and relevant SVPWM module are described. The interface between CPU and FPGA, as well as the interfaces between FPGA top-module and sub-module are defined in Figure 8-4. The “PWM_Mode” is a switch of option for modes of SPWM, SVPWM or DSC. The “Frequency” is used to set PWM frequency. The other input signals can be configured to synchronize the PWM module with parallel modules. The output signals of the PWM module is composed of three PWM signals and an interrupt signal “irq”. The “irq” is sent back to CPU as the sampling clock, which

guarantees synchronization between CPU and FPGA (Beig et al., 2007; Naderi & Rahmati, 2008; Chen et al., 2013).

8.2.3 Resolver demodulation

Generally, an encoder or resolver is used in the rotor position or speed measurement of an electrical drive system. The encoder can be understood as a simple coding device which is cheaper but less accurate than resolver. It outputs pulse signals with regard to the real time speed or position of the machine rotor. However, the resolver requires sine/cosine excitation signals and then sine/cosine output signals should be decoded. Only after decoding, output signals can be transferred into digital rotor position/speed signals which are used by digital controller (Ben-Brahim & Tadakuma, 1998; Jones et al., 2009).

In the existing real time system, the FPGA contains only one encoder demodulation module. One encoder is needed in the remaining context of experiment. Considering the system compatibility and flexibility, a resolver demodulation module in FPGA is utilised. The decoding device AD2S1210 is a device with flexibility on output format, range of configuration and interface protocols, etc. Its ability of flexibility is reflected through the fault diagnosis ability and decoding accuracy. As well as that, it makes the encoder signals compatible to different controller interfaces(Chen et al., 2013).

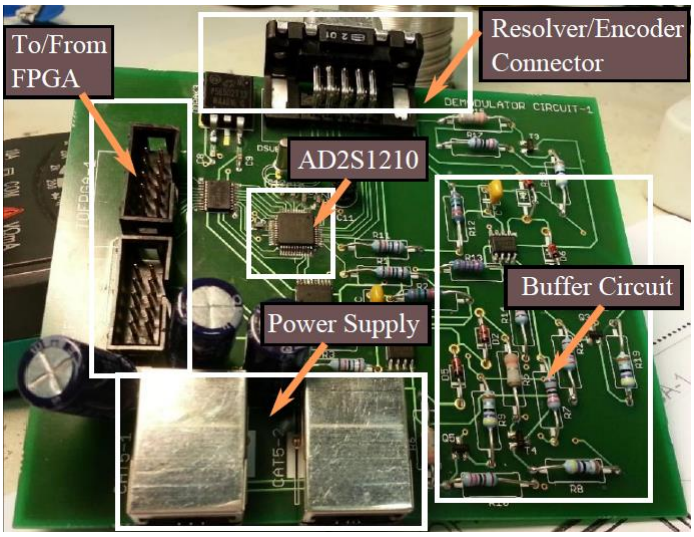

Figure 8-5 Resolver circuit(Chen et al., 2013)

The design has been shown in the Figure 8-5. A decoding circuit is a middleware between resolver module of FPGA and position/speed sensor of induction motor. The

configuration and control of the AD2S1210 is attained in resolver module within FPGA, then a serial digital position or speed signal are fed back to the resolver of FPGA for formatting and ratio adaption. In the next step, a 12 bit parallel unsigned position or speed signal is sent to CPU for further processing where control algorithms are applied.

Therefore, the FPGA can work independently as a core-processor and deal with the obtained rotor position or speed signal. In this condition, CPU only need to monitor and supervise the system conditions. Then the transform of position signal, speed signal and 3-phase currents are not needed in CPU.

8.3 C Code generation from Matlab/Simulink

The C language can be used to write executable code in a CPU or other type of DSP. Researchers with programming experience understand that writing C code manually is a time-consuming and energy-intensive job, and debugging takes a lot of time. In recent years, Matlab / Simulink software has developed a number of features based on the original platform, including a model-based C code generation tool. This makes this platform more useful for simulation and industrial applications. The dSPACE environment products based on Matlab / Simulink have been used as a successful example. It is an effective connection between Matlab / Simulink models and a DSP or FPGA. Although dSPACE is expensive to use, it can effectively implement complex control algorithms. Matlab Coder toolbox in Matlabr/Simulink is used in this study (Redfern & Campbell, 2012; Chen et al., 2013).

The procedures for C code generation are illustrated in this Section. The process includes three steps: modelling, configuration and generation of C code. Firstly, the Matlab / Simulink code should be simulated to ensure it and gives satisfactory results. Then the configuration of input and output signals, objective language or related properties should be achieved using the Matlab Coder. Finally, after the setting of path, the C code can be generated (Redfern & Campbell, 2012; Chen et al., 2013).

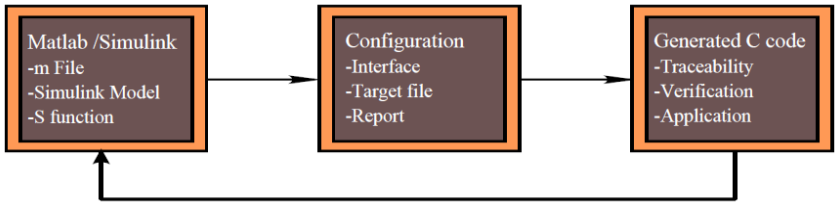

Figure 8-6 C code generation from Matlab/Simulink (Redfern & Campbell, 2012)

8.4 VHDL code generation from Matlab/Simulink

In the classic two types of drive control system, DSP uses C as the language to realize the algorithm; and FPGA using VHDL or Verilog as programming languages. Matlab / Simulink has a toolbox that generates VHDL or Verilog code, that is, HDL encoders and HDL validators. This Section describes the key technologies of HDL encoders and HDL validators (Roy & Banerjee, 2005; Chen et al., 2013).

VHDL code generation can be simply divided into three steps. Firstly, the Matlab / Simulink program based on floating point data is modelled and simulated. Then, the optimized fixed point model is obtained by using the "fixed point tool" toolbox. Second, readable and traceable VHDL or Verilog code for the FPGA is generated. Generating reports helps users understand the generated VHDL code. At the same time in this process, the pop-up window has a high-level resource utilization report. In the third step, collaborative simulation is used to verify the generated VHDL code and the original Matlab code function exactly the same.

There is a standard procedure for generating VHDL code generally. It is organised as the following steps. First of all, controller is designed for a dynamic system based on floating point data, and the mathematical modelling and control algorithm design should satisfy the requirements of the whole control system. Then the floating point model is transformed into optimized fixed point model using the toolbox “Fixed Point Tool”. In the second stage, readable and traceable VHDL is produced for FPGA. In order to realize the bi-directional traceability and to help user understand VHDL code, a report is produced at the end of this stage. A High-Level Resource Report showing resource utilization is generated with the VHDL code, which is convenient for optimization of streaming, sharing etc. In the third stage (after the above optimization), a Matlab-

Modelsim/Questa/Cadence co-simulation is generated. It is understood as a tool for verifying the function of the generated VHDL code using original Matlab/Simulink model. As well as that, FPGA hardware-in-the-loop simulation supplies with further VHDL code verification (Redfern & Campbell, 2012; Chen et al., 2013).

The VHDL generation helps to design various control algorithms based on FPGA. The design of induction motor controller is applied in the industry using VHDL. However, debugging brings in difficulty and its performance is not as good as CPU-based controller. Therefore, in the experiments covered in this Chapter, the CPU is still the core processor.

8.5 Experimental analysis

As introduced at the beginning of this Chapter, the test-bench experiment is utilized to verify the performance of the back-stepping control approach which is introduced in the Chapter 7. The paramter is introduced within Table 8-1.

Table 8-1	
Nominal power P_{nom}	2.2 kW
Nominal speed ω_{nom}	1420 rpm
Number of pole pairs n_p	1
Stator resistance R_s	2.6827 Ω
Rotor resistance R_r	2.1290 Ω
Stator inductance L_s	283.4 mH
Rotor inductance L_r	283.4 mH
Mutual inductance M	275.1 mH
Moment of inertia J	0.005 kg · m^2
Rated load torque T_L	7.5 Nm

It is important that the induction motor parameters have been introduced in Table 2-2 of the Chapter 2, hereby we use the second type of data setting according to the experiment environment. The experiments are divided into *two* groups:

1) The first group of experiments are aimed at fault-free scenarios, it is used to verify the effectiveness of the induction motor control system under both low speed and higher speed conditions. This is illustrated in Figures 8-7 and 8-8.
2) The second group of experiments are aimed at the verification of the effectiveness of back-stepping FTC approach. The unmatched fault, that is the load torque variation

ΔT_L, appears in three different types i.e. the constant signal, step signal and the ramp signal.

Figure 8-7 shows the induction motor control performance under the condition of no load, which means that this is also a no-fault scenario; however, the speed is required to be maintained at 100 RPM. This test shows the low speed tracking performance, the 100 RPM is seed as a reference. The estimated speed, actual speed and error are shown. This demonstrates the good control cabability in low speed operation. Furthrmore, this also supports the remaining experiments, since both the hardware/software system and the chosen control startegy all work well.

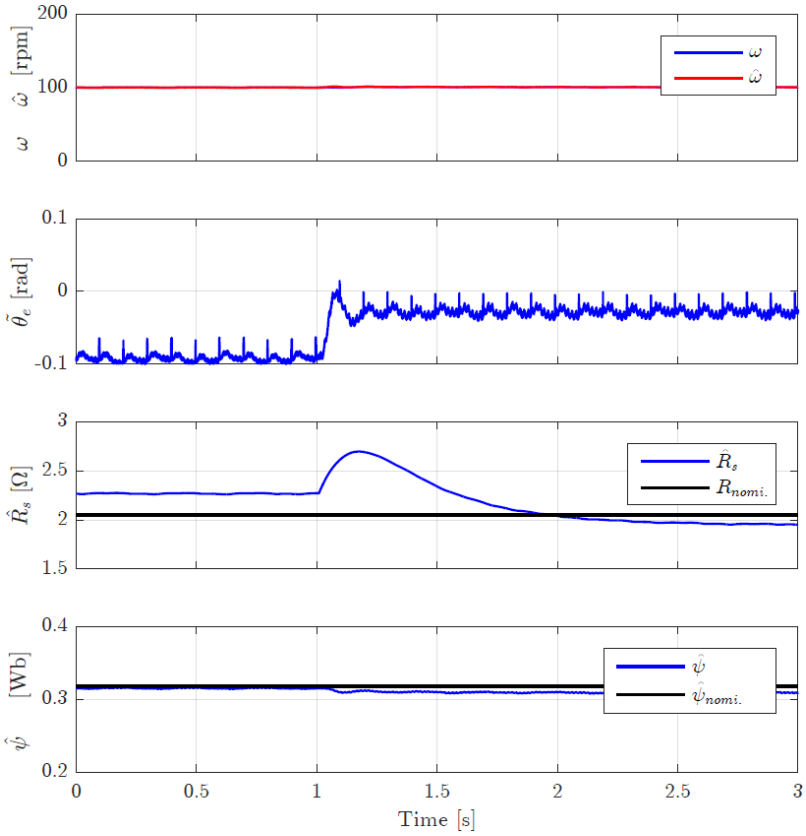

Figure 8-7 Fault-free scenario at 100 RPM

Figure 8-8 shows again the condition without load torque, which means the unmatched fault – load torque is not applied on the system. A speed requirement has been applied. The speed is required to rise from 150 RPM to 500 RPM. The system dynamic resonse is shown in Figure 8-8. Figures 8-7, Figure 8-8 together verify that the system works well under the fault-free condition and with the chosen control.

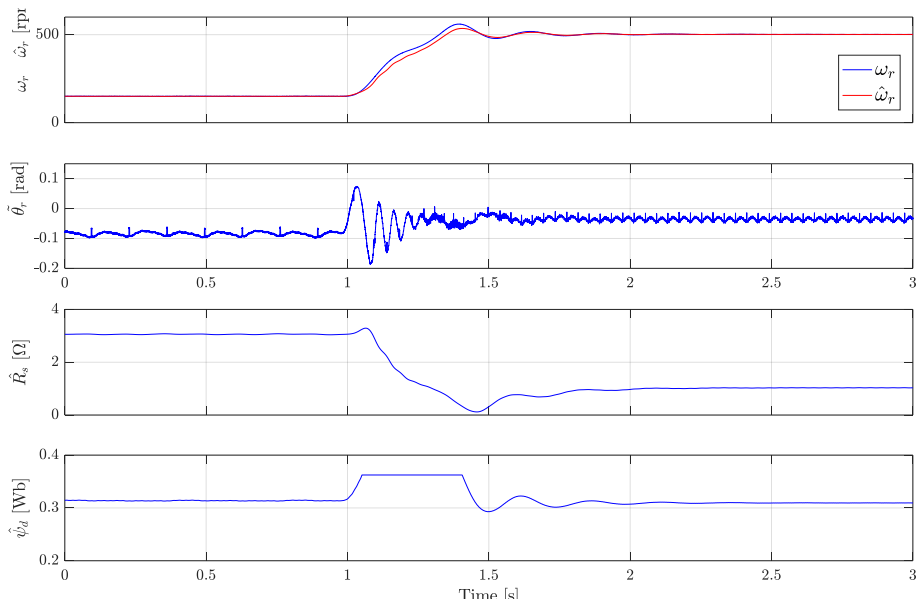

Figure 8-8 Fault free scenario with speed rising from 150 RPM to 500 RPM

Figures 8-9 and 8-10 show the control performance under fault scenarios where the effect of the unmatched fault – the load torque variation ΔT_L is considered. The estimated speed, actual speed and error are shown.In Figure 8-9, a step load torque is applied on the induction motor, jumping from zero to half of the rated load, and the constant reference speed is still 500 RPM. In Figure 8-10, a ramp change in load torque is applied on the induction motor, rising gradually from zero to half of the rated load, and the constant reference speed is still 500 RPM.

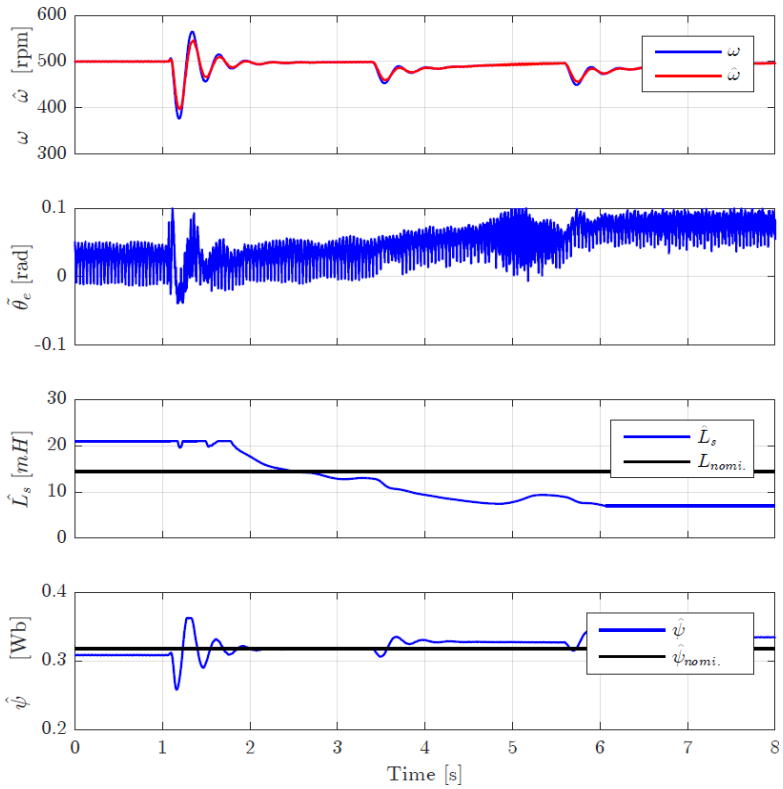

Figure 8-9 Faulty scenario 2: step load (0 - ½ rated load torque), reference speed of 500 RPM

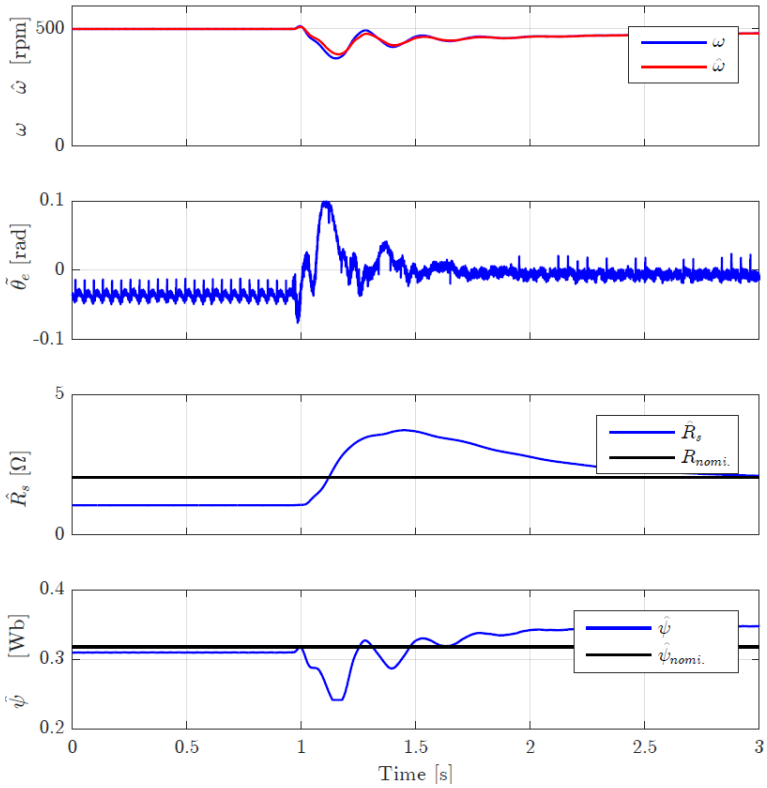

Figure 8-10 Faulty scenario 3: ramp load (0 - ½ rated load torque), reference speed of 500 RPM

8.6 Summary

The test-bench for the experiment has been introduced in this Chapter, including the hardware and software components. The experimental implementation is based on the induction motor which has been introduced in detail in Chapter 2, including the fault scenarios described in Chapter 3. The aim of the experiments is to verify the effectiveness of the control strategies under a wide speed range, and the unmatched faults scenarios has been utilized in this experiment design. The induction motor control system is based on several important components, including a Field Programmable Gate Array (FPGA) and Very High Speed Integrated Circuit Hardware Description Language (VHDL). Both of these have been introduced. In the test-bench experiment, the FPGA and the Central Processing Unit (CPU) work together to implement the active FTC scheme.

In this experimental framework, the back-stepping control approach is implemented through 4 groups of experiments, the first two groups were conducted under fault-free conditions, which is mainly used to prove the performance of control strategies under both low speed and high speed. Then the remaining 2 groups of experiments are conducted with consideration of unmatched faults.

Chapter 9: Conclusion and statement of future work

9.1 Thesis summary

Since the pioneering work of Tesla the physical structure of the uncontrolled induction motor system has been known since early in the 20th Century (Hunt, 1907; Stanley, 1938; Wagner, 1939). Scalar and vector control of induction machines (both motors and generators) developed following the introduction of control strategies together with improvements in electro-magentic and mecahnical properties during the 1950s (Dolan & Herbert, 1948; Nelsen & Acker, 1950; Carlsen, 1959). With the wide development of induction motor applications in industrial and rail vehicle systems interest in fault diagnosis and condition monitoring methods became important in order to maintain a good standard of operation reliability (Benbouzid, 2000; Nandi et al., 2005; Siddique et al., 2005). However, many of the fault diagnosis methods developed are based on data (i.e. data-driven) without the use of physical/electro-mecahnical system information. Simlarly, diagnosis methods based on signal processing developed in so-called condition monitoring have been widely considered. However, it can be seen that many faults occur within control systems and the effect that these faults have on the machine system itself can be modified through suitable control system design. Hence, in this research the model-based approach to fault diagnosis has been chosen rather than condition monitoring or the use of data-driven methods, keeping the fault modelling, fault estimation close to the control requirements of the real physical system.

The thesis has shown that there are are a number of commonly encountered induction motor faults, such as broken rotor bars, mass imbalance, stator faults, single-phasing, bearing faults, unbalanced power supply, short circuit in different components, etc. The research has stepped beyond the monitoring or diagnosis of machine faults into the realm of FTC for automatic system reconfiguration or compensation for the effects of faults. The subject of active FTC or AFTC in the thesis has been motivated by practical concerns for maintained machine availability as well as reducing the cost of system maintenance and cost of operation. The detection/isolation (FDI) of machine faults has been done in

this study using fault estimation (FE) instead of the old and more traditional approach of residual-based fault diagnosis for two main reasons: (1) FDI is a difficult subject from the point of view of robustness to modelling uncertainty, and (2) the AFTC system based on FDI is complex to realise involving system reconfiguration and variable time delay. The FE and compensation route gives a simpler strategy for AFTC. The detection and isolation steps of FDI are replaced immediately by the FE since the reconstructed/estimated fault(s) do not require an isolation procedure; the FE provides itself use of FE in AFTC is preferable to the use of fault detection and isolation (FDI) since the.

The thesis reviews the subject of deriving fault information, derived from FE as well as the literature describing methods of achievinf robust and rwliable AFTC action via fault compensation. The FE and compensation route gives a simpler strategy for AFTC use of FE in AFTC is preferable to the use of fault detection and isolation (FDI) since the.

Hence, the subject of induction motor FTC/FE in this thesis has been motivated by practical concerns, not only relaibility but ease of implementation as well as reduction in maintenance and operating cost when faults occur. The research has been developed keeping the requirements of the physical/practical system in mind with a strong focus on model and AFTC validation using experimental testing. The study of AFTC for induction motors deserves practical research through simulation and experiment.

In this thesis, relatively new control methods has been applied in simulations. For example, the LPV framework and back-stepping control approach provide two frameworks for nonlinear induction motor control, developed hand in hand with better modelling approaches and good strategies for combination with other control approaches (adaptive control and sliding mode control, etc). In the thesis, adaptive observer and sliding mode fault estimation observer approaches are used to estimate the sensor, actuator and component faults. These faults are subdivided into matched or unmatched faults, depending on the way in which the faults enter the dynamical system.

Instead of designing specific control approaches for snduction motor problems a more general approach to control and estimation has been adopted and developed within the framework of AFTC. Multiplicative faults have been transformed into and handled by an additive fault approach. Multiplicative faults usually belong to the class of unmatched

faults so this approach provides a more general strategy for the AFTC also made possible through the use of adaptive estimation and back-stepping control.

In Chapter 3 different types of electrical and mechanical system faults that arise commonly in the induction motor are investigated along with their modelling strategies.

Chapter 4 provides an overview and taxonomy of FTC methods as a background for the AFTC study in Chapters 6, 7, and 8.

The fault-free 4^{th} order electrical system model has been studied in Chapter 5 by combining the application of the well known adaptive and sliding mode observers.

In Chapter 6, the appropriate nonlinear 5^{th} order induction motor model has been studied by using LPV fault estimation observers. The induction motor model is shown to be nonlinear due to the specific faults and coupling of parameters.

Following this the Chapter 7 researched on the back-stepping FTC approach for a nonlinear induction motor system with strong coupling or unmatched uncertainties.

The simulation study of Chapters 5, 6 & 7 lead to the experimental work described in Chapter 8. The mathematical model work in Chapters 5,6 & 7 is based on the parameters of the laboratory induction motor system described in Chapter 8. The work in Chapter 8 involves a collaboration with Dr Chen at the Technical University of Munich using designs made by the author. Hence, the thesis provides a good basis for (a) modelling, control, fault tolerant control, and (b) model and AFTC verification on the real laboratory system.

The main contributions of this thesis are listed as follows:

Methods / Fault Types	Chapter 5			Chapter 6	Chapter 7 & 8	
	AFE	IAFE	SMO	SMO for LPV system	Adaptive back-stepping FTC	
Sensor fault	√	√	√	√	**Control objectives**	1) Speed control 2) State observation at high & low speed
Actuator fault	√	√	√	√	**Unmatched fault estimation**	Load Torque variation ΔT_L
Component fault	√	N/A	√	N/A	**Matched component fault estimation**	Resistance variation ΔR_s

Firstly, the adaptive observer combined with the SMO has been used to estimate the induction motor faults under the assumption that the rotor speed is relatively constant. Both additive and multiplicative faults in the induction motor system were studied. The combination of the adaptive and SMO methods is a new approach to induction motor fault estimation/monitoring.

In Chapter 5, a linear adaptive observer technique has been developed for FE in the electrical system of the induction motor; and an improved Adaptive FE (AFE) algorithm using an LMI design strategy has been proposed based on the AFE approach. In particular, compared with the first FE algorithm, it is shown clearly that the improved AFE algorithm can improve the application scope for FE, including the estimation of both the constant and time-varying faults.

The proposed startegy requires no assumption concerning constraints on fault shapes in the improved AFE algorithm. A sliding mode obserer is combined with the adaptive observer in order to handle estimation problem of both the constant fault and fast varying fault.

Simulation results of all the three applications of adaptive observer approaches show that both additive faults and multiplicative faults can be estimated with satisfactory rapidity and accuracy.

Secondly, the induction motor system has been extended into a *linear time-varying* LPV framework and the LPV sliding mode observer was studied under this condition, while assuming that the rotor speed is a varying parameter. This is applied with the combination of actuator fault and sensor fault estimation through sliding mode LPV observer design.

Thirdly, due to the shortcomings (modelling imperfections of nonlinearities) of LPV modelling, an adaptive back-stepping control approach has been applied on a nonlinear induction motor system with unmatched faults. The induction motor performance at low and high speeds has been studied through simulation. It has been pointed out that the state variables at low speed satisfy the requirements for industrial induction motor application.

Finally, as a verification of the adaptive back-stepping control approach, an experimental study of induction motor FTC has been investigated through a collaboration with the Technical University of Munich. The results included the verification of the effectiveness of the induction motor for reasonably significant (practical) rotation speed variations, considering control performance in unmatched fault cases. The results illustrate clearly the powerful performance of the back-stepping AFTC of the induction motor system under different speed ranges and fault scenarios.

9.2 Future work

The possible future work following this thesis could be:

1) The LPV sliding mode observer has been used in this thesis, and the sliding mode approach has already been proved to be insensitive to a particular class of uncertainties based on significant international research. This research on induction motor system would make this research more general and related more closely to real-world applications, when considering uncertainties. However, industrial environments, when more types of disturbances, such as vibrations and environmnetal effects (e.g. moisture), have been considered, more effective approaches should be considered. The remote control and multi-agent control methods may also be of value.

2) It is essential to investigate the induction motor performance under the back-stepping control with inclusion of supervision of the back-stepping observer; this approach has been said to be effective in some research studies. Since the thesis has demonstrated that adaptive back-stepping control is effective for low rotor speed operation, the integration of both the back-stepping control and back-stepping observer is a topic deserving new research attention.
3) Both LPV and Back-stepping can be used as a framework, and can be used through combination with other control or estimation approaches, since they are both methods used to deal with complex models. The advantages and disadvantages of the back-stepping framework can be compared with that of the LPV.

REFERENCES

Agamloh, E. (2014) A guide for the ranking and selection of induction motors, *Conference Record of 2014 Annual Pulp and Paper Industry Technical Conference*. IEEE Xplore.

Alwi, H. & Edwards, C. (2014) Robust fault reconstruction for linear parameter varying systems using sliding mode observers. *International Journal of Robust and Nonlinear Control*, 24(14), 1947-1968.

Alwi, H., Edwards, C. & Marcos, A. (2012) Fault reconstruction using a LPV sliding mode observer for a class of LPV systems. *Journal of the Franklin Institute*, 349(2), 510-530.

Apkarian, P. & Adams, R. J. (2000) Advanced gain-scheduling techniques for uncertain systems, *Advances in linear matrix inequality methods in control*, 209-228.

Apkarian, P. & Gahinet, P. (1995) A convex characterization of gain-scheduled H/sub/spl infin//controllers. *IEEE Transactions on Automatic Control*, 40(5), 853-864.

Apkarian, P., Gahinet, P. & Becker, G. (1995) Self-scheduled H∞ control of linear parameter-varying systems: a design example. *Automatica*, 31(9), 1251-1261.

Azizi, S. & Khorasani, K. (2009) A distributed Kalman filter for actuator fault estimation of deep space formation flying satellites, *The 3rd Annual IEEE Systems Conference*. IEEE.

Ballesteros, P. & Bohn, C. (2011) A frequency-tunable LPV controller for narrowband active noise and vibration control, *American Control Conference (ACC 2011)*. IEEE Xplore.

Bartolini, G., Ferrara, A. & Usai, E. (1998) Chattering avoidance by second-order sliding mode control. *IEEE Transactions on Automatic Control*, 43(2), 241-246.

Barut, M., Bogosyan, S. & Gokasan, M. (2007) Speed-sensorless estimation for induction motors using extended Kalman filters. *IEEE Transactions on Industrial Electronics*, 54(1), 272-280.

Becker, G. & Packard, A. (1994) Robust performance of linear parametrically varying systems using parametrically-dependent linear feedback. *Systems & Control Letters*, 23(3), 205-215.

Beig, A. R., Narayanan, G. & Ranganathan, V. (2007) Modified SVPWM algorithm for three level VSI with synchronized and symmetrical waveforms. *IEEE Transactions on Industrial Electronics*, 54(1), 486-494.

Ben-Brahim, L. & Tadakuma, S. (1998) Speed control of induction motor without rotational transducers, *33rd IAS Annual Meeting Industry on Applications*. IEEE Xplore.

Benbouzid, M. E. H. (2000) A review of induction motors signature analysis as a medium for faults detection. *IEEE Transactions on Industrial Electronics*, 47(5), 984-993.

Benchaib, A., Rachid, A., Audrezet, E. & Tadjine, M. (1999) Real-time sliding-mode observer and control of an induction motor. *IEEE Transactions on Industrial Electronics*, 46(1), 128-138.

Bennett, S. (1998) *Model based methods for sensor fault-tolerant control of rail vehicle traction.* PhD Thesis. University of Hull.

Bennett, S., Patton, R. & Daley, S. (1999) Sensor fault-tolerant control of a rail traction drive. *Control Engineering Practice*, 7(2), 217-225.

Bindu, S. & Thomas, V. V. (2014) Diagnoses of internal faults of three phase squirrel cage induction motor—A review, *2014 International Conference on Advances in Energy Conversion Technologies (ICAECT)*. IEEE Xplore.

Blanke, M., Kinnaert, M., Lunze, J., Staroswiecki, M. & Schröder, J. (2006) *Diagnosis and fault-tolerant control*, *691*.Springer.

Boiko, I., Fridman, L. & Iriarte, R. (2005) Analysis of chattering in continuous sliding mode control, *American Control Conference, 2005.* Portland USA: IEEE Xplore.

Boulkroune, A., Tadjine, M., M'Saad, M. & Farza, M. (2014) Design of a unified adaptive fuzzy observer for uncertain nonlinear systems. *Information Sciences*, 265, 139-153.

Briat, C. (2014) Linear parameter-varying and time-delay systems. *Analysis, Observation, Filtering & Control*, 3.

Cai, G., Song, J. & Chen, X. (2014) Flight control system design for hypersonic reentry vehicle based on LFT–LPV method. *Proceedings of the Institution of Mechanical Engineers, Part G: Journal of Aerospace Engineering*, 228(7), 1130-1140.

Campos-Delgado, D., Espinoza-Trejo, D. & Palacios, E. (2008) Fault-tolerant control in variable speed drives: a survey. *IET Electric Power Applications*, 2(2), 121-134.

Campos-Delgado, D. U., Martinez-Martinez, S. & Zhou, K. (2005) Integrated fault-tolerant scheme for a DC speed drive. *IEEE/ASME Transactions on Mechatronics*, 10(4), 419-427.

Carlsen, V. (1959) Induction motor armature control. Google Patents.

Casella, F. & Lovera, M. (2008) LPV/LFT modelling and identification: overview, synergies and a case study, *IEEE International Conference on Computer-Aided Control Systems*. IEEE Xplore.

Chakraborty, C. & Verma, V. (2015) Speed and current sensor fault detection and isolation technique for induction motor drive using axes transformation. *IEEE Transactions on Industrial Electronics*, 62(3), 1943-1954.

Chalmers, B. & Sarkar, B. (1968) Induction-motor losses due to nonsinusoidal supply waveforms, *Proceedings of the Institution of Electrical Engineers*. IET.

Chan, T. F. & Shi, K. (2011) *Applied intelligent control of induction motor drives.*John Wiley & Sons.

Chen, H., Jiang, B., Lu, N. & Mao, Z. (2016) Data-based incipient actuator fault detection and diagnosis for three-phase PWM voltage source inverter, *35th Chinese Control Conference (CCC)* IEEE.

Chen, J. & Patton, R. J. (1996) Optimal filtering and robust fault diagnosis of stochastic systems with unknown disturbances. *IEE Proceedings-Control Theory and Applications*, 143(1), 31-36.

Chen, J. & Patton, R. J. (1999) *Robust model-based fault diagnosis for dynamic systems, 3*. Repoduced on-line by Springer in 2012: Springer Science & Business Media.

Chen, W. & Saif, M. (2006) Unknown input observer design for a class of nonlinear systems: an LMI approach, *American Control Conference, 2006*. IEEE Xplore.

Chen, Z., Gao, J., Wang, F., Ma, Z., Zhang, Z. & Kennel, R. (2014) Sensorless control for SPMSM with concentrated windings using multisignal injection method. *IEEE Transactions on Industrial Electronics*, 61(12), 6624-6634.

Chen, Z., LIU, X.-d., JIN, Y.-q. & DAI, Y.-p. (2008) Direct torque control of permanent magnet synchronous motors based on extended Kalman filter observer of flux linkage. *Proceedings of the CSEE*, 33, 017.

Chen, Z., Wang, F., Stolze, P. & Kennel, R. (2013) Using compensated MRAS for model predictive control of induction machine, *Power Electronics and Applications (EPE), 2013 15th European Conference on*. IEEE.

Choi, H. H. (2007) LMI-based nonlinear fuzzy observer-controller design for uncertain MIMO nonlinear systems. *IEEE Transactions on Fuzzy Systems*, 15(5), 956-971.

Comtet-Varga, G., Christophe, C., Cocquempot, V. & Staroswiecki, M. (1999) FDI For the induction motor using elimination theory, *1999 European Control Conference (ECC)*. Karlsruhe, Germany: IEEE Xplore.

Cornell, E. P. & Lipo, T. A. (1977) Modeling and design of controlled current induction motor drive systems. *IEEE Transactions on Industry Applications*(4), 321-330.

Davari, S. A., Khaburi, D. A., Wang, F. & Kennel, R. M. (2012) Using full order and reduced order observers for robust sensorless predictive torque control of induction motors. *IEEE Transactions on Power Electronics*, 27(7), 3424-3433.

Deng, L. & Yu, D. (2014) Deep learning: methods and applications. *Foundations and Trends® in Signal Processing*, 7(3–4), 197-387.

Deshpande, A. P., Patwardhan, S. C. & Narasimhan, S. S. (2009) Intelligent state estimation for fault tolerant nonlinear predictive control. *Journal of Process control*, 19(2), 187-204.

Ding, S., Jeinsch, T., Frank, P. & Ding, E. (2000) A unified approach to the optimization of fault detection systems. *International journal of Adaptive Control and Signal Processing*, 14(7), 725-745.

Ding, S. X. (2009) Integrated design of feedback controllers and fault detectors. *Annual Reviews in Control*, 33(2), 124-135.

Dolan, H. & Herbert, S. C. (1948) Induction motor control by electric brake. Google Patents.

Drakunov, S. & Utkin, V. (1995) Sliding mode observers. Tutorial, *Decision and Control, 1995., Proceedings of the 34th IEEE Conference on*. IEEE.

Drakunov, S. V. & Utkin, V. I. (1992) Sliding mode control in dynamic systems. *International Journal of Control*, 55(4), 1029-1037.

Drif, M. h. & Cardoso, A. J. M. (2014) Stator fault diagnostics in squirrel cage three-phase induction motor drives using the instantaneous active and reactive power signature analyses. *IEEE Transactions on Industrial Informatics*, 10(2), 1348-1360.

Edwards, C. & Spurgeon, S. (1998) *Sliding mode control: theory and applications*.Crc Press.

Edwards, C. & Spurgeon, S. K. (1994) On the development of discontinuous observers. *International Journal of control*, 59(5), 1211-1229.

Edwards, C., Spurgeon, S. K. & Patton, R. J. (2000) Sliding mode observers for fault detection and isolation. *Automatica*, 36(4), 541-553.

Edwards, C. & Tan, C. P. (2006) Sensor fault tolerant control using sliding mode observers. *Control Engineering Practice*, 14(8), 897-908.

Eftekhari, M., Moallem, M., Sadri, S. & Shojaei, A. (2013) Review of induction motor testing and monitoring methods for inter-turn stator winding faults, *21st Iranian Conference on Electrical Engineering (ICEE)*. IEEE Xplore.

Ekramian, M., Sheikholeslam, F., Hosseinnia, S. & Yazdanpanah, M. J. (2013) Adaptive state observer for Lipschitz nonlinear systems. *Systems & Control Letters*, 62(4), 319-323.

Emedi, Z. & Karimi, A. (2014) Robust fixed-order discrete-time LPV controller design. *IFAC Proceedings Volumes*, 47(3), 6914-6919.

Estrada, A. & Fridman, L. (2010a) Quasi-continuous HOSM control for systems with unmatched perturbations. *Automatica*, 46(11), 1916-1919.

Estrada, A. & Fridman, L. M. (2010b) Integral HOSM semiglobal controller for finite-time exact compensation of unmatched perturbations. *IEEE Transactions on Automatic Control*, 55(11), 2645-2649.

Faiz, J., Ghorbanian, V. & Ebrahimi, B. M. (2014) EMD-based analysis of industrial induction motors with broken rotor bars for identification of operating point at different supply modes. *IEEE Transactions on Industrial Informatics*, 10(2), 957-966.

Fan, J., Zhang, Y. & Zheng, Z. (2013) Adaptive observer-based integrated fault diagnosis and fault-tolerant control systems against actuator faults and saturation. *Journal of Dynamic Systems, Measurement, and Control*, 135(4), 041008.

Fekih, A. (2008) Effective fault tolerant control design for nonlinear systems: application to a class of motor control system. *IET Control Theory & Applications*, 2(9), 762-772.

Feng, X. (2014) *Predictive control approaches to fault tolerant control of wind turbines*University of Hull.

Feng, X., Patton, R. & Wang, Z. (2014) Sensor fault tolerant control of a wind turbine via Takagi-Sugeno fuzzy observer and model predictive control, *2014 UKACC International Conference on Control*. Loughborough, UK: IEEE Xplore.

Filippetti, F., Franceschini, G., Tassoni, C. & Vas, P. (2000) Recent developments of induction motor drives fault diagnosis using AI techniques. *IEEE Transactions on Industrial Electronics*, 47(5), 994-1004.

Fridman, L. (2016) Technical Committee on Variable Structure and Sliding-Mode Control [Technical Activities]. *IEEE Control Systems*, 36(3), 18-20.

Fridman, L., Shtessel, Y., Edwards, C. & Yan, X. G. (2008) Higher‐order sliding‐mode observer for state estimation and input reconstruction in nonlinear systems. *International Journal of Robust and Nonlinear Control*, 18(4‐5), 399-412.

Gahinet, P. & Apkarian, P. (1994) A linear matrix inequality approach to H∞ control. *International Journal of Robust and Nonlinear Control*, 4(4), 421-448.

Garcia, E. A. & Frank, P. (1997) Deterministic nonlinear observer-based approaches to fault diagnosis: a survey. *Control Engineering Practice*, 5(5), 663-670.

Guzman, H., Duran, M. J., Barrero, F., Bogado, B. & Toral, S. (2014) Speed control of five-phase induction motors with integrated open-phase fault operation using model-based predictive current control techniques. *IEEE Transactions on Industrial Electronics*, 61(9), 4474-4484.

Hammond, P. & Mokrytzki, B. (1973) *Induction motor control system*

Hansen, C. & Debs, A. (1995) Power system state estimation using three-phase models. *IEEE Transactions on Power Systems*, 10(2), 818-824.

Hasegawa, M., Furutani, S., Doki, S. & Okuma, S. (2003) Robust vector control of induction motors using full-order observer in consideration of core loss. *IEEE Transactions on Industrial Electronics*, 50(5), 912-919.

Hinkkanen, M., Harnefors, L. & Luomi, J. (2010) Reduced-order flux observers with stator-resistance adaptation for speed-sensorless induction motor drives. *IEEE Transactions on Power Electronics*, 25(5), 1173-1183.

Hunt, L. J. (1907) A new type of induction motor. *Journal of the Institution of Electrical Engineers*, 39(186), 648-667.

Immovilli, F., Bianchini, C., Cocconcelli, M., Bellini, A. & Rubini, R. (2013) Bearing fault model for induction motor with externally induced vibration. *IEEE Transactions on Industrial Electronics*, 60(8), 3408-3418.

Isermann, R. (1984) Process fault detection based on modeling and estimation methods—a survey. *Automatica*, 20(4), 387-404.

Isermann, R. (2011) *Fault-diagnosis applications: model-based condition monitoring: actuators, drives, machinery, plants, sensors, and fault-tolerant systems*.Springer Science & Business Media.

Isermann, R. & Ballé, P. (1997) Trends in the application of model-based fault detection and diagnosis of technical processes. *Control Engineering Practice*, 5(5), 709-719.

Jiang, B. & Staroswiecki, M. (2002) Adaptive observer design for robust fault estimation. *International Journal of Systems Science*, 33(9), 767-775.

Jiang, B., Staroswiecki, M. & Cocquempot, V. (2004) Fault estimation in nonlinear uncertain systems using robust/sliding-mode observers. *IEE Proceedings-Control Theory and Applications*, 151(1), 29-37.

Joksimović, G. M. (2005) Dynamic simulation of cage induction machine with air gap eccentricity. *IEE Proceedings-Electric Power Applications*, 152(4), 803-811.

Jones, M., Vukosavic, S. N., Dujic, D. & Levi, E. (2009) A synchronous current control scheme for multiphase induction motor drives. *IEEE Transactions on Energy Conversion*, 24(4), 860-868.

Kaikaa, M. Y., Hadjami, M. & Khezzar, A. (2014) Effects of the simultaneous presence of static eccentricity and broken rotor bars on the stator current of induction machine. *IEEE Transactions on Industrial Electronics*, 61(5), 2452-2463.

Karmakar, S., Chattopadhyay, S., Mitra, M. & Sengupta, S. (2016a) Broken Rotor Bar, *Induction Motor Fault Diagnosis,*Springer, 57-78.

Karmakar, S., Chattopadhyay, S., Mitra, M. & Sengupta, S. (2016b) Induction Motor Fault Diagnosis.

Kastha, D. & Bose, B. K. (1994) Investigation of fault modes of voltage-fed inverter system for induction motor drive. *IEEE Transactions on Industry Applications*, 30(4), 1028-1038.

Khamari, D., Makouf, A. & Drid, S. (2011) Control of induction motor using polytopic LPV models, *2011 International Conference on Communications, Computing and Control Applications (CCCA)*. IEEE Xplore.

Khoob, A. R. (2008) Artificial neural network estimation of reference evapotranspiration from pan evaporation in a semi-arid environment. *Irrigation Science,* 27(1), 35-39.

Kim, K.-H. & Youn, M.-J. (2002) Performance comparison of PWM inverter and variable DC link inverter schemes for high-speed sensorless control of BLDC motor. *Electronics Letters*, 38(21), 1294-1295.

Kim, Y.-R., Sul, S.-K. & Park, M.-H. (1994) Speed sensorless vector control of induction motor using extended Kalman filter. *IEEE Transactions on Industry Applications*, 30(5), 1225-1233.

Kim, Y. H. & Lewis, F. L. (1999) Neural network output feedback control of robot manipulators. *IEEE Transactions on Robotics and Automation*, 15(2), 301-309.

Kioskeridis, I. & Margaris, N. (1996) Loss minimization in scalar-controlled induction motor drives with search controllers. *IEEE Transactions on Power Electronics*, 11(2), 213-220.

Klingshirn, E. A. & Jordan, H. E. (1968) Polyphase induction motor performance and losses on nonsinusoidal voltage sources. *IEEE Transactions on Power Apparatus and Systems*(3), 624-631.

Kommuri, S. K., Rath, J. J., Veluvolu, K. C. & Defoort, M. (2014) An induction motor sensor fault detection and isolation based on higher order sliding mode decoupled current controller, *2014 European Control Conference (ECC)*. IEEE.

Koshkouei, A. J. & Zinober, A. S. (2000a) Adaptive backstepping control of nonlinear systems with unmatched uncertainty, *Proceedings of the 39th IEEE Conference on Decision and Control.*: IEEE.

Koshkouei, A. J. & Zinober, A. S. (2000b) Adaptive backstepping control of nonlinear systems with unmatched uncertainty, *Proceedings of the 39th IEEE Conference on Decision and Control*. IEEE.

Krzemiński, Z. (1987) Nonlinear control of induction motor. *IFAC Proceedings Volumes*, 20(5), 357-362.

Kubota, H., Matsuse, K. & Nakano, T. (1993) DSP-based speed adaptive flux observer of induction motor. *IEEE Transactions on Industry Applications*, 29(2), 344-348.

Kwon, T.-S., Shin, M.-H. & Hyun, D.-S. (2005) Speed sensorless stator flux-oriented control of induction motor in the field weakening region using Luenberger observer. *IEEE Transactions on Power Electronics*, 20(4), 864-869.

Laghrouche, S., Plestan, F. & Glumineau, A. (2007) Higher order sliding mode control based on integral sliding mode. *Automatica*, 43(3), 531-537.

Lan, J. & Patton, R. J. (2015) Integrated design of robust fault estimation and fault-tolerant control for linear systems, *IEEE 54th Annual Conference on Decision and Control (CDC)*. Osaka, Japan: IEEE.

Lan, J. & Patton, R. J. (2016) A new strategy for integration of fault estimation within fault-tolerant control. *Automatica*, 69, 48-59.

Lan, J. & Patton, R. J. (2017) Integrated fault estimation and fault‐tolerant control for uncertain Lipschitz nonlinear systems. *International Journal of Robust and Nonlinear Control*, 27(5), 761-780.

Lascu, C., Boldea, I. & Blaabjerg, F. (1998) A modified direct torque control (DTC) for induction motor sensorless drive, *Industry Applications Conference, 33rd IAS Annual Meeting.*: IEEE.

Lascu, C., Boldea, I. & Blaabjerg, F. (2004) Direct torque control of sensorless induction motor drives: a sliding-mode approach. *IEEE Transactions on Industry Applications*, 40(2), 582-590.

Lascu, C., Boldea, I. & Blaabjerg, F. (2009) A class of speed-sensorless sliding-mode observers for high-performance induction motor drives. *IEEE Transactions on Industrial Electronics*, 56(9), 3394-3403.

Lavi, A. & Polge, R. (1966) Induction motor speed control with static inverter in the rotor. *IEEE Transactions on Power Apparatus and Systems*(1), 76-84.

Lee, H. & Utkin, V. I. (2007) Chattering suppression methods in sliding mode control systems. *Annual Reviews in Control*, 31(2), 179-188.

Leite, V. C., da Silva, J. G. B., Veloso, G. F. C., da Silva, L. E. B., Lambert-Torres, G., Bonaldi, E. L. & de Oliveira, L. E. d. L. (2015) Detection of localized bearing faults in induction machines by spectral kurtosis and envelope analysis of stator current. *IEEE Transactions on Industrial Electronics*, 62(3), 1855-1865.

Lin, F.-J., Shen, P.-H. & Hsu, S.-P. (2002) Adaptive backstepping sliding mode control for linear induction motor drive. *IEE Proceedings-Electric Power Applications*, 149(3), 184-194.

Lipo, T. A. & Krause, P. C. (1969) Stability analysis of a rectifier-inverter induction motor drive. *IEEE Transactions on Power Apparatus and Systems*(1), 55-66.

Lopez-Toribio, C., Patton, R. J. & Daley, S. (2000) Takagi–Sugeno fuzzy fault-tolerant control of an induction motor. *Neural Computing & Applications*, 9(1), 19-28.

Lu, B. & Wu, F. (2004) Switching LPV control designs using multiple parameter-dependent Lyapunov functions. *Automatica*, 40(11), 1973-1980.

Maes, J. & Melkebeek, J. A. (2000) Speed-sensorless direct torque control of induction motors using an adaptive flux observer. *IEEE Transactions on Industry Applications*, 36(3), 778-785.

Maiti, S., Chakraborty, C., Hori, Y. & Ta, M. C. (2008) Model reference adaptive controller-based rotor resistance and speed estimation techniques for vector controlled induction motor drive utilizing reactive power. *IEEE Transactions on Industrial Electronics*, 55(2), 594-601.

Mangoubi, R., Appleby, B. & Farrell, J. (1992) Robust estimation in fault detection, *Decision and Control, 1992., Proceedings of the 31st IEEE Conference on*. IEEE.

Marino, R., Sergei, P. & Paolo, V. (1993) Adaptive input-output linearization control of induction motor. *IEEE Transactions on Automation Control*, 38(2), 208-212.

Marino, R., Tomei, P. & Verrelli, C. M. (2010) *Induction motor control design*.Springer Science & Business Media.

Martins, J. F., Pires, V. F. & Pires, A. (2007) Unsupervised neural-network-based algorithm for an on-line diagnosis of three-phase induction motor stator fault. *IEEE Transactions on Industrial Electronics*, 54(1), 259-264.

Mendes, A. M. & Cardoso, A. M. (2006) Fault-tolerant operating strategies applied to three-phase induction-motor drives. *IEEE Transactions on Industrial Electronics*, 53(6), 1807-1817.

Mendrela, E., Fleszar, J. & Gierczak, E. (2012) *Modeling of induction motors with one and two degrees of mechanical freedom,*.Springer Science & Business Media.

Morari, M. & Lee, J. H. (1999) Model predictive control: past, present and future. *Computers & Chemical Engineering*, 23(4), 667-682.

Morawiec, M. (2015) Z-type observer backstepping for induction machines. *IEEE Transactions on Industrial Electronics*, 62(4), 2090-2102.

Moreno, J. A. & Osorio, M. (2008) A Lyapunov approach to second-order sliding mode controllers and observers, *Decision and Control, 2008. CDC 2008. 47th IEEE Conference on*. IEEE.

Naderi, R. & Rahmati, A. (2008) Phase-shifted carrier PWM technique for general cascaded inverters. *IEEE Transactions on Power Electronics*, 23(3), 1257-1269.

Nandi, S., Toliyat, H. A. & Li, X. (2005) Condition monitoring and fault diagnosis of electrical motors—A review. *IEEE transactions on Energy Conversion*, 20(4), 719-729.

Narita, M., Chen, G. & Takami, I. (2017) Gain scheduling controller synthesis for active magnetic bearing based on parameter dependent LMI with convexity condition, *2nd International Conference on Control and Robotics Engineering (ICCRE)*. IEEE.

Nash, J. N. (1997) Direct torque control, induction motor vector control without an encoder. *IEEE Transactions on Industry Applications*, 33(2), 333-341.

Nelsen, M. G. & Acker, R. S. (1950) Motor control relay and circuit. Google Patents.

Odgaard, P. F. & Johnson, K. E. (2013) Wind turbine fault detection and fault tolerant control-an enhanced benchmark challenge, *American Control Conference (ACC), 2013*. IEEE.

Ohnishi, K., Ueda, Y. & Miyachi, K. (1986) Model reference adaptive system against rotor resistance variation in induction motor drive. *IEEE Transactions on Industrial Electronics*(3), 217-223.

Ohtani, T., Takada, N. & Tanaka, K. (1992) Vector control of induction motor without shaft encoder. *IEEE Transactions on Industry Applications*, 28(1), 157-164.

Oliveira, R. C. & Peres, P. L. (2005) Stability of polytopes of matrices via affine parameter-dependent Lyapunov functions: Asymptotically exact LMI conditions. *Linear algebra and its applications*, 405, 209-228.

Orlowska-Kowalska, T. (1989) Application of extended Luenberger observer for flux and rotor time-constant estimation in induction motor drives, *IEE Proceedings D (Control Theory and Applications)*. IET.

Orlowska-Kowalska, T. & Dybkowski, M. (2010) Stator-current-based MRAS estimator for a wide range speed-sensorless induction-motor drive. *IEEE Transactions on Industrial Electronics*, 57(4), 1296-1308.

Oudghiri, M., Chadli, M. & El Hajjaji, A. (2008) Robust observer-based fault-tolerant control for vehicle lateral dynamics. *International Journal of Vehicle Design*, 48(3-4), 173-189.

Paice, D. A. (1968) Induction motor speed control by stator voltage control. *IEEE Transactions on Power Apparatus and systems*(2), 585-590.

Park, M.-H. & Kim, K.-S. (1991) Chattering reduction in the position control of induction motor using the sliding mode. *IEEE Transactions on Power Electronics*, 6(3), 317-325.

Patton, R. J. (1997a) Fault-tolerant control: the 1997 situation. *IFAC Safeprocess '97, The University of Hull*, 30(18), 1029-1051.

Patton, R. J. (1997b) Robustness in model-based fault diagnosis: the 1995 situation. *Annual Reviews in Control*, 21, 103-123.

Patton, R. J. (2015) Fault-tolerant control. *Encyclopedia of Systems and Control*, 422-428.

Pellanda, P. C., Apkarian, P. & Tuan, H. D. (2002) Missile autopilot design via a multi‐channel LFT/LPV control method. *International Journal of Robust and Nonlinear Control*, 12(1), 1-20.

Pfifer, H. (2013) *LPV/LFT Modeling and its Application in Aerospace*. Munich, Germany: Technical University of Munich.

Plunkett, A. B. (1977) Direct flux and torque regulation in a PWM inverter-induction motor drive. *IEEE Transactions on Industry Applications*(2), 139-146.

Prempain, E., Postlethwaite, I. & Benchaib, A. (2002) A linear parameter variant H∞ control design for an induction motor. *Control Engineering Practice*, 10(6), 633-644.

Raisemche, A., Boukhnifer, M., Larouci, C. & Diallo, D. (2014) Two active fault-tolerant control schemes of induction-motor drive in EV or HEV. *IEEE Transactions on Vehicular Technology*, 63(1), 19-29.

Redfern, D. & Campbell, C. (2012) *The MATLAB® 5 Handbook*.Springer Science & Business Media.

Rehman, S. & Mohandes, M. (2008) Artificial neural network estimation of global solar radiation using air temperature and relative humidity. *Energy Policy*, 36(2), 571-576.

Romero, M., Seron, M. & De Dona, J. (2010) Sensor fault-tolerant vector control of induction motors. *IET Control Theory & Applications*, 4(9), 1707-1724.

Rosales, A., Shtessel, Y., Fridman, L. & Panathula, C. B. (2016) Chattering Analysis of HOSM Controlled Systems: Frequency Domain Approach. *IEEE Transactions on Automatic Control*.

Roy, S. & Banerjee, P. (2005) An algorithm for trading off quantization error with hardware resources for MATLAB-based FPGA design. *IEEE Transactions on Computers*, 54(7), 886-896.

Sami, M. & Patton, R. J. (2012) Wind turbine power maximisation based on adaptive sensor fault tolerant sliding mode control, *20th Mediterranean Conference on Control & Automation (MED)*. IEEE.

Sami, M. & Patton, R. J. (2013) Active fault tolerant control for nonlinear systems with simultaneous actuator and sensor faults. *International Journal of Control, Automation and Systems*, 11(6), 1149-1161.

Schauder, C. (1992) Adaptive speed identification for vector control of induction motors without rotational transducers. *IEEE Transactions on Industry Applications*, 28(5), 1054-1061.

Schmidhuber, J. (2015) Deep learning in neural networks: An overview. *Neural networks*, 61, 85-117.

Schoen, R. R., Lin, B. K., Habetler, T. G., Schlag, J. H. & Farag, S. (1995) An unsupervised, on-line system for induction motor fault detection using stator current monitoring. *IEEE Transactions on Industry Applications*, 31(6), 1280-1286.

Shaker, M. S. & Patton, R. J. (2014) Active sensor fault tolerant output feedback tracking control for wind turbine systems via T–S model. *Engineering Applications of Artificial Intelligence*, 34, 1-12.

Shamma, J. S. & Athans, M. (1991) Guaranteed properties of gain scheduled control for linear parameter-varying plants. *Automatica*, 27(3), 559-564.

Shashidhara, S. & Raju, P. (2013) Stator Winding Fault Diagnosis of Three Phase Induction Motor by Park's Vector Approach. *International Journal of Advanced Research in Electrical, Electronics and Instrumentation Engineering*, 2(7), 2901-6.

Shen, Q. & Shi, P. (2015) Distributed command filtered backstepping consensus tracking control of nonlinear multiple-agent systems in strict-feedback form. *Automatica*, 53, 120-124.

Shi, F. & Patton, R. (2014) Active fault tolerant control of LPV descriptor systems based on extended state observers, *American Control Conference (ACC), 2014*. IEEE.

Shi, F. & Patton, R. J. (2015) Fault estimation and active fault tolerant control for linear parameter varying descriptor systems. *International Journal of Robust and Nonlinear Control*, 25(5), 689-706.

Shi, K., Chan, T., Wong, Y. & Ho, S. (2002) Speed estimation of an induction motor drive using an optimized extended Kalman filter. *IEEE Transactions on Industrial Electronics*, 49(1), 124-133.

Shieh, H.-J. & Shyu, K.-K. (1999) Nonlinear sliding-mode torque control with adaptive backstepping approach for induction motor drive. *IEEE Transactions on Industrial Electronics*, 46(2), 380-389.

Shipurkar, U., Strous, T. D., Polinder, H., Ferreira, J. B. & Veltman, A. (2017) Achieving Sensorless Control for the Brushless Doubly-Fed Induction Machine. *IEEE Transactions on Energy Conversion*.

Shyu, K.-K. & Shieh, H.-J. (1996) A new switching surface sliding-mode speed control for induction motor drive systems. *IEEE Transactions on Power Electronics*, 11(4), 660-667.

Siddique, A., Yadava, G. & Singh, B. (2005) A review of stator fault monitoring techniques of induction motors. *IEEE Transactions on Energy Conversion*, 20(1), 106-114.

Sonmez, H., Gokceoglu, C., Nefeslioglu, H. & Kayabasi, A. (2006) Estimation of rock modulus: for intact rocks with an artificial neural network and for rock masses with a new empirical equation. *International Journal of Rock Mechanics and Mining Sciences*, 43(2), 224-235.

Soualhi, A., Clerc, G. & Razik, H. (2013) Detection and diagnosis of faults in induction motor using an improved artificial ant clustering technique. *IEEE Transactions on Industrial Electronics*, 60(9), 4053-4062.

Stando, D., Kaźmierkowski, M. P. & Chudzik, P. (2014) Sensorless predictive torque control of induction motor drive operating in wide speed range—Simulation study, *Power Electronics and Motion Control Conference and Exposition (PEMC), 2014 16th International*. IEEE.

Stanley, H. C. (1938) An analysis of the induction machine. *Electrical Engineering*, 57(12), 751-757.

Stoustrup, J. & H Niemann, H. (2002) Fault estimation—a standard problem approach. *International Journal of Robust and Nonlinear Control*, 12(8), 649-673.

Sun, F., Sun, Z. & Woo, P.-Y. (2001) Neural network-based adaptive controller design of robotic manipulators with an observer. *IEEE Transactions on Neural networks*, 12(1), 54-67.

Tabbache, B., Rizoug, N., Benbouzid, M. E. H. & Kheloui, A. (2013) A control reconfiguration strategy for post-sensor FTC in induction motor-based EVs. *IEEE Transactions on Vehicular Technology*, 62(3), 965-971.

Takahashi, I. & Noguchi, T. (1986) A new quick-response and high-efficiency control strategy of an induction motor. *IEEE Transactions on Industry Applications*(5), 820-827.

Tan, C. P. & Edwards, C. (2002) Sliding mode observers for detection and reconstruction of sensor faults. *Automatica*, 38(10), 1815-1821.

Tan, C. P. & Edwards, C. (2003) Sliding mode observers for robust detection and reconstruction of actuator and sensor faults. *International Journal of Robust and Nonlinear Control*, 13(5), 443-463.

Tan, C. P. & Edwards, C. (2004) Multiplicative fault reconstruction using sliding mode observers, *Control Conference, 2004. 5th Asian*. IEEE.

Tan, D. & Patton, R. J. (2015) Integrated fault estimation and fault tolerant control: A joint design. *IFAC-PapersOnLine*, 48(21), 517-522.

Tan, H. (1999) Field orientation and adaptive backstepping for induction motor control, *Industry Applications Conference, 1999. Thirty-Fourth IAS Annual Meeting. Conference Record of the 1999 IEEE*. IEEE.

Tan, H. & Chang, J. (1999) Adaptive backstepping control of induction motor with uncertainties, *American Control Conference, 1999. Proceedings of the 1999*. IEEE.

Tayarani-Bathaie, S. S., Vanini, Z. S. & Khorasani, K. (2014) Dynamic neural network-based fault diagnosis of gas turbine engines. *Neurocomputing*, 125, 153-165.

Teja, A. R., Chakraborty, C., Maiti, S. & Hori, Y. (2012) A new model reference adaptive controller for four quadrant vector controlled induction motor drives. *IEEE Transactions on Industrial Electronics*, 59(10), 3757-3767.

Theocharis, J. & Petridis, V. (1994) Neural network observer for induction motor control. *IEEE Control Systems*, 14(2), 26-37.

Thomson, W. T. & Fenger, M. (2001) Current signature analysis to detect induction motor faults. *IEEE Industry Applications Magazine*, 7(4), 26-34.

Trzynadlowski, A. M. (2000) *Control of induction motors*.Academic press.

Ventura, U. P. & Fridman, L. (2016) Chattering measurement in SMC and HOSMC, *Variable Structure Systems (VSS), 2016 14th International Workshop on*. IEEE.

Vogelsberger, M. A., Grubic, S., Habetler, T. G. & Wolbank, T. M. (2010) Using PWM-induced transient excitation and advanced signal processing for zero-speed sensorless control of AC machines. *IEEE Transactions on Industrial Electronics*, 57(1), 365-374.

Wagner, C. (1939) Self-excitation of induction motors. *Electrical Engineering*, 58(2), 47-51.

Walcott, B. & Zak, S. (1987) State observation of nonlinear uncertain dynamical systems. *IEEE Transactions on Automatic Control*, 32(2), 166-170.

Walcott, B. L. & Zak, S. H. (1988) Combined observer-controller synthesis for uncertain dynamical systems with applications. *IEEE Transactions on Systems, Man, and Cybernetics*, 18(1), 88-104.

Wang, F., Chen, Z., Stolze, P., Stumper, J.-F., Rodriguez, J. & Kennel, R. (2014) Encoderless finite-state predictive torque control for induction machine with a compensated MRAS. *IEEE Transactions on Industrial Informatics*, 10(2), 1097-1106.

Wang, H. & Daley, S. (1996) Actuator fault diagnosis: An adaptive observer-based technique. *IEEE transactions on Automatic Control*, 41(7), 1073-1078.

Wang, J. L., Yang, G.-H. & Liu, J. (2007) An LMI approach to H-index and mixed H-/H ∞ fault detection observer design. *Automatica*, 43(9), 1656-1665.

Ward, E. & Härer, H. (1969) Preliminary investigation of an invertor-fed 5-phase induction motor, *Proceedings of the Institution of Electrical Engineers*. IET.

Xiao-Zheng, J. & Guang-Hong, Y. (2009) Robust adaptive fault-tolerant compensation control with actuator failures and bounded disturbances. *Acta Automatica Sinica*, 35(3), 305-309.

Xiao, B., Hu, Q. & Zhang, Y. (2012) Adaptive sliding mode fault tolerant attitude tracking control for flexible spacecraft under actuator saturation. *IEEE Transactions on Control Systems Technology*, 20(6), 1605-1612.

Xu, Z. & Rahman, M. (2003) An extended kalman filter observer for the direct torque controlled interior permanent magnet synchronous motor drive, *Power Electronics and Drive Systems, 2003. PEDS 2003. The Fifth International Conference on*. IEEE.

Yan, X.-G. & Edwards, C. (2007) Nonlinear robust fault reconstruction and estimation using a sliding mode observer. *Automatica*, 43(9), 1605-1614.

Yan, Z., Jin, C. & Utkin, V. (2000) Sensorless sliding-mode control of induction motors. *IEEE Transactions on Industrial Electronics*, 47(6), 1286-1297.

Yao, J., Jiao, Z. & Ma, D. (2014) Extended-state-observer-based output feedback nonlinear robust control of hydraulic systems with backstepping. *IEEE Transactions on Industrial Electronics*, 61(11), 6285-6293.

Yin, S., Luo, H. & Ding, S. X. (2014) Real-time implementation of fault-tolerant control systems with performance optimization. *IEEE Transactions on Industrial Electronics*, 61(5), 2402-2411.

Yu, Z., Chen, H. & Woo, P. y. (2002) Gain scheduled LPV H∞ control based on LMI approach for a robotic manipulator. *Journal of Field Robotics*, 19(12), 585-593.

Zai, L.-C., DeMarco, C. L. & Lipo, T. A. (1992) An extended Kalman filter approach to rotor time constant measurement in PWM induction motor drives. *IEEE Transactions on Industry Applications*, 28(1), 96-104.

Zhang, K., Jiang, B. & Cocquempot, V. (2008) Adaptive observer-based fast fault estimation. *International Journal of Control Automation and Systems*, 6(3), 320.

Zhang, X., Polycarpou, M. M. & Parisini, T. (2002) A robust detection and isolation scheme for abrupt and incipient faults in nonlinear systems. *IEEE Transactions on Automatic Control*, 47(4), 576-593.

Zhang, Y. & Jiang, J. (2006) Issues on integration of fault diagnosis and reconfigurable control in active fault-tolerant control systems. *IFAC Proceedings Volumes*, 39(13), 1437-1448.

Zhang, Y. & Jiang, J. (2008) Bibliographical review on reconfigurable fault-tolerant control systems. *Annual Reviews in Control*, 32(2), 229-252.

Zhang, Y., Zhao, Z., Lu, T., Yuan, L., Xu, W. & Zhu, J. (2009) A comparative study of Luenberger observer, sliding mode observer and extended Kalman filter for sensorless

vector control of induction motor drives, *Energy Conversion Congress and Exposition, 2009. ECCE 2009. IEEE*. IEEE.

Zhang, Y., Zhu, J., Zhao, Z., Xu, W. & Dorrell, D. G. (2012) An improved direct torque control for three-level inverter-fed induction motor sensorless drive. *IEEE Transactions on Power Electronics*, 27(3), 1502-1513.

Zhang, Z., Tang, R., Bai, B. & Xie, D. (2010) Novel direct torque control based on space vector modulation with adaptive stator flux observer for induction motors. *IEEE Transactions on Magnetics*, 46(8), 3133-3136.